ABSTRACT

Title of Dissertation:	MECHANISTIC STUDY AND THE DESIGN OF IRON-CATALYZED MULTI-COMPONENT CROSS-COUPLING REACTION
	Wes Lee, Doctor of Philosophy, 2021
Dissertation directed by:	Associate Professor Osvaldo Gutierrez, Department of Chemistry and Biochemistry

Cross-coupling reactions (CCRs) are one of the most versatile methods for the formation of C-C bonds. Traditionally, palladium and nickel are broadly used as the catalyst in this type of transformation. However, due to the low cost, low toxicity, and high natural abundance, iron has become an alternative metal catalyst for CCRs.

The first iron-catalyzed asymmetric cross-coupling reaction was reported by Nakamura in 2015 but the mechanism remained unknown. Since then, our lab has been working on 1) the elucidation of the mechanism using quantum mechanical calculations and experimental probes; and 2) the rational design and development of new types of iron-catalyzed cross-coupling reactions.

Quantum mechanical calculations were applied to study the mechanism (**Chapter 1**). With multiple possible pathways computed and extensive conformational search, we determined that the lowest energy pathway proceeds via radical formation by Fe(I), radical addition to Fe(II), and reductive elimination from Fe(III) to form the

desired cross-coupled product. With the mechanism in hand, we then designed and developed many new types of iron-catalyzed CCRs (**Chapter 2-5**), that included an intra- and inter-molecular dicarbofunctionalization of vinyl cyclopropanes, a three-component difunctionalization of unactivated alkenes, and a multicomponent radical cascade/annulation reaction. Finally, in **Chapter 6**, we introduced the [1.1.1]propellane as the σ-type radical acceptor in the three-component difunctionalization of iron-catalyzed cross-coupling reaction.

These reactions showcases the potential of iron-catalyzed CCRs and expanded the toolbox for organic synthesis.

MECHANISTIC STUDY AND THE DESIGN OF IRON-CATALYZED MULTI-COMPONENT CROSS-COUPLING REACTION

by

Wes Lee

Dissertation submitted to the Faculty of the Graduate School of the
University of Maryland, College Park, in partial fulfillment
of the requirements for the degree of
Doctor of Philosophy
2021

Advisory Committee:
Professor Osvaldo Gutierrez, Chair
Professor Jeffery Davis
Professor Andrei Vedernikov
Professor Daniel Falvey
Professor Dongxia Liu

Acknowledgements

I really enjoyed the years I spent in the chemistry department. Mainly because of all the supportive people around me.

First and foremost, I want to thank Dr. Osvaldo Gutierrez. I didn't expect to have such a great mentor like him. In both research and life, his optimistic attitude always gives me the confidence to accomplish any goals. The presentation skill he spent hours teaching me is something I will never forget.

Thank you to my committee members – Dr. Davis, Dr. Vedernikov, Dr. Falvey, and Dr. Liu. They never hesitate to help me when I contact them.

The staff in our department have been helpful all the time – Dr. Fu and Dr. Wang maintained the NMR instrument well. Dr. Li trained me on HRMS. Scott taught me FTIR and helped me connect the gas tank adaptor. Thanks to Monique in the business office for placing the chemical orders, thanks to Bill and LaVelle for receiving and delivering the packages and gas tanks.

I am also thankful for being a TA in Dr. Koppel and Dr. DeShong's classes, their teaching passion and style taught me to become a more effective teacher.

Thanks to all my lab mates, especially Lei who trained me in synthesis and listened to my practice talk many times. Thanks to Angel, Dinu, Madeline, Ryan, Mingbin, Zhihui, Robert, Cassy, and Shuai for all the conversation, discussion, and collaboration we had on many projects. Thanks to Michael, Ben, and Chris for the columns you ran and the calculations you submitted.

One of the best things in my graduate life is to become friends with Matt. Thanks to treat me like your younger brother. Having a Christmas dinner with your family is a special experience that I always remember. Thanks to Keith for inviting me to play intramural volleyball and board games. Thanks to Vinny and Doyeon who played basketball with me when I was depressed.

To Rosie. Thanks for bringing me joy and laughter. My weekends would be less interesting without you. I study chemistry by logic, I study you by emotion.

To my parents Yean-Jang Lee and Chu-Jyu Chao, thanks for giving me a balance of guidance and freedom to explore what I want and listening to all the good and bad that happened in my life. To my sister Yu-Chien Lee who is so smart and self-disciplined, thanks for being a model that I can learn from, and the one I can share every secret with.

Table of Contents

List of Tables

List of Figures

Chapter 1: Iron-Catalyzed Cross-Coupling Reactions

The following work has been published (Lee, W.; Zhou, J.; Gutierrez, O. *J. Am. Chem. Soc.* **2017**, *139*, 16126-16133.)

1.1 Cross-Coupling Reactions

Cross-coupling reactions (CCRs) are one of the most powerful methods in organic chemistry for the construction of C-C bonds.[1] In this vein, palladium- and nickel-complexes are by far the most popular transition metals for this type of transformation for applications in industry and academia.[2] However, due to the rising costs of precious transition metals (i.e., palladium)[34,35] the investigation on other transition metals for CCRs becomes crucial. In this context, iron is an inexpensive, abundant, and benign metal that can serve as an alternative catalyst to promote these transformations. Notably, iron complexes are well-known for the coupling of non-activated alkyl halides that are difficult using traditional palladium-based cross-coupling method due to propensity to undergo β-hydride elimination.[3,4,5,6,7,8,35]

The first Fe-catalyzed cross-coupling reaction was reported by Kharasch in 1941 (**Figure 1.1**). In particular, the authors reported the $C(sp^2)$-$C(sp^2)$ coupling between phenyl magnesium bromide and bromobenzene.[9] More than thirty years later, Kochi expanded the scope of this reaction and reported the coupling of alkenyl halides with aryl Grignard reagents.[10]

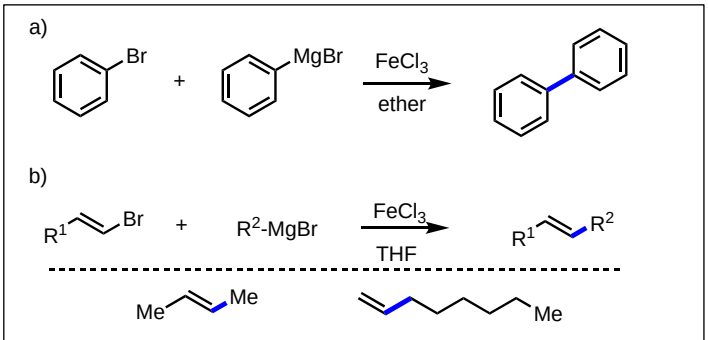

Figure 1.1. (a) First iron-catalyzed cross-coupling reaction by Kharasch in 1941. (b) Alkenyl halides with Grignard reagents reported by Kochi in 1971.

More recently, there been numerous reports by Chai,[11] Bedford,[12,13] and Nakamura[14,15,16,17] (among others) that use bisphosphine as ligands in Fe-catalyzed cross-coupling reactions. Notably, the use of bisphosphine ligands such as SciOPP, dppe, and Xantphos in combination with simple iron salts (e.g., $FeCl_3$) has accelerated

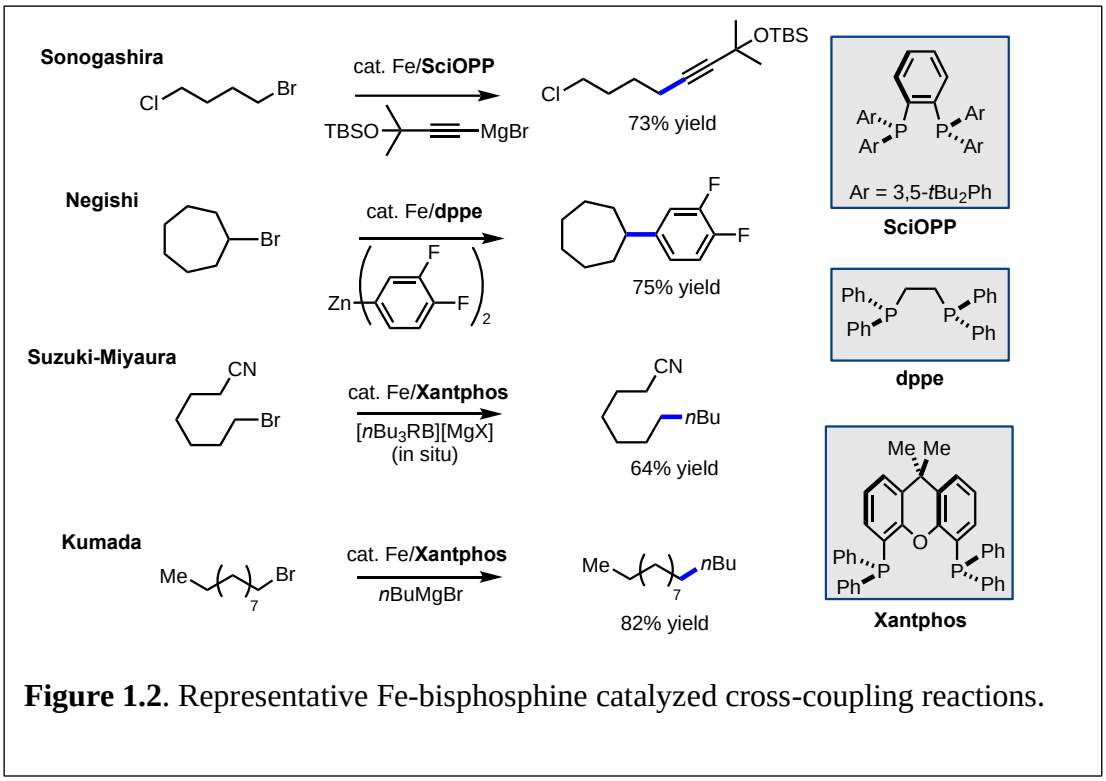

Figure 1.2. Representative Fe-bisphosphine catalyzed cross-coupling reactions.

the development of practical methods for Kumada-,[11] Negishi-,[12,14] Sonogashira-,[15] and Suzuki-Miyaura type[16,17] cross-coupling reactions (**Figure 1.2**).

In 2010 and 2014, Fu[18] and Bian,[19] respectively, reported the Kumada-type asymmetric cross-coupling reactions between α-halo-esters with Grignard reagents with nickel and cobalt catalyst (**Figure 1.3**). Subsequently, Nakamura[20] reported the

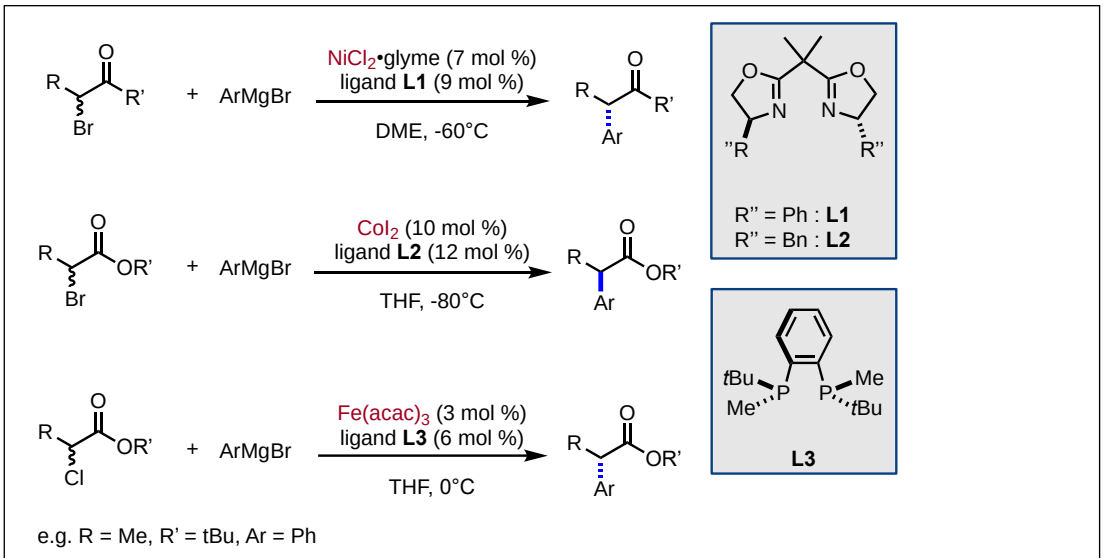

Figure 1.3. Representative late-first row asymmetric Kumada cross-coupling reactions.

first iron-catalyzed enantioselective cross-coupling reaction. This method promoted the coupling between a wide variety of α-chloroesters with Grignard reagents using catalytic amounts of iron in combination with chiral bisphosphine ligand **L3** to deliver asymmetric CCR product with high yields (up to 92% yield) and modest enantioselectivity [up to 90% enantiomeric excess (e.e.)]. Overall, contrary to well-established nickel- and palladium-catalyzed asymmetric cross-couplings, asymmetric iron-catalyzed cross-couplings reactions remain extremely rare. To this end, my goal is to use a computational and experimental approach towards the rational design and development of iron-catalyzed asymmetric multicomponent cross-couplings reactions.

Although several catalytic cycles have been proposed in the literature (**Figure 1.4**), in general, the mechanisms and, in particular, molecular-level information of the

carbon-carbon bond formation of iron-catalyzed cross-coupling reactions remain unknown. Moreover, until my report, there were only a few reports using transition-

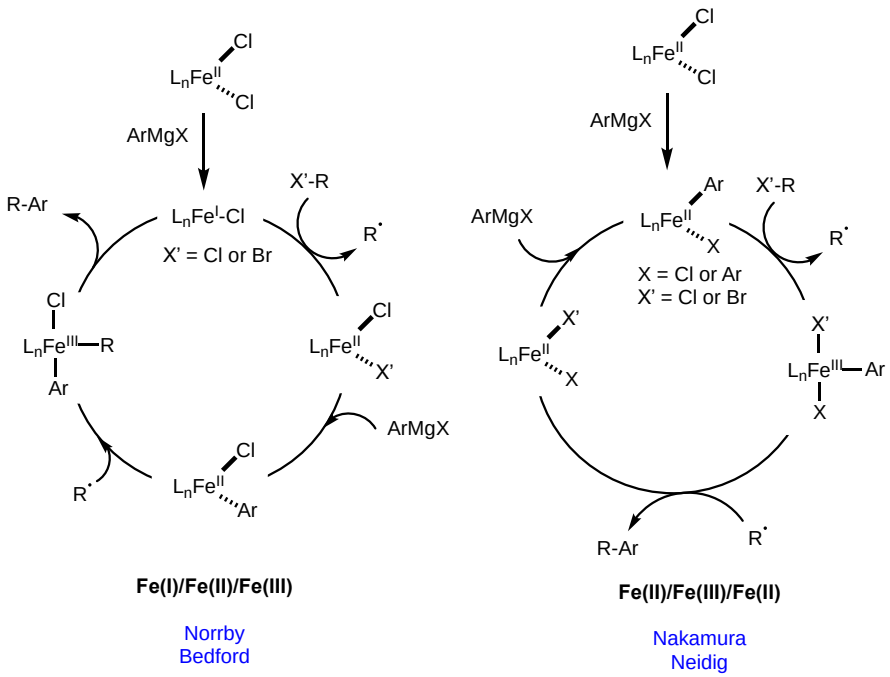

Figure 1.4. Commonly proposed mechanisms for iron-catalyzed cross-coupling reactions with Grignard reagents.

state calculations to gain insights into the mechanisms of iron-catalyzed cross-couplings.[21,22] The lack of molecular-level information limits the rational design of substrates and ligands for iron-catalyzed cross-coupling reactions. Therefore, I began to use transition-state calculations to investigate the mechanism of iron-catalyzed asymmetric CCRs with bisphosphine ligands in order to 1) understand the mechanism of these transformations and 2) gain insights into the factors controlling reactivity and enantioselectivity.

1.2 Computational Method Used to Study the Mechanism

In order to elucidate the mechanism of asymmetric iron-catalyzed cross-coupling, I began to explore the free-energy reaction pathway using the robust and well-studied unrestricted B3LYP[23] functional with a modest basis set [6-31G(d)]. To determine the spin state of each intermediate and transition state structure the expectation values of ⟨S2⟩ were used as a diagnostic tool. For example, based on the ⟨S2⟩ equation (⟨S2⟩=S(S+1)), accordingly a singlet will have a ⟨S2⟩=0. While a doublet, triplet, quartet, quintet, and sextet will have ⟨S2⟩ values of 0.75, 2, 3.75, 6, 8.75 respectively (**Table 1.1**).

	S	**2S+1**		**⟨S2⟩ = S(S+1)**
Unpaired electrion	*Spin (number)*	*multiplicity*	*Spin state*	*total spin*
0	0	1	*singlet*	0
1	1/2	2	*doublet*	0.75
2	1	3	*triplet*	2
3	3/2	4	*quartet*	3.75
4	2	5	*quintet*	6
5	5/2	6	*sextet*	8.75

Table 1.1. Relationship between spin state and the expectation value ⟨S2⟩.

Frequency calculations were subsequently preformed at the same level of theory to verify nature of stationary points and acquire thermal corrections. However, due to the well-known errors[24] associated with B3LYP including systematic bias for high-spin structures in iron complexes[24b,c] and failure to account well for dispersion interactions[24d] (crucial aspects to assess competing pathways in iron catalysis and in accounting for stereoselectivity), a range of DFT functionals ((UM06L,[25] UPBEPBE,[26] and UM06[27]) and large basis sets (6-311+G(d,p)-SDD (for Fe) and/or 6-311+G(d,p) with SMD[28] continuum solvation model in implicit THF solvent were used. These

methods are routinely used to study organometallic systems[29] and iron-catalyzed transformations including CCRs.[30,31] As such we refined all energies and assessed the relative barriers for all competing pathways by performing single-point energy calculations at the UM06L/6-311+G(d,p)-SDD (for Fe)-THF(SMD), UPBEPBE/6-311+G(d,p)-SDD (for Fe)-THF(SMD), UM06/6-311+G(d,p)-SDD (for Fe)-THF(SMD), and UM06/6-311+G(d,p)-THF(SMD) levels of theory for comparison. In our calculations, we considered all commonly proposed pathways (shown in **Figure 1.4**), including stepwise and concerted C−C bond-forming events, and computed all low, medium, and high spin states in determining the lowest free energy pathway. Only the lowest energy spin states and conformers are shown and discussed in the text and the rest of the pathways are presented in the **Chapter 7** (**Figure 7.1**, **7.2**). Unsurprisingly, we found that the absolute barriers varied significantly with the DFT functional but the overall conclusions of the reaction pathway remain the same (**Figure 7.1**, **7.2**). All calculations were performed using Guassian09,[32a] and structural figures were generated using CYLview.[33a]

1.3 Competing Pathway Leading to Biaryl Formation

In the process of mapping possible mechanism pathways, the truncated and symmetrical 1,2 bis(tetramethylphosphineo)benzene ligand was applied in the calculation (**Figure 1.5**) to reduce computational cost and accelerate mapping of competing pathways. We hypothesize that this truncation would be

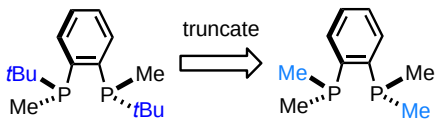

Figure 1.5. Computational truncated ligand.

appropriate because the *tert*-butyl group, presumably, mainly would affect the enantioselectivity but not the reactivity. Notably, our overall mechanism[41] using this truncated model agrees well with the mechanism reported in parallel to our studies by Nakamura and Morokuma using the full C_2 symmetric chiral ligand.[36]

Although the mechanism of iron-catalyzed cross-coupling reactions are not known, there is evidence for the participation of alkyl radical intermediates[20] (presumably originating from single electron halogen abstraction or via single electron transfer followed by halide dissociation promoted by Fe(I) or Fe(II) intermediates). Further, in the bisphosphine-iron-catalyzed cross-coupling reactions, two possible iron complexes (i.e., chloro-phenyl-iron(II) and diphenyl-iron(II) complexes) are commonly proposed as the active species and similar species have been isolated, characterized, and their reactivity explored (**Figure 1.6**)[39,40]. Naturally, we initiated our mechanistic investigation by examining the barriers for halogen abstraction using both Fe(I) and Fe(II) complexes with various coordination spheres. Energies are shown with four different methods with the lowest energy spin state found.

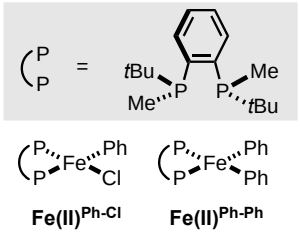

Figure 1.6. Possible iron active species.

(STOP) For clarity, I will discuss the results based on calculations using the method UPBEPBE/6-311+G(d,p)-SDD(Fe)-SMD(THF)//UB3LYP/6-31G(d) since these were found to best correlate with experimental results (see below). As shown in the free energy reaction coordinate in **Figure 1.7**, halogen abstraction by diphenyl iron(II) **Fe(II)$^{Ph-Ph}$** is ca. 20.7 kcal/mol leading to alkyl radical and trivalent iron(III)

Fe(III)$^{Ph\text{-}Ph\text{-}Cl}$ downhill in energy (3.9 kcal/mol). Next, rather than radical addition

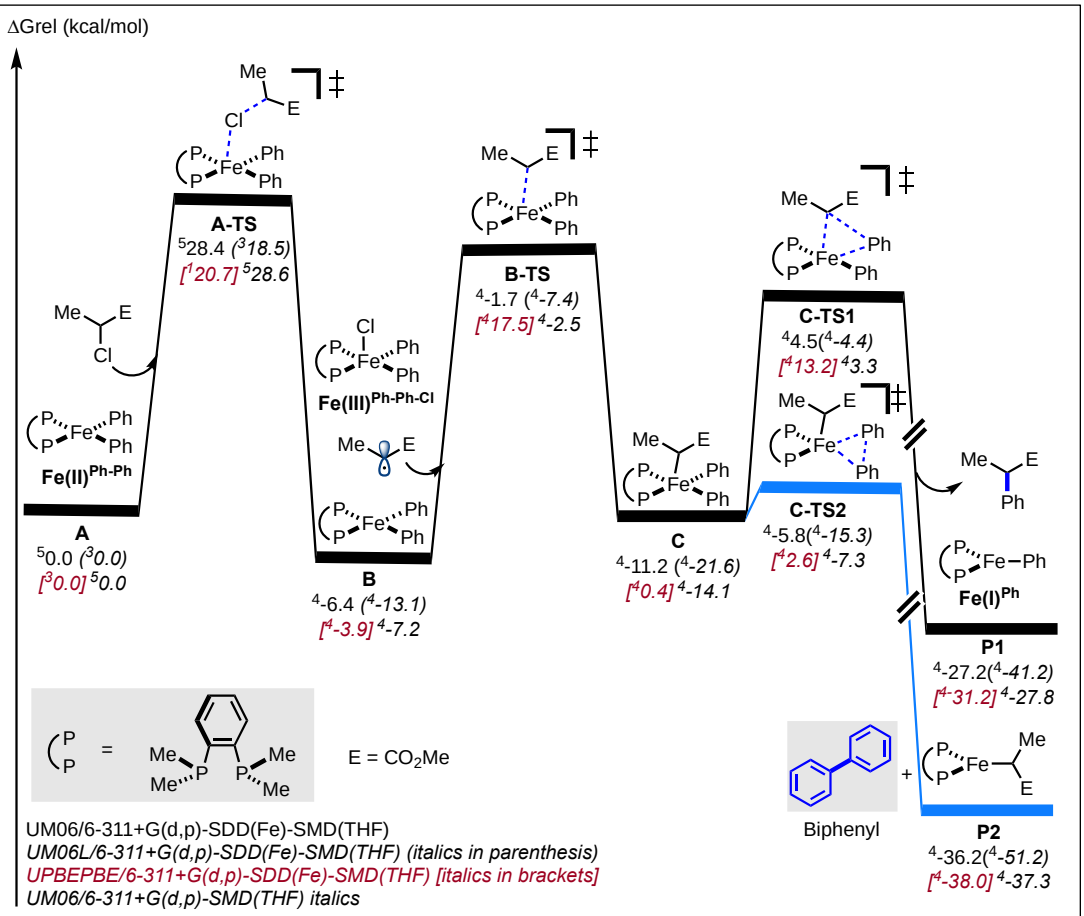

Figure 1.7. Energy diagram of the reaction with diphenyl-iron(II) complex Fe(II)$^{Ph\text{-}Ph}$ leads to biphenyl side product. Numbers shown are four methods in single point energy calculation from UB3LYP/6-31G(d) optimized structure.

(29.1 kcal/mol, see S1) to the **Fe(III)$^{Ph\text{-}Ph\text{-}Cl}$** to form Fe(IV) intermediate, the alkyl radical species favors to interact with another Fe(II) species (step **B** to **B-TS**). Specifically, the alkyl radical can add to another molecule of iron(II) diphenyl **Fe(II)$^{Ph\text{-}Ph}$** to form intermediate **C** with the barrier of 21.4 kcal/mol from **B**. However, the barrier for the reductive elimination to form the desired C(sp^2)-C(sp^3) cross-coupling product (**P1**) is much higher than C(sp^2)-C(sp^2) reductive elimination that would lead to the undesired biphenyl (**P2**) product by 10.6 kcal/mol (12.8. vs. 2.2 kcal/mol). Overall, our

calculations suggest that if diphenyl **Fe(II)$^{\mathbf{Ph\text{-}Ph}}$** is present in the solution, biphenyl will be the major product. Experimentally, if Grignard reagent is added rapidly, significant formation of biphenyl is observed. We speculate that rapid addition of phenyl Grignard leads to the formation of diphenyl Fe(II) species which could quickly trap the alkyl radical and undergo selective and undesired C(sp^2)-C(sp^2) bond formation. Overall these computational results rule against the formation of diphenyl-iron(II) complex as the active species in the formation of the desired C(sp^2)-C(sp^3) cross-coupling reactions (under slow addition of Grignard).

1.4 Productive Pathway Forming the Cross-Coupled Product

Fe(I) has been implicated in many iron-catalyzed cross-coupling reactions although there is no evidence that this species is responsible for catalytic activity.[22] Nonetheless, I investigated the energy barriers starting with phenyl-iron(I) complex (**Figure 1.8**). Phenyl-iron(I) **Fe(I)^{Ph}** species can promote halogen abstraction (barrier

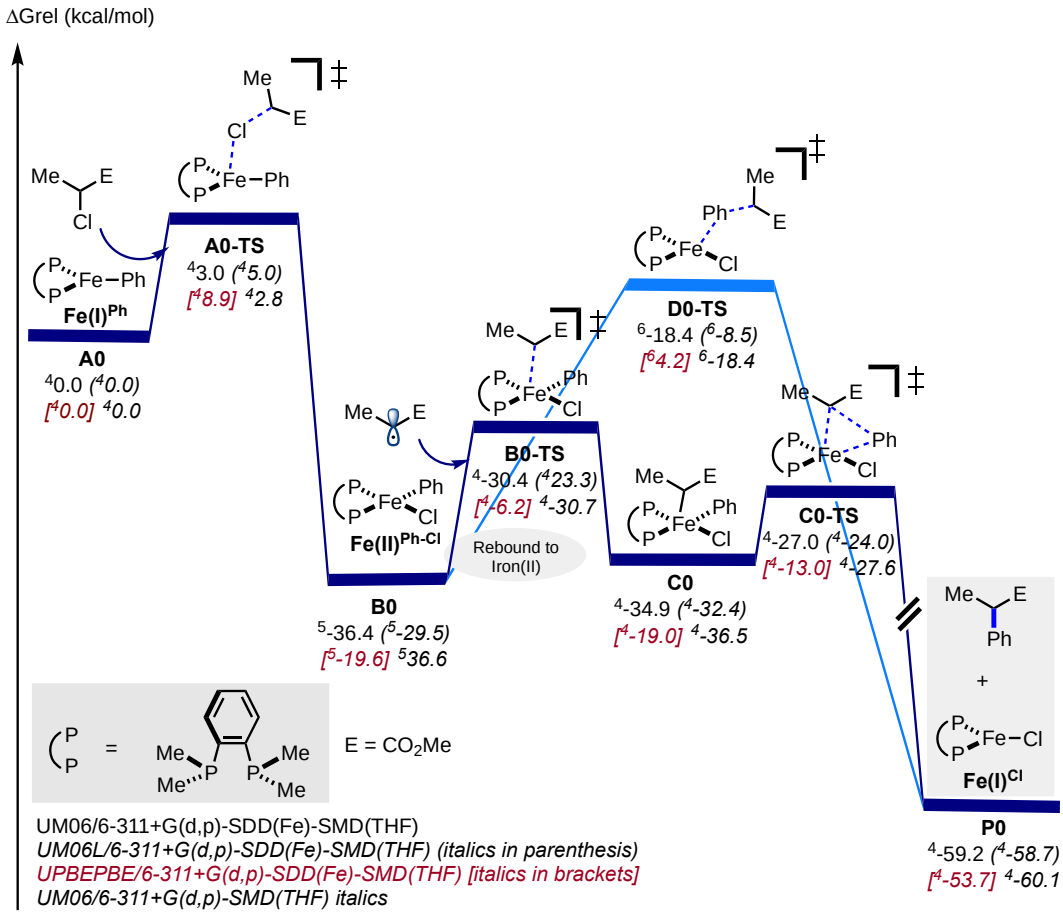

Figure 1.8. The lowest energy pathway starting with monophenyl-iron(I) complex that leads to the cross-coupling product.

ca. 8.9 kcal/mol) to form chloro-phenyl-iron(II) complex **Fe(II)$^{Ph-Cl}$**. In turn, the radical can rebound to iron(II) **Fe(II)$^{Ph-Cl}$** (via radical addition, **B0-TS**) via a barrier of ca. 13.4 kcal/mol to form intermediate **C0**. Finally, intermediate **C0** will undergo a very rapid reductive elimination to generate the desired C(sp^2)-C(sp^3) cross-coupling product and

the chloro-iron(I) complex **Fe(I)^{Cl}**. Chloro-iron(I) complex can re-generate the phenyl-iron(I) complex **Fe(I)^{Ph}** by transmetalation with phenyl Grignard reagent (details are still under debate[37]). Given that the reaction is highly exergonic (-53.7 kcal/mol), calculations suggest that once the product is formed, the reaction will be irreversible at room temperature. Further, closer inspection of this pathway, by comparing the two transition states corresponding to radical addition and reductive elimination, reveals that the radical addition step is more likely to be the enantiodetermining step because of its higher energy barrier (-6.2 vs. -13.0 kcal/mol) but calculations using full chiral ligand are necessary to determine the enantioselectivity determining step (more below).

Interestingly, there is an alternative pathway we explored and found a different transition state that also leads to the C(sp^2)-C(sp^3) cross-coupling product (i.e., **D0-TS**, **Figure 1.8**). This transition state corresponds to the concerted process in which the radical, instead of adding to iron, is undergoing outer-sphere-arylation (pathway highlighted in blue) leading to the experimentally observed C(sp^2)-C(sp^3) cross-coupling product. However, this transition state is only found in the sextet spin state and the energy is much higher (4.2 kcal/mol) therefore not expected to be productive. This example highlights the importance of spin state on the reaction mechanism (inner-sphere vs. outer-sphere) in iron-catalyzed cross-coupling reactions akin to the "two-state reactivity" in C-H oxidations by iron catalysts.[38]

1.5 The Origin of Enantioselectivity

We carefully examined the two lowest energy diastereomeric transition states (radical addition and reductive elimination) to gain insight into the origin of enantioselectivity using the full chiral bisphosphine ligand. **Figure 1.9** shows the four

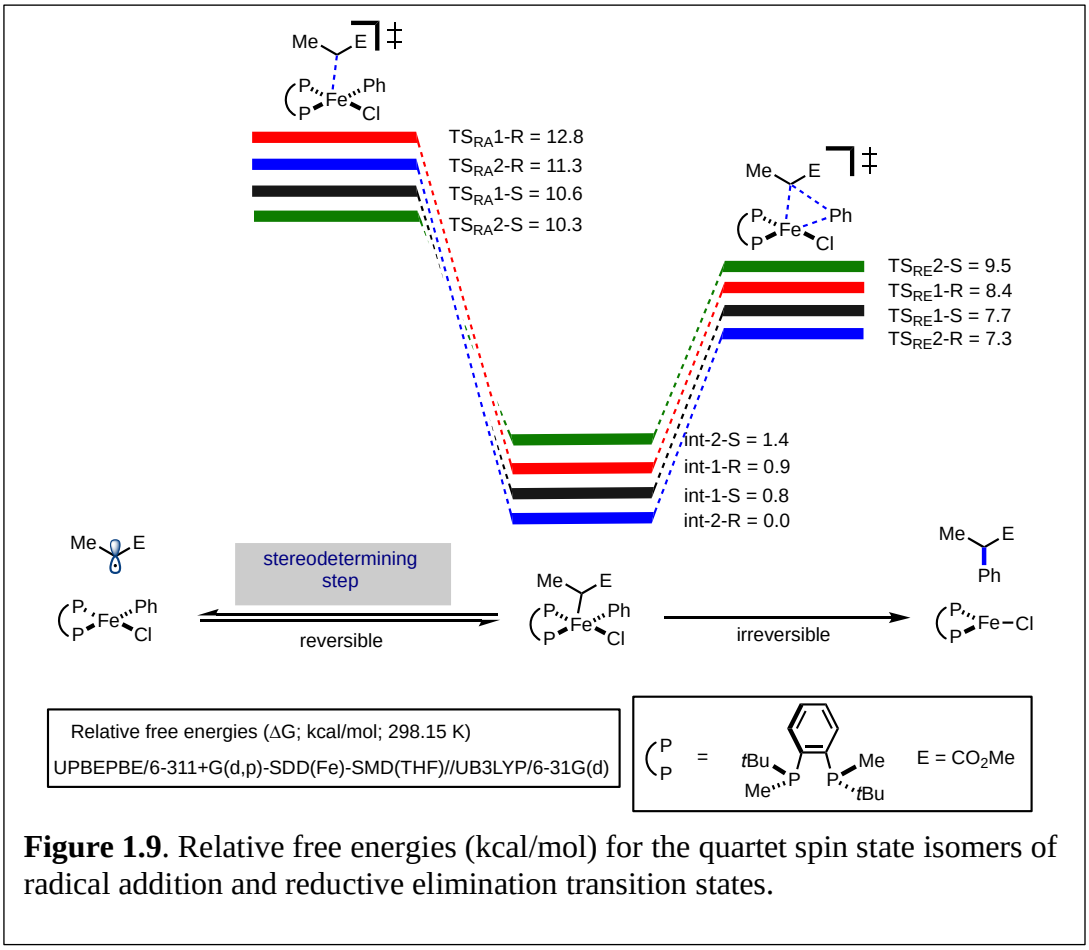

Figure 1.9. Relative free energies (kcal/mol) for the quartet spin state isomers of radical addition and reductive elimination transition states.

lowest energy diastereomeric transition states (two of the isomers will lead to the *S*, black and green, configuration product; the other two will lead to the *R*, red and blue, configuration product) corresponding both the radical addition and reductive elimination steps. In all, the radical addition step is higher in energy than the reductive elimination. Therefore, these calculations further support the hypothesis that radical addition is the stereodetermining step. Finally, we performed a Boltzmann distribution

(**Table 1.2**) using various computational methods extensively used in the study of

		UPBEPBE/6-311+G(d,p)-SDD(Fe)-SMD(THF)		UM06L/6-311+G(d,p)-SDD(Fe)-SMD(THF)	
		Radical addition	*Reductive elimination*	*Radical addition*	*Reductive elimination*
S:R ratio	0°C (273 K)	91:9	31:69	98:2	41:59
	25°C (298 K)	89:11	32:68	97:3	41:59

Table 1.2. Boltzmann distribution of radical addition and reductive elimination that predict different configuration products.

organometallic systems (UPBEPBE, UM06L, and UM06) and, in general, all the methods predict the major enantiomer as observed via experiment.

Specifically, Boltzmann distribution with the lower transition structures we located, the radical addition predicts the major product in *S* configuration, which is consistent with Nakamura's experimental result. In contrast, using the same methods, the reductive elimination would predict the configuration different from the experiment. Therefore, these calculations provide strong support for radical addition as the stereodetermining step.

Calculations with the full ligand system provides us information of the noncovalent interactions involved in controlling the enantioselectivity. We find that both electronic and steric effects influence the enantioselectivity. Specifically, as shown in **Figure 1.10**, the TS-S, which leads to the major experimentally determined

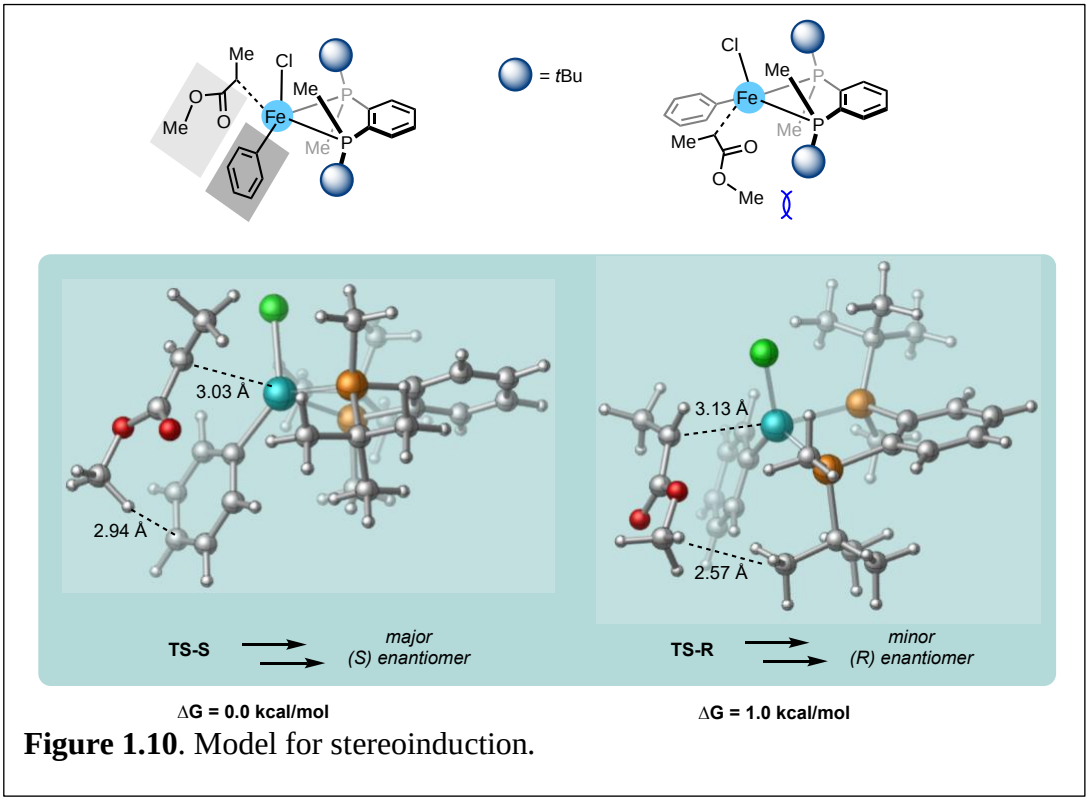

Figure 1.10. Model for stereoinduction.

S enantiomer, is ~1 kcal lower in energy than the TS-R which will lead to the opposite (and minor) enantiomer. We attribute the energy difference to the C-H ••• π interaction. This interaction will stabilize the transition structure of the radical addition. Thus, the energy barrier becomes lower in the pathway of forming S configuration product. In contrast, the transition structure that will lead to the R enantiomer is higher in energy because the *tert*-butyl group on the chiral ligand is interacting with the methoxy group on the substrate that destabilizes the structure.

1.6 Overall Catalytic Cycle

Based on all the studies above, the mechanism that we proposed is shown in **Figure 1.11**. Started with iron(I) species, phenyl-Fe(I) complex will abstract the

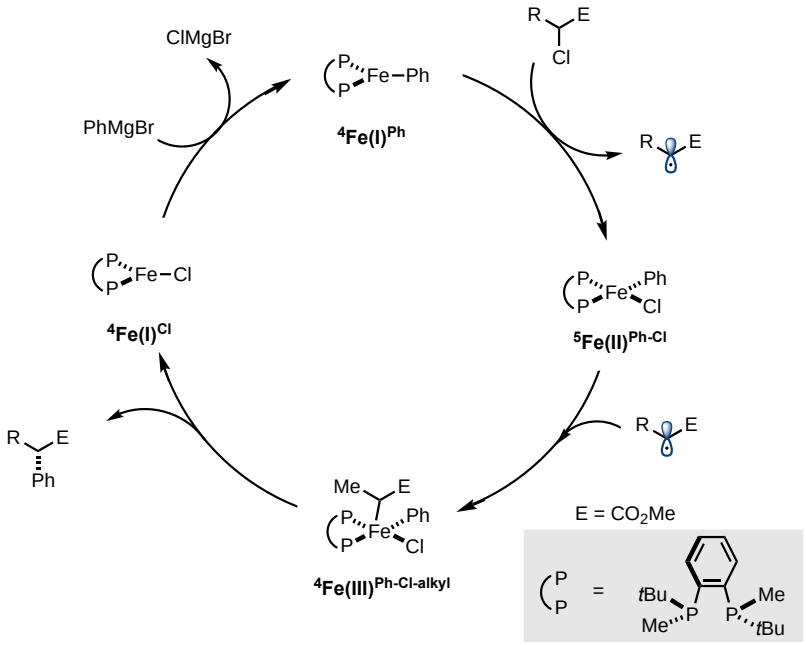

Figure 1.11. Catalytic cycle of Kumada-type iron-catalyzed asymmetric cross-coupling reaction.

halogen from the substrate and form chloro-phenyl-Fe(II) complex that allows the radical to rebound to iron by radical addition. And then the reductive elimination can occur to release the C(sp^2)-C(sp^3) cross-coupling product. At the same time, chloro-Fe(I) complex is generated. Chloro-Fe(I) complex can go through transmetalation by phenyl Grignard to regenerate Fe(I)-Ph and repeat the cycle. With this information in hand, I next focus on modulating the relative rates of radical addition to the Fe(II) versus reductive elimination to design new multicomponent iron-catalyzed cross-coupling reactions. Further, I also focused on the chiral environment posed by the chiral ligand to allow multicomponent asymmetric iron-catalyzed cross-coupling reactions.

1.7 References

(1) Taylor, B. L. H.; Jarvo, E. R. *Synlett*, **2011**, 2761−2765.

(2) *Metal-Catalyzed Cross-Coupling Reactions and More*; de Meijere, A.; Bräse, S.; Oestreich, M.; Eds.; Wiley-VCH Verlag GmbH: Weinheim, **2014**.

(3) Bolm, C.; Legros, J.; Paih, J. L.; Zani, L. *Chem. Rev*. **2004**, *104*, 6217−6254.

(4) Sherry, B. D.; Furstner, A. *Acc. Chem. Res*. **2008**, *41*, 1500−1511.

(5) Czaplik, W. M.; Mayer, M.; Cvengros, J.; Wangelin, A. J. v. *ChemSusChem*, **2009**, *2*, 396−417.

(6) Jana, R.; Pathak, T. P.; Sigman, M. S. *Chem. Rev*. **2011**, *111*, 1417−1492.

(7) Bauer, I.; Knolker, H.-J. *Chem. Rev*. **2015**, *115*, 3170−3387.

(8) Nakamura, E.; Yoshikai, N. *J. Org. Chem*. **2010**, *75*, 6061−6067.

(9) Kharasch, M. S.; Fields, E. K. *J. Am. Chem. Soc*. **1941**, *63*, 2316−2320.

(10) Tamura, M.; Kochi, J. K. *J. Am. Chem. Soc*. **1971**, *93*, 1487−1489.

(11) Dongol, K. G.; Koh, H.; Sau, M.; Chai, C. L. *Adv.Synth.Catal.* **2007** *349*, 1015−1018.

(12) Bedford, R. B.; Huwe, M.; Wilkinson, M. C. *Chem. Commun*. **2009**, 600−602.

(13) Adams, C. J.; Bedford, R. B.; Carter, E.; Gower, N. J.; Haddow, M. F.; Harvey, J. N.; Huwe, M.; Cartes, M. A.; Mansell, S. M.; Mendoza, C.; Murphy, D. M.; Neeve, E. C.; Nunn, J. *J. Am. Chem. Soc*. **2012**, *134*, 10333−10336.

(14) Hatakeyama, T.; Kondo, Y.; Fujiwara, Y.; Takaya, H.; Ito, S.; Nakamura, E.; Nakamura, M. *Chem. Commun*. **2009**, 1216−1218.

(15) Hatakeyama, T.; Okada, Y.; Yoshimoto, Y.; Nakamura, M. *Angew. Chem., Int. Ed.* **2011**, *123*, 11165-11168.

(16) Hatakeyama, T.; Hashimoto, T.; Kondo, Y.; Fujiwara, Y.; Seike, H.; Takaya, H.; Tamada, Y.; Ono, T.; Nakamura, M. *J. Am. Chem. Soc.* **2010**, *132*, 10674-10676.

(17) Hatakeyama, T.; Hashimoto, T.; Kathriarachchi, K. K.; Zenmyo, T.; Seike, H.; Nakamura, M. *Angew. Chem., Int. Ed.* **2012**, *124*, 8964-8967.

(18) Lou, S.; Fu, G. C. *J. Am. Chem. Soc.* **2010**, *132*, 1264.

(19) Mao, J.; Liu, F.; Wang, M.; Wu, L.; Zheng, B.; Liu, S.; Zhong, J.; Bian, Q.; Walsh, P. J. *J. Am. Chem. Soc.* **2014**, *136*, 17662.

(20) Jin, M.; Adak, L.; Nakamura, M. *J. Am. Chem. Soc*. **2015**, *137*, 7128−7134.

(21) Ren, Q.; Guan, S.; Jiang, F.; Fang, J. *J. Phys. Chem. A*, **2013**,*117*, 756−764.

(22) Hedström, A.; Lindstedt, E.; & Norrby, P. O. *J. Organomet. Chem.* **2013**, *748*, 51−55.

(23) Becke, A. D. *J. Chem. Phys*. **1993**, *98*, 5648−5652.

(24) (a) Cohen, A. J.; Mori-Sanchez, P.; Yang, W. *Chem. Rev*. **2012**, *112*, 289−320. (b) Reiher, M.; Salomon, O.; Artur Hess, B. *Theor. Chem. Acc*. **2001**, *107*, 48−55. (c) Bowman, D. N.; Jakubikova, E. *Inorg. Chem*. **2012**, *51*, 6011−6019. (d) Grimme, S. WIREs Comput. Mol. Sci. **2011**, *1*, 211−228.

(25) Zhao, Y.; Truhlar, D. G. *J. Chem. Phys*. **2006**, *125*, 194101−194118.

(26) (a) Perdew, J. P.; Burke, K.; Ernzerhof, M. *Phys. Rev. Lett*. **1996**, *77*, 3865−3868; (b) Perdew, J. P.; Burke, K.; Ernzerhof, M. *Phys. Rev. Lett*. **1997**, *78*, 1396−1396.

(27) Zhao, Y.; Truhlar, D. G. *Theor. Chem. Acc*. **2008**, *120*, 215−241.

(28) Marenich, A. V.; Cramer, C. J.; Truhlar, D. G. *J. Phys. Chem. B* **2009**, *113*, 6378−6396.

(29) (a) Sperger, T.; Sanhueza, I. A.; Kalvet, I.; Schoenebeck, F. *Chem. Rev*. **2015**, *115*, 9532−9586. (b) Sperger, T.; Sanhueza, I. A.; Schoenebeck, F. *Acc. Chem. Res*. **2016**, *49*, 1311−1319.

(30) (a) Kleimark, J.; Hedström, A.; Larsson, P. F.; Johansson, C.; Norrby, P. O. *ChemCatChem*. **2009**, *1*, 152−161. (b) Hedström, A.; Izakian, Z.; Vreto, I.; Wallentin, C. J.; Norrby, P. O. *Chem. Eur. J*. **2015**, *21*, 5946−5953. (c) Bauer, G.; Wodrich, M. D.; Scopelliti, R.; Hu, X. *Organometallics* **2015**, *34*, 289−298.

(31) For selected examples on computational analysis of ironcatalyzed reactions, see: (a) Wang, Y.; Janardanan, D.; Usharani, D.; Han, K.; Que, L., Jr.; Shaik, S. *ACS Catal*. **2013**, *3*, 1334−1341. (b) Sameera, W. M. C.; Hatanaka, M.; Kitanosono, T.; Kobayashi, S.; Morokuma, K. *J. Am. Chem. Soc*. **2015**, *137*, 11085−11094. (c) Heggen, B.; Thiel, W. J. *Organomet. Chem*. **2016**, *804*, 42−47. (d) Sun, Y.; Tang, H.; Chen, K.; Hu, L.; Yao, J.; Shaik, S.; Chen, H. *J. Am. Chem. Soc*. **2016**, *138*, 3715−3730. (e) Ren, Q.; Guan, S.; Shen, X.; Fang, J. *Organometallics* **2014**, *33*, 1423−1430. (f) Ren, Q.; Wu, N.; Cai, Y.; Fang, J. *Organometallics* **2016**, *35*, 3932−3938. (g) Kneebone, J. L.; Fleischauer, V. E.; Daifuku, S. L.; Shaps, A. A.; Bailey, J. M.; Iannuzzi, T. E.; Neidig, M. L. *Inorg. Chem*. **2016**, *55*, 272−282.

(32) (a) Frisch, M. J., et al. *Gaussian 09*. Revision D.01; Gaussian, Inc.: Wallingford, CT, 2009. (b) Frisch, M. J., et al. *Gaussian 16*. Revision C.01; Gaussian, Inc.: Wallingford, CT, 2016.

(33) (a) *CYLview, 1.0b*; Legault, C. Y., Université de Sherbrooke, 2009 (b) *CYLview20*; Legault, C. Y., Université de Sherbrooke, 2020 (http://www.cylview.org)

(34) Palladium. https://tradingeconomics.com/commodity/palladium (accessed Mar 30, 2021).

(35) Campeau, L. C.; Hazari, N. *Organometallics*, **2018**, *38*, 3−35.

(36) Sharma, A. K.; Sameera, W. M. C.; Jin, M.; Adak, L.; Okuzono, C.; Iwamoto, T.; Kato, M.; Nakamura, M.; Morokuma, K. *J. Am. Chem. Soc*. **2017**, *139*, 16117−16125.

(37) Peltzer, R. M.; Gauss, J.; Eisenstein, O.; Cascella, M. *J. Am. Chem. Soc*. **2020**, *142*, 2984−2994.

(38) Sun, Y.; Tang, H.; Chen, K.; Hu, L.; Yao, J.; Shaik, S.; Chen, H. *J. Am. Chem. Soc*. **2016**, *138*, 3715−3730.

(39) Daifuku, S. L.; Kneebone, J. L.; Snyder, B. E.; Neidig, M. L. *J. Am. Chem. Soc*. **2015**, *137*, 11432-11444.

(40) Messinis, A. M.; Luckham, S. L.; Bedford, R. B.; et al. *Nat. Catal*. **2019**, *2*, 123-133.

(41) Lee, W.; Zhou, J.; Gutierrez, O. *J. Am. Chem. Soc*. **2017**, *139*, 16126-16133.

Chapter 2: Radical-Clock α-Halo-Esters as Mechanistic Probes for Bisphosphine Iron-Catalyzed Cross-Coupling Reactions

Excerpts from this chapter were published in: Liu, L.; Lee, W.; Zhou, J.; Bandyopadhyay, S.; Gutierrez, O. *Tetrahedron*, **2019**, *75*, 129−136.

2.1 Mechanistic Probe of Radical Formation

In the previous chapter, through the investigation of quantum mechanical calculations, the mechanism of chiral bisphosphine iron-catalyzed C(sp^2)-C(sp^3) cross-coupling reactions was discussed. Our study[1] (**Figure 2.1 A**) and Nakaura-Morokuma's [2] study (**Figure 2.1 B**) revealed similar Fe(I)/Fe(II)/Fe(III) catalytic cycles for this transformation. Although evidence for the participation of alky radical is strong, the factors that control alkyl radical (e.g., in-cage or out-of-cage) arylation are not

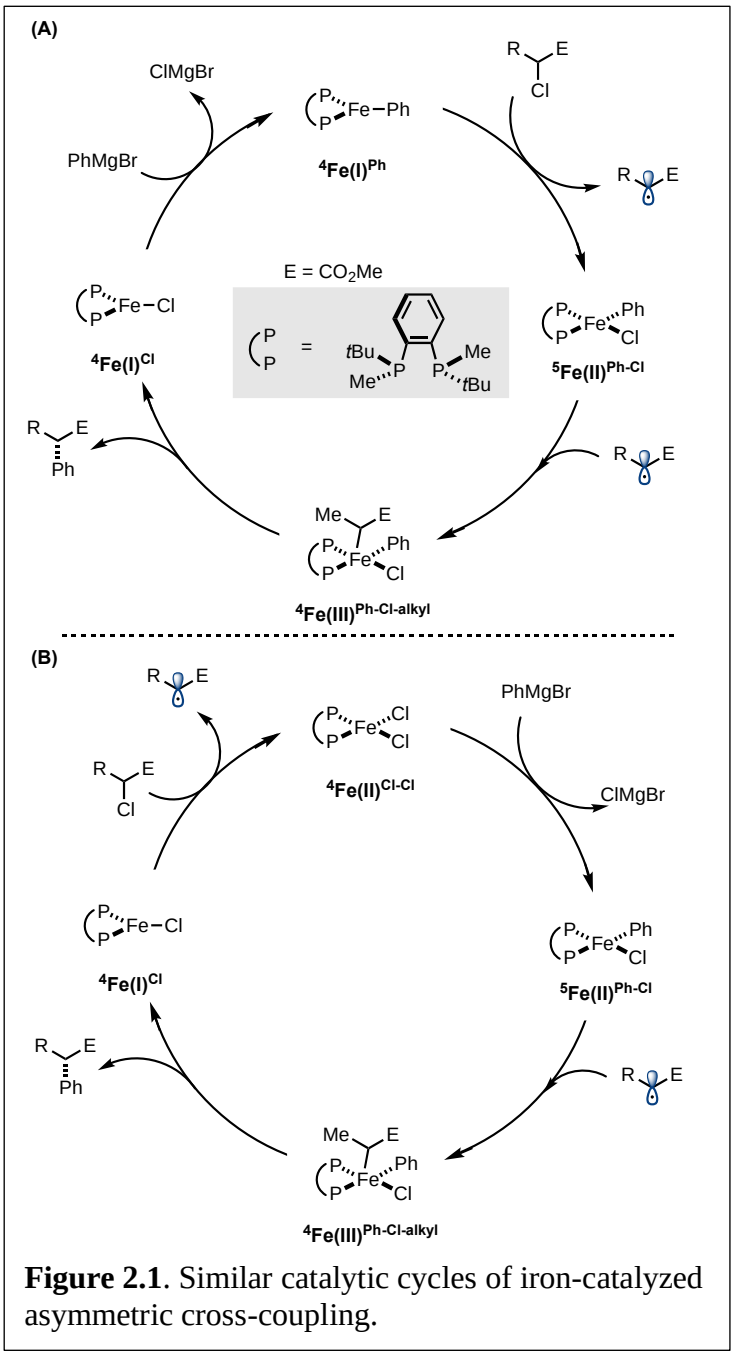

Figure 2.1. Similar catalytic cycles of iron-catalyzed asymmetric cross-coupling.

known. Previously, Nakamura used **1a** and **1b** as mechanistic probes in the asymmetric iron-catalyzed cross-coupling reaction using chiral bisphosphine ligand **BenzP***

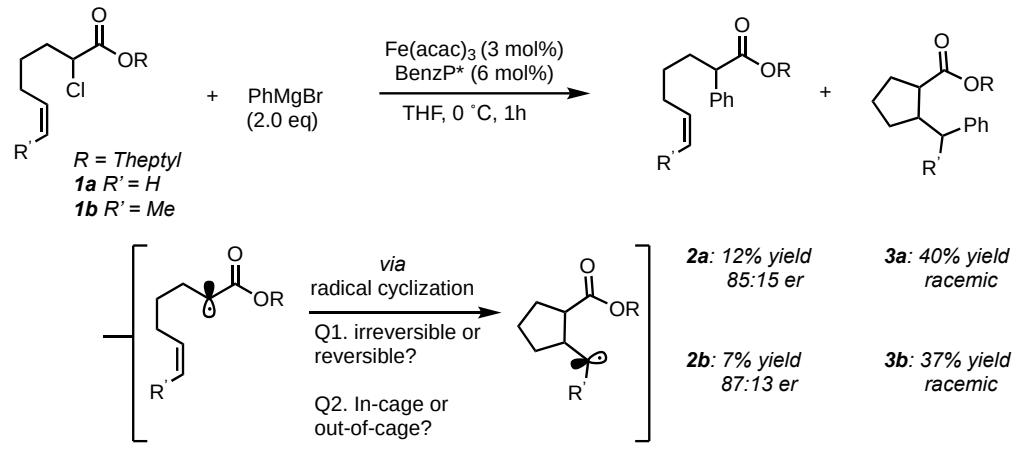

Figure 2.2. Mechanistic probe used that indicates the participation of alky radical.

(**Figure 2.2**).[3] Under standard conditions (e.g., slow addition of aryl Grignard), α-chloro ester **1a** formed a mixture of the acyclic (enantioenriched) and cyclic (racemic) cross-coupled products **2a** and **3a** in low yields, 12% and 40%, respectively (**Figure 2.2**). Moreover, a first-order relationship between the ratio of acyclic/cyclic cross-coupled product (**2a**/**3a**) and catalyst concentration supported a competing out-of-cage radical pathway in which apparent radical lifetime is inversely proportional to the degree of radical clock rearrangement.[4] Substrate **1b** that bear pendant olefin with Z stereochemistry also provided a mixture of the corresponding acyclic (enantioenriched) and cyclic (racemic) cross-coupled products, **2b** and **3b** respectively. Moreover, the observation that both acyclic cross-coupled product **2b** and recovered starting material **1b** retained *Z* stereochemistry suggests that after cyclization occurs the process is irreversible (**Figure 2.2**). Herein, we use a series of sensitive α-halo esters as mechanistic probes together with quantum mechanical calculations to elucidate at the fate of the alkyl radicals in bisphosphineiron catalyzed cross-coupling reactions.

Implications for the rational design of iron-catalyzed enantioselective tandem radical cyclization-arylation reaction are discussed.

2.2 Computational Study of Radical Cyclization

We began our study by computing the energetics for radical cyclization of the alkyl radicals **2a** and **2b**, presumably formed directly from probes **1a** and **1b**, respectively, via halogen abstraction by iron(I) (**Figure 2.1**). All energies discussed are

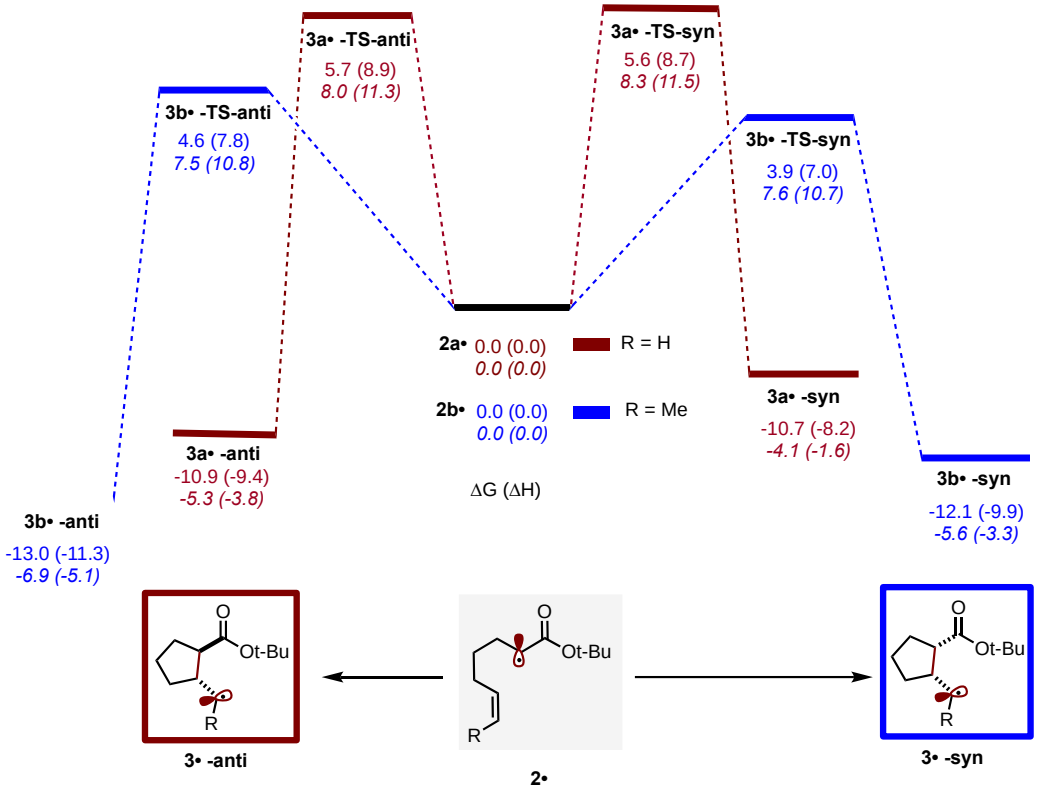

Figure 2.3. Energetics for radical cyclization of **1a** (red) and **1b** (blue) calculated at the (U)DLPNO-CCSD(T)/def2-TZVPP//UB3LYP/6-31G(d) and UB3LYP/6-31G(d) [italics] level of theory. Enthalpies and free energies are in kcal/mol.

for singlet spin states (for non-transition metals) were performed at the (U) DLPNO-CCSD(T)/def2-TZVPP//UB3LYP/6-31G(d) level of theory. DFT optimizations were performed using Guassian09,[5] and (U) DLPNO-CCSD(T) single point energy

calculations were performed using ORCA.[6] For simplicity, primarily (U)DLPNO-CCSD(T) energies will be discussed. As shown in **Figure. 2.3**, for the unsubstituted probe 1a, the lowest energy barrier for radical cyclization of **2a•** is 5.7 kcal/mol (via **3a• -TS-anti**), which will lead to the formation of **3a• -anti** (downhill in energy by 10.9 kcal/mol). This barrier is in excellent agreement with the experimental activation barrier ~6 kcal/mol (rate constant $k \sim 10^5\ s^{-1}$) for the analogous α-radical (R = Et) and allows us to calibrate our computational methods.[7] Not surprisingly, the cyclization barrier for the methyl-substituted Z olefin **2b•** (from probe **1b**) is significantly lower (~2 kcal/mol; via **3b•-TS-syn**) and more exergonic (12.1 kcal/mol) reflecting the additional stability provided by the methyl to the incipient cyclized radical. Notably, the lowest energy barrier to undergo reversible cyclization (i.e., from **3b•-syn** to **2b•**) is only 16.0 kcal/mol. Given both acyclic cross-coupled product **2b** and recovered starting material **1b** retained *Z* stereochemistry, these computational results suggest that 1) the barrier for direct (in-cage) arylation must be in the 4−5 kcal/mol range (i.e., relatively similar in magnitude as radical cyclization); and 2) downstream arylation (in-cage or out-of-cage) of the cyclized radical must be faster than the reverse ring-opening barrier (less than ca. 17 kcal/mol).

2.3 Synthesis of New Mechanistic Probe

We hypothesize that a more sensitive radical clock substrate could lead to the exclusive formation of cyclized product(s) by outcompeting the direct (in-cage) arylation of acyclic alkyl radical and, in turn, define the upper limit for in-cage arylation in these systems. Newcomb and co-workers have measured the rate constants for

substituted alkyl radicals to undergo 5-exo cyclizations in the range of k = 10^5–10^8 s^{-1} (at room temperature).[7] These studies also show that the rates for radical cyclization are faster for substrates that bear groups that stabilize the incipient cyclized radicals. For instance, the rate for 5-exo cyclization of ethyl hept-6-enoate radical is 1.4 × 10^5 s^{-1} while that of the corresponding radical ethyl 1,1-diphenyl-hept-6-enoate is more than two orders of magnitude faster (i.e., k = 5 × 10^7 s^{-1}). As such, Dr. Lei Liu and I synthesized a series of α-alkyl esters with pendant esters (**7a-c**; **Figure 2.4A**) using a short and highly versatile synthetic route (**Figure 2.4B**). We chose these substrates due

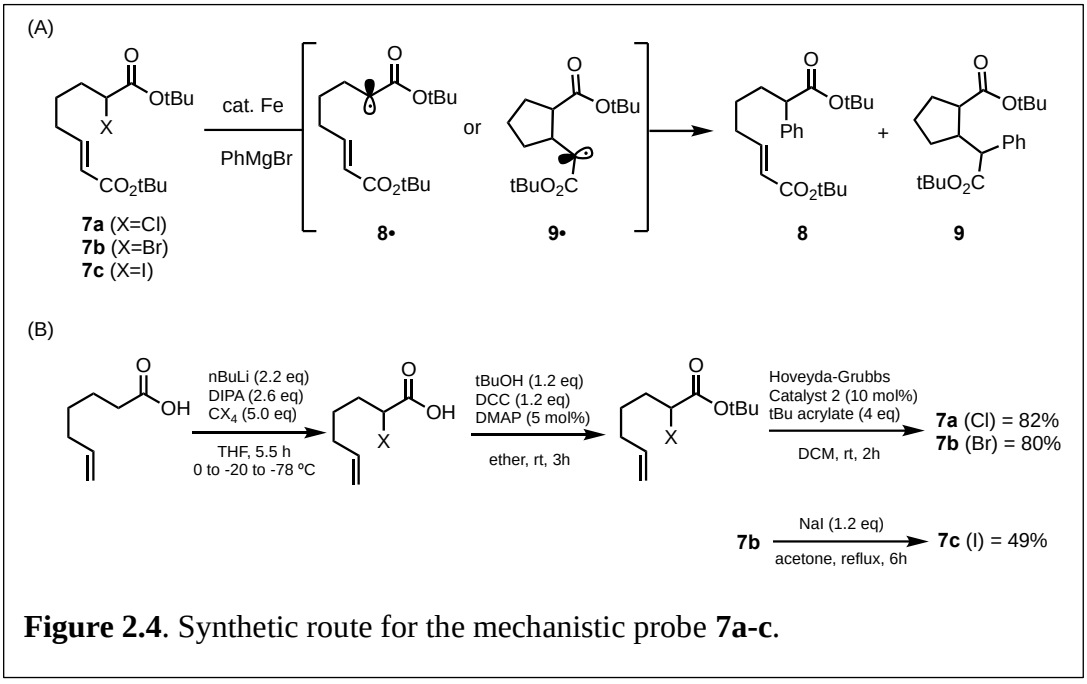

Figure 2.4. Synthetic route for the mechanistic probe **7a-c**.

to ease of synthesis, presumed barrier lowering of the 5-exo radical cyclization (**8•** to **9•**) by the ester moiety via stabilization of the incipient radical, and potential for pendant ester group to induce asymmetry in the tandem cyclization-arylation reaction.

As shown in **Figure 2.4**, Dr. Lei Liu and I synthesized the desired α-halo esters in 3−4 steps from commercially starting materials in modest to good yields. To the best of our knowledge, the effect of pendant ester moiety on 5-exo radical cyclizations has

not been determined. Therefore, I computed the energetics for 5-exo radical cyclization starting from **8•** (presumably formed directly from halogen abstraction of a-alkyl esters **7a-c**) to explore the effect of the ester group. As shown in **Figure 2.5**, the barrier for

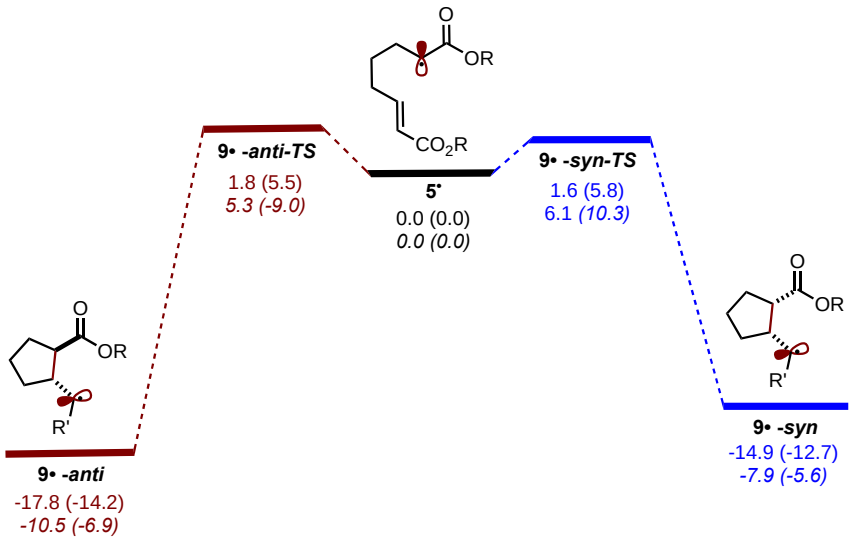

Figure 2.5. Energetics for radical cyclization of 8• (R = tert-butyl) calculated at the (U)DLPNO-CCSD(T)/def2-TZVPP//UB3LYP/6 31G(d) and UB3LYP/6-31G(d) [italics] level of theory. Enthalpies and free energies are in kcal/mol.

5-exo radical cyclization of ester-substituted **8•** is much lower (~2−4 kcal/mol) in energy than of previous used radical probes **2a•** and **2b•** (**Figure. 2.3**) and also 4−7 kcal/mol more exothermic. We attribute the lower barrier and larger exothermicity to the resonance stabilization of the incipient radical by ester group. These computations suggest that the relative rate of 5-exo radical cyclization of **8•** should be at least 100-times faster than direct (in-cage) arylation leading to the corresponding cyclized radicals.[8] Moreover, since the barrier for cyclization of **8•** is much lower than previously explored systems (**Figure 2.3**), we hypothesize that **8•** will quickly cyclize (to **9•**) rather than undergoing direct (in-cage) arylation. Ultimately, cyclic radical **9•** will undergo arylation to form **9**. Alternatively, if acyclic product **8** is observed, it will

suggest that subsequent C−C bond formation of the cyclized radicals is much higher in energy than the combined energy penalty to undergo reverse ring-opening (16−19 kcal/mol) followed by C−C bond formation of acyclic radical **8•**.

2.4 Different Ligands and Alkyl Halides

With mechanistic probes in hand, Dr. Lei Liu subjected **7a-c** to standard iron-catalyzed cross-coupling conditions (**Figure 2.6**). In agreement low barrier for radical

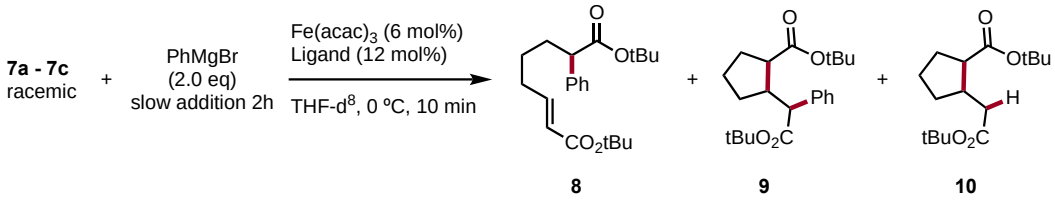

Entry	**7**	ligand	yield **8** (%)	yield **9** (%)	yield **10** (%)
1	7a	BenzP*	NA	28 (1:4:1.5:1.5)	30 (1.5:1)
2	7a	NA	NA	NA	25 (1.5:1)
3	7a	QuinoxP*	NA	NA	62 (1.4:1)
4	7b	QuinoxP*	NA	16 (1:4:1.5:1.5)	52 (1.6:1)
5	7b	NA	NA	NA	41 (1.4:1)
6	7c	QuinoxP*	NA	38 (1:2:1:1)	55 (1.5:1)
7	7c	NA	NA	34 (1:6.7:2:1.7)	56 (1.5:1)

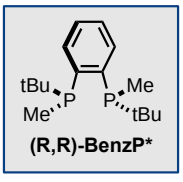

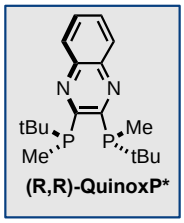

Figure 2.6. Mechanistic experiments of bisphosphine iron-catalyzed cross-coupling reactions.

cyclization of **8•** (**Figure 2.5**), the formation of acyclic cross-coupled product **8** was not observed, presumably from direct (in-cage) arylation. Instead, the tandem radical cyclization-arylation product **9** as a mixture of four diastereomers was found, albeit in low (28%) yield (entry 1). Nonetheless, these results indicate that the radical cyclization outcompetes in-cage arylation of **8•** and sets the upper limit for the rate of

direct arylation at **8•** at ~10^5 s^{-1}. Notably, Dr. Lei Liu also found 30% yield of the cyclized protonated product **10** (entry 1). Control experiments without bisphosphine ligand (entry 2) show similar yields of **10** but no formation of the cyclic cross-coupled product **8**. Overall, these results indicate that formation of cyclized protonated product **10** is likely a result of ferrate chemistry (e.g., dehalogenation, conjugate addition, and protonation) although the mechanism is not well elucidated.[9]

Previously, Nakamura reported that chiral ligand **BenzP*** and **QuinoxP*** deliver nearly identical enantioselectivities albeit slightly lower yields.[3] Thus, we also explored the reactivity and selectivity of this ligand with mechanistic probes **7a-c**. To our surprise, changing the ligand from **BenzP*** to **QuinoxP*** completely shut down the tandem cyclization-arylation pathway while still forming (likely via ferrate chemistry) product 10 in 62% yield (entry 3). Notably, we were able to turn back on the reactivity of the tandem cyclization-arylation pathway by switching the substrate from α-chloro **7a** to α-bromo ester **7b** (entry 4), which resulted in the formation of **9** albeit lower yields than the α-chloro **7a** and **BenzP*** ligand combination. Moreover, as with α-chloro esters, control experiment (entry 5) revealed that the bisphosphine ligand is crucial to promote tandem cyclization-arylation reaction with α-bromo **7b**. Notably, iodo ester **7c** provided both **9** and **10** in 38% and 55% yield, respectively (entry 6). However, the observed reactivity with iodo probe (i.e., the formation of **9** and **10**) is likely a result of ligand-less (e.g., ferrate) chemistry as evident from nearly identical results in the absence of bisphosphine ligand (entry 7).[10] Overall, these results suggest that the reactivity of the tandem cyclization-arylation is highly dependent on subtle changes to the bisphosphine ligand and nature of alkyl halide. Notably, model

calculations (**Figure 2.7**) revealed no effect of the ligand electronics (**BenzP*** vs. **QuinoxP***) or halogen on the arylation step (i.e., radical addition or reductive

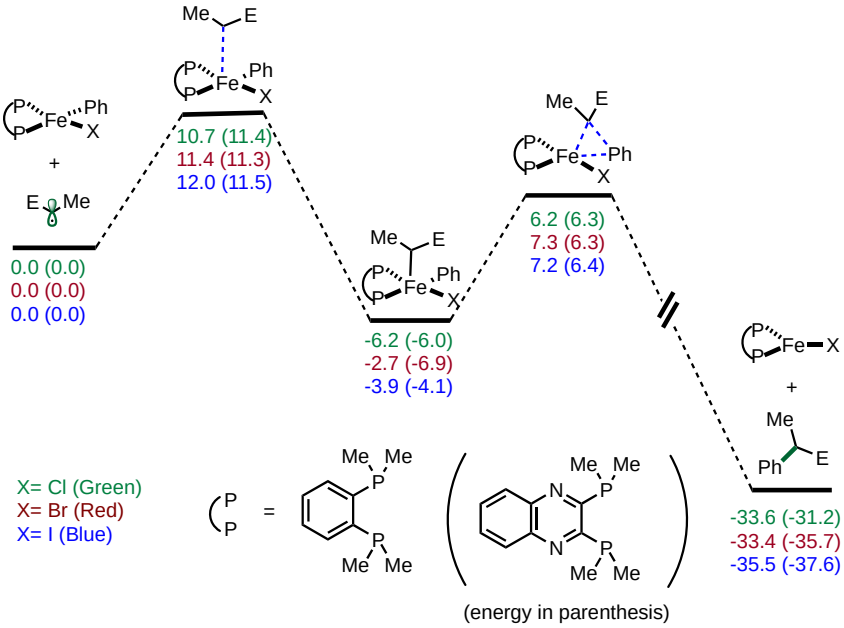

Figure 2.7. Halogen and ligand effect on the iron-catalyzed C-C bond formation step via quartet spin state. Free energies are in kcal/mol. (U)PBEPBE/6-311+G(d,p)-SDD(Fe,Cl,Br,I)-THF(SMD)//(U)B3LYP/6-31G(d)-LANL2DZ(Cl,Br,I).

elimination). These results are consistent with the formation of α-alkyl radicals (i.e., halogen abstraction) as the rate-determining step and more sensitive to the nature of the ligand and the alkyl halide in the tandem cyclizationarylation reaction (vide infra). Calculations are underway to explore the effect of ligand and halide in the formation of alkyl radicals and determining the barriers for C−C bond formation using the full cyclized systems.

2.5 Introducing Vinyl Cyclopropane to the Mechanistic Probe

We envisioned probing the effect of reversibility 5-exo cyclization of iron-catalyzed cross coupling reactions using **13** as a mechanistic probe (**Figure 2.8**).

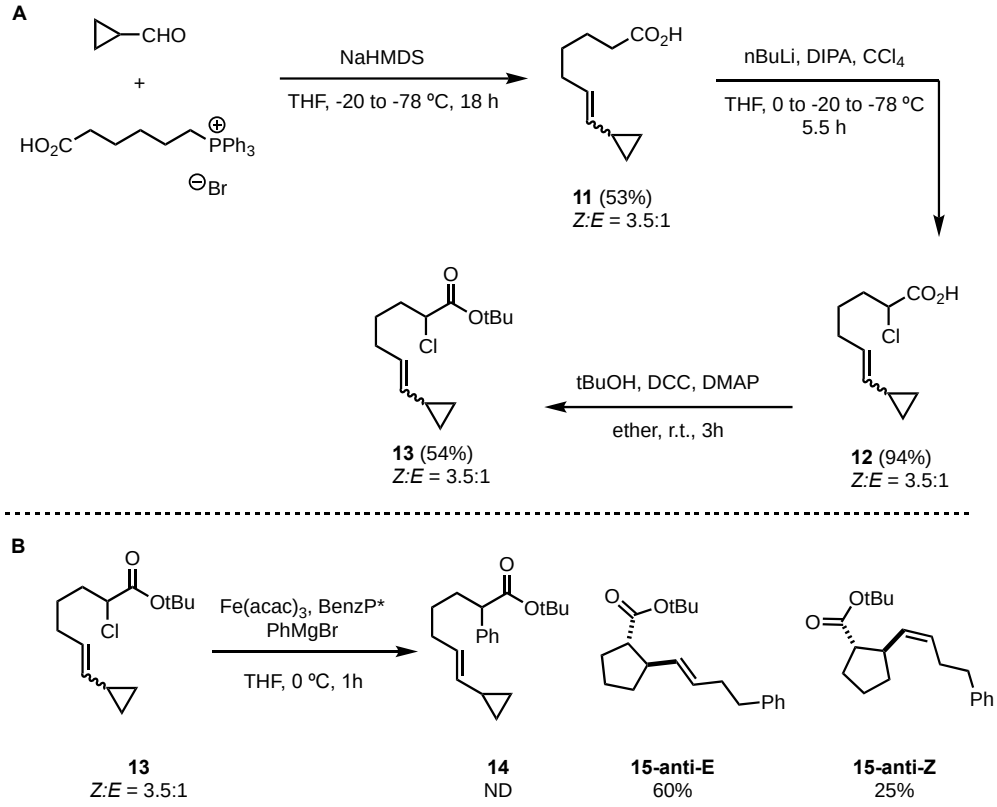

Figure 2.8. Synthesis of the desired α-chloro ester with pendant vinyl cyclopropyl group (mechanistic probe **13**).

Specifically, we hypothesized that radical cyclization should follow ring-opening of the cyclopropyl group to form the thermodynamically more stable cyclic ring-opened alkyl radical thus increasing both the thermodynamic drive and barrier for reverse reaction. Using a similar synthetic route (**Figure 2.4**), we synthesized the desired α-chloro ester with pendant vinyl cyclopropyl group mechanistic probe **13** as an inseparable 3.5:1 (*Z:E*) mixture (**Figure 2.8A**). As shown in **Figure 2.8B**, the reaction with **13** formed nearly exclusive cascade cyclization-ring-opening-arylation products

(85% combined yield)! Specifically, we found the formation of the corresponding anti cyclic/ring-opened products **15-anti-E** in 60% yield and 25% yield of **15-anti-Z**. Notably, this result provides further support for the participation of cyclic alkyl radicals before (out-of-cage) arylation. The lack of acyclic cross-coupled product **14** implies that the direct (in-cage) arylation is slower than the cascade radical cyclization, ring-opening, arylation process (vide supra). To gain insights into the reversibility of the radical cyclization in this system, we turned to quantum mechanical calculations. As shown in **Figure. 2.9**, the barrier for 5-exo radical cyclization is only ca. 4 kcal/mol and exothermic by ca. 13−15 kcal/mol leading to both syn- and anti-cyclic alkyl radicals **15•Z-anti** and **15•Z-syn**. Further, although radical **13•Z** (from probe **13**) is analogous to radical **2b•**, the barrier for cyclization of **13** is slightly lower (0.2 kcal/mol) than radical cyclization of **2b•**. Notably, **1b** formed direct arylation product **2b** (from **2b•**) while no direct cross-coupled product was observed with **13** (from **13•Z**). This result implies that by lowering the barrier for radical cyclization, it is possible to outcompete (and even shut down) the direct (in-cage) arylation pathway. Finally, cyclopropyl ring-opening will lead to the much more thermodynamically stable ring-opened products **15• -anti-E/Z** and **15• -syn-E/Z** (either directly from **15•Z-anti** and **15•Z-syn** or from rotation to **15•E-anti** and **15•E-syn** followed by ring-opening). Importantly, the barriers for the reverse reaction (ca. 21 kcal/mol) to get back to **13•** are insurmountable at experimental conditions and therefore, contrary to previous probes, convincingly irreversible (not under a Curtin-Hammett scenario). Although, **15• -anti-E** and **15• -anti-Z** can interconvert (under Curtin-Hammett scenario) via the 3-member ring closing/ring opening. Experimentally, we observed the 5-member anti

as the major products (up to 85% yield) and only observed minor amounts of the syn

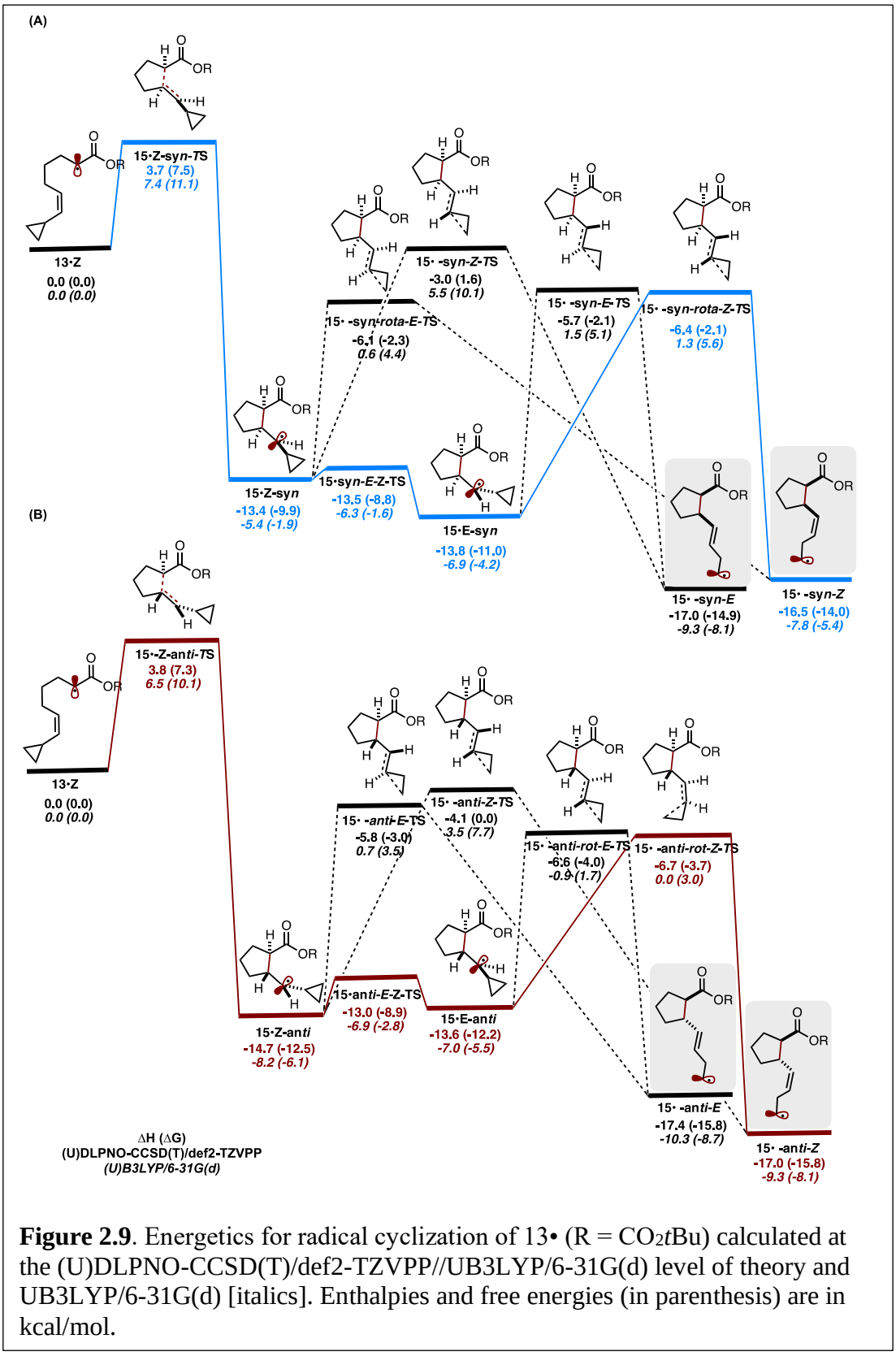

Figure 2.9. Energetics for radical cyclization of 13• (R = CO_2tBu) calculated at the (U)DLPNO-CCSD(T)/def2-TZVPP//UB3LYP/6-31G(d) level of theory and UB3LYP/6-31G(d) [italics]. Enthalpies and free energies (in parenthesis) are in kcal/mol.

5-member cyclized products. This observation is more consistent with the B3LYP computations, which predict a ca. 1 kcal/mol lower barrier for the anti-cyclization (**15•-Z-anti-TS**) in comparison to the syn-cyclization. Overall, the observed product distributions can be rationalized based on the preference for the irreversible anti 5-member cyclization-ring-opening and subsequent relative barriers for the competing C−C bond formation of the cyclic/ring-opened alkyl radicals **15• -anti-E/Z**.

2.6 The Radical Competing Pathways

Through the synthesis of new radical clock mechanistic probes and quantum mechanical calculations, we have bracketed the rate for alkyl radical arylation to ca. 5 kcal/mol at the (U)DLPNOCCSD(T)/def2-TZVPP//UB3LYP/6-31G(d) level of theory. Taken together, we propose the working hypothesis presented in **Figure 2.10**. in which competing in-cage and out-of-cage arylation pathways are operative. (A) For *short-lived* alkyl radicals [e.g., at this level of theory, when the barrier for radical cyclization is higher than 5 kcal/mol], direct (in-cage) arylation of alkyl radical **A•** will form acyclic cross-coupled product **A** with apparent "retention" of stereochemistry [probe **1a** and **1b**]. Nonetheless, although the strength of the cage (e.g., local viscosity of solvent) is likely to play a significant role in the efficiency of direct arylation (i.e., from rapid, radical rebound)[11], the rate of diffusion should be much faster ($k = \times 10^9$

s^{-1})[12] and thus some leakage of alkyl radicals will inherently occur. For alkyl radicals

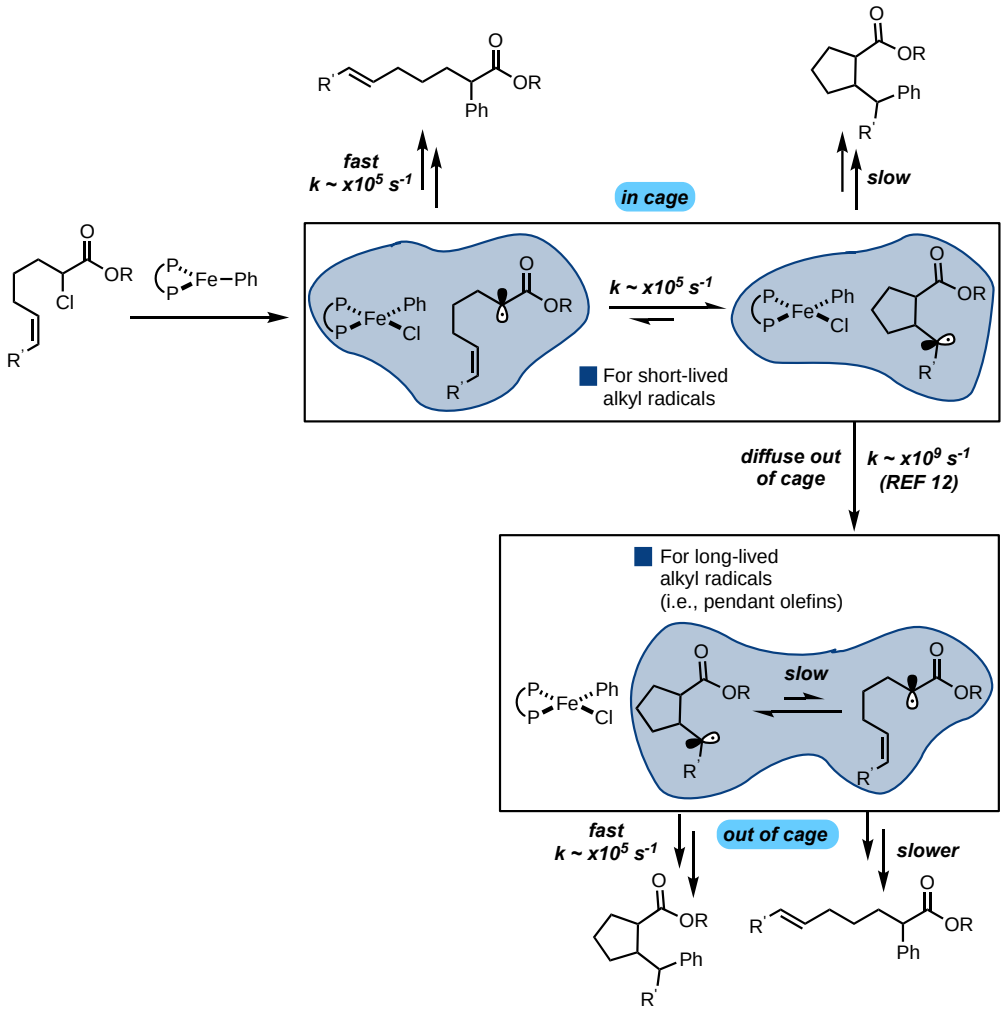

Figure 2.10. Working hypothesis.

without pendant olefins, cross-coupled products from competing in-cage (direct) and out-of-cage arylation will form the same acyclic arylated product. The competition between in-cage and out-of-cage is consistent with the first-order relationship between the ratio of acyclic/cyclic cross-coupled products and catalyst loading. (B) As the barrier for radical cyclization lowers (e.g., by tuning the properties of the pendant olefin) a higher concentration of acyclic radical **2•** will (in-cage) cyclize to (more thermodynamically stable) cyclic radical thus increasing the apparent lifetime of the

radical [probe **8**]. As such, this persistent cyclic alkyl radical[13] can escape the solvent cage and capture the transient aryl iron species to undergo C−C bond formation. Given the structural similarities between **A•** and **B•**, we can assume that the relative barriers for C−C bond formation are similar. Therefore, combined with the fact that the cyclic radical is thermodynamically lower in energy than acyclic radical, **B•** will undergo, preferentially faster, out-of-cage radical arylation leading to the formation of cyclic cross-coupled product **B**. As the thermodynamic drive for cyclic radicals increases (non-Curtin-Hammett scenario) to prevent reversible cyclization (e.g., with pendant cyclopropyl group) only cyclic cross-coupled products will form from arylation of downstream alkyl radicals [probe **13**].

2.7 Summary

The mechanism of chiral bisphosphine iron-catalyzed $C(sp^2)$-$C(sp^3)$ cross-coupling reactions has been studied via the synthesis of novel radical-clock mechanistic probes and DLPNO-CCSD(T) calculations. From a broader perspective, these results indicate that, in principle, alkyl halides can participate in selective tandem cyclization-arylation reactions, which remain a challenge in iron catalysis. We next explored the scope of this transformation and the development of enantioselective tandemcyclization/arylation reactions and reported in the next chapter (**Chapter 3**).

2.8 References

(1) Lee, W.; Zhou, J.; Gutierrez, O. *J. Am. Chem. Soc*. **2017**, *139*, 16126−16133.

(2) Sharma, A. K.; Sameera, W. M. C.; Jin, M.; Adak, L.; Okuzono, C.; Iwamoto, T.; Kato, M.; Nakamura, M.; Morokuma, K. *J. Am. Chem. Soc*. **2017**, *139*, 16117−16125.

(3) Jin, M.; Adak, L.; Nakamura, M. *J. Am. Chem. Soc*. **2015**, *137*, 7128−7134.

(4) (a) Choi, J.; Martín-Gago, P.; Fu, G. C. *J. Am. Chem. Soc*. **2014**, *136*, 12161−12165. (b) Biswas, S.; Weix, D. J. *J. Am. Chem. Soc*. **2013**, *135*, 16192−16197.

(5) Frisch, M. J.; Trucks, G. W.; Schlegel, H. B.; Scuseria, G. E.; Robb, M. A.; Cheeseman, J. R.; Scalmani, G.; Barone, V.; Mennucci, B.; Petersson, G. A.; Nakatsuji, H.; Caricato, M.; Li, X.; Hratchian, H. P.; Izmaylov, A. F.; Bloino, J.; Zheng, G.; Sonnenberg, J. L.; Hada, M.; Ehara, M.; Toyota, K.; Fukuda, R.; Hasegawa, J.; Ishida, M.; Nakajima, T.; Honda, Y.; Kitao, O.; Nakai, H.; Vreven, T.; Montgomery, J. A., Jr.; Peralta, J. E.; Ogliaro, F.; Bearpark, M.; Heyd, J. J.; Brothers, E.; Kudin, K. N.; Staroverov, V. N.; Kobayashi, R.; Normand, J.; Raghavachari, K.; Rendell, A.; Burant, J. C.; Iyengar, S. S.; Tomasi, J.; Cossi, M.; Rega, N.; Millam, J. M.; Klene, M.; Knox, J. E.; Cross, J. B.; Bakken, V.; Adamo, C.; Jaramillo, J.; Gomperts, R.; Stratmann, R. E.; Yazyev, O.; Austin, A. J.; Cammi, R.; Pomelli, C.; Ochterski, J. W.; Martin, R. L.; Morokuma, K.; Zakrzewski, V. G.; Voth, G. A.; Salvador, P.; Dannenberg, J. J.; Dapprich, S.; Daniels, A. D.; Farkas, Ö.; Foresman, J. B.; Ortiz, J. V.; Cioslowski, J.; Fox, D. J. Gaussian, Inc., Wallingford CT, 2009.

(6) Neese, F. *Wiley Interdiscip. Rev. Comput. Mol. Sci*. **2012**, *2*, 73−78.

(7) Newcomb, M. *Encyclopedia of Radicals in Chemistry, Biology and Materials*. **2012**.

(8) Guan, X.; Phillips, D. L.; Yang, D. *J. Org. Chem*. **2006**, *71*, 1984−1988.

(9) Alonso, F.; Beletskaya, I. P.; Yus, M. *Chem. Rev*. **2002**, *102*, 4009−4092.

(10) Jin, M.; Nakamura, M. *Chem. Lett*. **2011**, *40*, 1012−1014.

(11) (a) Barry, J. T.; Berg, D. J.; Tyler, D. R. *J. Am. Chem. Soc*. **2016**, *138*, 9389−9392. (b) Barry, J. T.; Berg, D. J.; Tyler, D. R. *J. Am. Chem. Soc*. **2017**, *139*, 14399−14405.

(12) Paquette, L. A. *Synlett*. **2001**, *2001*, 0001−0012.

(13) Fischer, H. *Chem. Rev*. **2001**, *101*, 3581−3610.

Chapter 3: Intra- and Intermolecular Fe-Catalyzed Dicarbofunctionalization of Vinyl Cyclopropanes

Excerpts from this chapter were published in: Liu, L.; Lee, W.; Yuan, M.; Acha, C.; Geherty, M. B.; Williams, B. Gutierrez, O. *Chem. Sci*. **2020**, *11*, 3146−3151.

3.1 Vinyl Cyclopropanes Used in Iron-Catalyzed Radical Cascade Reactions

Iron-catalyzed C–C cross-coupling reactions have attracted much attention due to the higher abundance, cost effectiveness, and lower toxicity of iron in comparison to precious transition metals.[1] Methods for ligand-supported (e.g., N-heterocycles, bisphosphines, and diamines) and ligand-free systems for iron-catalyzed C–C cross-coupling reactions using C(sp), C(sp^2), and C(sp^3) partners have been developed.[2] In particular, bisphosphine-iron systems have emerged as highly versatile and promising candidates for the formation of new C–C bonds with a range of organometallic nucleophiles including Mg- (Kumada),[3] Zn- (Negishi),[4] B- (Suzuki–Miyaura),[5] and Al[6] reagents with alkyl halides and redox active esters.[4a] Electron-poor vinyl cyclopropanes have also been used as π-coupling partners in Fe-catalyzed C(sp^2)–C(sp^3) bond formation (**Figure 3.1A**). In particular, Furstner used low valent iron ferrates to promote tandem ring-opening/monoarylation of electron-poor vinyl cyclopropanes (VCPs) using aryl Grignard reagents.[7] In a related study, Plietker used a low valent, electron rich ferrate complex ($Bu_4N[Fe(CO)_3(NO)]$) to promote ringopening/monoarylation of electron-deficient VCPs with acidic pronucleophiles.[8] Despite these advancements, to the best of our knowledge, there were only two reports of asymmetric iron-catalyzed cross-couplings: between aryl Grignard reagents or lithium aryl borates as nucleophiles and α-halo esters as electrophiles (**Figure 3.1A**).[9,10] Further, despite the use of vinylcyclopropanes as useful reagents in organic synthesis,

the application of VCPs in Fe-catalyzed conjunctive cross-couplings is not known.

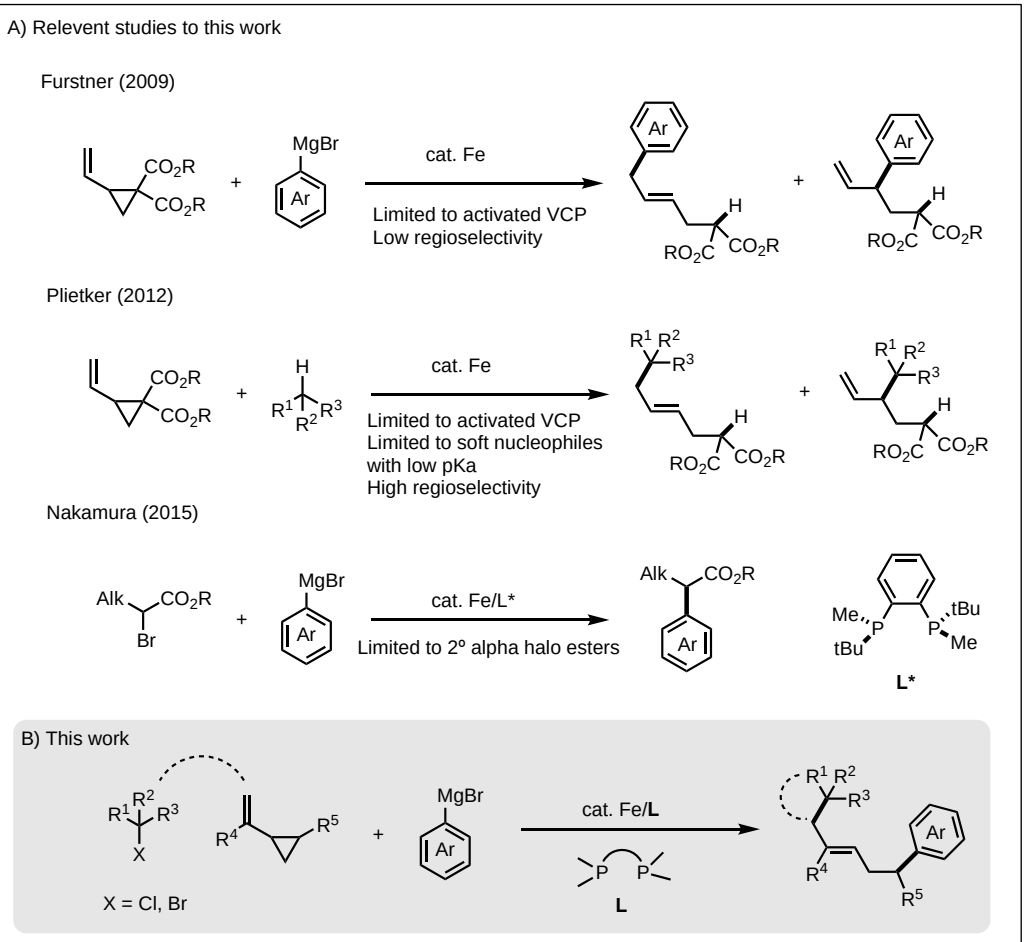

Figure 3.1. Design and development of Fe-catalyzed intra- and intermolecular difunctionalization of vinyl cyclopropanes via a new radical cascade reaction.

Thus, in this chapter, I will discuss my efforts to develop a new (asymmetric) iron-catalyzed radical cascade/C(sp^2)–C(sp^3) cross-coupling reactions.[11] In particular, we used a mechanistically guided approach to design and develop a new and selective Fe-catalyzed intra- and inter-molecular dicarbofunctionalization of synthetically versatile vinyl cyclopropanes (**Figure 3.1B**).[12,13] Overall, this work establishes the use of readily accessible vinyl cyclopropanes in Fe-catalyzed conjunctive cross-coupling reactions.

3.2 Proposed Mechanism

Contributing to the scarcity of iron-catalyzed asymmetric reactions is likely the fact that mechanistic details of iron-catalyzed cross-coupling are not well understood.[14] Pioneering mechanistic studies by Kochi[15] in the 1970s and more recent reports by

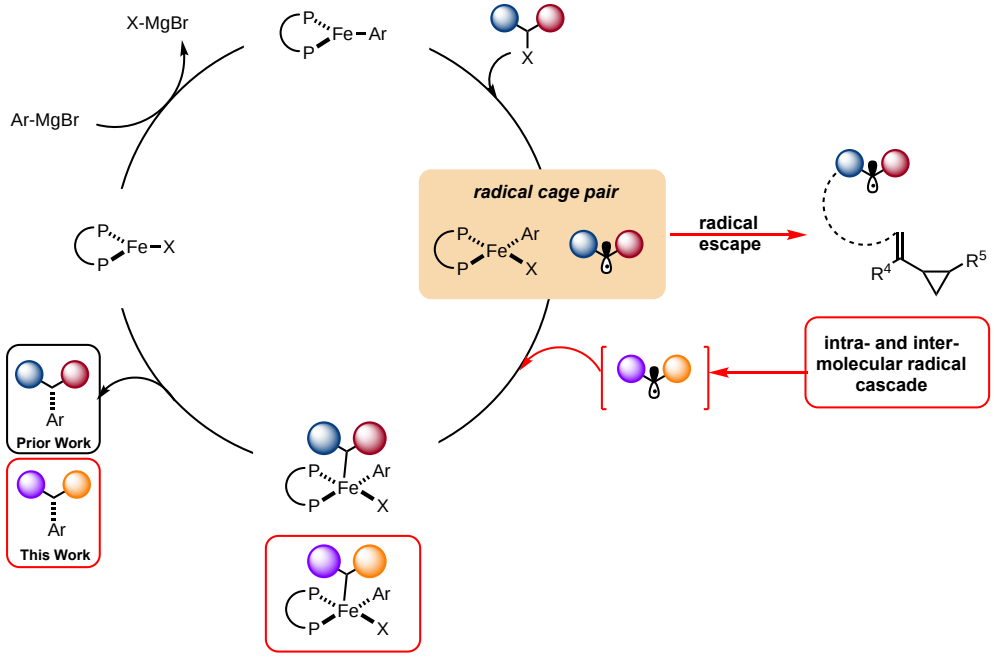

Figure 3.2. A proposed mechanism of iron-catalyzed cross-coupling reactions.

Bedford,[16] Nakamura,[17] Norrby,[18] Furstner,[19] Tonzetich,[20] Koszinowski,[21] and Neidig[22] have led to a greater understanding of these transformations. As discussed first in Chapter 1, in 2017, parallel quantum mechanical studies in our lab[23] and by Morokuma[24] were reported on the mechanism of chiral bisphosphine cross-coupling reactions between α-chloro esters and aryl Grignard reagents. These studies revealed a mechanism involving halogen abstraction by an aryl Fe(I) complex, leading to an alkyl radical and halo aryl Fe(II) species (**Figure 3.2**). In turn, these two species could combine, leading to an Fe(III) intermediate which will then undergo reductive

elimination, leading to the desired cross-coupled product. More experimental studies (i.e., spectroscopic and kinetic) are needed to assess the validity of the computational models, and the mechanism likely depends on subtle changes to the alkyl halide, Grignard, and ligand structures. Nonetheless, based on these mechanistic studies, we hypothesized the possibility of diverting the reactivity from the Fe radical cross-coupling catalytic cycle (black) to a programmed intra- and intermolecular radical cascade (red) with vinyl cyclopropanes, leading to a new alkyl radical that could then re-enter the catalytic cycle and undergo stereoselective $C(sp^2)$–$C(sp^3)$ bond formation. Given that most of the transition-metal catalyzed cascade reactions terminate with C–H bond formation[25] and fail to control the stereoselectivity at the termination step, if successful, this approach could lead to a rapid increase in molecular diversity.

3.3 Computation of Intra-Molecular Dicarbofunctionalization of VCPs

Li's group demonstrated the use of cyclopropyl olefins to promote a radical alkylation, ring-opening, intramolecular arylation cascade reaction under photoredox conditions.[26] Fu and co-workers reported that chiral nickel catalysts could achieve enantioselective cross-coupling of a wide range of racemic alkyl halides (as radical precursors) with organometallic nucleophiles[27] including those involving stereoconvergent radical cyclization/arylation.[28] We hypothesized that upon radical formation and in the presence of a pendant vinyl cyclopropane (**Figure 3.2** and **Figure 3.3**; right, red), we could divert reactivity from the cross-coupling cycle to promote an intra-molecular radical cascade reaction. Specifically, we envisage a 5-exo-trig

cyclization outcompeting radical rebound to an aryl Fe species and divert reactivity towards Fe-catalyzed 1,5-dicarbofunctionalization of vinyl cyclopropanes.

Indeed, as shown in **Figure 3.3**, quantum mechanical calculations by Mingbin Yuan and I support our hypothesis. Specifically, the barrier for radical 5-exo-

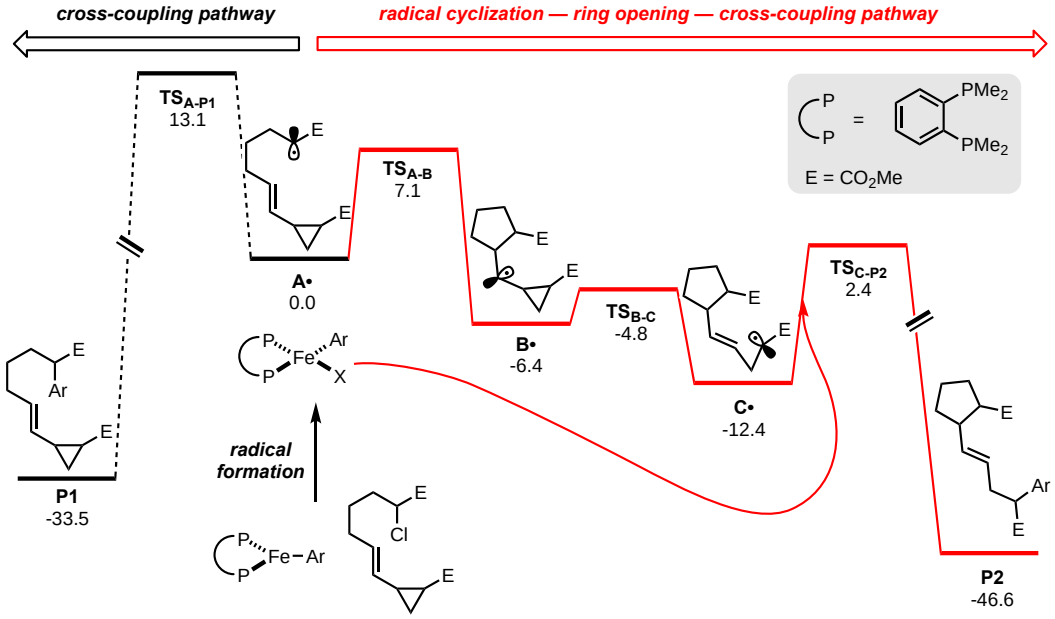

Figure 3.3. Energetics for the in-cage (black) and out-of-cage (red) arylation computed at the UPBEPBE/6-311+G(d,p)-SDD(Fe)-THF(SMD)//UB3LYP/6-31G(d) levels of theory.

cyclization (via $\mathbf{TS_{A\text{-}B}}$) to form **B•** is 6.0 kcal mol–1 lower in energy than the barrier for the radical rebound transition state $\mathbf{TS_{A\text{-}P1}}$ that will lead to cross-coupling product **P1** (7.1 kcal mol–1 vs. 13.1 kcal mol–1, respectively). In turn, the kinetically favored cyclic alkyl radical **B•** will then undergo radical ring-opening (the barrier is only 1.6 kcal mol–1) to form the thermodynamically favored alkyl radical **C•**. Finally, **C•** could then re-enter the iron cross-coupling cycle and undergo C(sp^2)–C(sp^3) bond formation (via $\mathbf{TS_{C\text{-}P2}}$; the barrier is 14.8 kcal mol–1 from **C•**) leading, after reductive elimination (not shown), to the radical cascade product **P2**. Overall, these calculations suggest that

the radical cyclization/ring-opening/cross-coupling pathway (leading to **P2**) is kinetically favored over cross-coupling (leading to **P1**). Moreover, we anticipate that the chiral aryl iron species could control the final radical coupling step (with **C•**) and permit high-levels of stereocontrol.

3.4 Stereoselective Intra-Molecular Dicarbofunctionalization of VCPs

Gratifyingly, we found that we can divert reactivity towards the asymmetric intra-molecular 1,5-difunctionalization of vinyl cyclopropanes using **3.4.a** as the substrate (**Figure 3.4**). Specifically, using the standard conditions for Fe-catalyzed α-

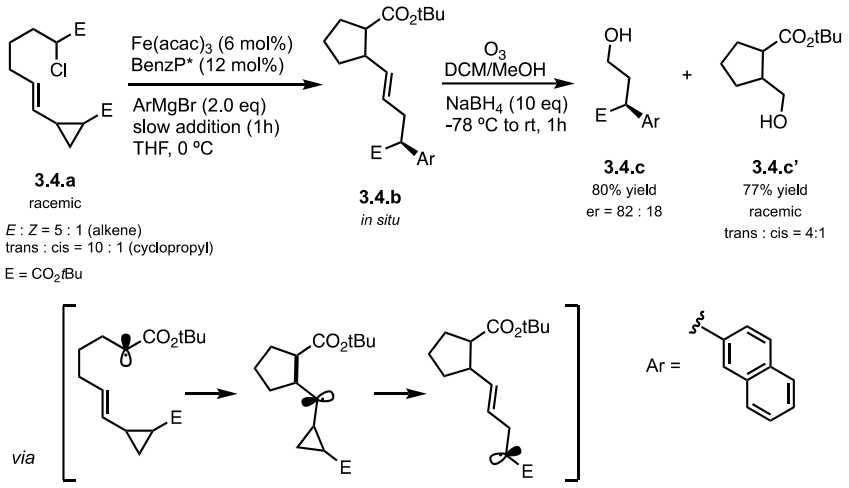

Figure 3.4. Design and application of asymmetric Fe-catalyzed intramolecular dicarbofunctionalization of vinyl cyclopropanes.

arylation,[29] the reaction of **3.4.a** with 2-napthylmagnesium bromide gave a mixture of diastereomeric radical cascade products **3.4.b**. At this moment, noting that most of the transition-metal catalyzed cascade reactions terminate with C–H bond formation[25] and fail to control stereoselectivity at the termination step, we were primarily concerned with determining if the chiral iron species controlled the stereochemistry of the

terminating $C(sp^2)$–$C(sp^3)$ arylation. As a proof-of-concept, to determine stereochemistry at the terminating C–C bond forming step, Dr. Lei Liu subjected **3.4.b** to a one-pot procedure of ozonolysis followed by reduction with $NaBH_4$ that led to the corresponding product **3.4.c** in good yields and enantioselectivities. Notably, as expected from the radical cyclization event in the absence of chiral iron species (**Figure 3.3**), the corresponding racemic cyclopentane fragment **3.4.c'** was isolated in 77% yield in 4:1 dr. Having established, as a proof of-concept, that we could control the enantioselectivity at the terminating step in the cascade reaction, we examine the aryl Grignard reagent scope in this transformation and its effect on enantioselectivity. As

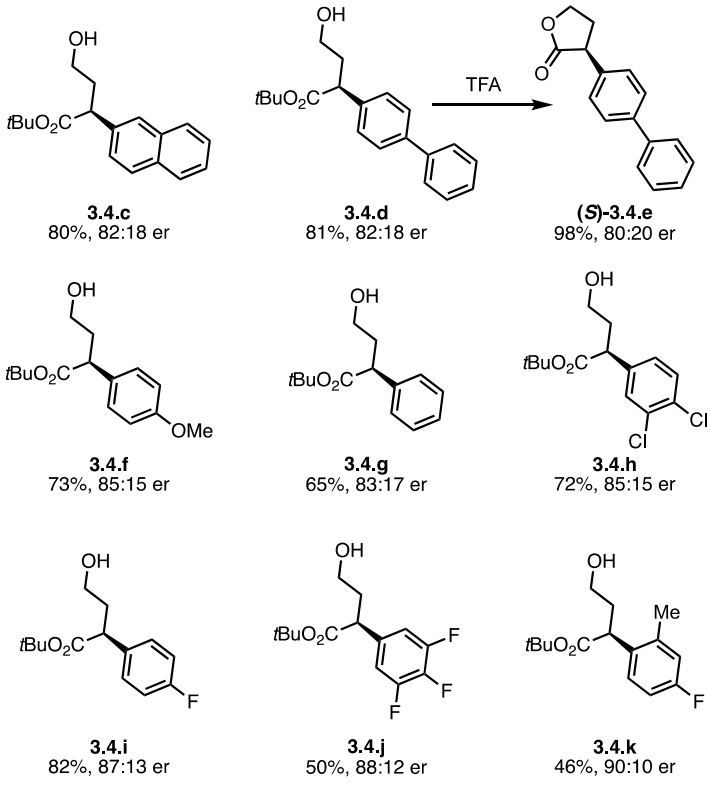

Figure 3.5. Scope of the nucleophile.

shown in **Figure 3.5**, the aryl Grignard reagent scope is broad. Both electron-poor and electron-rich aryl Grignard reagents participate in the diverted Fe-catalyzed intra-

molecular difunctionalization of vinyl cyclopropanes to give the desired products in good yields (up to 82% **3.4.i** over three steps) and enantioselectivities (up to 90 : 10 er). We established the absolute stereochemistry as (*S*) from the cyclized lactone (*S*)-**3.4.e** from **3.4.d**. Notably, Grignard reagents that failed in the asymmetric Fe-catalyzed cross-coupling reactions were compatible reagents in these radical cascade/cross-coupling transformations. Specifically, highly electron-deficient (i.e.,3,4,5-trifluorophenyl **3.4.j**) and even sterically congested (e.g., *ortho*-methyl aryl **3.4.k**) aryl Grignard reagents formed the desired products with good enantioselectivities (90 : 10 er) albeit in lower yields (46%). However, at this moment, this method is limited to 5-exo-trig radical cyclization. Lengthening the tether with an extra methylene group leads to the formation of the Fe radical cross-coupled product and no products from diverted 6-exo-trig radical cyclization are observed. Presumably, the much higher energy barrier to undergo radical 6-exo-trig cyclization in comparison to 5-exo-trig radical cyclization (**Figure 3.3**) prevents the formation of radical cascade/arylation (**Figure 3.6**).

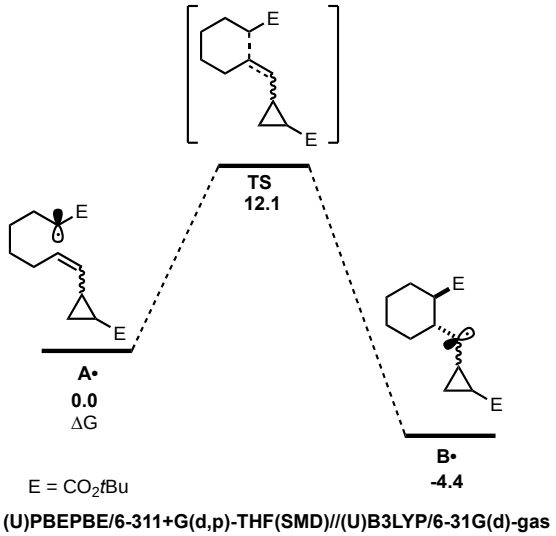

Figure 3.6. Energetics for the 6-exo-cyclization.

3.5 Design of the Inter-Molecular Dicarbofunctionalization of VCPs

Given the scarcity of stereoconvergent transition metal-catalyzed radical cyclization-arylation cascades and under utilization of vinyl cyclopropanes in transition metal-catalyzed conjunctive cross-couplings, our proof-of-principle results with intramolecular functionalization of VCPs (**Figure 3.4**) represent an attractive strategy towards this unmet need.[30] Specifically, we envisage that by tuning the properties of alkyl halides, we could divert reactivity towards regioselective intermolecular ring-opening/dicarbofunctionalization of VCPs. Specifically, we hypothesize that sterically hindered tertiary alkyl halides will lead to higher barriers for Fe radical coupling (e.g., two component cross-coupling) and, instead, favor intermolecular radical addition to

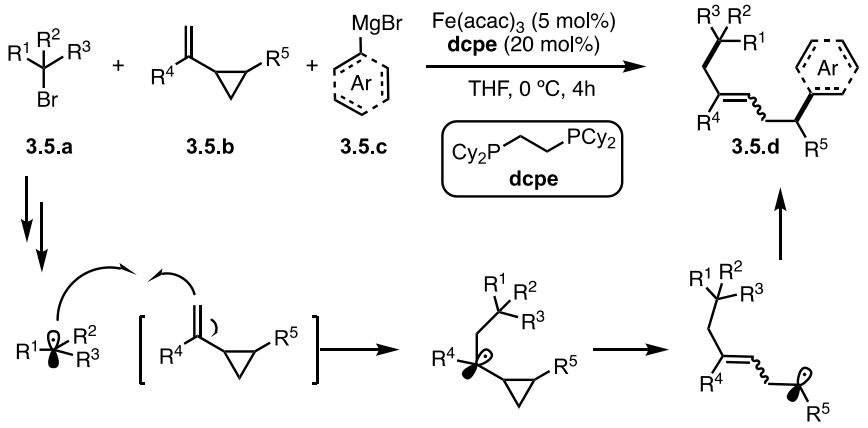

Figure 3.7. Proposed mechanism for iron-catalyzed three-component cross-coupling reaction.

the vinyl cyclopropane (**Figure 3.7**). In turn, the incipient radical could then undergo cyclopropyl ring-opening and re-enter the Fe radical cross-coupling cycle to undergo (stereoselective) $C(sp^2)$–$C(sp^3)$ arylation at the least sterically hindered site (i.e., three-component cross-coupling). Previous work by Furstner and Plietker using iron as the catalyst with vinyl cyclopropanes (VCPs) resulted in ring-

opening/monocarbofunctionalization, required electron-deficient VCPs, and terminated in protonation (**Figure 3.1A**).[7,8] Thus, with our success, this approach expanded the range of Fe-catalyzed transformations using vinyl cyclopropanes as valuable synthons in chemical synthesis. Also, this work represents the first example of (asymmetric) Fe-catalyzed 3-component cross-coupling.

3.6 Scope of the Inter-Molecular Dicarbofunctionalization of VCPs

We initiated our optimization studies using sterically hindered tert-butyl 2-bromo-2-methylpropanoate **3.6.a**, (1-cyclopropylvinyl)-benzene **3.6.b** and aryl 4-fuorophenyl magnesium bromide **3.6.c** as model substrates. Gratifyingly, after extensive ligand screening using bisphosphine, monophosphine, and diamine ligands

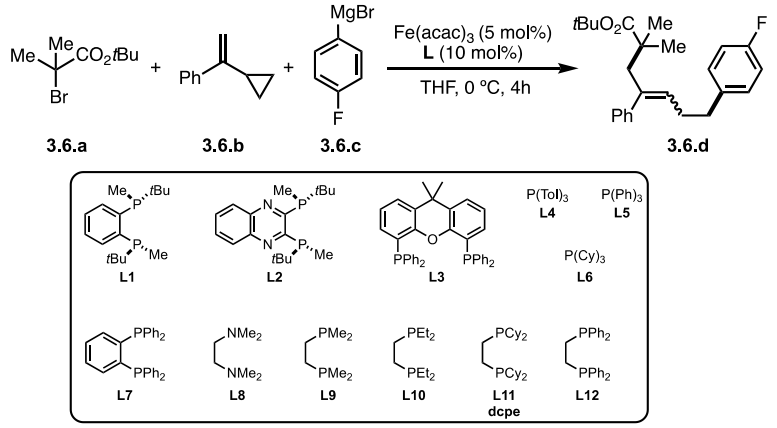

Entry	Ligand	Yield(%)	*E*:*Z*
1	**L1**	92	3.3:1
2	**L2**	70	3.3:1
3	**L3**	0	NA
4	**L4**	0	NA
5	**L5**	0	NA
6	**L6**	0	NA
7	**L7**	40	2.5:1
8	**L7** (room temp)	34	1.4:1
9	**L7** (6h)	40	2.5:1
10	**L8**	55	3.8:1
11	**L9**	0	NA
12	**L10**	0	NA
13	**L11**	73	3.7:1
14	**L11** (20 mol%)	82	3.6:1
15	**L12**	0	NA
16	none (no Fe)	0	NA
17	none (with Fe)	0	NA

Table 3.1. Screening of ligands for iron-catalyzed intermolecular difunctionalization of vinyl cyclopropane.

(**Table 3.1**) and optimization studies, we identified acyclic 1,2-bis(dicyclohexylphosphino) ethane ligand (**dcpe**) **L11** to be suitable to promote the desired and highly selective ring-opening/1,5-alkylarylation of vinyl cyclopropanes, forming compound **3.4.d** in 82% isolated yield and 3.6 : 1 *E*/*Z* ratio (Entry 14). With optimized conditions in hand, we next investigated the reaction scope of this transformation. As shown in **Figure 3.8**, the scope of this Fe-catalyzed 3-component

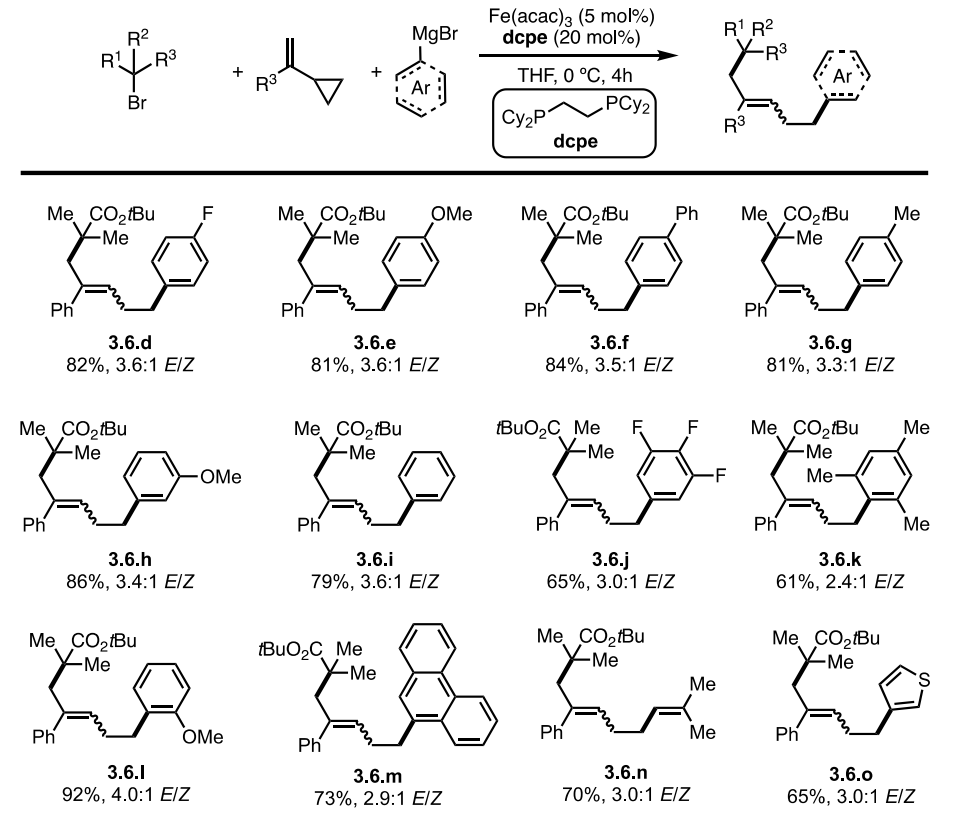

Figure 3.8. Reaction scope of the aryl Grignard reagent in Fe-catalyzed intermolecular dicarbofunctionalization of vinyl cyclopropanes.

dicarbofunctionalization is broad with respect to the Grignard nucleophile. Specifically, the reaction tolerated both electron-withdrawing and electron-donating aryl nucleophiles, forming the desired 1,5-alkylaryl products in 61–92% yield. Notably, the reaction tolerated sterically hindered *ortho*-substituted aryl Grignard reagents

(**3.6.k**, **3.6.l**, and **3.6.m**) that proved to be problematic in previous direct Fe-catalyzed cross-coupling reactions.[31] To highlight the versatility of this method, we also used both vinyl and heteroaryl Grignard reagents and, gratifyingly, obtained the desired products **3.6.n** and **3.6.o**, in good yields, 70% and 65% yield, respectively. Next, we explored the scope of vinyl cyclopropane and alkyl radical precursors (**Figure 3.9**).

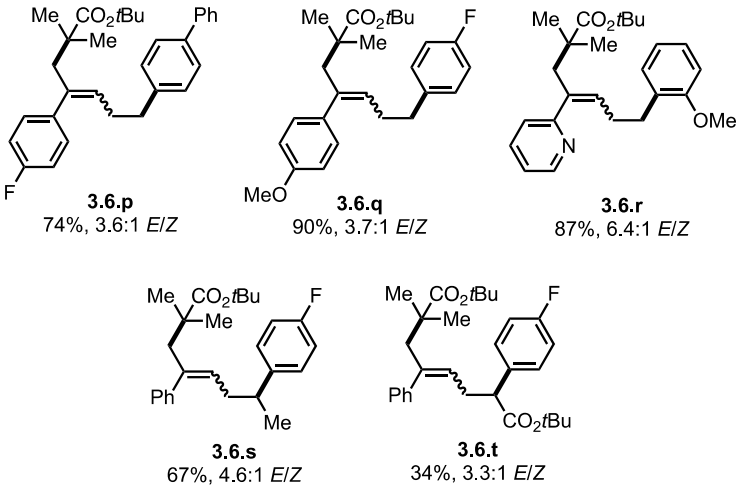

Figure 3.9. Scope of vinyl cyclopropane.

Installing electron-rich or electron-poor aryl groups in the vinyl cyclopropane moiety (R^4) allows the formation of the desired products in good to excellent yields. Notably, the reaction tolerates medicinally relevant pyridyl moieties (**3.6.r**). Moreover, the substituted cyclopropanes (R^5) were suitable for this catalytic system, affording **3.6.s** and **3.6.t** in 67% and 34% yield, respectively. In contrast to previously reported Fe-catalyzed cross-couplings, we found a wide range of alkyl bromides to be suitable radical precursors in this Fe-catalyzed conjunctive cross-coupling (**Figure 3.10**). Specifically, we found that alkyl fluorinated radical precursors are effective partners in the Fe-catalyzed intermolecular dicarbofunctionalization of VCPs, yielding the desired

products **3.4.u** and **3.4.v** in 42% and 75% yield, respectively. Further, we observed a much higher *E/Z* ratio for **3.4.v** (12 : 1 *E/Z*), although the origin of this high selectivity

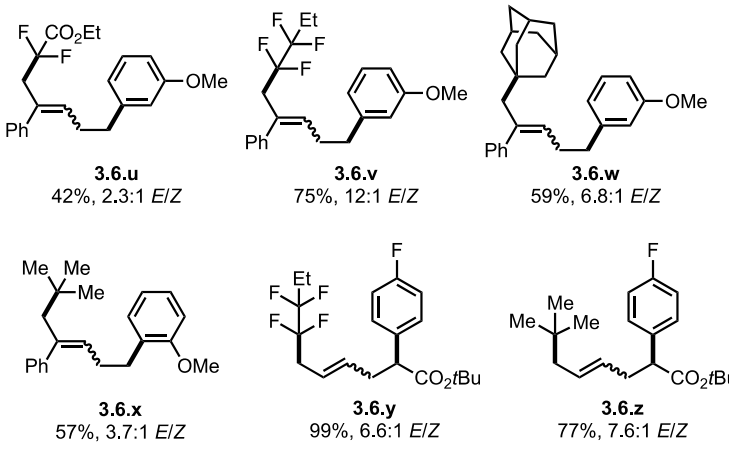

Figure 3.10. Scope of Alkyl Radical Precursors.

is currently unknown. Finally, this method tolerated simple alkyl radical precursors which led to the desired 3-component products **3.6.w** and **3.6.x**. Interestingly, fluorinated and *tert*-butyl radical precursors in combination with unactivated vinyl cyclopropanes led to the desired products **3.6.y**, and **3.6.z** in excellent yields (99% and 77%). Mingbin Yuan performed quantum mechanical calculations on the inter-molecular dicarbofunctionalization, and the calculated results are consistent with our hypothesis and the experimental result (**Figure 3.11**). Specifically, tertiary alkyl radicals preferably undergo *inter*-molecular radical addition (with a barrier of 14.0 kcal

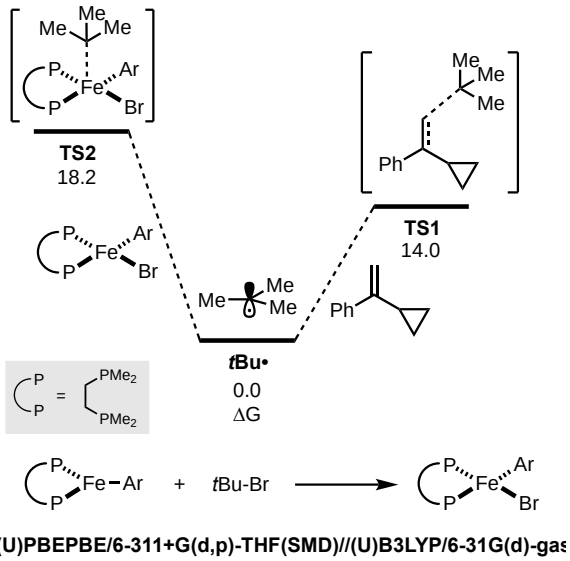

Figure 3.11. A comparison of the energetics of the radical adding to vinyl cyclopropane or adding to the iron(II) active species.

mol^{-1}) to the vinyl cyclopropane over radical coupling with Fe (with a barrier of 18.2 kcal mol^{-1}).

3.7 Application of the Inter-Molecular Dicarbofunctionalization of VCPs

To demonstrate the synthetic versatility of the five-carbon unsaturated chain – potentially useful transformation, Dr. Lei Liu performed the gram-scale synthesis of **3.7.a** (1.37 g, 87% yield) and performed several diversifications (**Figure 3.12**). First,

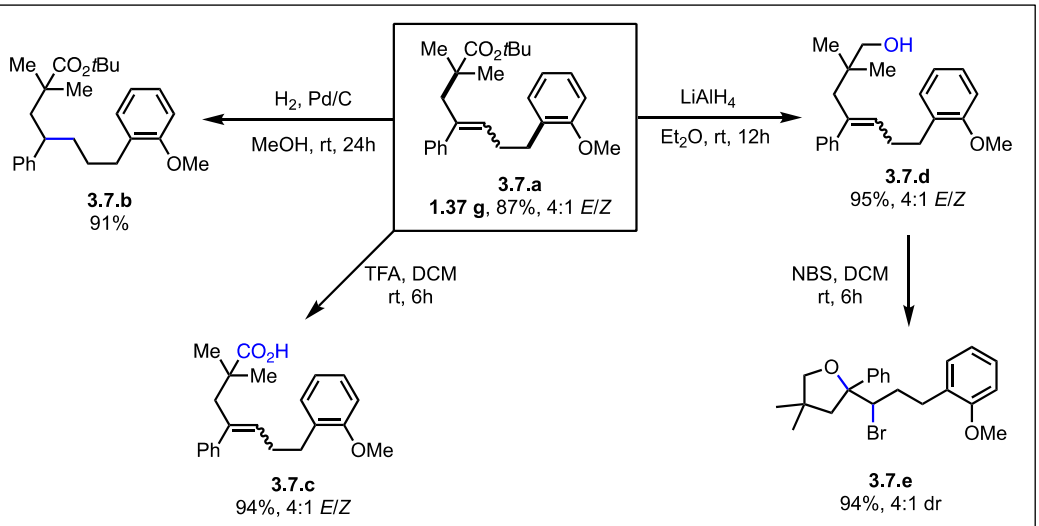

Figure 3.12. Synthetic applications of five-carbon unsaturated chain ester.

reduction of the alkene (Pd/C) provided the alkyl ester (**3.7.b**). Next, he performed hydrolysis of the ester to carboxylic acid (**3.7.c**) which could be a useful substrate in subsequent decarboxylative radical cross-coupling reactions.[32] Notably, derivatization of **3.7.a** to the carboxylic acid analog **3.7.c** permitted facile separation and purification of the major isomer (*E*). Finally, reduction of the ester formed the corresponding primary alcohol (**3.7.d**) which could undergo bromocyclization with N-bromosuccinimide (NBS) leading to the substituted tetrahydropyran with two stereogenic centers (**3.7.e**).

3.8 Summary

In summary, Fe-catalyzed intra- and inter-molecular dicarbofunctionalizations of vinyl cyclopropanes have now been realized. In particular, we have used a mechanistically driven (computational and experimental) approach to divert the reactivity of the alkyl radical from the Fe radical cross-coupling cycle to undergo intra- and inter-molecular radical cascade reactions with activated and unactivated vinyl cyclopropanes. In turn, the incipient alkyl radical then re-enters the Fe cross-coupling cycle and undergoes (stereoselective) $C(sp^2)$–$C(sp^3)$ bond formation. Finally, for the first time, as a proof-of-concept we show that VCPs can be used as effective conjunctive partners in asymmetric Fe-catalyzed 3-component cross-coupling reactions. We anticipate that the intermolecular 3-component Fe-catalyzed dicarbofunctionalization reaction will impact the synthesis of medicinally relevant molecules. However, at present, some drawbacks of this method are the use of Grignard reagents that limits functional group incorporation into the nucleophile/radical precursors along with *E/Z* mixtures. Overall, these results represent the first examples of an asymmetric Fe-catalyzed conjunctive cross-coupling. The next chapter (**Chapter 4**) will be showing the work geared towards expanding this transformation.

3.9 References

(1) Piontek, A.; Bisz, E.; Szostak, M. Angew. Chem., Int. Ed. **2018**, *57*, 11116–11128.

(2) (a) Cassani, C.; Bergonzini, G.; Wallentin, C. J. *ACS Catal.* **2016**, *6*, 1640–1648; (b) Bedford, R. B, *Acc. Chem. Res*. **2015**, *48*, 1485–1493; (c) Bauer, I.; Knölker, H. J. *Chem. Rev.* **2015**, *115*, 3170–3387; (d) Czaplik, W. M.; Mayer, M.; Cvengroš, J.; von Wangelin, A. J. *ChemSusChem*, **2009**, *2*, 396–417; (e) Sherry, B. D.; Fürstner, A. *Acc. Chem. Res*. **2008**, *41*, 1500–1511.

(3) (a) Sun, C. L.; Krause, H.; Fürstner, A. *Adv. Synth. Catal*. **2014**, *356*, 1281–1291.; (b) Kawamura, S.; Nakamura, M. *Chem. Lett*. **2013**, *42*, 183–185; (c) Hatakeyama, T.; Fujiwara, Y. I.; Okada, Y.; Itoh, T.; Hashimoto, T.; Kawamura, S.; Takaya, H.; Nakamura, M. *Chem. Lett*. **2011**, *40*, 1030–1032; (d) Hatakeyama, T; Okada, Y.; Yoshimoto, Y.; Nakamura, M. *Angew. Chem., Int. Ed*. **2011**, *50*, 10973–10976; (e) Dongol, K. G.; Koh, H.; Sau, M.; Chai, C. L. *Adv. Synth. Catal*. **2007**, *349*, 1015–1018.

(4) (a) Toriyama, F.; Cornella, J.; Wimmer, L.; Chen, T. G.; Dixon, D. D.; Creech, G.; Baran, P. S. *J. Am. Chem. Soc*. **2016**, *138*, 11132–11135; (b) Bedford, R. B.; Carter, E.; Cogswell, P. M.; Gower, N. J.; Haddow, M. F.; Harvey, J. N.; Murphy, D. M.; Neeve, E. C.; Nunn, J. *Angew. Chem., Int. Ed*. **2013**, *52*, 1285–1288; (c) Adams, C. J.; Bedford, R. B.; Carter, E.; Gower, N. J.; Haddow, M. F.; Harvey, J. N.; Huwe, M.; Cartes, M. A.; Mansell, S. M.; Mendoza, C.; Murphy, D. M.; Neeve, E. C.; Nunn, J. *J. Am. Chem. Soc*. **2012**, *134*, 10333–10336; (d) Hatakeyama, T.; Kondo, Y.; Fujiwara, Y. I.; Takaya, H.; Ito, S.; Nakamura, E.; Nakamura, M. *Chem. Commun*. **2009**, 1216–1218; (e) Bedford, R. B.; Huwe, M.; Wilkinson, M. C. *Chem. Commun*. **2009**, 600–602.

(5) (a) Nakagawa, N.; Hatakeyama, T.; Nakamura, M. *Chem. Lett*. **2015**, *44*, 486–488; (b) Hatakeyama, T.; Hashimoto, T.; Kathriarachchi, K. K.; Zenmyo, T.; Seike, H.; Nakamura, M. *Angew. Chem., Int. Ed*. **2012**, *51*, 8834–8837; (c) Hashimoto, T.; Hatakeyama, T.; Nakamura, M. *J. Org. Chem*. **2012**, *77*, 1168–1173; (d) Hatakeyama, T.; Hashimoto, T.; Kondo, Y.; Fujiwara, Y.; Seike, H.; Takaya, H.; Tamad, Y.; Ono, T.; Nakamura M. *J. Am. Chem. Soc*. **2010**, *132*, 10674–10676.

(6) (a) Kawamura, S.; Kawabata, T.; Ishizuka, K.; Nakamura, M. *Chem. Commun*. **2012**, *48*, 9376–9378; (b) Kawamura, S.; Ishizuka, K.; Takaya, H.; Nakamura, M. *Chem. Commun*. **2010**, *46*, 6054–6056.

(7) Sherry, B. D.; Fürstner, A. *Chem. Commun*. **2009**, 7116–7118.

(8) Dieskau, A. P.; Holzwarth, M. S.; Plietker, B. *J. Am. Chem. Soc*. **2012**, *134*, 5048–5051.

(9) (a) Iwamoto, T.; Okuzono, C.; Adak, L.; Jin, M.; Nakamura, M. *Chem. Commun*. **2019**, *55*, 1128–1131; (b) Jin, M.; Adak, L.; Nakamura, M. *J. Am. Chem. Soc*. **2015**, *137*, 7128–7134.

(10) Pellissier, H. *Coord. Chem. Rev*. **2019**, *386*, 1–31.

(11) (a) Choi, J.; Fu, G. C. *Science*, **2017**, *356*; (b) Cherney, A. H.; Kadunce, N. T.; Reisman, S. E. *Chem. Rev*. **2015**, *115*, 9587–9652.

(12) Meazza, M.; Guo, H.; Rios, R. *Org. Biomol. Chem*. **2017**, *15*, 2479–2490.

(13) Chen, C.; Shen, X.; Chen, J.; Hong, X.; Lu, Z. *Org. Lett*. **2017**, *19*, 5422–5425.

(14) (a) Neidig, M. L.; Carpenter, S. H.; Curran, D. J.; DeMuth, J. C.; Fleischauer, V. E.; Iannuzzi, T. E.; Neate, P. G. N.; Sears, J. D.; Wolford, N. J. *Acc. Chem.*

Res. **2019**, *52*, 140–150; (b) Sears, J. D.; Neate, P. G.; Neidig, M. L. *J. Am. Chem. Soc*. **2018**, *140*, 11872–11883; (c) Liu, L.; Lee, W.; Yuan, M.; Gutierrez, O. *Comments Inorg. Chem*. **2018**, *38*, 210–237; (d) Mako, T. L.; Byers, J. A. *Inorg. Chem. Front*. **2016**, *3*, 766–790.

(15) Smith, R. S.; Kochi, J. K. *J. Org. Chem*. **1976**, *41*, 502–509.

(16) Bedford, R. B.; Brenner, P. B.; Carter, E.; Cogswell, P. M.; Haddow, M. F.; Harvey, J. N.; Murphy, D. M.; Nunn, J.; Woodall, C. H. *Angew. Chem., Int. Ed*. **2014**, *53*, 1804–1808.

(17) (a) Takaya, H.; Nakajima, S.; Nakagawa, N.; Isozaki, K.; Iwamoto, T.; Imayoshi, R.; Gower, N. J.; Adak, L.; Hatakeyama, T.; Honma, T.; Takagaki, M.; Sunada, Y.; Nagashima, H.; Hashizume, D.; Takahashi, O.; Nakamura, M. *Chem. Soc. Jpn*. **2015**, *88*, 410–418; (b) Noda, D.; Sunada, Y.; Hatakeyama, T.; Nakamura, M.; Nagashima, H. *J. Am. Chem. Soc*. **2009**, *131*, 6078–6079.

(18) (a) Bekhradnia, A.; Norrby, P. O. *Dalton Trans*. **2015**, *44*, 3959–3962; (b) Hedström, A.; Izakian, Z.; Vreto, I.; Wallentin, C. J.; Norrby, P. O. *Chem.–Eur. J*. **2015**, *21*, 5946–5953; (c) Kleimark, J.; Hedström, A.; Larsson, P. F.; Johansson, C.; Norrby, P. O. *ChemCatChem*, **2009**, *1*, 152–161; (d) Hedström, A.; Bollmann, U.; Bravidor, J.; Norrby, P. O. *Chem.–Eur. J*. **2011**, *17*, 11991.

(19) (a) Casitas, A.; Rees, J. A.; Goddard, R.; Bill, E.; DeBeer, S.; Fürstner, A. *Angew. Chem., Int. Ed*. **2017**, *56*, 10108–10113; (b) Fürstner, A.; Krause, H.; Lehmann, C. W. *Angew. Chem., Int. Ed*. **2006**, *45*, 440–444.

(20) Przyojski, J. A.; Veggeberg, K. P.; Arman, H. D.; Tonzetich, Z. J. *ACS Catal*. **2015**, *5*, 5938–5946.

(21) (a) Parchomyk, T.; Demeshko, S.; Meyer, F.; Koszinowski, K. *J. Am. Chem. Soc*. **2018**, *140*, 9709–9720; (b) Parchomyk, T.; Koszinowski, K. *Chem.–Eur. J.* **2016**, *22*, 15609–15613.

(22) (a) Carpenter, S. H.; Baker, T. M.; Muñoz, S. B.; Brennessel, W. W.; Neidig, M. L, *Chem. Sci*. **2018**, *9*, 7931–7939; (b) Muñoz III, S. B.; Daifuku, S. L.; Sears, J. D.; Baker, T. M.; Carpenter, S. H.; Brennessel, W. W.; Neidig, M. L. *Angew. Chem., Int. Ed*. **2018**, *57*, 6606–6610; (c) Fleischauer, V. E.; Muñoz III, S. B.; Neate, P. G.; Brennessel, W. W.; Neidig, M. L. *Chem. Sci.* **2018**, *9*, 1878–1891; (d) Kneebone, J. L.; Brennessel, W. W.; Neidig, M. L. *J. Am. Chem. Soc*. **2017**, *139*, 6988–7003; (e) Muñoz III, S. B.; Daifuku, S. L.; Brennessel, W. W.; Neidig, M. L. *J. Am. Chem. Soc*. **2016**, *138*, 7492–7495; (f) Daifuku, S. L.; Kneebone, J. L.; Snyder, B. E.; Neidig, M. L. *J. Am. Chem. Soc*. **2015**, *137*, 11432–11444; (g) Al-Afyouni, M. H.; Fillman, K. L.; Brennessel, W. W.; Neidig, M. L. *J. Am. Chem. Soc*. **2014**, *136*, 15457–15460; (h) Daifuku, S. L.; Al-Afyouni, M. H.; Snyder, B. E.; Kneebone, J. L.; Neidig, M. L. *J. Am. Chem. Soc*. **2014**, *136*, 9132–9143.

(23) Lee, W.; Zhou, J.; Gutierrez, O. *J. Am. Chem. Soc*. **2017**, *139*, 16126–16133.

(24) Sharma, A. K.; Sameera, W. M. C.; Jin, M.; Adak, L.; Okuzono, C.; Iwamoto, T.; Kato, M.; Nakamura, M.; Morokuma, K. *J. Am. Chem. Soc*. **2017**, *139*, 16117–16125.

(25) (a) Plesniak, M. P.; Huang, H. M.; Procter, D. J. *Nat. Rev. Chem*. **2017**, *1*, 1–16; (b) Quiclet-Sire, B.; Zard, S. Z. *Proc. R. Soc. A.* **2017**, *473*, 20160859; (c) Brill, Z. G.; Grover, H. K.; Maimone, T. J. *Science*, **2016**, *352*, 1078–1082; (d)

Wille, U. *Chem. Rev*. **2013**, *113*, 813–853; (e) Nicolaou, K. C.; Edmonds, D. J.; Bulger, P. G. *Angew. Chem., Int. Ed*. **2006**, *45*, 7134–7186.

(26) Li, J.; Chen, J.; Jiao, W.; Wang, G.; Li, Y.; Cheng, X.; Li, G. *J. Org. Chem*. **2016**, *81*, 9992–10001.

(27) Fu, G. C. *ACS Cent. Sci*. **2017**, *3*, 692–700

(28) Cong, H.; Fu, G. C. *J. Am. Chem. Soc*. **2014**, *136*, 3788–3791.

(29) Liu, L.; Lee, W.; Zhou, J.; Bandyopadhyay, S.; Gutierrez, O. *Tetrahedron*, **2019**, *75*, 129–136.

(30) (a) Leifert, D.; Studer, A. *Angew. Chem., Int. Ed*. **2020**, *59*, 74–108.; (b) Jiang, H.; Seidler, G.; Studer, A. *Angew. Chem., Int. Ed*. **2019**, *58*, 16528–16532.

(31) Jin, M.; Nakamura, M. *Chem. Lett*. **2011**, *40*, 1012–1014.

(32) (a) Qin, T.; Malins, L. R.; Edwards, J. T.; Merchant, R. R.; Novak, A. J.; Zhong, J. Z.; Mills, R. B.; Yan, M.; Yuan, C.; Eastgate M. D.; Baran, P. S. *Angew. Chem., Int. Ed*. **2017**, *56*, 260–265; (b) Arshadi, S.; Ebrahimiasl, S.; Hosseinian, A.; Monfared, A.; Vessally, E. *RSC Adv*. **2019**, *9*, 8964–8976.

Chapter 4: Fe-Catalyzed Three-Component Dicarbofunctionalization of Unactivated Alkenes with Alkyl Halides and Grignard Reagents

Excerpts from this chapter were published in: Liu, L.; Lee, W.; Youshaw, C. R.; Yuan, M.; Geherty, M. B.; Zavalij, P. Y.; Gutierrez, O. *Chem. Sci*. **2020**, *11*, 8301−8305.

4.1 Transition Metal-Catalyzed Difunctionalization of Olefins

Olefins are ubiquitous in natural products and bioactive compounds and serve as versatile commodity feedstocks. 1,2-difunctionalization of olefins represents one of the most widely used strategies to build synthetic complexity in organic synthesis and serves as a platform to introduce concepts of chemo-, regio-, and stereoselectivity.[1] Recently, there has been a surge in the development of three-component transition metal-catalyzed difunctionalization that employs olefins because of its potential to rapidly increase diversity in a single step (**Figure 4.1A**).[2–4] However, selective transition metal-catalyzed three-component alkylarylation of unactivated alkenes without electronically biased substrates or directing groups is rare.[5] Moreover, despite the inherent attractive features of iron as a catalyst (Earth abundant, less toxic, inexpensive, and environmentally benign in comparison to Pd or Ni) in pharmaceutical settings, there are no general methods for iron-catalyzed three-component 1,2-dicarbofunctionalization of olefins.[6–13] Recently, as described in the prior chapter, our group reported the use of a strained vinyl cyclopropanes to promote a three-component Fe-catalyzed reaction leading to 1,5-alkylarylation products (**Figure 4.1B**).[14,15] Unfortunately, despite numerous attempts, the 1,2-difunctionalization products were

not observed, presumably due to much more rapid ring-opening of the incipient alkyl radical followed by C–C bond formation. In this chapter, I will describe my efforts on developing the first iron-catalyzed 3-component dicarbofunctionalization of unactivated alkenes with both alkyl iodides and bromides with sp^2-hybridized Grignard

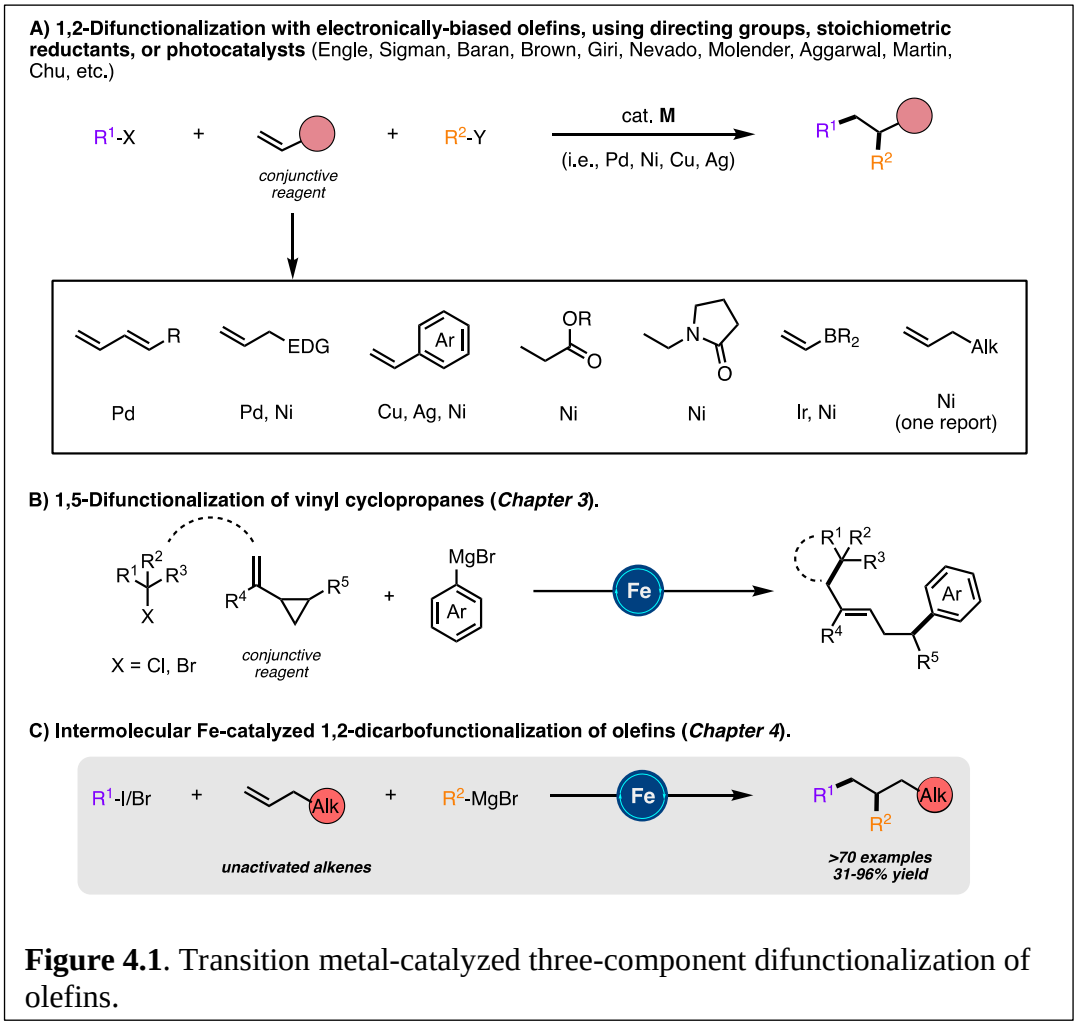

Figure 4.1. Transition metal-catalyzed three-component difunctionalization of olefins.

nucleophiles leading to 1,2-alkylarylation or 1,2-alkylvinylation of alkenes with broad scope and excellent regio- and chemoselectivity (**Figure 4.1C**). In addition, I will discuss how we applied this concept to develop a three-component radical alkylation/cyclization/arylation cascade leading to diverse (hetero)cyclic compounds.

We anticipate that this work will lead to greater application of Fe as a catalyst in three-component difunctionalization of olefins.

4.2 Proposed Mechanism

As shown in **Figure 4.2** , we hypothesize that alkyl halide **1** would react with Fe species **A** to form the alkyl radical **int-1** and **B**.[12,13] Due to the high barrier associated with sterically hindered alkyl radicals and aryl iron **B** to undergo direct cross-coupling,

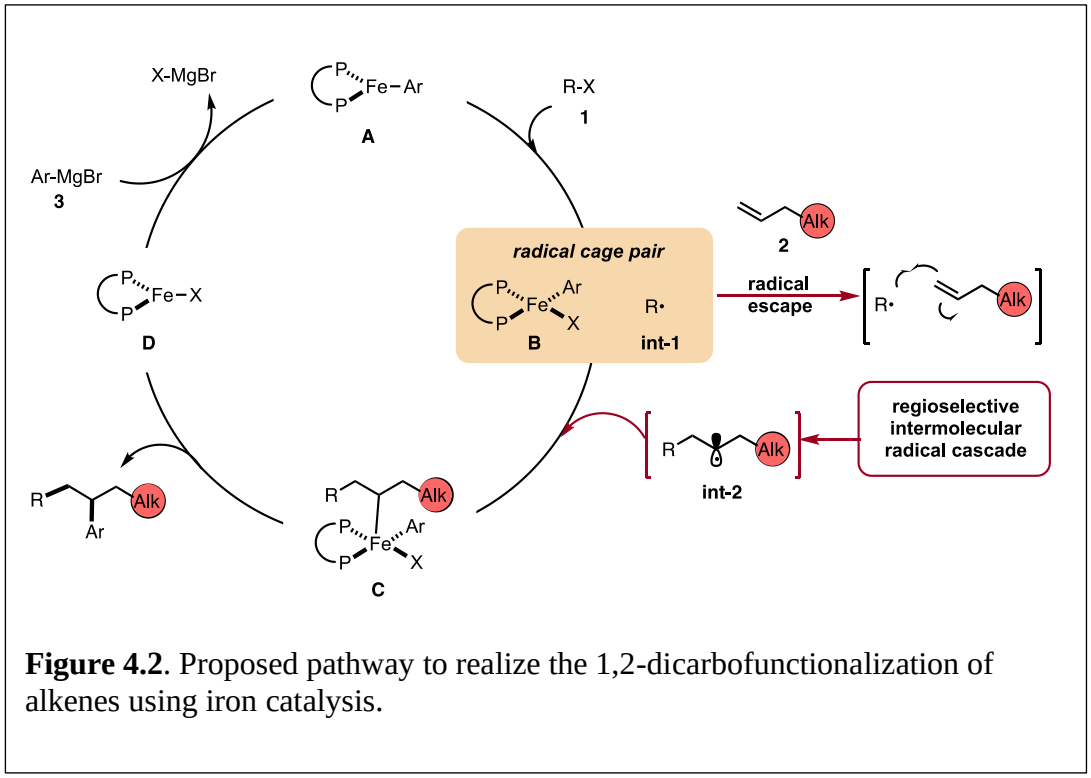

Figure 4.2. Proposed pathway to realize the 1,2-dicarbofunctionalization of alkenes using iron catalysis.

we anticipate that the tertiary radical **int-1** (or a fast reacting alkyl radical) would favor regioselective Giese addition to olefin **2** to form, in the absence of cyclopropyl groups, a transient secondary alkyl radical **int-2**.[16] Then the longer lived (persistent) aryl iron species **B** can trap the less sterically hindered 2º alkyl radical **int-2**, and undergo reductive elimination from **C** to form the desired 1,2-dicarbofunctionalization product and **D**. Finally, facile transmetallation with aryl Grignard **3** restarts the catalytic cycle.[17]

Recognizing that the success of the 3-component dicarbofunctionalization hinges on driving the equilibrium towards formation of **int-2**, presumably by favoring Giese addition over addition to aryl iron **B**, we initiated our studies under solvent-free conditions and at high concentrations of alkenes. The challenge remains whether (a) we can drive the kinetics towards the Giese addition to **2**, (b) **int-2** is sufficiently long-lived to be intercepted by the persistent iron species **B**, and (c) **C** will undergo reductive elimination to form the desired 1,2-dicarbofunctionalization product.

4.3 Reaction Optimization and the Scope of Grignard

Initially, we elected to use tert-butyl iodide **4.3.a**, 4-phenyl-1-butene **4.3.b**, and meta-methoxy phenyl Grignard **4.3.c** as model substrates (**Table 4.1**). Gratifyingly, under our modified conditions for radical cross-coupling with vinyl cyclopropanes (i.e., using $Fe(acac)_3$ as a precatalyst and 1,2-bis(dicyclohexylphosphino) ethane as a ligand),[14a] we observed the formation of the desired 1,2-alkylaryl product **4.3.d** in 86% yield and complete regioselectivity with unactivated olefin **4.3.b** (**Table 4.1,** entry 1). Notably, other bisphosphine ligands commonly employed in direct Fe-catalyzed cross-coupling reactions with alkyl halides[10] significantly decrease the yield (entries 2–5). Further, the use of the iron precatalyst bearing strongly coordinating ligands inhibits the reaction (entry 6) while other precatalysts were less efficient (entries 7 and 8). Moreover, the use of THF as solvent had a minor effect on the overall efficiency of the 3-component 1,2-dicarbofunctionalization (entry 9). Finally, we could also perform the

4.3.a 4.3.b 4.3.c 4.3.d

Entry	Deviations from above	Yield [%]
1	None	86
2	**L2** (20 mol%)	0
3	**L3** (20 mol%)	0
4	**L4** (20 mol%)	2
5	**L5** (20 mol%)	14
6	$Fe(OAc)_2$ (5 mol%)	<5
7	$FeBr_2$ (5 mol%)	80
8	$Fe(OTf)_2$ (5 mol%)	41
9	In THF (0.2 mL)	83
10	$Fe(acac)_3$ (3 mol%) and L1 (12 mol%)	85
11	No Ligand	<5
12	No $Fe(acac)_3$ and no Ligand	0

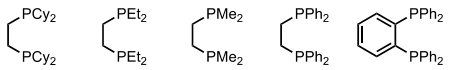

L1 L2 L3 L4 L5

The reaction was performed with *tert*-butyl iodide **4.3.a** (0.1 mmol, 1.0 equiv.), 4-phenyl-1-butene **4.3.b** (14 equiv.) and *meta*-methoxy phenyl Grignard **4.3.c** (1.4 equiv.) without any additional solvent. Aryla Grignard **4.3.c** was added dropwise via a syringe pump over 1 h.

Table 4.1. Evaluation of reaction conditions.

reaction in high yield under lower catalytic loading (entry 10). Control experiments show that the Fe and ligand are both critical for the reaction (entries 11 and 12). With a set of optimized reaction conditions in hand, an exploration of the reaction scope and limitations of this bisphosphine iron-catalyzed 3-component dicarbofunctionalization was undertaken. As shown in **Figure 4.3**, the reaction tolerated a wide range of electron-rich (e.g., **4.3.d – 4.3.j**) and electron-deficient aryl Grignard nucleophiles (e.g., **4.3.l – 4.3.n**) forming the desired 1,2-alkylaryl products. Further, various substituent positions on the aryl nucleophiles were tolerated including meta and para mono- and disubstituted aryl Grignard nucleophiles. Importantly, vinyl Grignard reagents are also competent nucleophilic partners forming the regioselective 1,2-alkylvinyl product

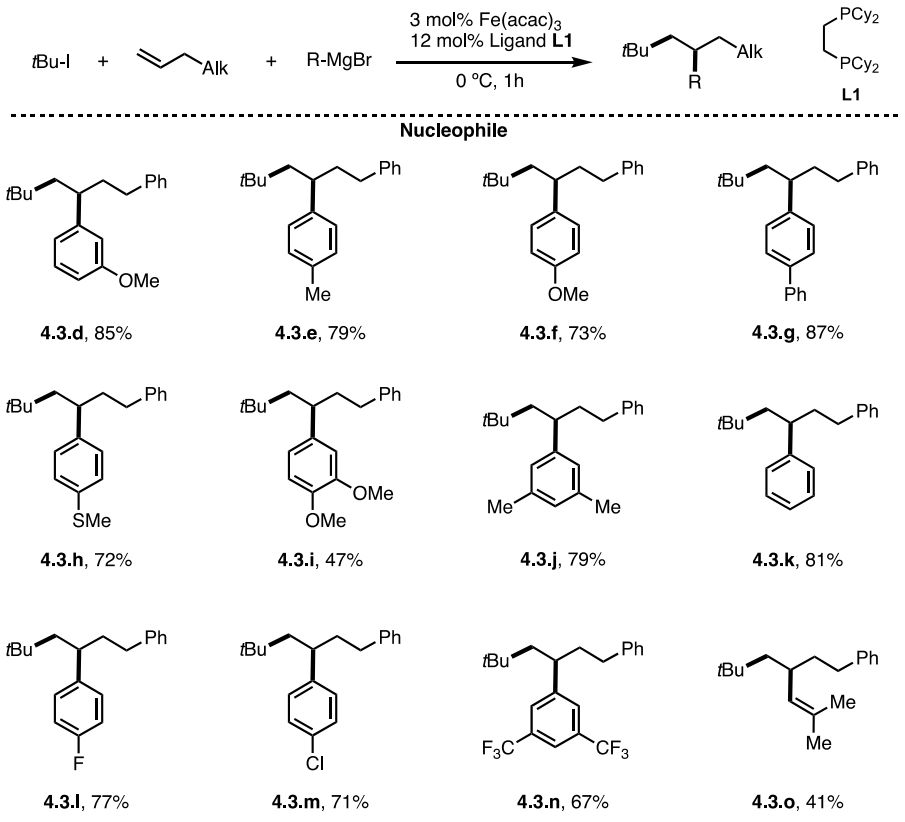

Figure 4.3. Scope of the Grignard nucleophile in the 3-component dicarbofuntionalization with unactivated alkenes.

4.3.o in 41% yield. This represents the first example of transition-metal catalyzed 1,2-alkylvinyl functionalization of unactivated olefins. Unfortunately, sterically hindered Grignard reagents are not compatible reagents in this transformation, presumably due to the high energy required to undergo inner-sphere reductive elimination.[11,12]

4.4 Scope of Alkenes

Next, we explored the olefin scope using tert-butyl iodide **4.3.a** and *meta*-methoxy phenyl Grignard **4.3.c** as dicarbofunctionalization partners (**Figure 4.4**). In

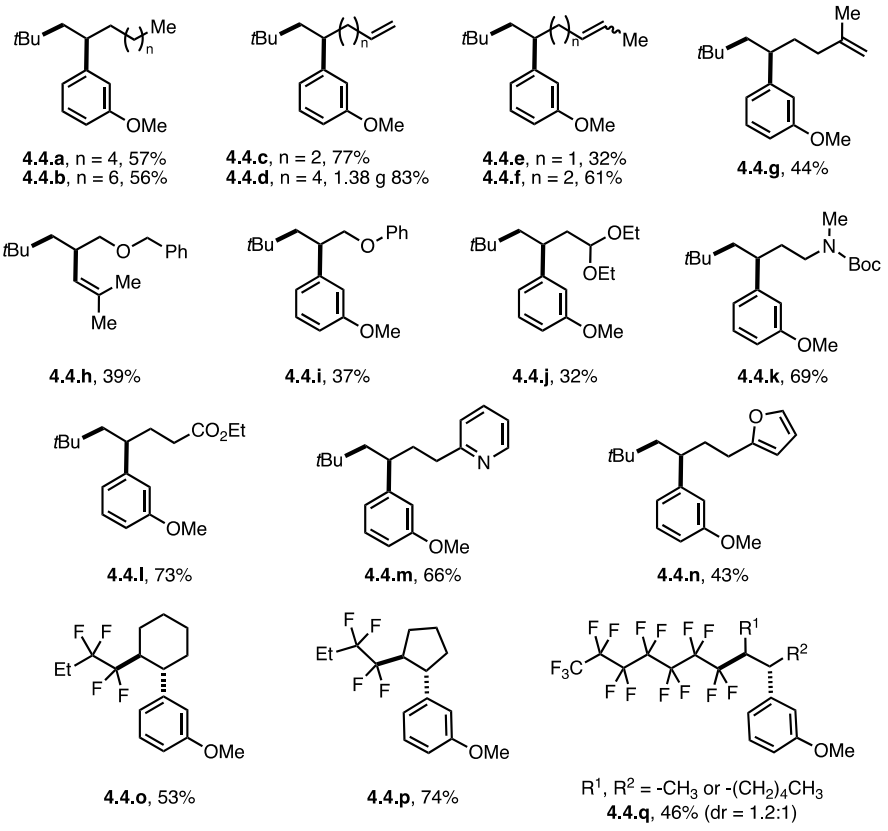

Figure 4.4. Scope of alkenes in the reaction.

general, a wide range of unactivated olefinic partners were tolerated. Compatible partners include olefins with tethered aliphatic chains, alkenes, alkoxy, protected alcohols, aldehydes and amines, esters, and even pyridine and furan moieties producing

the desired products in 32–83% yield (**4.4.a**–**4.4.n**). Importantly, this Fe-catalyzed three-component method provides unique reactivity with dienes. In particular, we found that the method is highly chemo- and regioselective for monofunctionalization

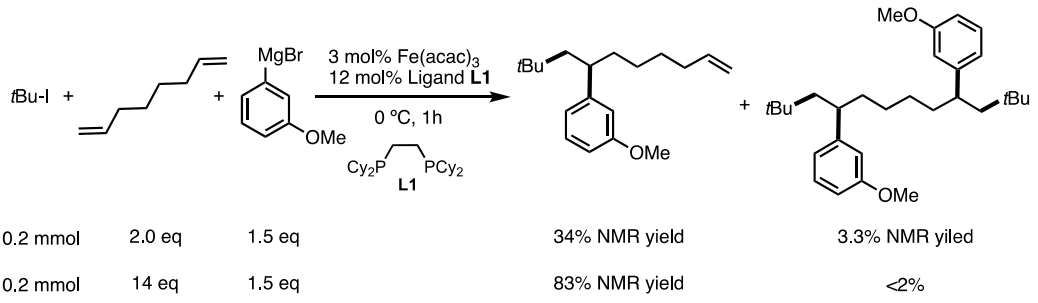

Figure 4.5. The selectivity for monofunctionalization of diene.

of less substituted alkenes (**4.4.e** – **4.4.g**) even at lower concentrations of alkenes (**Figure 4.5**). To showcase the practical application of this method, we also scaled up the reaction that formed the monofunctionalized product **4.4.d** in 83% yield (1.38 g). Furthermore, we also found that the per-fluororated n-alkyl bromides were competent partners with unactivated cyclic alkenes (**4.4.o** and **4.4.p**) yielding the desired products as single diastereoisomers in 53% and 74% yield. For aliphatic chain internal alkene (**4.4.q**) using the per-fluororated n-alkyl radical, we obtained the desired products as a mixture of diastereomers (dr = 1.2 : 1) in 46% yield.

4.5 Scope of Alkenes and Alkyl Halides

As shown in **Figure 4.6**, contrary to current state-of-the-art transition metal-catalyzed three-component dicarbofunctionalization, this method tolerates a range of

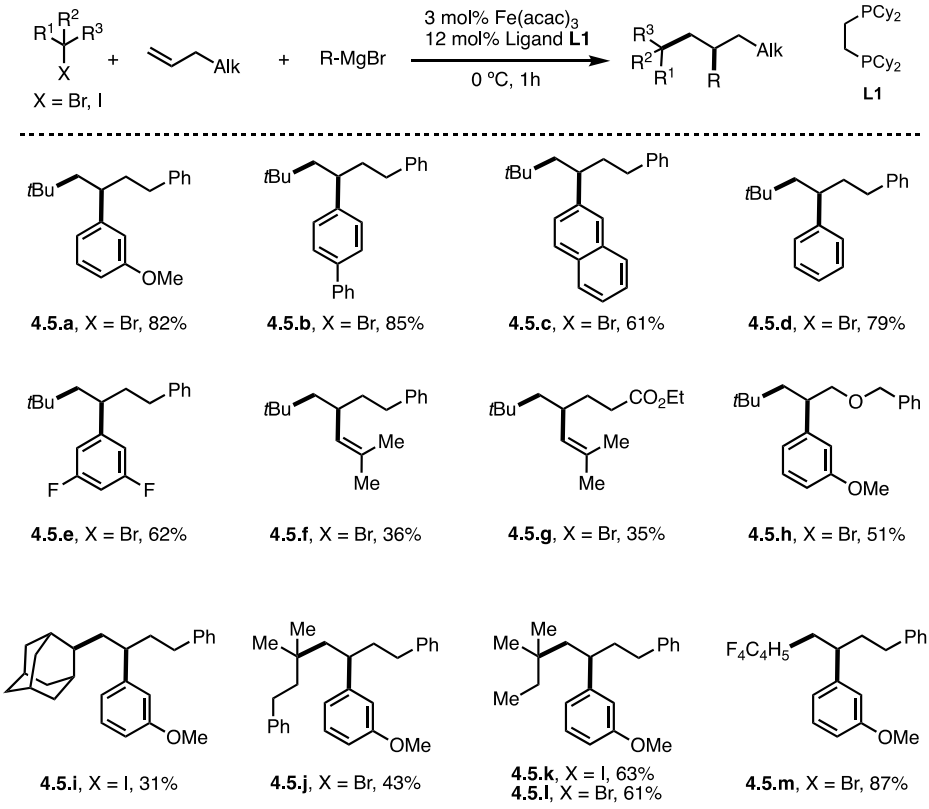

Figure 4.6. Scope of alkenes in the reaction.

diverse radical precursors and operates under short reaction times and at low temperatures. Specifically, tertiary alkyl bromides also form the desired 1,2-alkylaryl products **4.5.a** – **4.5.h** with similar efficiency to alkyl iodides. These results represent the first examples of using alkyl bromides in a transition metal-catalyzed 3-component intermolecular 1,2-alkylarylation of unactivated olefins and can complement existing methods using reductive cross-couplings as reported by Nevado.[5] Furthermore, other tertiary alkyl iodides/bromides are compatible in this transformation yielding the desired products **4.5.i** – **4.5.l** in 31–63% yield. Finally, consistent with our hypothesis

(**Figure 4.2**), we also found that perfluororated n-alkyl radicals (much more reactive towards Giese addition to alkenes)[18] were competent in this Fe-catalyzed three-component dicarbofunctionalization reaction yielding the desired products **4.5.m** in

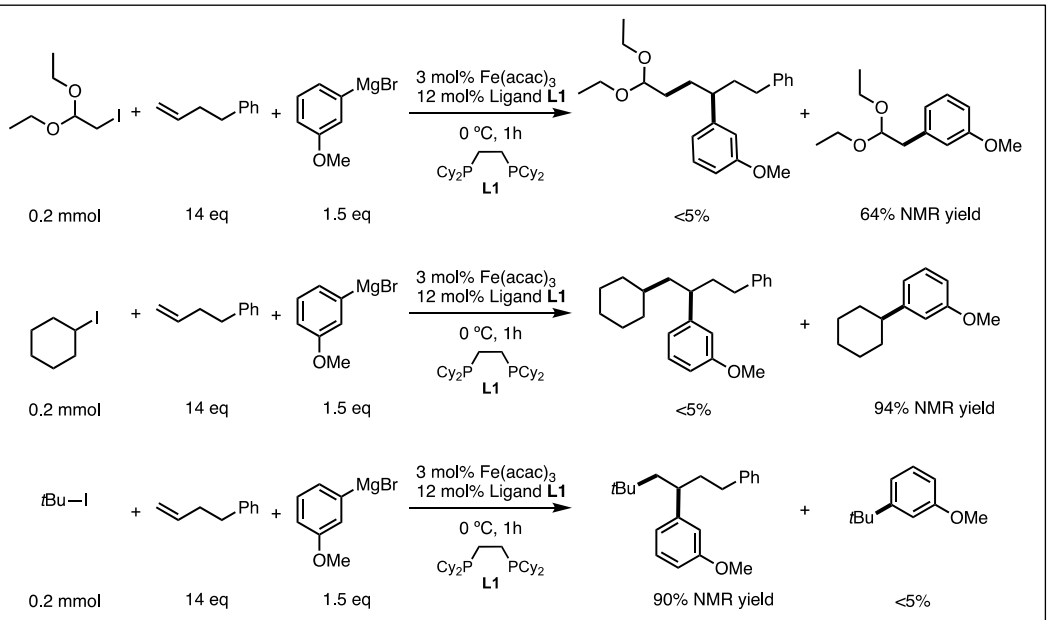

Figure 4.7. Comparison of 1,2-alkylarylation and direct arylation.

87% yield. Unfortunately, other primary and secondary alkyl halides are not compatible in this transformation due to the competing direct cross-coupling formation (**Figure 4.7**).

4.6 Radical Cascade Cyclization/Arylation

To expand the synthetic utility of this Fe-catalyzed three-component dicarbofunctionalization, we next explored the possibility of performing a radical cascade cyclization/arylation with a series of 1,6-dienes leading to the formation of three carbon–carbon bonds in one synthetic step (**Figure 4.8**). We hypothesize that regioselective Giese addition to the olefin will form the secondary alkyl radical intermediate **G•**. If the rates of Fe-arylation are slower than the rate of ring-closure,

then we should only observe the ring-closed arylated product (i.e., **58**). However, if the rate for Fe-arylation of **G•** is faster than the rate for Fe-arylation of radical 5-exo-trig,

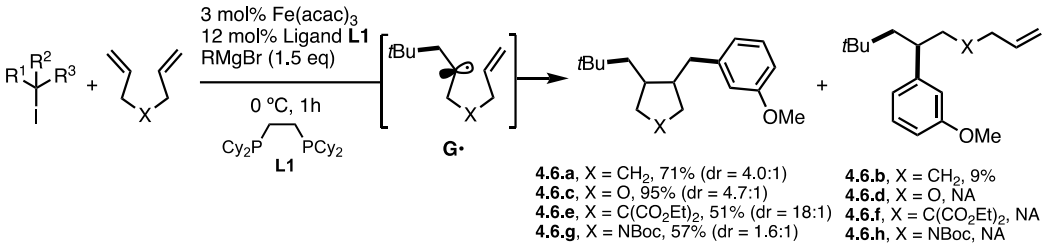

Figure 4.8. Radical cascade cyclization/arylation.

then we should observe only the uncyclized product (i.e., **4.6.b**). As shown in **Figure 4.8**, we found that this method delivered the desired carbocycle **4.6.a** in good yield (71%). We also observed the uncyclized product **4.6.b**, presumably from direct arylation of **G•**, albeit in low yield (9%). Notably, incorporation of heteroatoms (O or N) or addition of diester linkage results in exclusive formation of the cyclic product. Specifically, we found the desired formation of alkyl-aryl tetrahydrofuran **4.6.c**, di-ester substituted carbocycle **4.6.e**, and pyrrolidine **4.6.g** in good to excellent yield (51–95%) and without the formation of the uncyclized product. DFT calculations [UPBEPBE-D3/6-311+G(d,p)-CPCM(THF)//UB3LYP/6-31G(d)] using the *t*Bu radical and 1,6-heptadiene predict a barrier of 13.2 kcal mol^{-1} for irreversible Giese addition leading to **G•**, 5.2 kcal mol^{-1} downhill in energy. In agreement with the experiment, **G•** preferentially favors radical cyclization leading to a cis isomer, while (irreversible) radical cyclization leading to a trans isomer is only 1.2 kcal mol^{-1} higher in energy (**Figure 4.9A**). However, consistent with the experiment, the rates for radical cyclization for X=O substituted diene are faster and the energy difference between cis and trans radical cyclization is much higher (1.7 kcal mol; **Figure 4.9B**). However, at

this stage, we cannot rule out alternative mechanistic pathways such as olefin

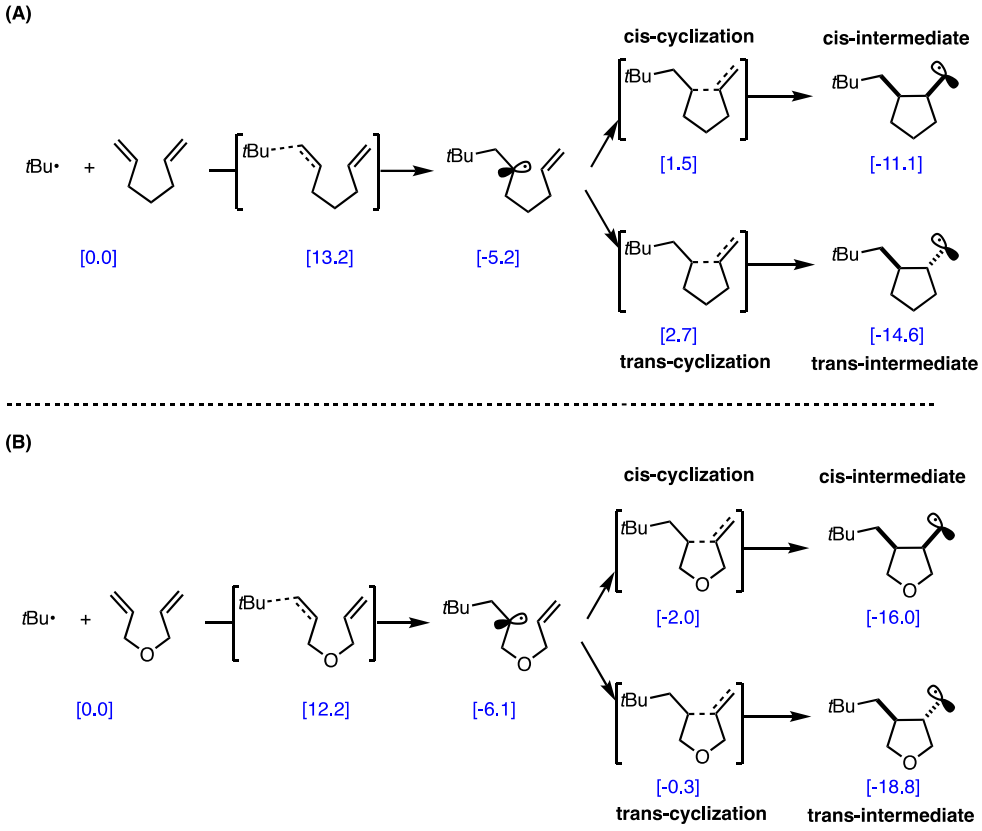

Figure 4.9. Calculation of radical addition and cyclization steps of 1,6-heptadiene vs 1-propenyl ether. ΔG (kcal/mol; 298 K).

coordination to the metal center preceding alkyl radical addition or 1,2-migratory insertion of the iron-aryl into the alkene. Future work on elucidating the mechanism of this transformation is ongoing and will be reported in due course. Given the prevalence of saturated heterocyclic compounds (tetrahydrofurans and pyrrolidines) in pharmaceuticals, we used an oxygensubstituted diene as a model compound to explore the reaction scope of this Fe-catalyzed three-component radical cascade cyclization/arylation. As shown in **Figure 4.10**, this reaction is very robust with aryl Grignard nucleophiles forming the desired products in excellent yields, and the cis-isomer is the major product. The use of sterically hindered, heteroaryl or vinyl

nucleophiles was also tolerated (**4.6.k** – **4.6.n**). Moreover, other tertiary alkyl iodides and per-fluorinated alkyl and tertiary bromides also work in this transformation

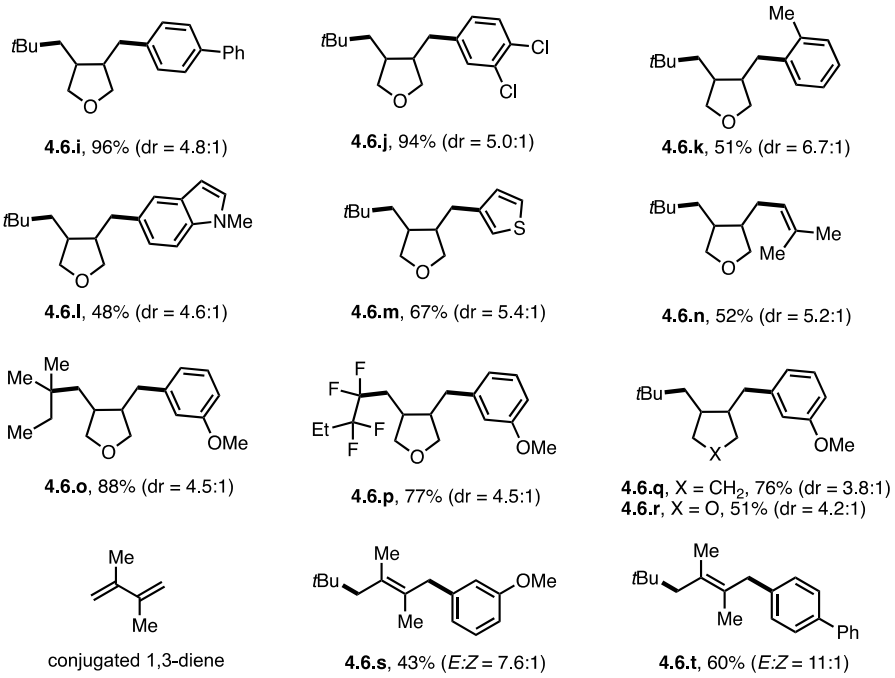

Figure 4.10. Scope of the Radical cascade cyclization/arylation.

forming the radical cascade cyclization/arylation products **4.6.o** – **4.6.r** in 51–88% yield. Finally, the method is regioselective for addition to conjugated 1,3-diene to form 1,4-alkylaryl products **4.6.s** – **4.6.t** in good yield (up to 11 : 1 *E* : *Z*, **Figure 10**).

4.7 Summary

In summary, we have developed a three-component 1,2-alkylarylation of unactivated olefins using bisphosphine iron as the catalyst. Further, we demonstrated that this protocol can forge three carbon–carbon bonds in one synthetic step leading to a diverse set of carbo- and heterocyclic compounds. We expect that this method will be adapted by the pharmaceutical community for the synthesis of bioactive products,

fine chemicals, and late-stage diversification of promising leads. Although this method is currently limited to the use of a large excess of olefins, preliminary experiments show that the use of activated alkenes could circumvent the need for excess alkenes, and this will be reported in **Chapter 5**. Future work is ongoing to elucidate the mechanism of this transformation using computational, experimental, and spectroscopic tools. We actively pursued other three-component Fe-catalyzed reactions with other π-acceptors, nucleophiles, and electrophiles including asymmetric variants and will report in the following chapters.

4.8 References

(1) For representative reviews on alkene functionalization, see: (a) Saini, V.; Stokes, B. J.; Sigman, M. S. *Angew. Chem., Int. Ed*. **2013**, *52*, 11206−11220; (b) Coombs, J. R.; Morken, J. P. *Angew. Chem., Int. Ed*. **2016**, *55*, 2636−2649.

(2) For representative reviews on dicarbofunctionalization of alkenes, see: (a) Derosa, J.; Tran, V. T.; van der Puyl, V. A.; Engle, K. M., *Aldrichimica Acta*. **2018**, *51*, 21−32; (b) Giri, R.; Kc, S. *J. Org. Chem*. **2018**, *83*, 3013−3022.

(3) For some examples leading to dicarbofunctionalization of alkenes, see: (a) Liao, L.; Jana, R.; Urkalan, K. B.; Sigman, M. S. *J. Am. Chem. Soc*. **2011**, *133*, 5784−5787; (b) Qin, T.; Cornella, J.; Li, C.; Malins, L. R.; Edwards, J. T.; Kawamura, S.; Maxwell, B. D.; Eastgate, M. D.; Baran, P. S. *Science*, **2016**, *352*, 801−805; (c) García-Domínguez, A.; Li, Z.; Nevado, C. *J. Am. Chem. Soc*. **2017**, *139*, 6835−6838; (d) Kc, S.; Dhungana, R. K.; Shrestha, B.; Thapa, S.; Khanal, N.; Basnet, P.; Lebrun, R. W.; Giri, R. *J. Am. Chem. Soc*. **2018**, *140*,

9801−9805; (e) Gao, P.; Chen, L. A.; Brown, M. K, *J. Am. Chem. Soc*. **2018**, *140*, 10653−10657; (f) Chierchia, M.; Xu, P.; Lovinger, G. J.; Morken, J. P. *Angew. Chem., Int. Ed.* **2019**, *58*, 14245−14249; (g) Campbell, M. W.; Compton, J. S.; Kelly, C. B.; Molander, G. A. *J. Am. Chem. Soc*. **2019**, *141*, 20069−20078; (h) Mega, R. S.; Duong, V. K.; Noble, A.; Aggarwal, V. K. *Angew. Chem., Int. Ed*. **2020**, *59*, 4375−4379; (i) Sun, S. Z.; Duan, Y.; Mega, R. S.; Somerville, R. J.; Martin, R. *Angew. Chem., Int. Ed*. **2020**, *59*, 4370−4374; (j) Kc, S.; Dhungana, R. K.; Khanal, N.; Giri, R. *Angew. Chem., Int. Ed*., **2020**, 59, 8047−8051.

(4) For recent examples using directing groups, see: (a) Derosa, J.; Kang, T.; Tran, V. T.; Wisniewski, S. R.; Karunananda, M. K.; Jankins, T. C.; Xu, K. L.; Engle, K. M. *Angew. Chem., Int. Ed.* **2020**, *59*, 1201−1205; (b) Yang, T.; Chen, X.; Rao, W.; Koh, M. J. *Chem*, **2020**, *6*, 738−751.

(5) Shu, W.; García-Domínguez, A.; Quirós, M. T.; Mondal, R.; Cárdenas, D. J.; Nevado, C. *J. Am. Chem. Soc*., **2019**, *141*, 13812−13821.

(6) For a recent review, see: Piontek, A.; Bisz, E.; Szostak, M. *Angew. Chem., Int. Ed*. **2018**, *57*, 11116−11128.

(7) (a) Sun, C. L.; Krause, H.; Fürstner, A. *Adv. Synth. Catal*., **2014**, *356*, 1281−1291; (b) Hatakeyama, T.; Okada, Y.; Yoshimoto, Y.; Nakamura, M. *Angew. Chem., Int. Ed.* **2011**, *50*, 10973−10976; (c) Dongol, K. G.; Koh, H.; Sau, M.; Chai, C. L. *Adv. Synth. Catal*. **2007**, *349*, 1015−1018.

(8) (a) Toriyama, F.; Cornella, J.; Wimmer, L.; Chen, T. G.; Dixon, D. D.; Creech, G.; Baran, P. S. *J. Am. Chem. Soc*. **2016**, *138*, 11132−11135; (b) Lo, J. C.; Kim,

D.; Pan, C. M.; Edwards, J. T.; Yabe, Y.; Gui, J.; Qin, T.; Gutierrez, S.; Giacoboni, J.; Smith, M. W.; Holland, P. L.; Baran, P. S. *J. Am. Chem. Soc*., **2017**, 139, 2484−2503; (c) Bedford, R. B.; Carter, E.; Cogswell, P. M.; Gower, N. J.; Haddow, M. F.; Harvey, J. N.; Murphy, D. M.; Neeve, E. C.; Nunn, J. *Angew. Chem., Int. Ed*. **2013**, *52*, 1285−1288; (d) Adams, C. J.; Bedford, R. B.; Carter, E.; Gower, N. J.; Haddow, M. F.; Harvey, J. N.; Huwe, M.; Cartes, M. A.; Mansell, S. M.; Mendoza, C.; Murphy, D. M.; Neeve, E. C.; Nunn, J. *J. Am. Chem. Soc*. **2012**, *134*, 10333−10336; (e) Hatakeyama, T.; Kondo, Y.; Fujiwara, Y. I.; Takaya, H.; Ito, S.; Nakamura, E.; Nakamura, M. *Chem. Commun*. **2009**, 1216−1218; (f) Bedford, R. B.; Huwe, M.; Wilkinson, M. C. *Chem. Commun*. **2009**, 600−602.

(9) (a) Nakagawa, N.; Hatakeyama, T.; Nakamura, M. *Chem. Lett*. **2015**, *44*, 486−488; (b) Hatakeyama, T.; Hashimoto, T.; Kathriarachchi, K. K. A. D. S.; Zenmyo, T.; Seike, H.; Nakamura, M. *Angew. Chem., Int. Ed*., **2012**, *51*, 8834−8837; (c) Hashimoto, T.; Hatakeyama, T.; Nakamura, M. *J. Org. Chem*. **2011**, *77*, 1168−1173; (d) Hatakeyama, T.; Hashimoto, T.; Kondo, Y.; Fujiwara, Y.; Seike, H.; Takaya, H.; Tamada, Y.; Ono, T.; Nakamura, M. *J. Am. Chem. Soc*. **2010**, *132*, 10674−10676.

(10) Mako, T. L.; Byers, J. A. *Inorg. Chem. Front*. **2016**, *3*, 766−790.

(11) Jin, M.; Adak, L.; Nakamura, M. *J. Am. Chem. Soc*., **2015**, *137*, 7128−7134.

(12) Lee, W.; Zhou, J.; Gutierrez, O. *J. Am. Chem. Soc*. **2017**, *139*, 16126−16133.

(13) Sharma, A. K.; Sameera, W. M. C.; Jin, M.; Adak, L.; Okuzono, C.; Iwamoto, T.; Kato, M.; Nakamura, M.; Morokuma, K. *J. Am. Chem. Soc*., **2017**, *139*, 16117−16125.

(14) (a) Liu, L.; Lee, W.; Yuan, M.; Acha, C.; Geherty, M. B.; Williams, B.; Gutierrez, O. *Chem. Sci*. **2020**, *11*, 3146−3151; (b) Liu, L.; Lee, W.; Zhou, J.; Bandyopadhyay, S.; Gutierrez, O. *Tetrahedron*, **2019**, *75*, 129−136.

(15) Zhang, Z. Q.; Meng, X. Y.; Sheng, J.; Lan, Q.; Wang, X. S. *Org. Lett*. **2019**, *21*, 8256−8260.

(16) Leifert, D.; Studer, A. *Angew. Chem., Int. Ed*. **2020**, *59*, 74−108.

(17) (a) Neidig, M. L.; Carpenter, S. H.; Curran, D. J.; DeMuth, J. C.; Fleischauer, V. E.; Iannuzzi, T. E.; Neate, P. G. N.; Sears, J. D.; Wolford, N. J. *Acc. Chem. Res*. **2019**, *52*, 140−150; (b) Sears, J. D.; Neate, P. G.; Neidig, M. L. *J. Am. Chem. Soc*. **2018**, *140*, 11872−11883; (c) Liu, L.; Lee, W.; Yuan, M.; Gutierrez, O. *Comments Inorg. Chem*. **2018**, *38*, 210−237.

(18) Avila, D. V.; Ingold, K. U.; Lusztyk, J.; Dolbier, W. R.; Pan, H. Q. *J. Am. Chem. Soc*. **1993**, *115*, 1577−1579.

Chapter 5: General Method for Multicomponent Radical Cascades/Cross-Couplings Enabled by Iron Catalysis

Excerpts from this chapter were submitted and the article is under review.

5.1 Organoboron Compounds in Organic Synthesis

Organoboron compounds are valuable and highly versatile reagents widely used in modern organic synthesis.[1] In particular, the inherent stability, ease of handling, and commercial accessibility of structurally-diverse organoboron compounds have established these reagents as the workhorse in 2-electron transition metal-catalyzed cross-coupling reactions (e.g., Pd catalysis) and constitutes one of the top five most used reactions in drug discovery for the construction of C-C bonds.[2] In the last decade, significant efforts in the area of photoredox catalysis have expanded the utility of alkyl organoboron compounds as versatile radical precursors for numerous transformations.[3] More recently, vinyl organoboron reagents have been used as effective lynchpins in three-component nickel(photoredox)-catalyzed cross-coupling reactions leading to valuable and versatile alkyl boryl scaffolds prime for further functionalization.4 Despite these efforts, the equivalent iron-catalyzed transformation remains highly desirable in pharmaceutical research due to iron's low cost, abundance, and potential for new and complementary modes of reactivity to existing catalytic methods.

5.2 The Expand Reaction Scope of Multicomponent Fe-Catalyzed Cross-Couplings

Fe-catalyzed cross-couplings has enabled the union of diverse carbon-centered radicals and organometallic partners (**Figure 5.1A**). However, while organoboron reagents have found utility in Fe-catalyzed two-component cross-couplings (i.e.,

Suzuki-Miyaura), the use of iron catalysts in multi-component cross-couplings with organoboron reagents remains an elusive transformation (**Figure 5.1B**).[5,6,7,8] Herein we

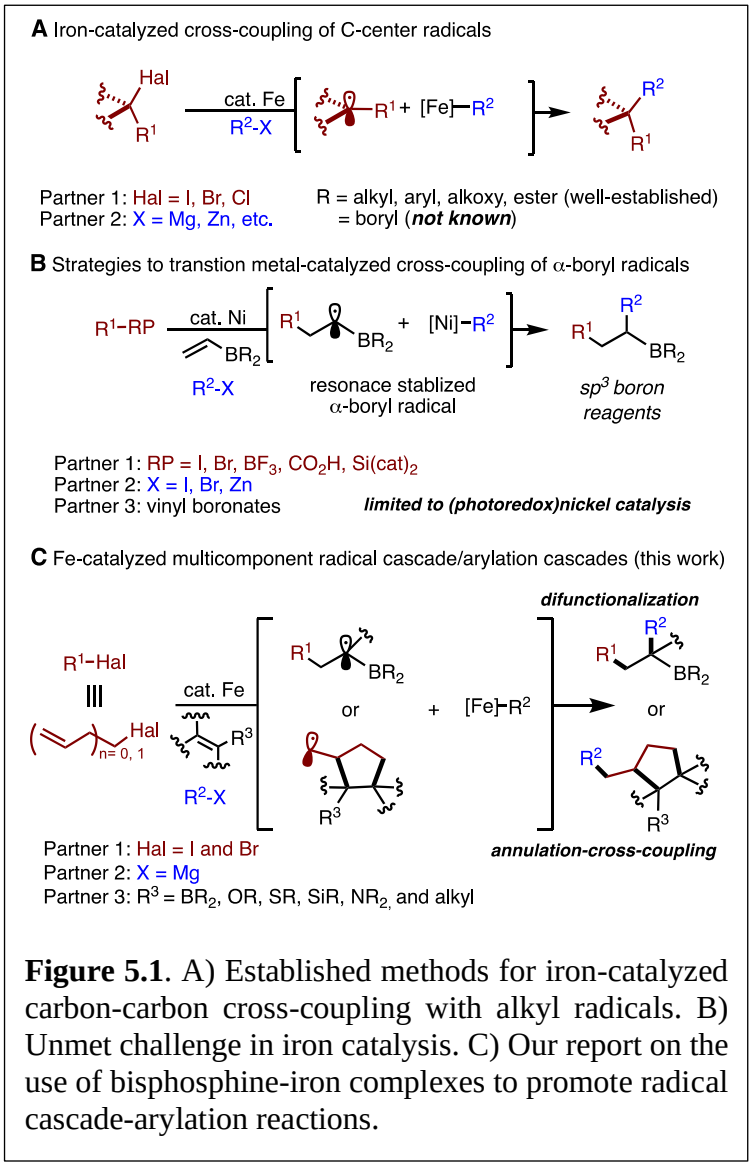

Figure 5.1. A) Established methods for iron-catalyzed carbon-carbon cross-coupling with alkyl radicals. B) Unmet challenge in iron catalysis. C) Our report on the use of bisphosphine-iron complexes to promote radical cascade-arylation reactions.

report the successful realization of Fe-catalyzed cross-coupling of α-boryl radicals, generated from selective radical addition to vinyl boronates, and organometallic reagents to form the desired dicarbofunctionalized (DCF) compounds (**Figure 5.1C**). Further, to address a long-standing challenge in multicomponent cross-couplings, we report a general Fe-catalyzed multicomponent annulation-arylation (MAC) protocol that facilitates the practical synthesis of previously difficult-to-make

tetrafluoroethylene-containing carbocycles and derivatives.[9] Finally, DFT and radical probes, shed light into the mechanism of this transformation. More broadly, this work provides a blueprint to expand the reaction scope of multicomponent Fe-catalyzed cross-couplings and, in particular, intermolecular annulation-arylation reactions with broad applications to the practical and large scale synthesis of pharmaceuticals, agrochemicals, pesticides, and materials.

5.3 Reaction Optimization

Based on recent multicomponent radical cross-couplings,[10,11] we hypothesized that electron-deficient nature of vinyl boronates and the rapid kinetics of observed for Fe-catalyzed Kumada cross-couplings could be coupled to engage transient α-boryl radicals in selective three-component radical cross-couplings. If successful, this radical cascade could lead to rapid construction of complex molecular structures and open new opportunities for sustainable synthesis of alkyl boron reagents for further synthetic manipulations.[12] In this vein, we first tested the proposed three-component radical cross-coupling using a sterically hindered alkyl halide under slow addition of aryl Grignard nucleophile to avoid competing two-component cross-coupling and biaryl formation. After extensive experimentation, we identified $FeCl_3$ (10 mol%) in combination with 1,2-bis(dicyclohexylphosphino)ethane **L1** (20 mol%) as an effective catalytic system that engages α-boryl radicals, presumably from regioselective Giese

addition of tert-butyl radical to vinyl boronate **2a** (vide infra) to form the desired product **4a** in 90 % yield (entry 3, **Table 5.1**) and, in stark contrast to existing nickel systems, at low temperatures and exceeding fast reaction times (<1 hr). Precatalysts

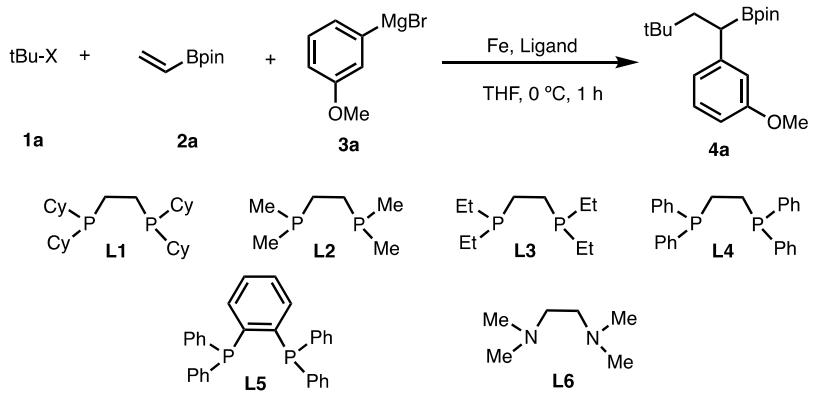

entry	X	Fe	Ligand	Fe/L (mol%)	yield (%)[a]
1	I	$Fe(acac)_3$	L1	10/20	77
2	I	$FeBr_2$	L1	10/20	80
3	I	$FeCl_3$	L1	10/20	90
4	I	$Fe(OTf)_2$	L1	10/20	27
5	I	$Fe(OAc)_2$	L1	10/20	36
6	I	$FeCl_2$	L1	10/20	80
7	I	$FeCl_3$	L2	10/20	< 5
8	I	$FeCl_3$	L3	10/20	< 5
9	I	$FeCl_3$	L4	10/20	7
10	I	$FeCl_3$	L5	10/20	28
11	I	$FeCl_3$	L6	10/20	34
12	I	$FeCl_3$	no ligand	30/0	< 5
13	I	no catalyst	no ligand	0/0	< 5
14	Br	$FeCl_3$	L1	10/20	89
15	Cl	$FeCl_3$	L1	10/20	12

Table 5.1. Reactions were carried out on a 0.20 mmol scale, Grignard addition for 1 h, 0.2 mL THF. a, Determined by crude 1H NMR with CH_2Br_2 as internal standard.

with weakly coordinating triflate or acetate groups diminished the efficiency of the system while halogen or acetyl acetone counterions had minor effect on the yields (entries 1-6). Notably, 1,2-bis(dicyclohexylphosphino)ethane **L1** is uniquely effective

in this radical cascade and all of the phosphine and amine ligands were less efficient (entries 6-11). Control experiments demonstrate that both the ligand and iron salt as crucial for the reaction (entries 12-13). Finally, in stark contrast to state-of-the-art (dual photoredox) Ni-catalyzed methods, both alkyl iodides and bromides also provide the desired product under these conditions (~90% yield) while diminished yields are observed with alkyl chlorides (entries 14-15).

5.4 Scope of DCF Reaction

Encouraged by these findings, we turned our attention to studying the generality of the three-component radical cascade transformation. As shown in **Figure 5.2**, we

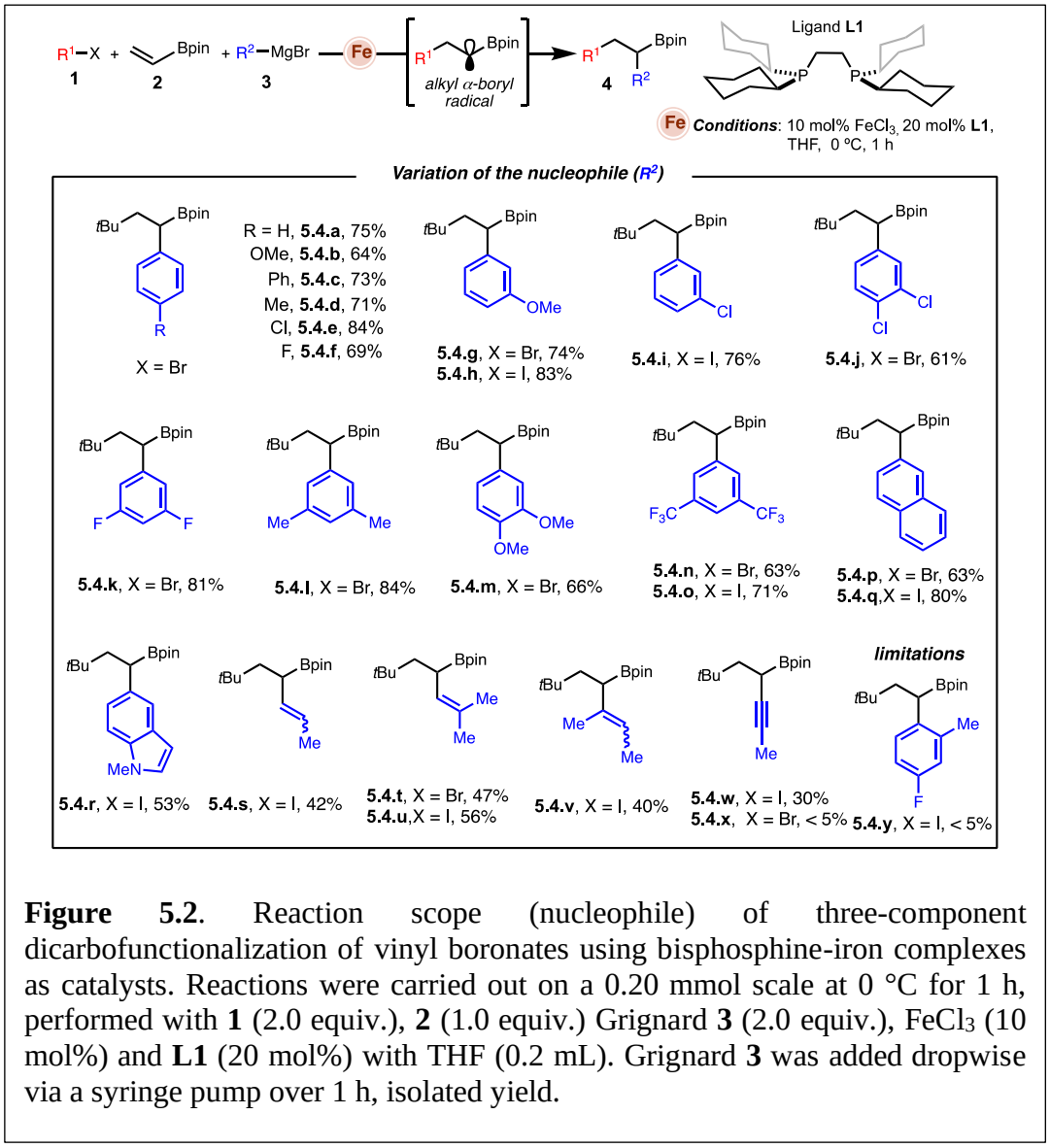

Figure 5.2. Reaction scope (nucleophile) of three-component dicarbofunctionalization of vinyl boronates using bisphosphine-iron complexes as catalysts. Reactions were carried out on a 0.20 mmol scale at 0 °C for 1 h, performed with **1** (2.0 equiv.), **2** (1.0 equiv.) Grignard **3** (2.0 equiv.), $FeCl_3$ (10 mol%) and **L1** (20 mol%) with THF (0.2 mL). Grignard **3** was added dropwise via a syringe pump over 1 h, isolated yield.

observed a wide range of organomagnesium compounds as suitable cross-coupling partners with alkyl α-boryl radicals. In particular, difunctionalization of vinyl boronates proceeded with good yields and excellent regioselectivity with mono- and disubstituted aryl Grignard nucleophiles that varied with electron density at the para- and meta position (**5.4.a** to **5.4.q**) and (hetero)aryls nucleophile (**5.4.r**). Further, in stark contrast

to nickel(photoredox)-catalytic systems, this protocol tolerates akenyl and alkynyl nucleophiles (**5.4.s** to **5.4.w**), albeit on average lower yields were observed for alkynyl nucleophiles in comparison to the aryl and vinyl counterparts. Unfortunately, ortho-substituted aryl Grignard reagents were less efficient presumably due to increase steric demand (**5.4.y**). Having established the reactivity with sp- and sp^2-hybridized Grignard nucleophiles, we next probed the alkyl halide scope (**Figure 5.3**). In the tertiary alkyl

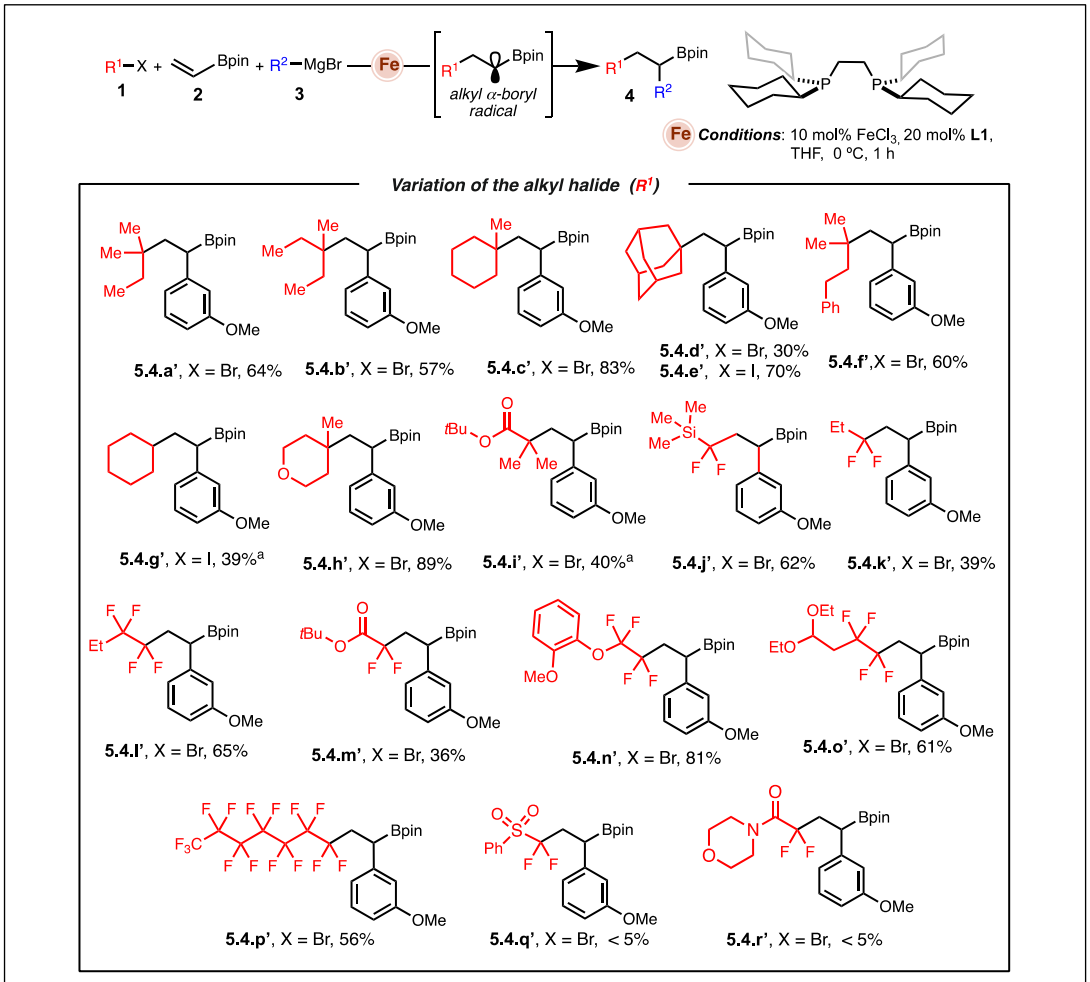

Figure 5.3. Reaction scope (alkyl halide) of three-component dicarbofunctionalization of vinyl boronates using bisphosphine-iron complexes as catalysts. Reactions were carried out on a 0.20 mmol scale at 0 °C for 1 h, performed with **1** (2.0 equiv.), **2** (1.0 equiv.) Grignard **3** (2.0 equiv.), $FeCl_3$ (10 mol%) and **L1** (20 mol%) with THF (0.2 mL). Grignard **3** was added dropwise via a syringe pump over 1 h, isolated yield. a, **1** (5.0 equiv.), Grignard **3** (5.5 equiv.) and 3h.

scope, a range of acyclic and cyclic aliphatic electrophiles afforded the desired products with good yields (**5.4.a'** to **5.4.f'**). Notably, secondary alkyl systems (**5.4.g'**) and tertiary alkyl halides bearing aryl or heteroatoms also formed the desired products (**5.4.f'** and **5.4.h'**). Finally, we were pleased to identify tertiary α-bromo esters as competent substrates which formed the synthetically useful product **5.4.i'** bearing both an ester and alkyl boron as versatile synthetic handles for further diversification. Despite significant advances in the synthesis of organofluorinated compounds,[13] selective and catalytic C(sp^3)-CF_2R bond formation remains challenging[14] and is exceedingly rare in Fe-catalyzed cross-couplings.[15,16] Further, there are no reports of transition metal-catalyzed three-component radical dicarbofunctionalization of vinyl boron alkenes that engage fluoro-n-alkyl radical precursors.[17] Presumably, the higher reactivity towards Giese addition to alkene is also plagued by the inherent faster reactivity to undergo H-atom abstraction,[18] propensity to undergo single electron transfer (SET), defluorination, and competing two-component cross-coupling.[19] Seeking to expand the alkyl radical scope, we question whether this protocol could provide direct access to versatile fluorinated alkyl boron compounds. Gratifyingly, as shown in **Figure 5.3**, a wide range of fluoro alkyl radical precursors including those containing alkyl, ester, silyl, heteroaryl, phenoxy, perfluroalkyl, and protected aldehydes, are competent partners leading to the desired 1,2-alkylfluorinated-aryl organoboron products (**5.4.j'** to **5.4.p'**) in good to excellent yield. Owning to the unique properties of C-F bonds[20,21,22,23] coupled with the versatility of the C(sp^3)-B bond and practicality of this method, we anticipate that this method will lead to rapid access to

fluoro alkyl boron building blocks with numerous applications in pharmaceuticals, biology, materials, and agrochemistry.

5.5 Tuning Reaction to Form MAC Product

With the aim at expanding the applications of multicomponent radical cross-couplings, we turned our attention to alkyl halides with pendant alkenes as bifunctional coupling partners.[24] Despite the utility of radical-based cyclization cascades and transition-metal catalyzed intra-molecular cyclization-arylation in organic synthesis,[25] the analogous inter-molecular three-component radical cycloaddition-arylations are proven surprisingly elusive. Further while stitching of -CF_3, C_2F_5, and perfluoroalkyl alkyl groups in medicinal research is common, synthetic methods for incorporation of tetrafluoroethylene (-CF_2-CF_2-) moiety into cyclic compounds, especially for the formation of five-member carbocycles, remains virtually unknown. In addition, traditional protocols to incorporation -CF_2-CF_2- in carbocycles suffer from the use of hazardous tetrafluoroethylene gas (TFE) or hypervalent iodine reagents (e.g., Togni's reagent) thus preventing broad applications.[26] To solve this unmet need in chemical synthesis, we envisioned that commercially available and safe to handle tetrafluoroethylene alkyl bromide **1b** could serve as a general and practical lynchpin for the construction of previously hard-to-make tetrafluoroethylene containing carbocycles. Gratifyingly, similar conditions employed for three-component radical cross-coupling led to the multicomponent annulation/cross-coupling (MAC) product **5b** albeit low yields due to competitive formation of dicarbofunctionalization product **4b** (**Figure 5.4A**). Notably, after screening of conditions we found that by lowering the

iron concentration and changing the catalyst-to-ligand ratio we could shut down the

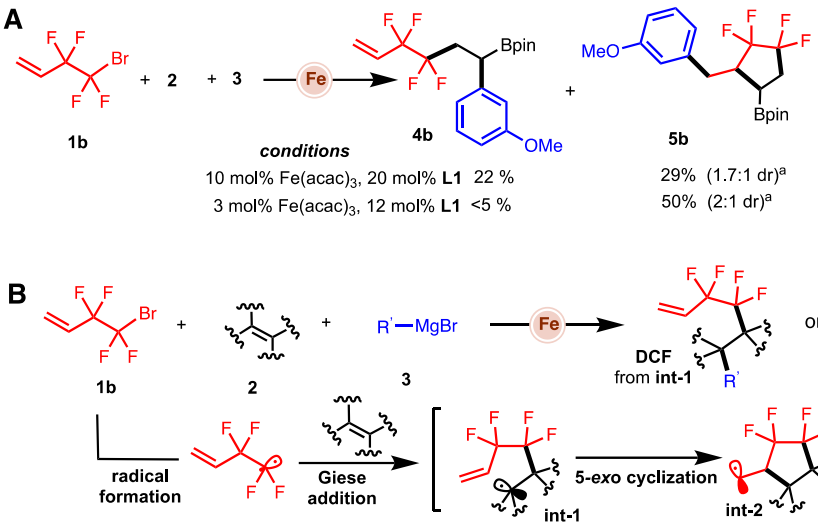

Figure 5.4. Lower concentration of iron increases the yield of the MAC product. Reactions were carried out on a 0.20 mmol scale at 0 °C for 1 h, performed with **1b** (1.0equiv.), **2** (1.5 equiv.) Grignard **3** (2.0 equiv.), $Fe(acac)_3$ (3 mol%) and **L1** (12 mol%) with THF (0.2 mL). Grignard **3** was added dropwise via a syringe pump over 1 h, isolated yield and dr.

dicarbofunctionalization pathway and increase yield of the MAC product **5b**. Presumably, lower catalyst concentration allows for more efficient 5-exo cyclization (vide infra) leading to **int-2** which in turn can undergo radical cross-coupling to form the MAC product (**Figure 5.4B**).

5.6 Scope of Alkenes in MAC Reaction

With optimized conditions in hand, we next turn to explore the generality of the Fe-MAC transformations with respect to alkene (**Figure 5.5**). Overall, a broad and impressive range of olefinic partners were found competent partners leading to tetrafluoroethylene containing drug-like scaffolds in one synthetic step. In particular, in addition to boron-substituted alkenes **5.6.a**, the list of suitable olefinic partners includes acyclic and cyclic alkenes bearing oxygen-, nitrogen-, sulfur-, and silicon

hetereoatoms. Specifically, cyclic vinyl silanes (**5.6.b**), ketene acetals (**5.6.c**), enols (**5.6.d**), thioenols (**5.6.e**). Further, we found that 4-, 5-, and 6-member (hetero)carbocycles bearing exo-cyclic alkenes (**5.6.f** – **5.6.h**) formed the

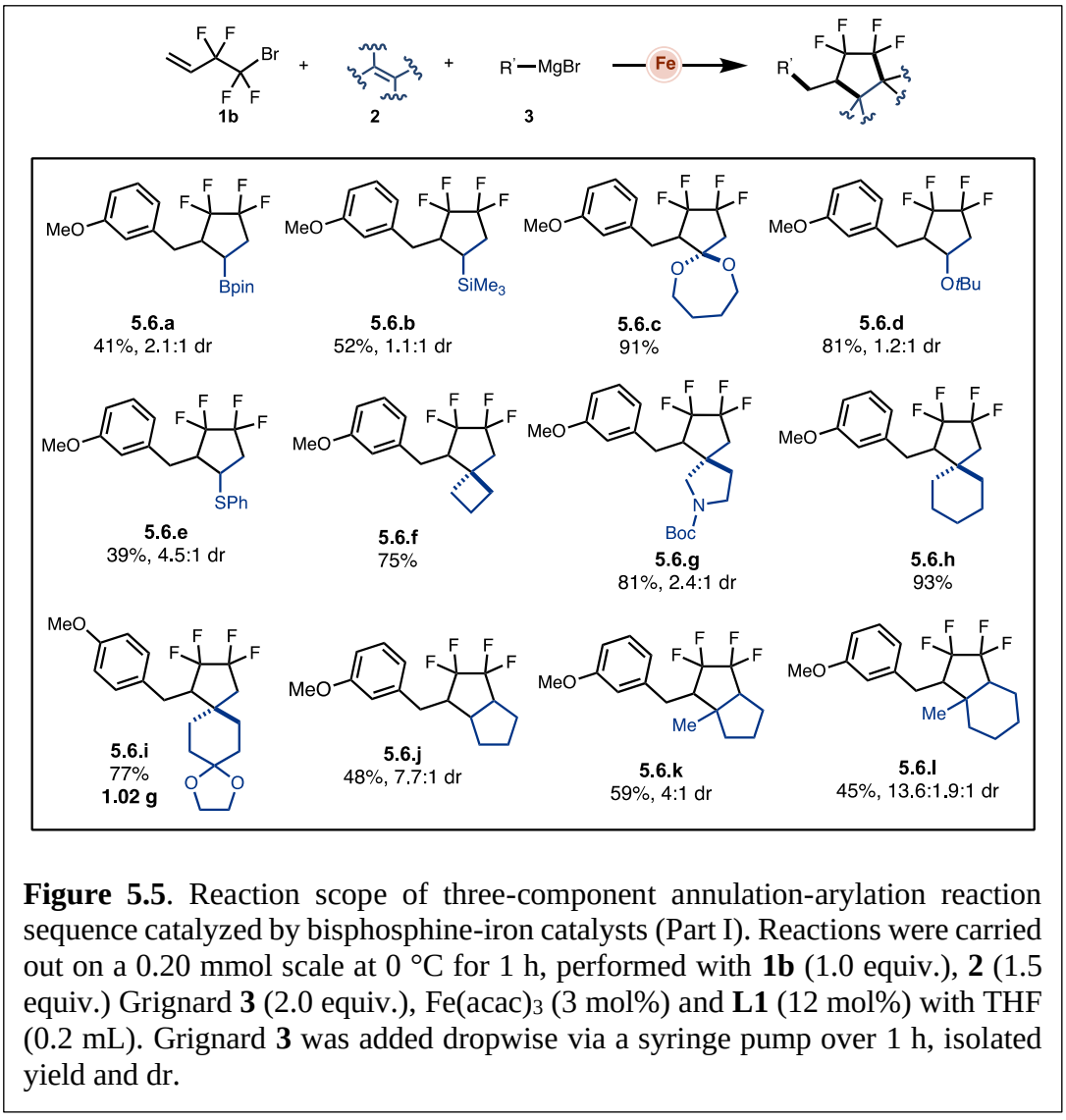

Figure 5.5. Reaction scope of three-component annulation-arylation reaction sequence catalyzed by bisphosphine-iron catalysts (Part I). Reactions were carried out on a 0.20 mmol scale at 0 °C for 1 h, performed with **1b** (1.0 equiv.), **2** (1.5 equiv.) Grignard **3** (2.0 equiv.), $Fe(acac)_3$ (3 mol%) and **L1** (12 mol%) with THF (0.2 mL). Grignard **3** was added dropwise via a syringe pump over 1 h, isolated yield and dr.

corresponding medicinally relevant arylated spirocyclic compounds in good to excellent yields (up to 93 % yield). In addition, this method allowed the gram scale synthesis of functional spirocyclic compound **5.6.i**, which is a derivative of sequosempervirin A, and fused bicyclic (hetero)cyclic structures using the corresponding di- and tri-substituted cyclic (hetero)alkenes with good yields and

modest to high regio- and diastereoselectivity (**5.6.j** – **5.6.l**). Notably, acyclic olefins bearing alkyl chains with pendant functional groups including aryl (**5.6.m**), primary chlorides (**5.6.n**), alkenes (**5.6.o**), unprotected alcohols (**5.6.p**) were also competent partners. Preliminary results also show that tetra-substituted alkenes and terminal

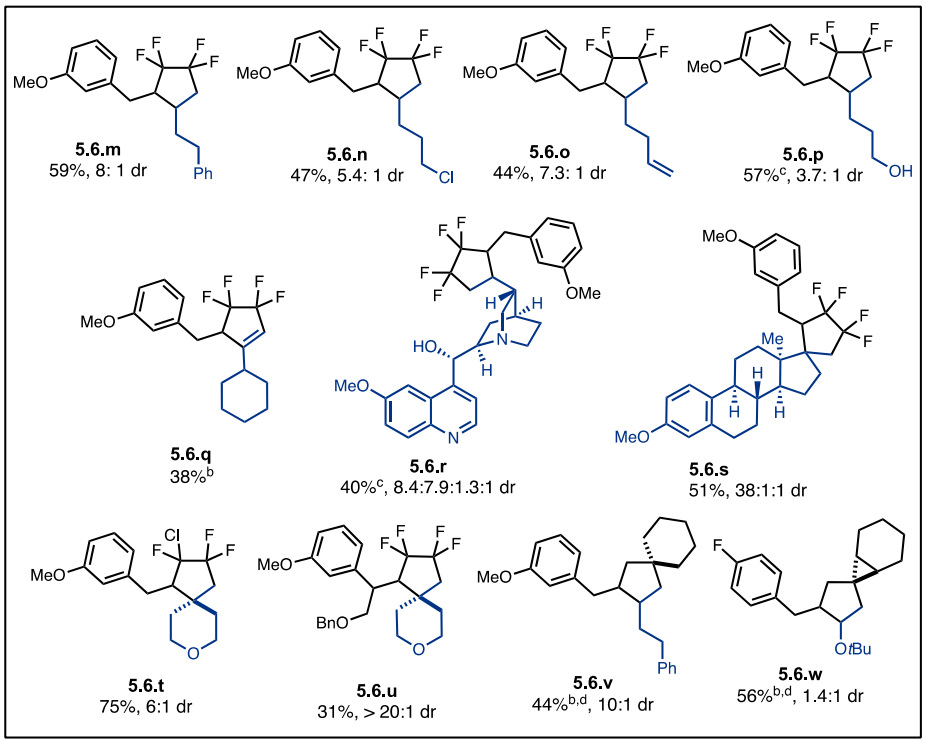

Figure 5.6. Reaction scope of three-component annulation-arylation reaction sequence catalyzed by bisphosphine-iron catalysts (Part II). b, Alkene or alkyne (14 equiv). c, Grignard 3 (3.0 equiv.). d, No additional solvent.

alkynes can participate in this radical annulation-arylation sequence yielding the desired annulation-arylation products (**5.6.q**) albeit lower yields. To demonstrate potential for late-stage modification of bioactive compounds, we applied this protocol to natural products bearing alkene groups that provided the desired products in good to excellent yields (**5.6.r** and **5.6.s**). We also explored the alkyl radical scope and found that other radical precursor can participate in the Fe-MAC transformation including alkyl bromides with C-Cl functionalities and alkyl substituted alkenes (**5.6.t** and **5.6.u**).

Finally, we also found that non-fluorinated tertiary alkyl halides bearing an allyl group also formed the desired product (**5.6.v** and **5.6.w**) by adding high equivalence (14 eq.) of alkene.

5.7 Scope of Nucleophiles in MAC Reaction

Having established a broad and general alkene scope in Fe-MACs, we next explored the reaction scope in terms of nucleophile (**Figure 5.7**). In general, we found

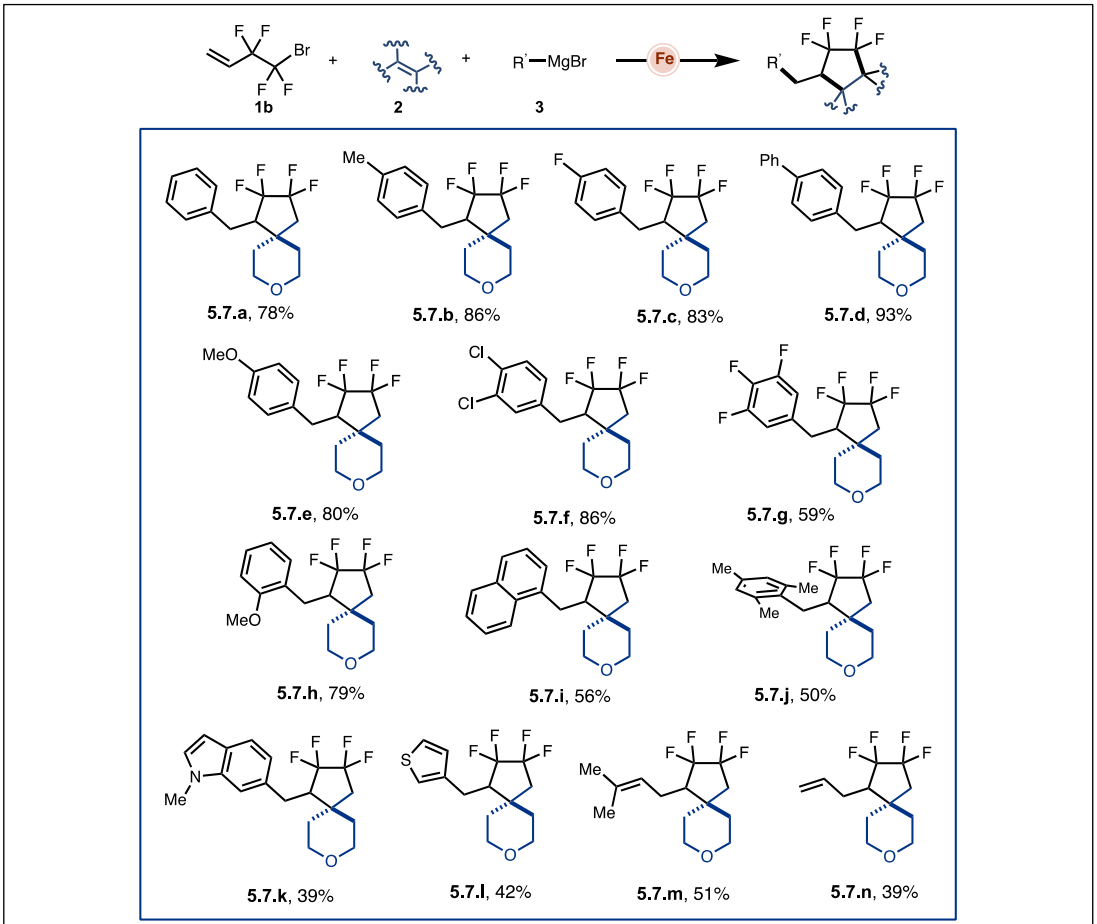

Figure 5.7. Reaction scope (nucleophile) of three-component annulation-arylation reaction sequence catalyzed by bisphosphine-iron catalysts. Reactions were carried out on a 0.20 mmol scale at 0 °C for 1 h, performed with **1b** (1.0 equiv.), **2** (1.5 equiv.) Grignard **3** (2.0 equiv.), $Fe(acac)_3$ (3 mol%) and **L1** (12 mol%) with THF (0.2 mL). Grignard **3** was added dropwise via a syringe pump over 1 h, isolated yield and dr.

that *para*-substituted electron rich and poor aryl Grignard reagents formed the desired products (**5.7.a** – **5.7.e**). In addition, we found good yields across the board with aryl magnesium nucleophiles bearing electron withdrawing groups (**5.7.f** and **5.7.g**), sterically hindered (*ortho*-substituted) systems (**5.7.h**, **5.7.i**, and **5.7.g**). Heteroaryls (**5.7.k** and **5.7.l**), and vinyl Grignard reagents (**5.7.m** and **5.7.n**) can also work. Given the generality of this Fe-catalyzed MAC transformation in terms of alkene and nucleophile scope, the use of inexpensive catalysts, readily accessible and non-toxic reagents, late-stage applications, and exceeding fast reaction times, we anticipate that this general method will accelerate the exploration of perfluoroethylated carbocycles in pharmaceutical, agrochemical, biology, and materials research.

5.8 Mechanistic Study by Experiment

To elucidate the mechanism of this multicomponent Fe-catalyzed cross-coupling, we combined computational and organic synthetic approach. First, using

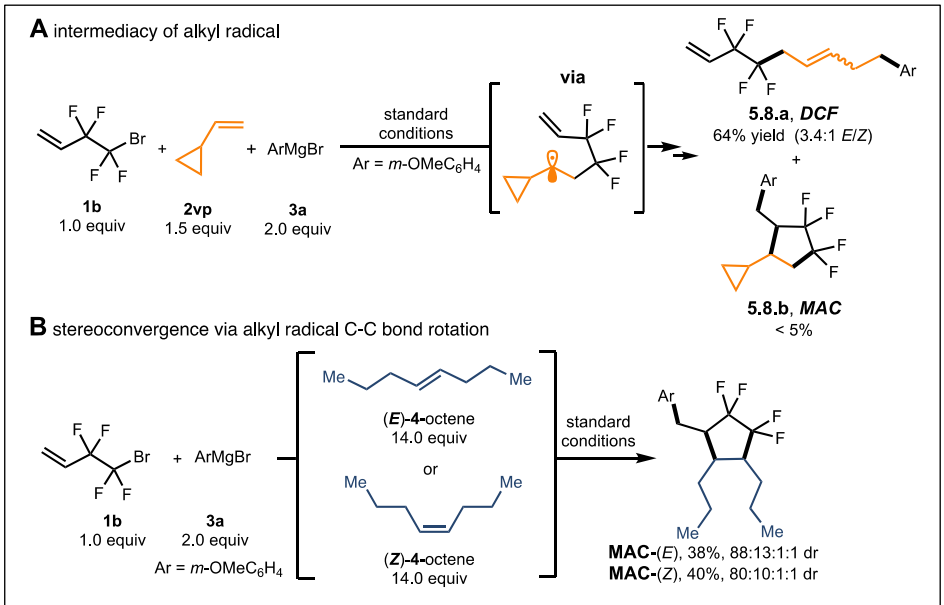

Figure 5.8. Experimental insights into the mechanism.

vinyl cyclopropane as radical probe **2vp** (**Figure 5.8A**), we observe the 1,5-dicarbofunctionalization **5.8.a** product and no MAC product **5.8.b** consistent with alkyl faster alkyl radical ring-opening ($k \sim 10^7\ s^{-1}$) than radical 5-exo cyclization ($k \sim 10^5\ s^{-1}$).[27] Second, consistent with the intermediacy of the alkyl radical, we also observed the stereoconvergence in the three-component Fe-MAC transformation leading to the same product outcome using either *E* or *Z* 4-octene, suggesting rapid equilibration (via sigma-bond rotation) prior to 5-exo radical cyclization/arylation (**Figure 5.8B**).

5.9 Mechanistic Study by Computation

Finally, to gain insight into the nature of carbon-carbon bond formation, we turn to broken symmetric DFT (BS-DFT) studies. Overall, the method is able to replicate both experimental structural and electronic parameters (**Figure 5.9**).

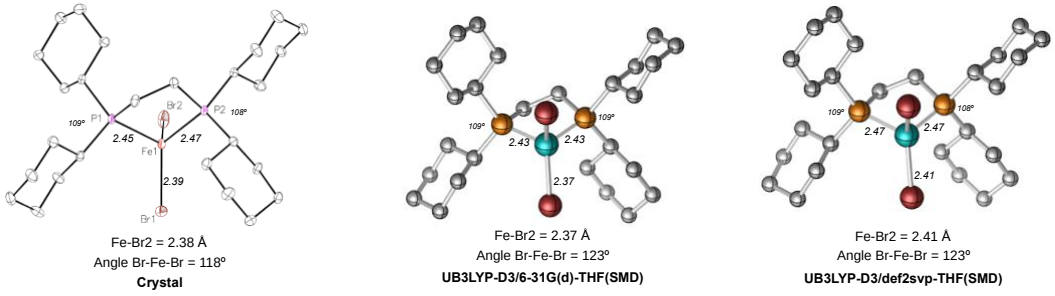

Figure 5.9. The justification of the selected computational method. The UB3LYP-D3/6-31G(d)-THF(SMD) and UB3LYP-D3/def2svp-THF(SMD) can closely predict the bond lengths and angles compared with the crystal structure as determined by Maria Camila Aguilera (Neidig group; Rochester University).

Consistent with these observations, DFT calculations supported radical formation from distorted square planar bisarylated Fe(II) species via halogen abstraction (barrier ~20 kcal/mol) leading to Fe(III) and tertiary radical. Notably, as shown in **Figure 5.10A**, we find that radical addition to vinyl boronate is fast (barrier is ~11 kcal/mol) and

irreversible leading to α-boryl radical R•. In turn, this radical can rapidly add (diffusion

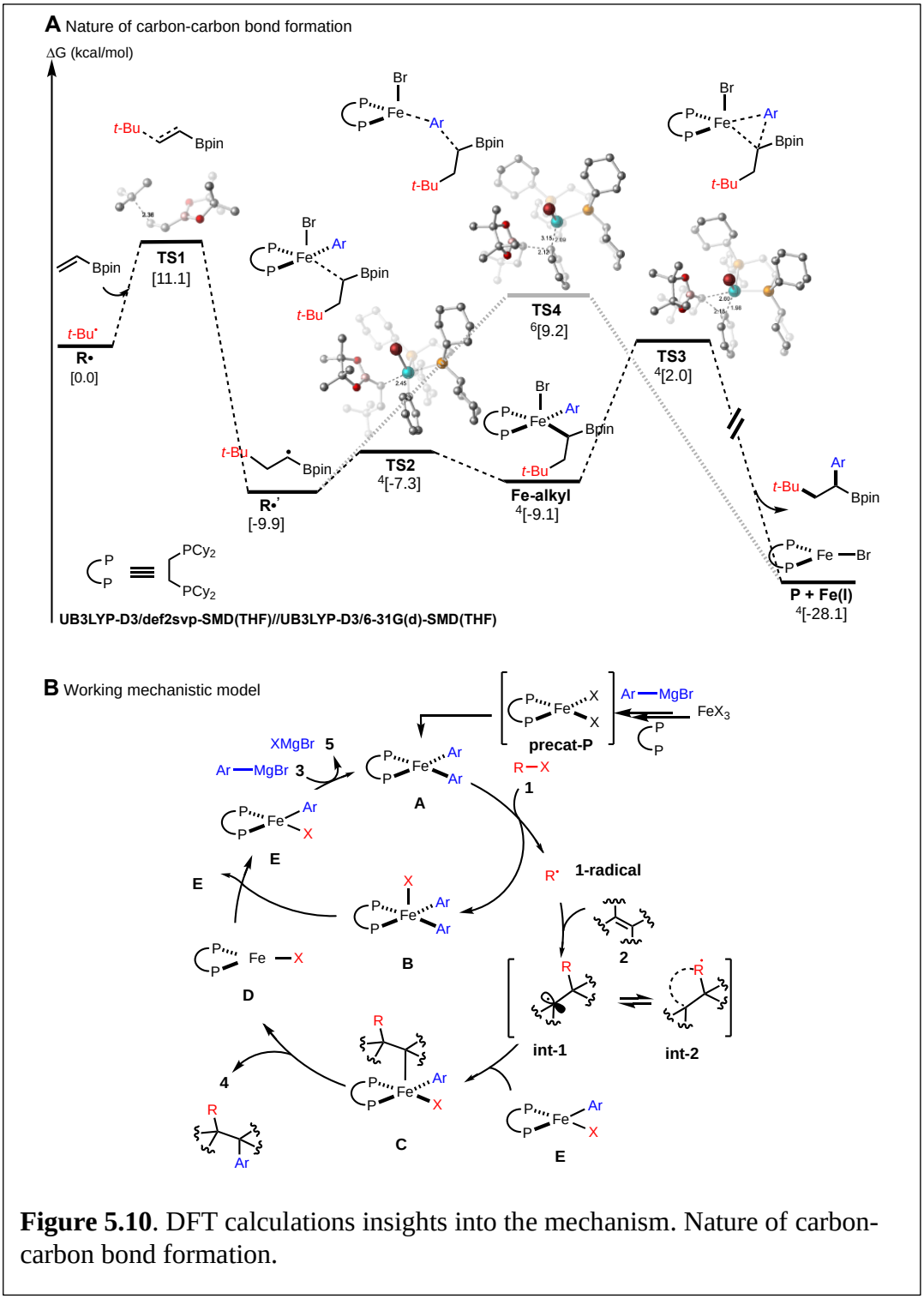

Figure 5.10. DFT calculations insights into the mechanism. Nature of carbon-carbon bond formation.

controlled) to the corresponding tetrahedral monoarylated Fe(II) species leading to square pyramidal Fe(III)-alkyl intermediate. Finally, subsequent reductive elimination

via quartet spin state will lead to the desired DCF product and Fe(I) species (barrier ~11 kcal/mol). We also located the competing outer-sphere C-C bond formation via the sextet spin state but is less likely due to a much higher barrier (> 7 kcal/mol) in comparison to the inner-sphere stepwise C-C bond formation (**Figure 5.10A**, **TS4** vs **TS3**). Overall, these mechanistic studies support the catalytic cycle shown **Figure 5.10B**. In particular, a distorted square planar bisarylated Fe(II) species **A** is responsible for halogen abstraction leading to alkyl radical formation **1-radical** and Fe(III) **B**. In turn, alkyl radical can participate in the radical cascade with the π-lynchpin then undergo inner-sphere C-C bond formation with an tetrahedral monoarylated Fe(II) species. Finally, disproportionation between Fe(I) **D** and Fe(III) **B** will lead to Fe(II), which under slow addition of Grignard reagent, could regenerate the catalytic cycle.

5.10 Summary

In summary, we have documented the first reports of Fe-catalyzed three-component alkylation- and annulation-arylation reactions of vinyl boronate esters leading to high-value and synthetically versatile alkyl boron compounds. Further, we extend this unique reactivity to permit Fe-catalyzed annulation-arylation radical cascade that engages a broad range of alkenes leading to previously difficult-to-make fluoroethylene containing-cyclic, spirocyclic, and fused bicyclic scaffolds. The salient features of this protocol are the use of inexpensive catalyst, low temperatures, rapid kinetics, high atom-economy, and environmentally benign side products (e.g., magnesium dihalide). As such, we anticipate that this method will provide a practical and general route to functionalization of electron-rich and electron-deficient alkenes

with various alkyl and hetero-substituents, and application to late-stage functionalization of bioactive molecules. These protocols expand the medicinal chemistry toolbox and expect to have an immediate impact in the access of diverse reagents and carbocycles.

5.11 References

(1) Fernández, E.; Whiting, A. (Eds.). *Synthesis and application of organoboron compounds*, **2015**.

(2) (a) J Wolfe, J. P.; Singer, R. A.; Yang, B. H.; Buchwald, S. L. *J. Am. Chem. Soc*. **1999**, *121*, 9550−9561. (b) Fihri, A.; Luart, D.; Len, C.; Solhy, A.; Chevrin, C.; Polshettiwar, V. *Dalton Trans*. **2011**, *40*, 3116−3121. (c) Brown, D. G.; Bostrom, J. *J. Med. Chem*. **2016**, *59*, 4443−4458.

(3) (a) Tellis, J. C.; Primer, D. N.; Molander, G. A. *Science*, **2014**, *345*, 443−436. (b) Primer, D. N.; Karakaya, I.; Tellis, J. C.; Molander, G. A. *J. Am. Chem. Soc*. **2015**, *137*, 2195−2198.

(4) (a) Campbell, M. W.; Compton, J. S.; Kelly, C. B.; Molander, G. A. *J. Am. Chem*. *Soc*. **2019**, *141*, 20069−20078. (b) Garcia-Dominguez, A.; Mondal, R.; Nevado, C. *Angew. Chem., Int. Ed.* **2019**, *58*, 12286−12290. (c) Mega, R. S.; Duong, V. K.; Noble, A.; Aggarwal, V. K. *Angew. Chem., Int. Ed*. **2020**, *59*, 4375−4379. (d) Sun, S.-Z.; Duan, Y.; Mega, R. S.; Somerville, R. J.; Martin, R. *Angew. Chem., Int. Ed*. **2020**, *59*, 4370−4374. (e) Chierchia, M.; Xu, P.; Lovinger, G. J.; Morken, J. P. *Angew. Chem., Int. Ed*. **2019**, *58*, 14245−14249. (f) Wang, X.-X.; Lu, X.; He, S.-J.; Fu, Y. *Chem. Sci*. **2020**, *11*, 7950−7956.

(5) (a) Hatakeyama, T.; Hashimoto, T.; Kondo, Y.; Fujiwara, Y.; Seike, H.; Takaya, H.; Tamada, Y.; Ono, T.; Nakamura, M. *J. Am. Chem. Soc*. **2010**, *132*, 10674−10676. (b) Hashimoto, T.; Hatakeyama, T.; Nakamura, M. *J. Org. Chem*. **2012**, *77*, 1168−1173. (c) Bedford, R. B.; Brenner, P. B.; Carter, E.; Carvell, T. W.; Cogswell, P. M.; Gallagher, T.; Harvey, J. N.; Murphy, D. M.; Neeve, E. C.; Nunn, J.; Pye, D. R. *Chem. Eur. J*. **2014**, *20*, 7935−7938. (d) O'Brien, H. M.; Manzotti, M.; Abrams, R. D.; Elorriaga, D.; Sparkes, H. A.; Davis, S. A.; Bedford, R. B. *Nat. Catal*. **2018**, *1*, 429−437. (e) Crockett, M. P.; Tyrol, C. C.; Wong, A. S.; Li, B.; Byers, J. A. *Org. Lett*. **2018**, *20*, 5233−5237. (f) Iwamoto, T.; Okuzono, C.; Adak, L.; Jin, M.; Nakamura, M. *Chem. Commun*. **2019**, *55*, 1128−1131. (g) Crockett, M. P.; Wong, A. S.; Li, B.; Byers, J. A. *Angew. Chem., Int. Ed*. **2020**, *59*, 5392−5397.

(6) Bedford, R. B.; Brenner, P. B.; Carter, E.; Gallagher, T.; Murphy, D. M.; Pye, D. R. *Organometallics*, **2014**, *33*, 5940−5943.

(7) Kumar, N.; Reddy, R. R.; Eghbarieh, N.; Masarwa, A. *Chem. Commun*. **2020**, *56*, 13−25.

(8) Lo, J. C.; Kim, D.; Pan,C.-M.; Edwards, J. T.; Yabe, Y.; Gui, J.; Qin, T.; Gutierrez, S.; Giacoboni, J.; Smith, M. W.; Holland, P. L.; Baran, P. S. *J. Am. Chem. Soc*. **2017**, *139*, 2484−2503.

(9) Vaclavik, J.; Klimankova, I.; Budinska, A.; Beier, P. *Eur. J. Org. Chem*. **2018**, *27-28*, 3554−3593.

(10) (a) Lee, W.; Zhou, J.; Gutierrez, O. *J. Am. Chem. Soc*. **2017**, *139*, 16126−16133. (b) Liu, L.; Lee, W.; Yuan, M.; Gutierrez, O. *Comment. Inorg. Chem*. **2018**, *38*,

210−237. (c) Liu, L.; Lee, W.; Zhou, J.; Bandyopadhyay, S.; Gutierrez, O. *Tetrahedron*, **2019**, *75*, 129−136. (d) Liu, L.; Lee, W.; Yuan, M.; Acha, C.; Geherty, M. B.; Williams, B.; Gutierrez, O. *Chem. Sci*. **2020**, *11*, 3146−3151. (e) Liu, L.; Lee, W.; Youshaw, C. R.; Yuan, M.; Geherty, M. B.; Zavalij, P. Y.; Gutierrez, O. *Chem. Sci*. **2020**, *11*, 8301−8305.

(11) (a) Neidig, M. L.; Carpenter, S. H.; Curran, D. J.; DeMuth, J. C.; Fleischauer, V. E.; Iannuzzi, T. E.; Neate, P. G. N.; Sears, J. D.; Wolford, N. *J. Acc. Chem. Res*. **2019**, *52*, 140-150. (b) Sears, J. D.; Neate, P. G. N.; Neidig, M. L. J. *Am. Chem. Soc*. **2018**, *140*, 11872−11883.

(12) Hall, D. G. Structure, properties, and preparation of boronic acid derivatives. in boronic acids (ed, Hall, D. G.) 1−133 (Wiley-VCH Verlag, 2011).

(13) (a) Hu, J.; Zhang, W.; Wang, F. *Chem. Commun*. **2009**, 7465–7478. (b) Chen, B.; Vicic, D. A. *Top. Organomet. Chem*. **2014**, *52*, 113–142. (d) Belhomme, M.-C.; Besset, T.; Poisson, T.; Pannecoucke, X. *Chem. Eur. J*. **2015**, *21*, 12836–12865.

(14) (a) Aikawa, K.; Maruyama, K.; Nitta, J.; Hashimoto, R.; Mikami, K. *Org. Lett.* 2016, *18*, 3354–3357. (b) An, L.; Xu, C.; Zhang, X. *Nat Commun.* **2017**, *8*, 1–9.

(15) An, L.; Xiao, Y.-L.; Zhang, S.; Zhang, X. *Angew. Chem., Int. Ed.* **2018**, *57*, 6921–6925. (b) Miao, W.; Zhao, Y.; Ni, C.; Gao, B.; Zhang, W.; Hu, J. *J. Am. Chem. Soc*. **2018**, *140*, 880-883.

(16) Rong, X. X., Pan, H.-Q., Dolbier Jr., W. R. & Smart, B. E. J. Am. Chem. Soc. 116, 4521−4522 (1994).

(17) Derosa, J.; Apolinar, O.; Kang, T.; Tran, V. T.; Engle, K. M. *Chem. Sci*. **2020**, *11*, 4287−4296.

(18) Avila, D. V.; Ingold, K. U.; Lusztyk, J.; Dolbier Jr., W. R.; Pan, H. Q.; Muir, M. *J. Am. Chem. Soc*. **1994**, *116*, 99−104.

(19) Lin, X.; Zheng, F.; Quing, F.-L. *Organometallics*, **2012**, *31*, 1578−1582.

(20) O'Hagan, D. *Chem. Soc. Rev*. **2008**, *37*, 308–319.

(21) Müller, K.; Faeh, C.; Diederich, F. *Science*, **2007**, *317*, 1881–1886.

(22) Purser, S.; Moore, P. R.; Swallow, S.; Gouverneur, V. *Chem. Soc. Rev*. **2008**, *37*, 320–330.

(23) Miller, M. A.; Sletten, E. M. *ChemBioChem*, **2020**, *21*, 3451–3462.

(24) Boström, J.; Brown, D. G.; Young, R. J.; Keserü, G. M. *Nature Reviews*. **2018**, *17*, 709−727.

(25) (a) Sebren, L. J.; Devery, J. J.; Stephenson, C. R. *ACS Catal*. **2014**, *4*, 703–716. (b) Studer, A.; Curran, D. *Angew. Chem., Int. Ed*. **2016**, *55*, 58–102.

(26) Li, L.; Ni, C.; Xie, Q.; Hu, M.; Wang, F.; Hu, J. *Angew. Chem., Int. Ed*. **2017**, *56*, 9971–9975.

(27) Newcomb, M. Radical Kinetics and Clocks. *Encyclopedia of Radicals in Chemistry, Biology and Materials*. **2012**.

Chapter 6: Synthesis of Bicyclo[1.1.1]pentanes by Iron-Catalyzed Three-Component Cross-Coupling Reaction

6.1 Biocyclo[1.1.1]Pentatnes in Organic Synthesis

Bicyclo[1.1.1]pentanes (BCPs) are widely used in medicinal chemistry (**Figure 6.1A**) as an analogue of the phenyl ring,[1] internal alkyne,[2] and tert-butyl group.[3] The fusion of this motif with drugs often leads to pharmacological benefits including the enhancement in solubility, membrane permeability, and metabolic stability.[4] 1,3-disubstituted BCP-bearing compounds can be synthesized from [1.1.1]propellane (**Figure 6.1B**).[5] Recent selected studies of this type of transformation has been done by Knochel,[2] Aggarwal,[6] Anderson,[7] MacMillan,[8] Uchiyama,[9] and Walsh[10] (**Figure 6.2A**). However, the development and synthetic routes to BCP analogues in drug-like molecules are still limited by many aspects such as the substrate scope and reaction condition. Herein, I will describe my efforts toward the first iron-catalyzed

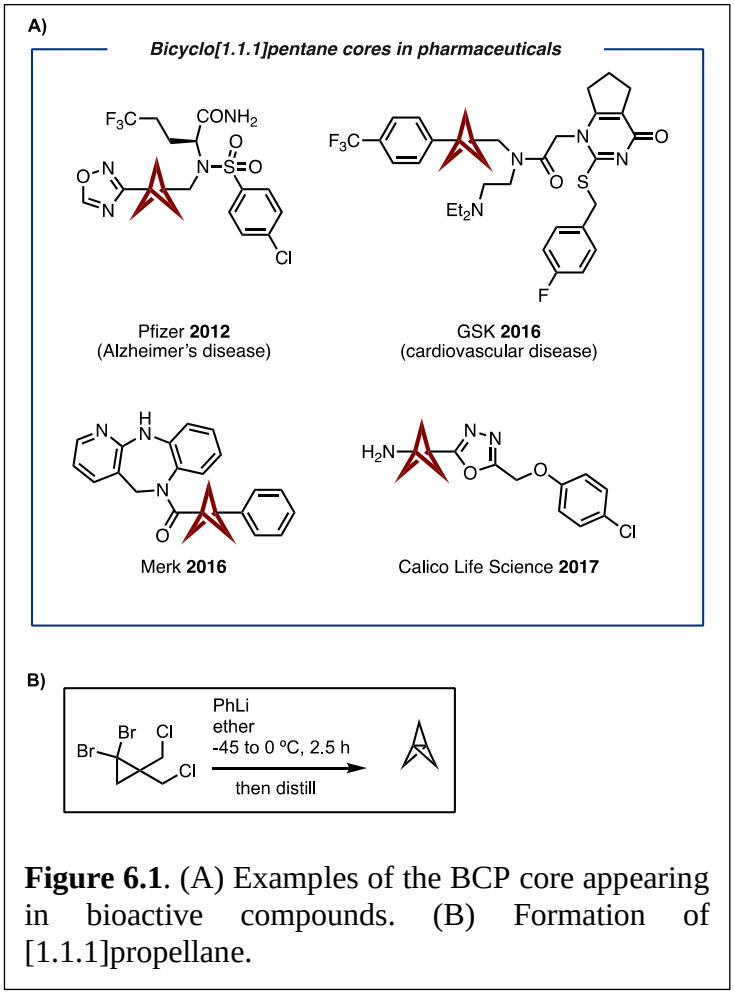

Figure 6.1. (A) Examples of the BCP core appearing in bioactive compounds. (B) Formation of [1.1.1]propellane.

three-component cross-coupling to generate the 1,3-difuncationalized BCP-bearing compounds with short reaction time, mild condition in the one-pot reaction (**Figure 6.2B**).

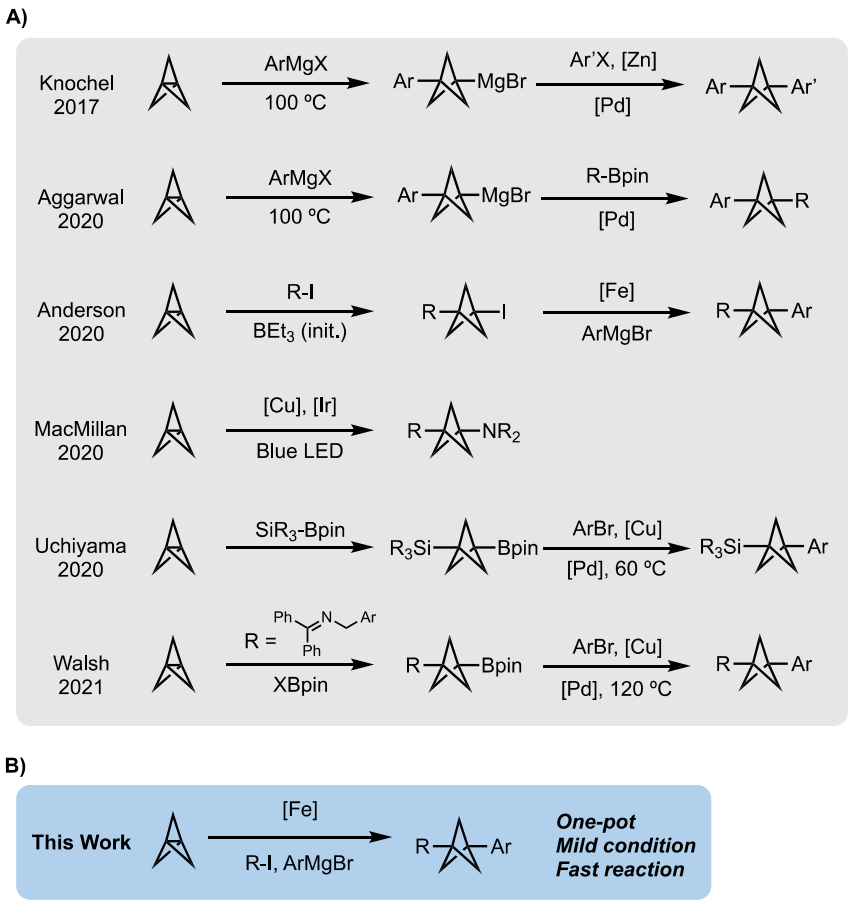

Figure 6.2. Selected studies of the formation of 1,3-disubstituted BCPs from [1.1.1]propellane.

6.2 Reaction Optimization

I initiated our study by optimizing the reaction condition using *tert*-butyl iodine **6.2.a** with fresh propellane **6.2.b**, and 3-methoxyphenylmagnesium bromide **6.2.c** under different conditions (**Table 6.1**). I started the screening with the Bis-(dicyclohexylphosphino)ethane (**dcpe**) ligand. Based on our previous experience, this

ligand usually works well in the iron-catalyzed Kumada type cross-coupling reactions.

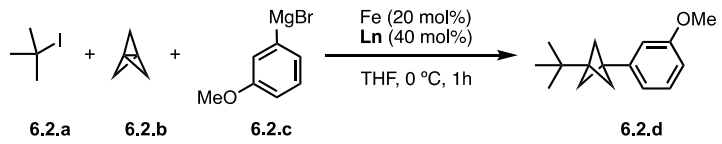

6.2.a **6.2.b** **6.2.c** **6.2.d**

entry	**6.2.a**	**6.2.b**	**6.2.c** (eq)	Fe	**Ln**	**6.2.d** (yield%)
1	1	1.1	1.2	$Fe(acac)_3$	**dcpe**	29%
2	1	2	3	$Fe(acac)_3$	**dcpe**	30%
3	1	4	3	$Fe(acac)_3$	**dcpe**	7%
4	2	1	4.2	$Fe(acac)_3$	**dcpe**	70%
5	2	1	2.2	$Fe(acac)_3$	**dcpe**	29%
6	4	1	4.2	$Fe(acac)_3$	**dcpe**	41%
7	2	1	4.2	NA	**dcpe**	ND
8	2	1	4.2	$Fe(acac)_3$	NA	13%
9	2	1	4.2	$FeBr_2$	**dcpe**	34%
10	2	1	4.2	$FeCl_3$	**dcpe**	9%
11	2	1	4.2	$Fe(acac)_3$	**L1**	67%
12	2	1	4.2	$Fe(acac)_3$	**L2**	77%
13	2	1	4.2	$Fe(acac)_3$	**L3**	ND
14	2	1	4.2	$Fe(acac)_3$	**L4**	ND
15	2	1	4.2	$Fe(acac)_3$	**L5**	ND
16	2	1	4.2	$Fe(acac)_3$	**L6**	53%

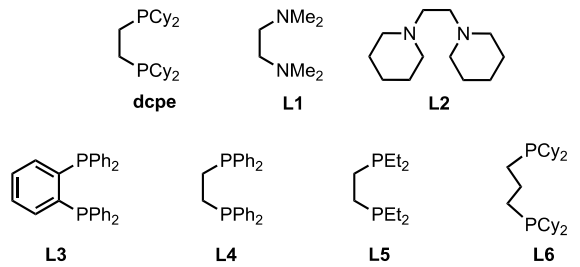

Table 6.1. Reaction optimization and the ligand screening.

Notably, by varying the ratio of compound **6.2.a**:**6.2.b**:**6.2.c** = 2:1:4.2, we were able to obtain 70% yield (4 repeat in average) in entry **6.2.d**. However, when we tried to decrease the Grignard loading in entry 5, the yield decreased. Also, higher equivalence of *tert*-butyl iodine wouldn't increase the yield (entry 6). Next, I screened different iron salts (entry 9 & 10) but they are not as good as $Fe(acac)_3$ in this reaction. Finally, I screened different diamine and bisphosphine ligands. Surprisingly, using the 1,2-

dipiperidinoethane ligand **L2** also lead to a high yield (77%) in entry 12. Therefore, I decided to use both ligands in all reactions and see how they behave.

6.3 Scope of Nucleophiles

With optimized conditions in hand, the scope of this transformation was examined. Shown in **Figure 6.3**, the scope of this Fe-catalyzed BCP 1,3-difunctionalization is broad with respect to the Grignard nucleophile. In some of the

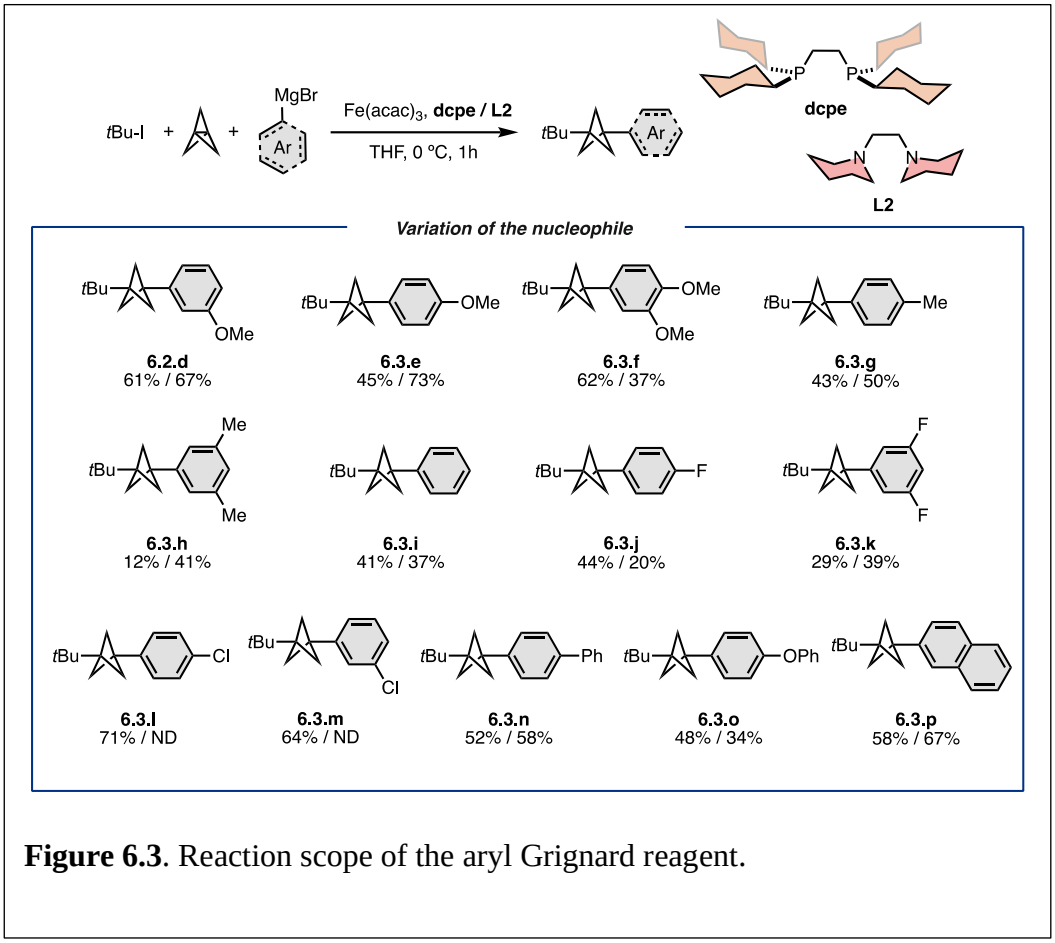

Figure 6.3. Reaction scope of the aryl Grignard reagent.

cases, **dcpe** and **L2** ligand lead to similar yields such as **6.2.d**, **6.3.g**, **6.3.i**, **6.3.n**. The difference between **dcpe** and **L2** can be seen in **6.3.e** that the condition with **L2** has a much better yield (45% vs 73%). However, in some extreme cases (**6.3.l** and **6.3.m**), using **dcpe** as the ligand can create product with 71% and 64% yield over the **L2** which

none of the product was observed. Currently we are using quantum mechanical calculation to explore the difference in the electronic effect between these two ligands.

6.4 Scope of Alkyl Halides

I then investigated the scope of the radical precursors. As shown in **Figure 6.4**, this method can be applied to a range of alkyl halides in a short reaction time and

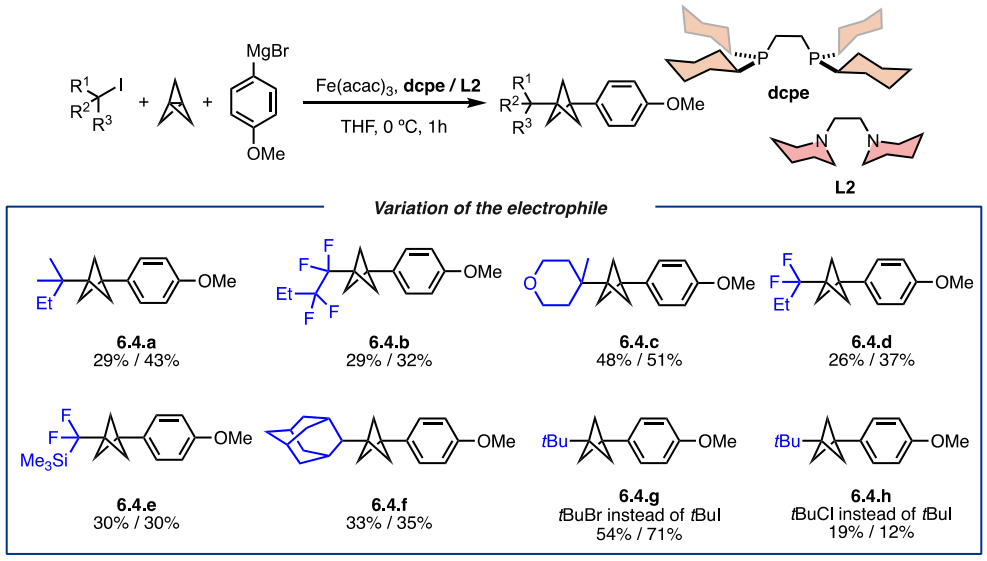

Figure 6.4. Scope of alkenes in the reaction.

temperature. In this part, the effect of different of radical precursor with two ligands is less significant compared with the electronic groups on Grignard reagents. Both ligands have tolerance with fluorinated alkyl halides (**6.4.b**, **6.4.d**, and **6.4.e**) and other tertiary alkyl halides (**6.4.a**, **6.4.c**, **6.4.f**, **6.4.g**, **6.4.h**) forming the C-C (sp^3-sp^3) bond which is rarely seen in other methods.

6.5 Proposed Mechanism

A proposed mechanism is shown in **Figure 6.5**. After the radical **int-1** is generated by iron active species **B**. The radical escaped from the solvent cage to react

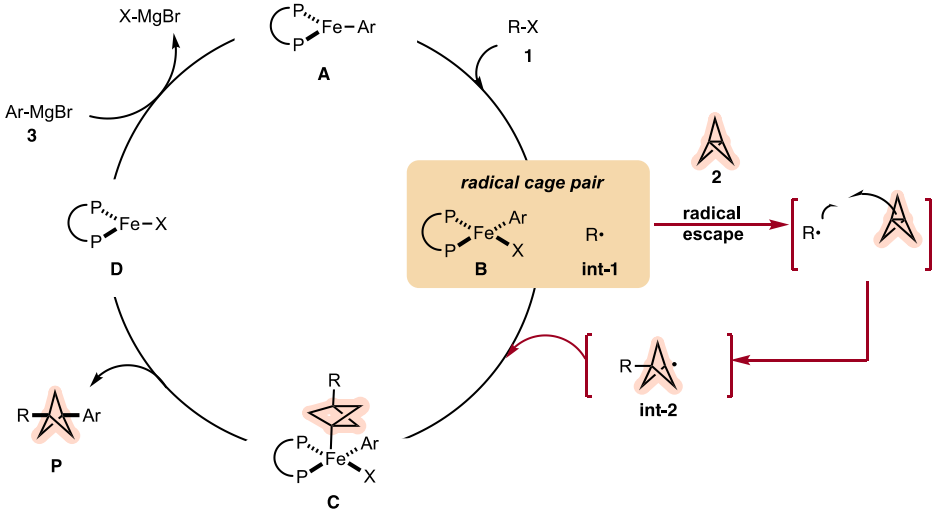

Figure 6.5. Proposed mechanism.

with the [1.1.1]propellane **2**. Through the right side in the figure, **int-2** is formed and it reacts with compound **B** to form iron(III) intermediate **C**. Finally, this iron(III) species will undergo reductive elimination and generate the 1,3-difunctionalized BCP product **P**. The iron(I)-mono-halide species **D** can turn back to Iron(I)-mono-aryl species **A** by transmetalation.

6.6 Summary

In summary, I have developed an iron-catalyzed three-component reaction that utilize [1.1.1]propellane to form 1,3-difunctionalized bycyclopentane using both diamine and bisphosphine ligands. I also demonstrated that this protocol can create two carbon-carbon bonds, one on each side of the BCP, in a one-pot reaction that takes only

an hour under low temperature (0 ºC). The reaction can tolerate aryl Grignard with substituents on the *para*- and *meta*-position and different radical precursors. Further study for the large-scale reaction and the late-stage functionalization is ongoing in our lab. Mechanistic study with DFT calculation is also progressing. 1,3-difunctionalization of BCP is one of the examples of iron-catalyzed cross-coupling reactions. There are more for us to explore in the future.

6.7 References

(1) (a) Pellicciari, R.; Raimondo, M.; Marinozzi, M.; Natalini, B.; Costantino, G.; Thomsen, C. J. Med. Chem. 1996, 39, 2874−2876; (b) Stepan, A. F.; Subramanyam, C.; Efremov, I. V.; Dutra, J. K.; O'Sullivan, T. J.; DiRico, K. J. et al. J. Med. Chem. 2012, 55, 3414−3424.

(2) Makarov, I. S.; Brocklehurst, C. E.; Karaghiosoff, K.; Koch, G.; Knochel, P. *Angew. Chem., Int. Ed.* **2017**, *56*, 12774−12777.

(3) Westphal, M. V.; Wolfstädter, B. T.; Plancher, J. M.; Gatfield, J.; Carreira, E. M. *ChemMedChem*. **2015**, *10*, 461−469.

(4) (a) Meanwell, N. A. *Chem. Res. Toxicol*. **2016**, *29*, 564−616; (b) For a review, see: Mykhailiuk, P. K. *Org. Biomol. Chem*. **2019**, *17*, 2839−2849; (c) Locke, G. M.; Bernhard, S. S.; Senge, M. O. *Chem. Eur. J.* **2019**, *25*, 4590−4647; (d) Lovering, F.; Bikker, J.; Humblet, C. *J. Med. Chem*. **2009**, *52*, 6752−6756.

(5) Hughes, J. M.; Scarlata, D. A.; Chen, A. C. Y.; Burch, J. D.; Gleason, J. L. *Org. Lett*. **2019**, *21*, 6800−6804.

(6) Yu, S.; Jing, C.; Noble, A.; Aggarwal, V. K. *Angew. Chem., Int. Ed.* **2020**, 132, 3945−3949.

(7) Nugent, J.; Shire, B. R.; Caputo, D. F.; Pickford, H. D.; Nightingale, F.; Houlsby, I. T.; Mousseau, J. J.; Anderson, E. A. *Angew. Chem., Int. Ed*. **2020**, *59*, 11866−11870.

(8) Zhang, X.; Smith, R. T.; Le, C.; McCarver, S. J.; Shireman, B. T.; Carruthers, N. I.; MacMillan, D. W. *Nature*, **2020**, *580*, 220−226.

(9) Kondo, M.; Kanazawa, J.; Ichikawa, T.; Shimokawa, T.; Nagashima, Y.; Miyamoto, K.; Uchiyama, M. *Angew. Chem., Int. Ed*., **2020**, *59*, 1970−1974.

(10) Shelp, R. A.; Ciro, A.; Pu, Y.; Merchant, R. R.; Hughes, J. M.; Walsh, P. J. *Chem. Sci*. **2021**, *12*, 7066−7072.

Chapter 7: Supplemental Information

7.1 Chapter 1 Detailed Energy Diagram with 4 Different Methods

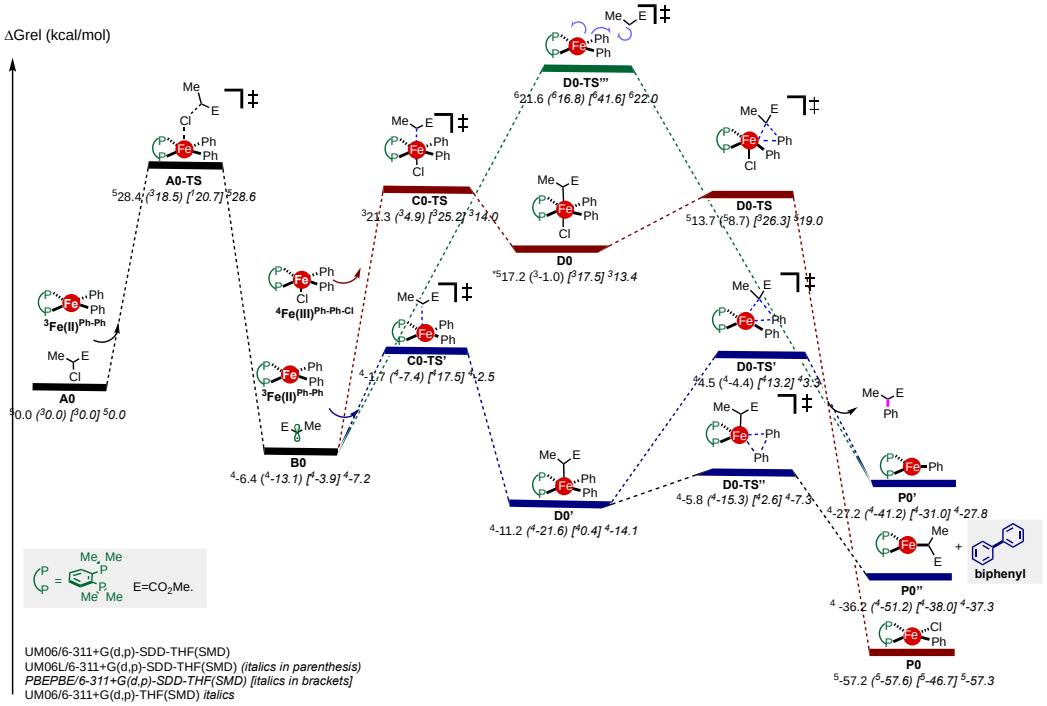

Figure 7.1. Formation of biphenyl.

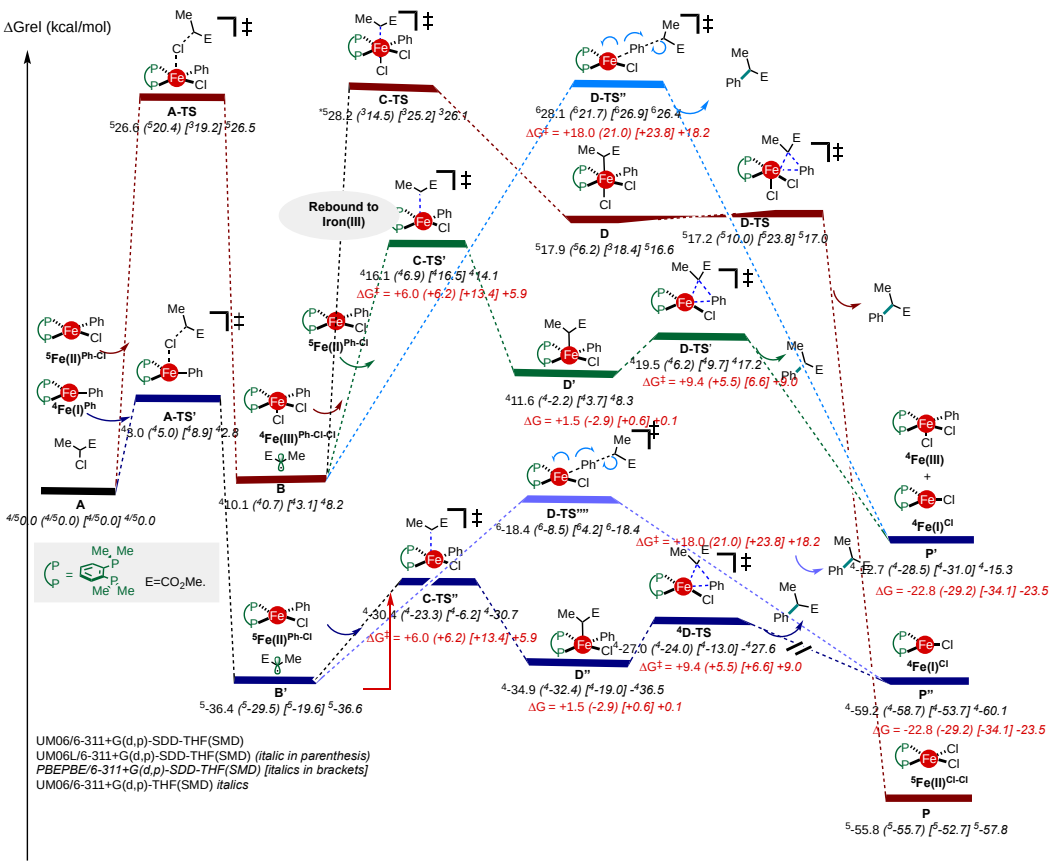

Figure 7.2. Iron(I) Inner-sphere pathway forming the desired cross-coupled product.

7.2 Computational Method

Unless otherwise stated, all optimizations were carried out without constraints at the UB3LYP/6-31G(d) level of theory with the "guess=mix" keyword as implemented in Gaussian09. We considered low, medium, and high spin species for all open-shell intermediates and transition state structures. The expectation values of <S2> were evaluated as a diagnostic value of the spin state of the systems. To refine energetics, we carried out single point energy calculations using UM06/6-311+G(d,p)

in a polarizable continuum solvent (THF) with SMD as solvation model to account for the condensed phase effects. We also carried out calculations using the uM06L functional, in conjunction with effective core potential basis set (SDD) for iron and 6-311++G(d,p) basis set for all other atoms in implicit solvent (THF-SMD) for selected structures. All structural figures were generated using CLYview. Vibrational frequencies were computed at the same level to obtain thermal corrections (at 298 K; enthalpic and free energy) and to characterize the stationary points as transition states (one and only one imaginary frequency) or minima (zero imaginary frequencies). Exhaustive conformational searches were performed for all intermediates to map out the lowest energy profile, and intrinsic reaction coordinate (IRCs) calculations were undertaken for selected transition state structures to ensure they connected the illustrated ground states.

7.3 General Procedure for the Synthesis of α-Halo Esters in Chapter 2

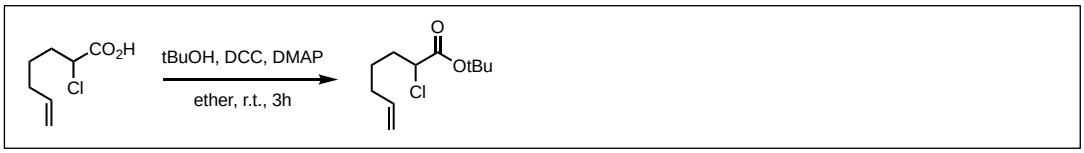

To a stirred solution of N,N'-dicyclohexylcarbodiimide (DCC) (1.24 g, 6 mmol) in diethyl ether (15 mL) was added *α*-halo hept-6-enoic acid (5 mmol) at room temperature. Then a mixed solution of the tert-butanol (6 mmol) and 4-dimethylaminopyridine (DMAP) (36.7 mg, 0.3 mmol) in diethyl ether (5 mL) was added via syringe dropwise. Upon addition of the mixed solution of *tert*-butanol and DMAP, a precipitate began to form. After the addition was complete, the reaction mixture was maintained for 3 h at the same temperature, then diluted with hexanes (20

mL). The resulting mixture was filtered through a celite pad and the filtrate was concentrated under reduced pressure. The crude product was purified by silica gel chromatography to yield the α-halo esters (hexane:EtOAc = 30:1).

7.4 General Procedure for the Iron-Catalyzed Intermolecular Difunctionalization of Vinyl Cyclopropane in Chapter 3

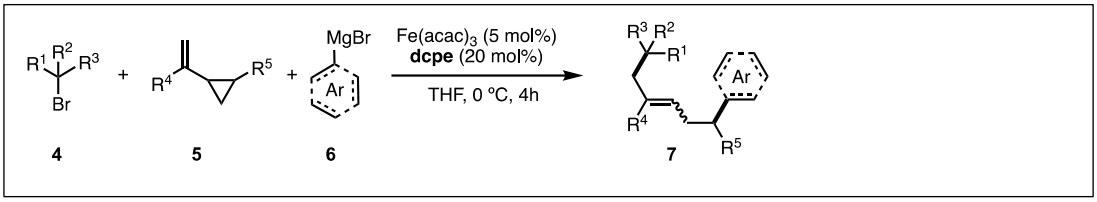

A flame-dried 5 mL microwave vial with a stir bar was brought into an argon-filled glovebox and the vial was charged with $Fe(acac)_3$ (3.5 mg, 5 mol%), 1,2-bis(dicyclohexylphosphanyl)ethane (**dcpe**) (16.9 mg, 20 mol%), vinyl cyclopropane **5** (0.2 mmol), and alkyl bromide **4** (1.1 mmol, 5.5 equiv). The vial was sealed with a Teflon cap and was brought out of the glovebox and 0.2 mL of THF was added. The red solution was stirred at room temperature for 5 min. The reaction mixture was then cooled to 0 ºC and a ArMgBr solution (0.3–1.0 M solution in THF, 8.0 equiv) was added slowly over 4 h using a syringe pump, over which time the heterogeneous solution turned from red to colorless to yellow, brown or grass green color (depending on ArMgBr and substrate). After the addition was complete, the reaction mixture was maintained at 0 ºC for an additional 10 min. Then the resulting mixture was quenched with a 1.0 M aqueous solution (0.4 mL) of hydrochloric acid or saturated aqueous NH_4Cl (depending on product properties), then extracted with ethyl acetate (3 x 2 mL). The organic layer was filtered through a plug of silica and concentrated in vacuo. The

resulting residue was purified by flash chromatography on silica gel with hexane/CH_2Cl_2.

7.5 General Procedure of Iron-Catalyzed Difunctionalization with Unactivated Alkene in Chapter 4

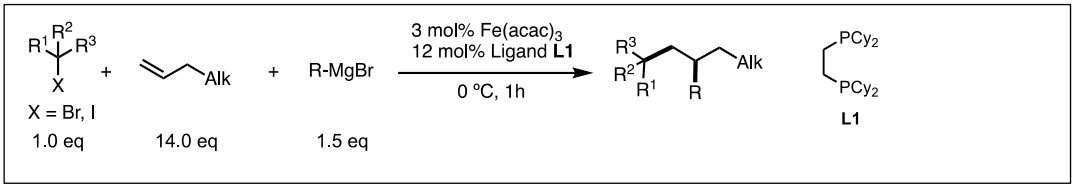

A flame-dried 5 mL microwave vial with a stir bar was brought into an argon-filled glovebox and the vial was charged with $Fe(acac)_3$ (2.1 mg, 3 mol%), 1,2-bis(dicyclohexylphosphanyl)ethane **L1** (10.1 mg, 12 mol%), alkyl halide (0.2 mmol, 1.0 equiv) and alkene (2.8 mmol, 14.0 equiv) (using oven-dried glass pipet to transfer alkyl halide and alkene to the vial which was on the balance). The vial was sealed with a Teflon cap and was brought out of the glovebox without solvent (0.2 mL of THF was added if need). The red solution was stirred at room temperature for 5 min. The reaction mixture was then cooled to 0 ºC and a ArMgBr solution (0.5–1.0 M solution in THF, 1.5 equiv) was added slowly for 1 h using a syringe pump, over which time the heterogeneous solution turned from red to colorless to yellow, brown, grass green or orange color (depending on ArMgBr and substrate). After the addition was complete, the reaction mixture was maintained at 0 ºC for an additional 20 min. Then the resulting mixture was quenched with a 1.0 M aqueous solution (0.5 mL) of hydrochloric acid and water (0.5 mL), or saturated aqueous NH_4Cl (1 mL) (depending on product properties), then extracted with ethyl acetate or diethyl ether (3 x 2 mL) depending on recovered alkene boiling point. The combined organic layer was filtered through a plug

of silica and concentrated in vacuo (the low boiling point recovered alkene was obtained by Vigreux column vacuum distillation). The resulting residue was purified by flash column chromatography on silica gel with hexane/CH_2Cl_2 or Isolera™ Flash Systems silica gel chromatography with prepacked silica-gel cartridges (SNAP Ultra; Biotage) and a gradient elution of hexane/Et_2O (hexane/EtOAc, or hexane/CH_2Cl_2) to obtain products and recovered alkene.

7.6 General Procedure of Iron-Catalyzed Difunctionalization with Vinylboronate in Chapter 5

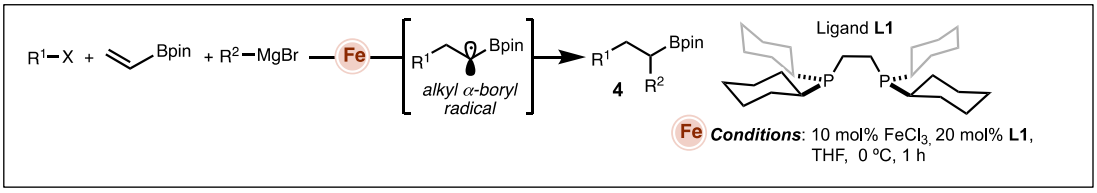

A flame-dried 5 mL microwave vial with a stir bar was brought into an argon-filled glovebox and the vial was charged with $FeCl_3$ (3.2 mg, 10 mol%), 1,2-bis(dicyclohexylphosphanyl)ethane **L1** (16.9 mg, 20 mol%), alkyl halide (0.4 mmol, 2.0 equiv) and vinylboronic acid pinacol ester (0.2 mmol, 1.0 equiv) (using oven-dried glass pipet to transfer alkyl halide and vinylboronic acid pinacol ester to the vial which was on the balance). The vial was sealed with a Teflon cap and was brought out of the glovebox and 0.2 mL of THF was added. The solution was stirred at room temperature for 5 min. The reaction mixture was then cooled to 0 °C and a ArMgBr solution (0.3–1.0 M solution in THF, 2.0 equiv) was added slowly for 1 h using a syringe pump. After the addition was complete, the reaction mixture was maintained at 0 °C for an additional 10 min. Then the resulting mixture was quenched with a 1.0 M aqueous solution (0.5 mL) of hydrochloric acid and water (0.5 mL), then extracted with ethyl

acetate (3 x 2 mL). The combined organic layer was filtered through a plug of silica and concentrated in vacuo. The resulting residue was purified by flash column chromatography on silica gel with hexane/EtOAc/CH_2Cl_2 or Isolera™ Flash Systems silica gel chromatography with prepacked silica-gel cartridges (SNAP Ultra; Biotage) and a gradient elution of hexane/EtOAc/CH_2Cl_2 to obtain products.

7.7 General Procedure of Iron-Catalyzed Multicomponent Annulation-Arylation in Chapter 5

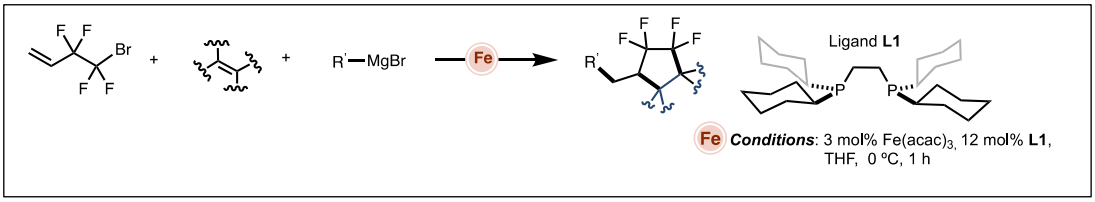

A flame-dried 5 mL microwave vial with a stir bar was brought into an argon-filled glovebox and the vial was charged with $Fe(acac)_3$ (2.1 mg, 3 mol%), 1,2-bis(dicyclohexylphosphanyl)ethane **L1** (10.1 mg, 12 mol%), alkyl halide (0.2 mmol, 1.0 equiv) and alkene (0.3 mmol, 1.5 equiv) (using oven-dried glass pipet to transfer alkyl halide and alkene to the vial which was on the balance). The vial was sealed with a Teflon cap and was brought out of the glovebox and 0.2 mL of THF were added. The solution was stirred at room temperature for 5 min. The reaction mixture was then cooled to 0 °C and a ArMgBr solution (0.3–1.0 M solution in THF, 2.0 equiv) was added slowly for 1 h using a syringe pump. After the addition was complete, the reaction mixture was maintained at 0 °C for an additional 10 min. Then the resulting mixture was quenched with a 1.0 M aqueous solution (0.5 mL) of hydrochloric acid and water (0.5 mL), or saturated aqueous NH_4Cl (1 mL) (depending on product properties), then extracted with ethyl acetate. The combined organic layer was filtered

through a plug of silica and concentrated in vacuo. The resulting residue was purified by flash column chromatography on silica gel with hexane/CH_2Cl_2 or Isolera™ Flash Systems silica gel chromatography with prepacked silica-gel cartridges (SNAP Ultra; Biotage) and a gradient elution of hexane/CH_2Cl_2 (hexane/EtOAc/CH_2Cl_2 or hexane/EtOAc) to obtain products.

7.8 General Procedure of Iron-Catalyzed Difunctionalization of [1.1.1]Propellane in Chapter 6

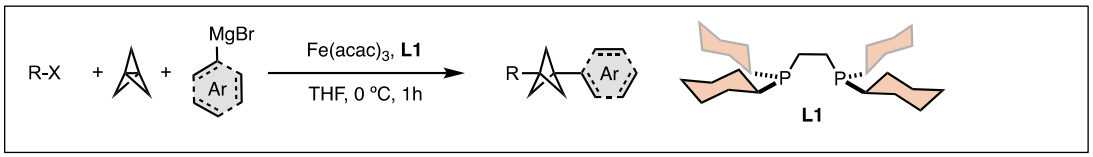

A flame-dried 5 mL microwave vial with a stir bar was brought into an argon-filled glovebox and the vial was charged with $Fe(acac)_3$ (7.1 mg, 10 mol%), 1,2-bis(dicyclohexylphosphanyl)ethane **L1** (33.8 mg, 20 mol%), alkyl halide (0.4 mmol, 2.0 equiv) and the [1.1.1.]propellane (0.5 – 1.0 M, 1.0 equiv) solution in ether (using oven-dried glass pipet to transfer alkyl halide and propellane to the vial which was on the balance). The vial was sealed with a Teflon cap and was brought out of the glovebox and 0.2 mL of THF were added. The solution was stirred at room temperature for 5 min. The reaction mixture was then cooled to 0 °C and a ArMgBr solution (0.5–1.0 M solution in THF, 4.0 equiv) was added slowly for 1 h using a syringe pump. After the addition was complete, the reaction mixture was maintained at 0 °C for an additional 10 min. Then the resulting mixture was quenched with a 1.0 M aqueous solution (0.5 mL) of hydrochloric acid and water (0.5 mL), then extracted with ethyl acetate. The combined organic layer was filtered through a plug of silica and concentrated in vacuo. The resulting residue was purified by flash column chromatography on silica gel with

hexane/CH_2Cl_2 or Isolera™ Flash Systems silica gel chromatography with prepacked silica-gel cartridges (SNAP Ultra; Biotage) and a gradient elution of hexane/CH_2Cl_2 to obtain products.

7.9 NMR Spectra of Compounds in Chapter 5

5.4.f

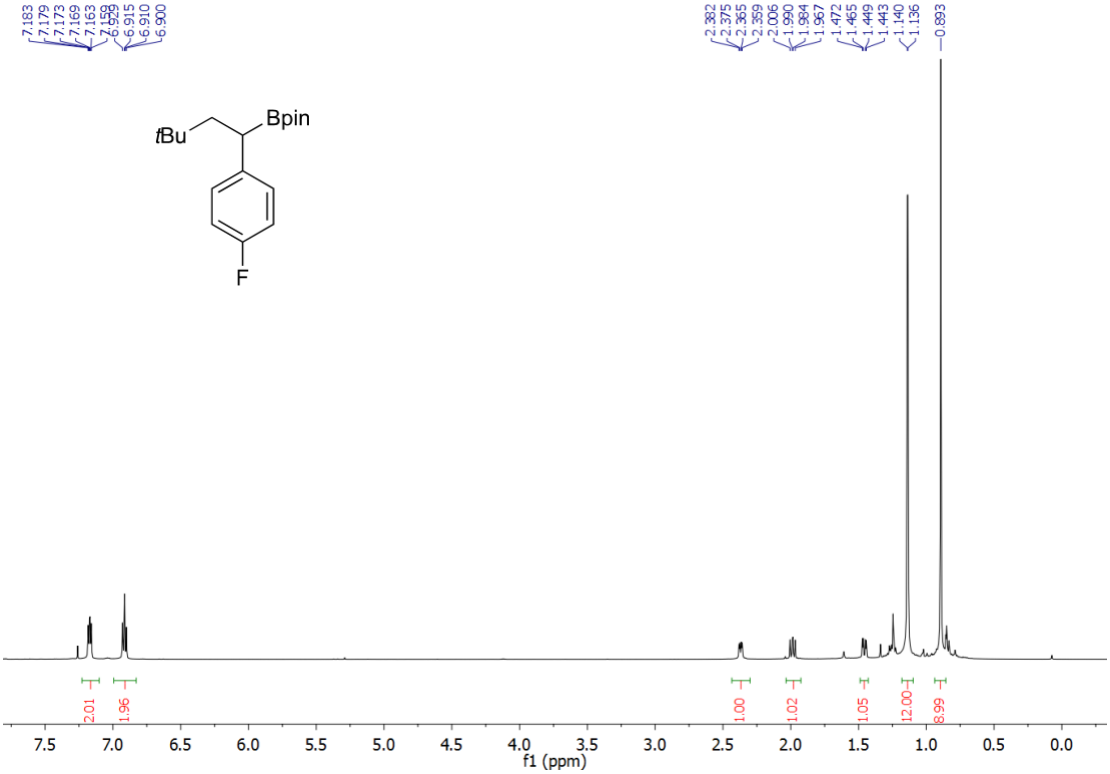

HRMS (DART) calcd for $C_{18}H_{29}BFO_2$ $[M+H]^+$ *m/z* = 307.2245; found 307.2248.

5.4.h

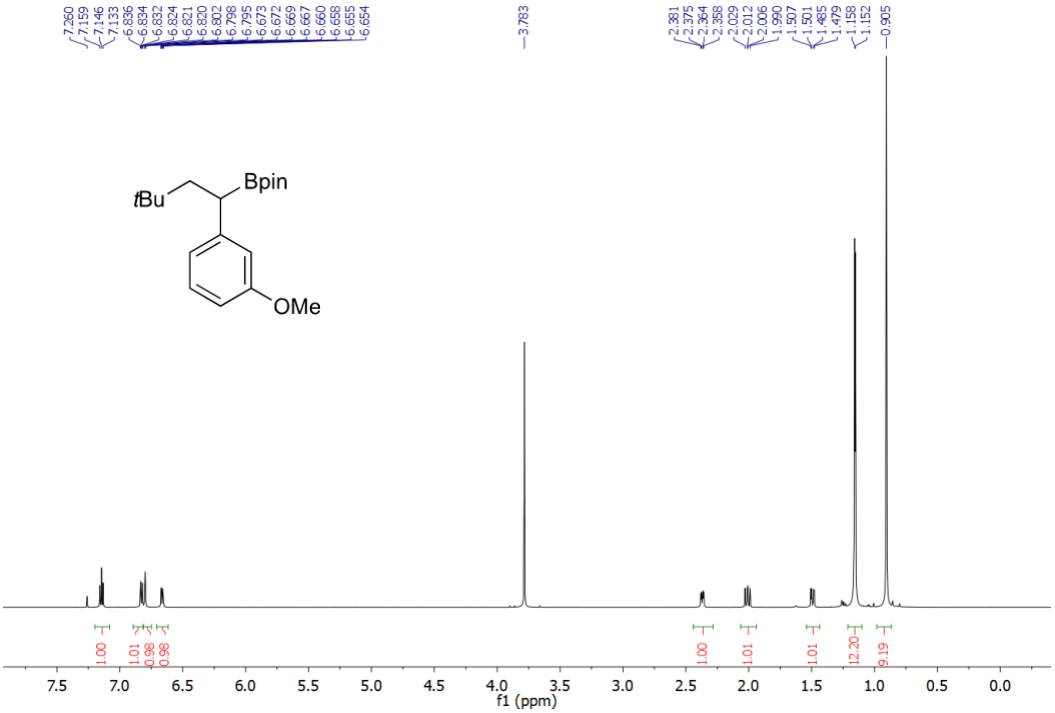

HRMS (DART) calcd for $C_{19}H_{32}BO_3$ $[M+H]^+$ *m/z* = 319.2445; found 319.2444.

5.4.i

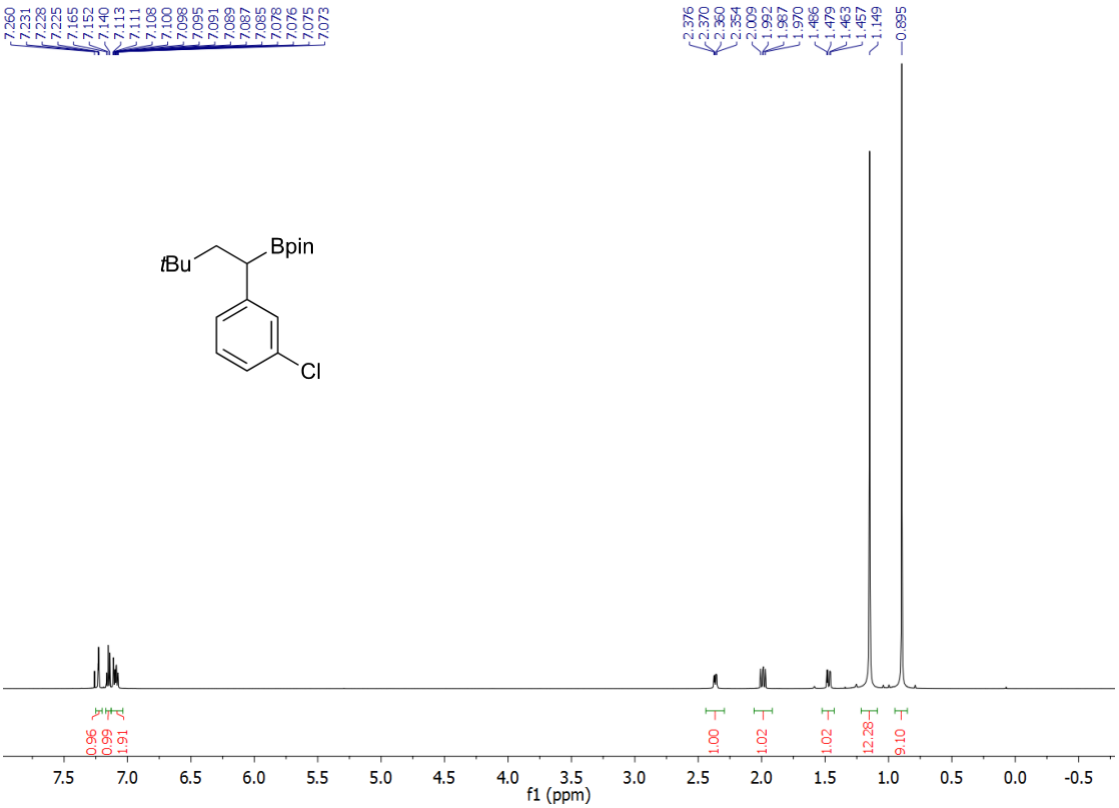

HRMS (DART) calcd for $C_{18}H_{29}BClO_2$ $[M+H]^+$ *m/z* = 323.1949; found 323.1945.

5.4.k

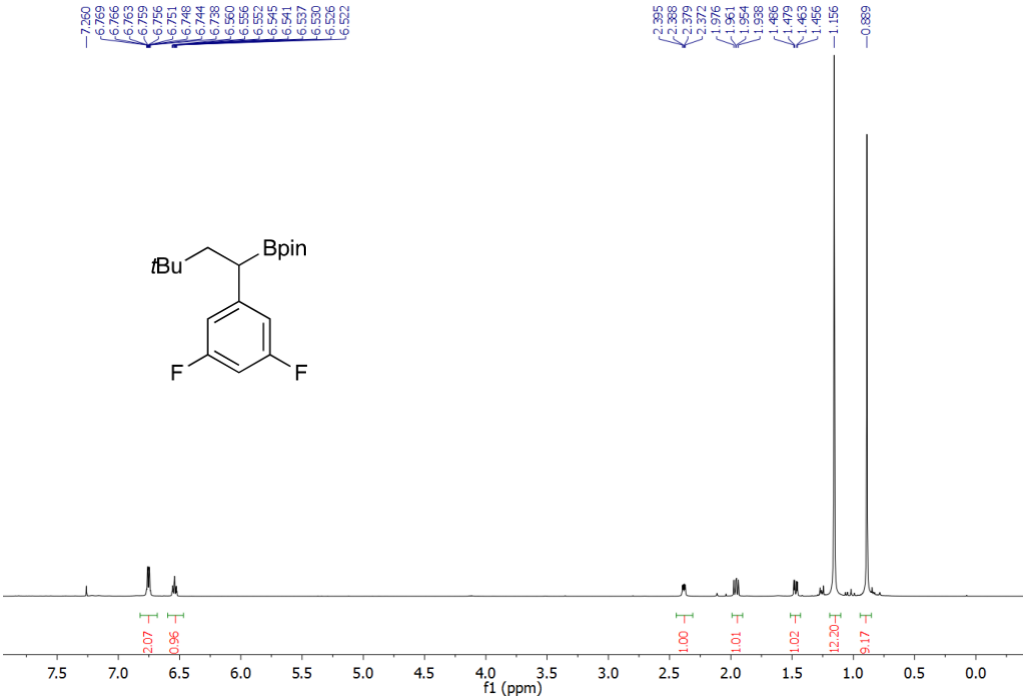

HRMS (DART) calcd for $C_{18}H_{28}BF_2O_2$ $[M+H]^+$ *m/z* = 325.2150; found 325.2150.

5.4.l

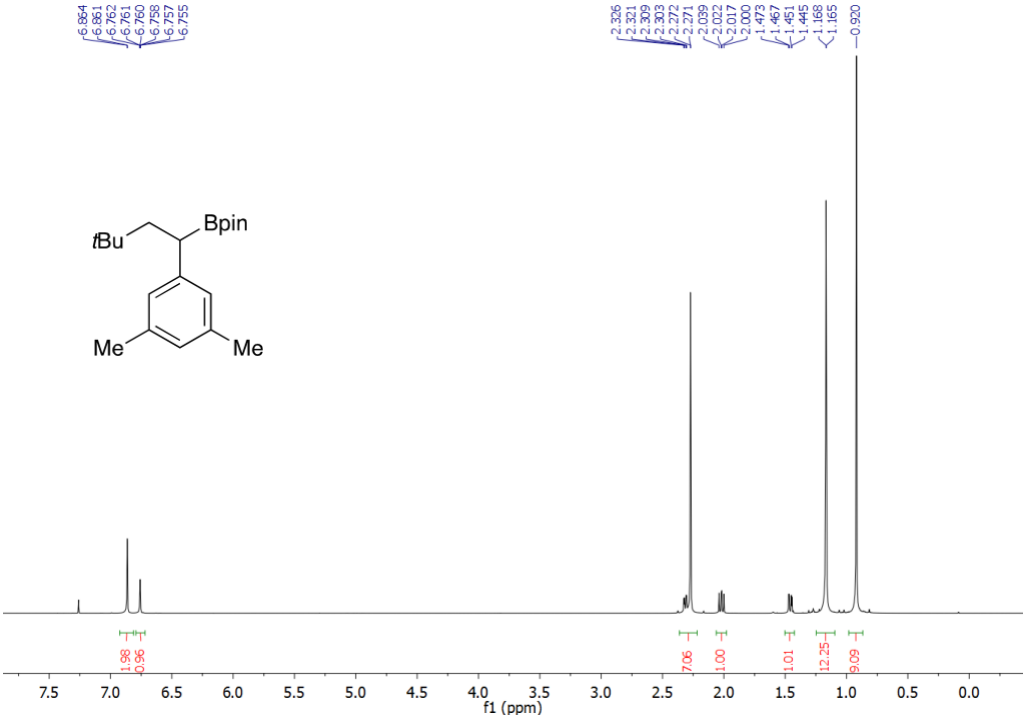

HRMS (DART) calcd for $C_{20}H_{34}BO_2$ $[M+H]^+$ *m/z* = 317.2652; found 317.2660.

5.4.m

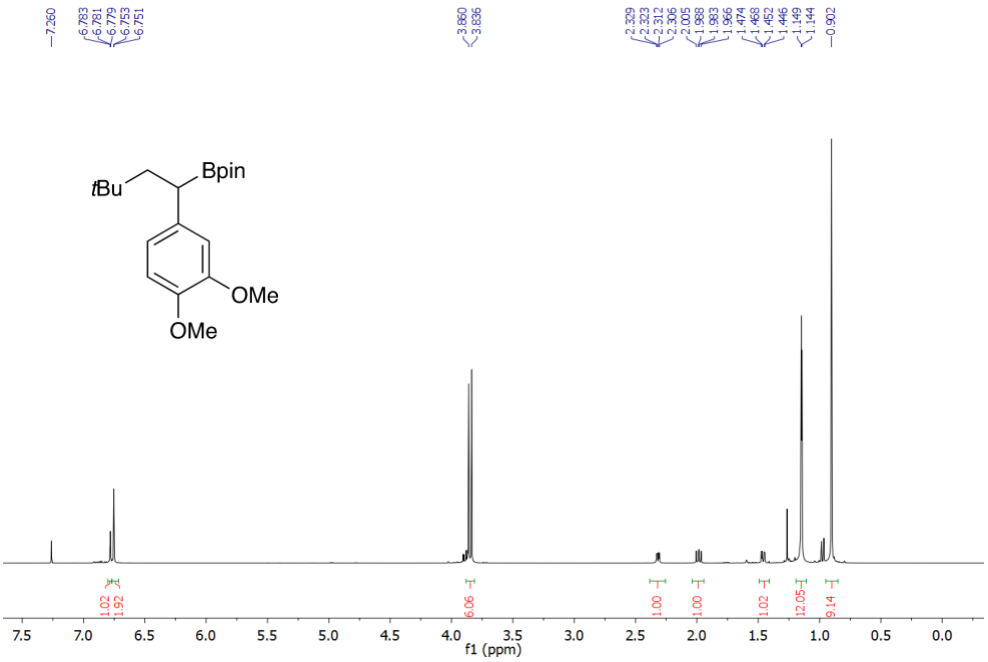

HRMS (DART) calcd for $C_{20}H_{34}BO_4$ $[M+H]^+$ *m/z* = 349.2550; found 349.2542.

5.4.o

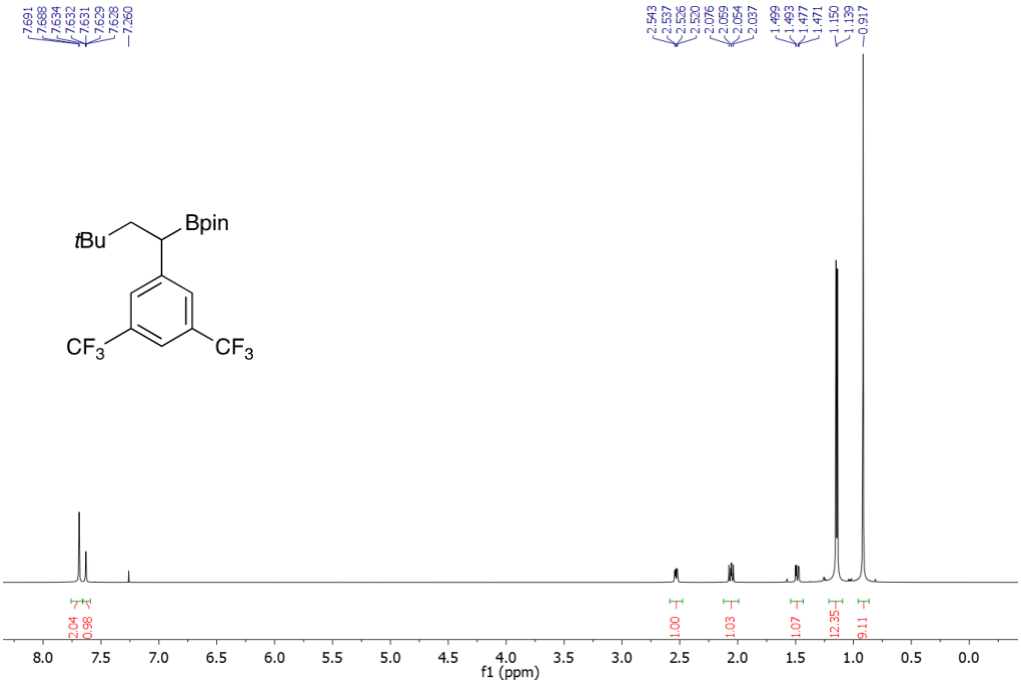

HRMS (DART) calcd for $C_{20}H_{28}BF_6O_2$ $[M+H]^+$ *m/z* = 425.2087; found 425.2084.

5.4.q

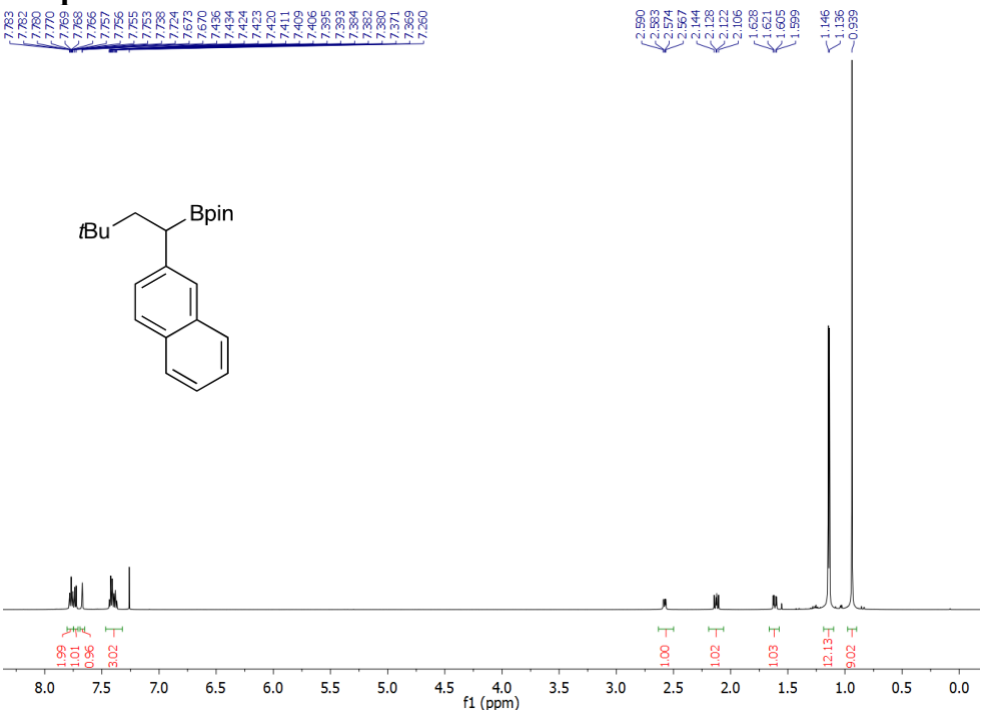

HRMS (DART) calcd for $C_{22}H_{32}BO_2$ $[M+H]^+$ *m/z* = 339.2495; found 339.2498.

5.4.r

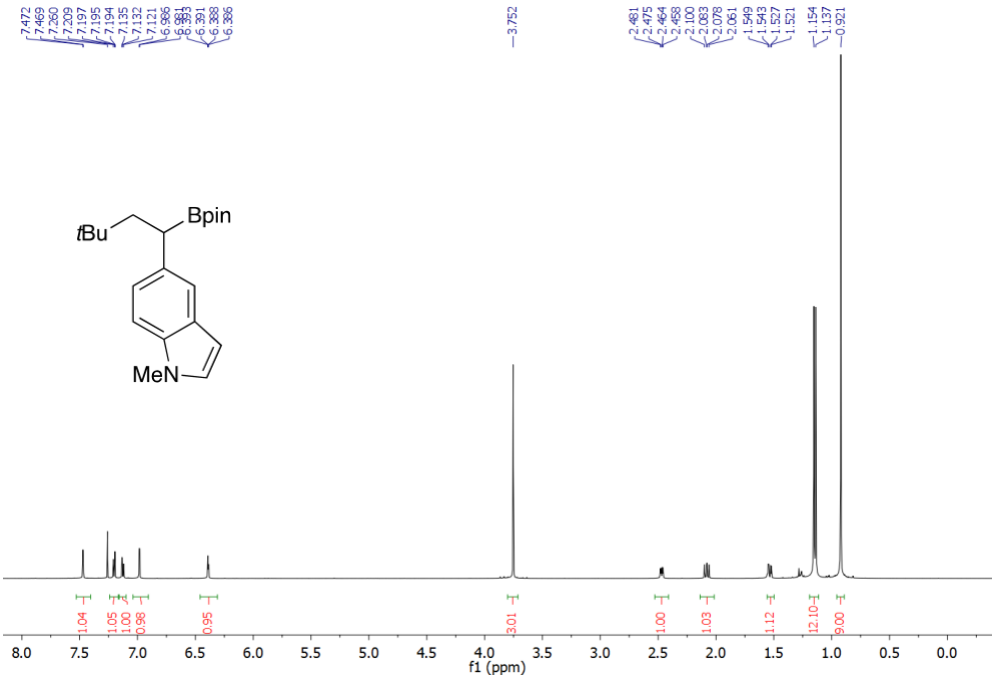

HRMS (DART) calcd for $C_{21}H_{33}BNO_2$ $[M+H]^+$ *m/z* = 342.2604; found 342.2606.

5.4.s

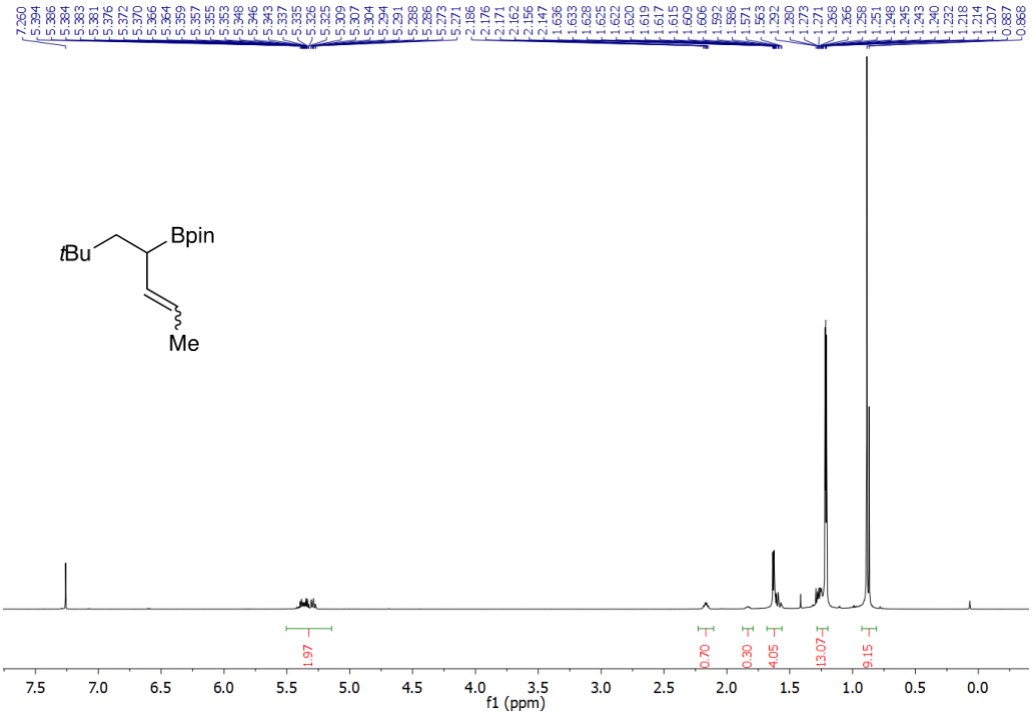

HRMS (DART) calcd for $C_{15}H_{30}BO_2$ $[M+H]^+$ *m/z* = 253.2339; found 253.2337.

5.4.u

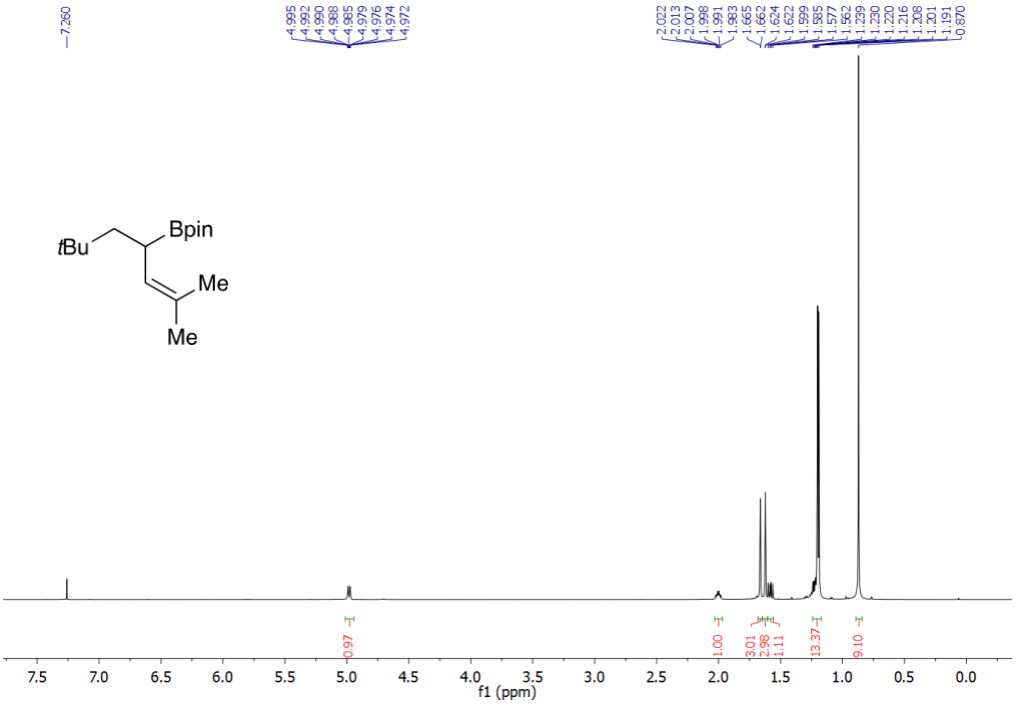

HRMS (DART) calcd for $C_{16}H_{32}BO_2$ $[M+H]^+$ *m/z* = 267.2495; found 267.2490.

5.4.v

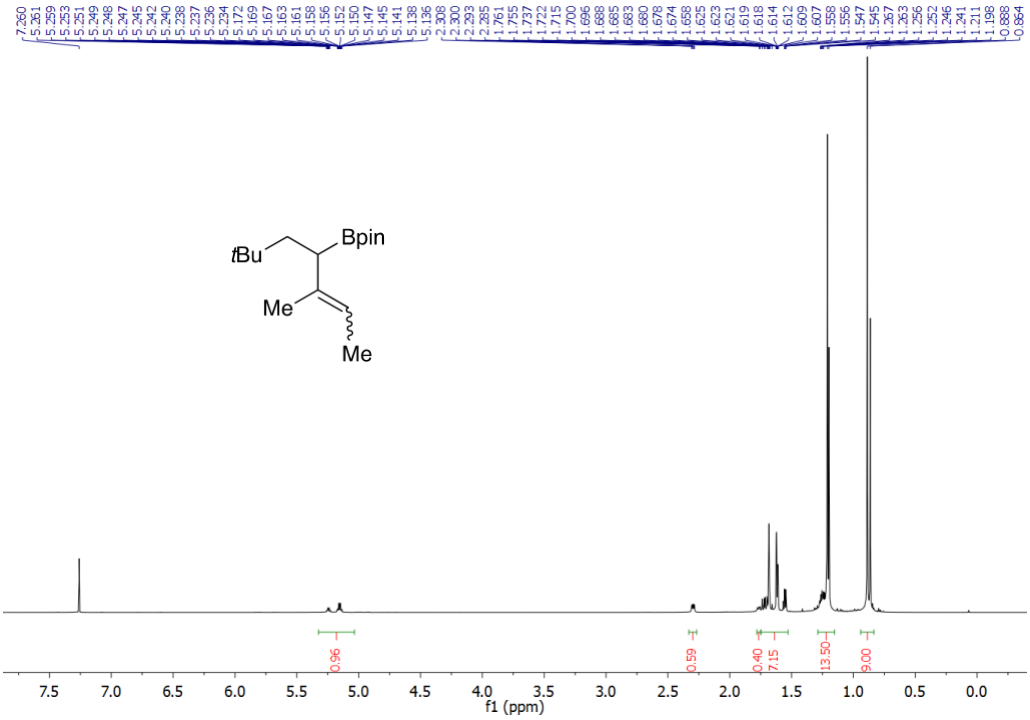

HRMS (DART) calcd for $C_{16}H_{32}BO_2$ $[M+H]^+$ *m/z* = 267.2495; found 267.2499.

5.4.w

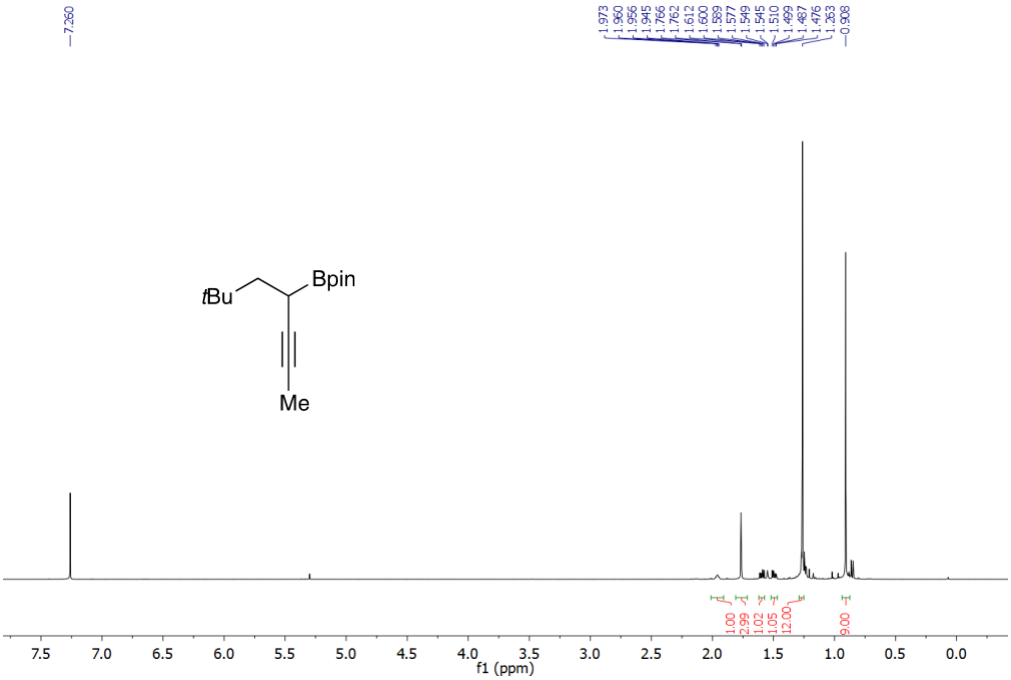

HRMS (DART) calcd for $C_{15}H_{28}BO_2$ $[M+H]^+$ *m/z* = 251.2182; found 251.2175.

5.4.a'

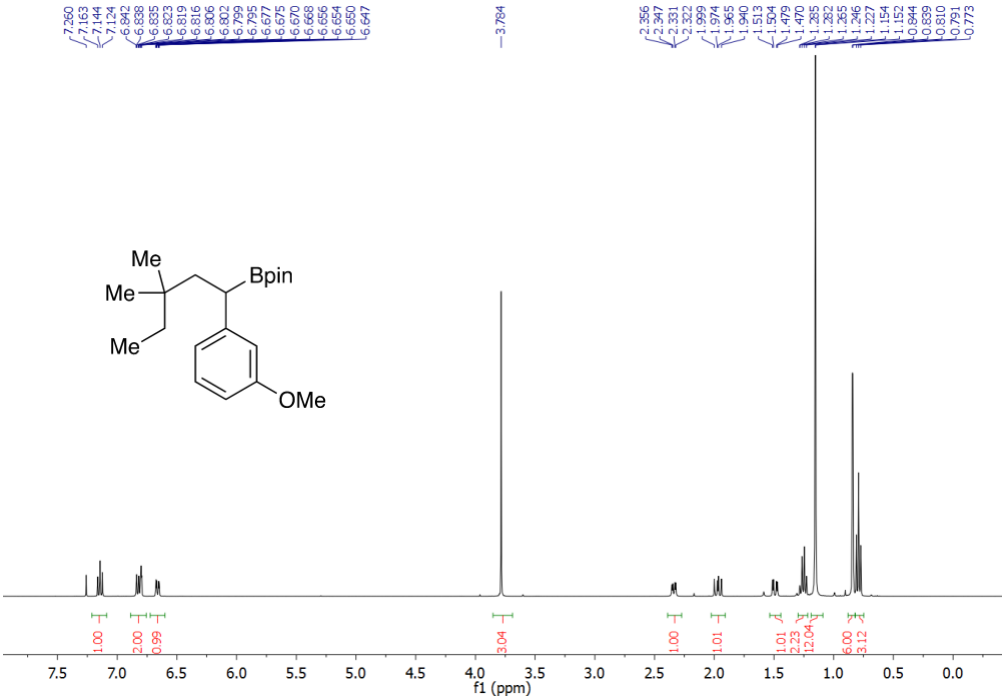

HRMS (DART) calcd for $C_{20}H_{34}BO_3$ $[M+H]^+$ *m/z* = 333.2601; found 333.2595.

5.4.b'

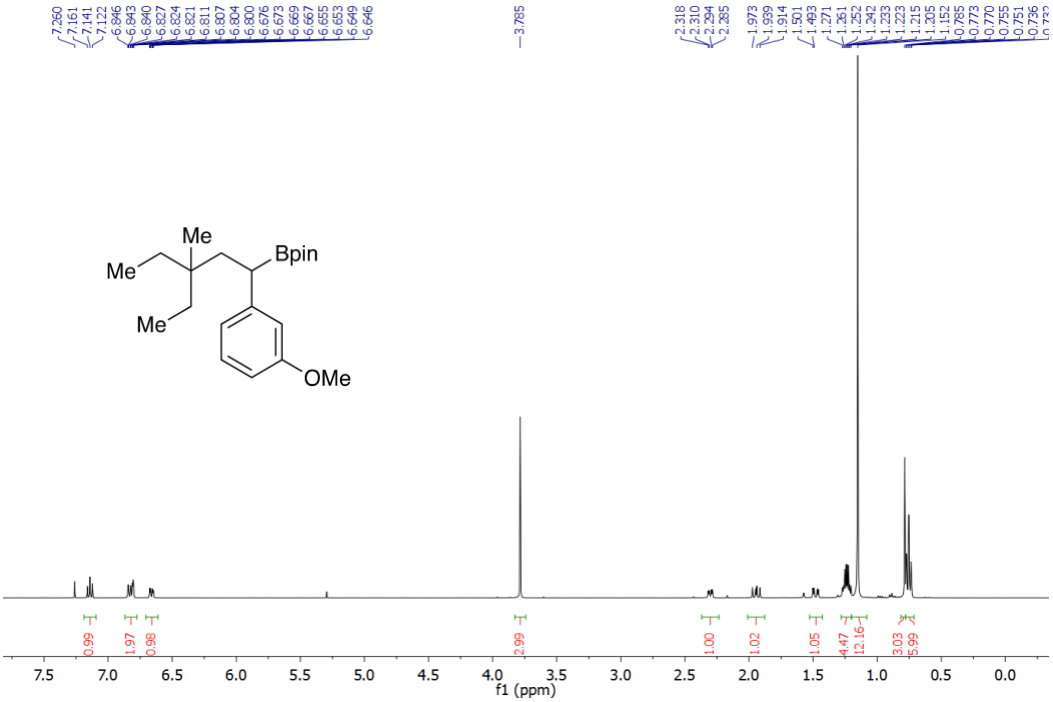

HRMS (DART) calcd for $C_{21}H_{36}BO_3$ $[M+H]^+$ *m/z* = 347.2758; found 347.2764.

5.4.g'

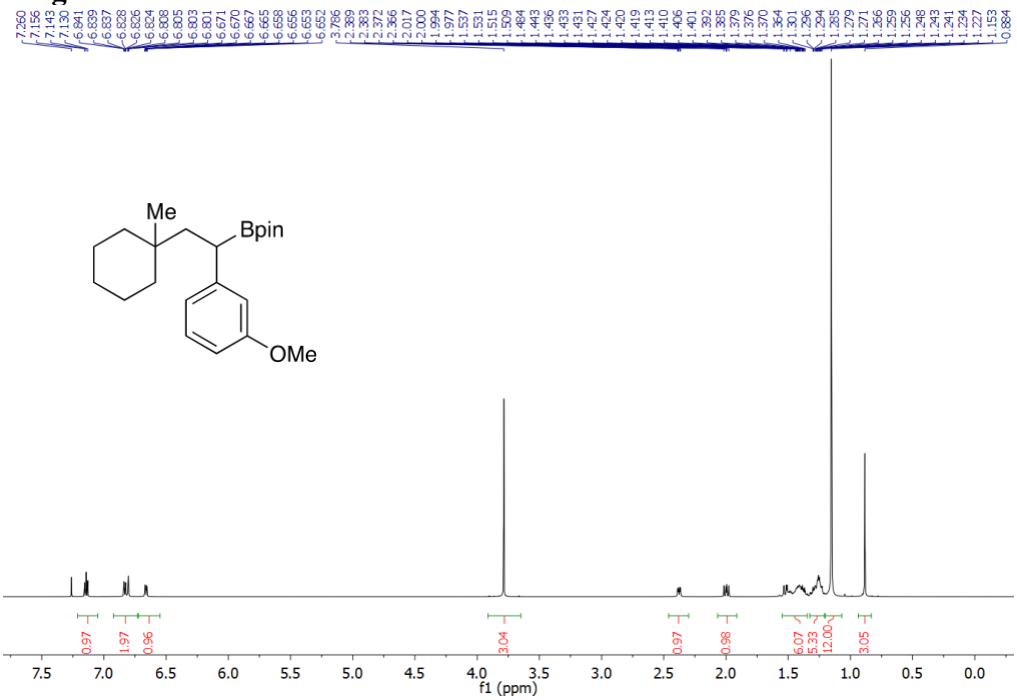

HRMS (DART) calcd for $C_{22}H_{36}BO_3$ $[M+H]^+$ *m/z* = 359.2758; found 359.2767.

5.4.e'

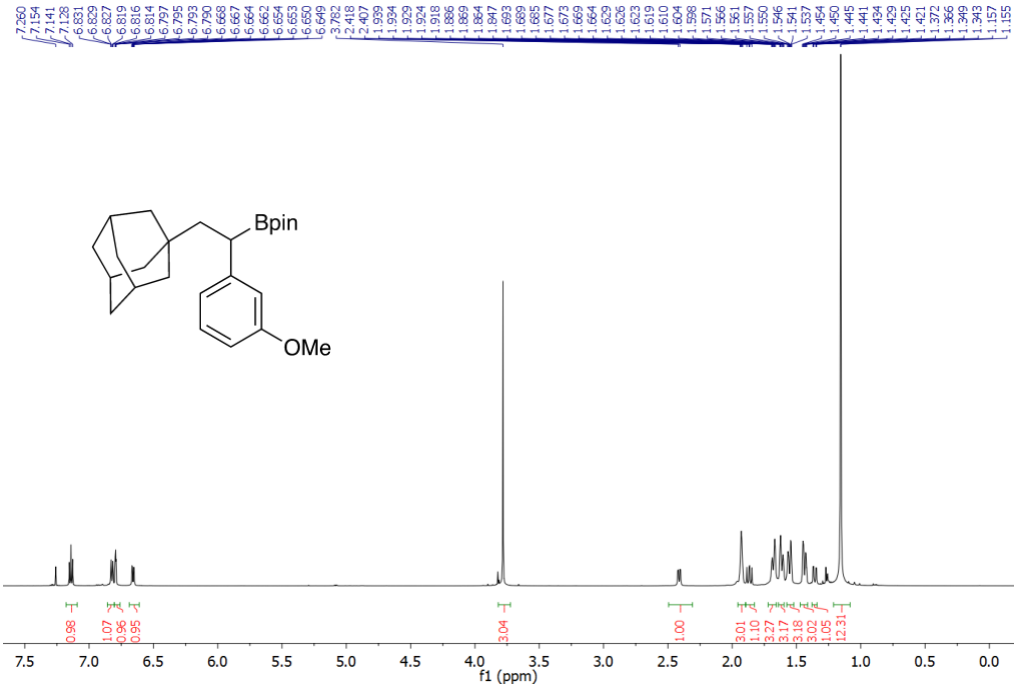

HRMS (DART) calcd for $C_{25}H_{38}BO_3$ $[M+H]^+$ *m/z* = 397.2914; found 397.2920.

5.4.f'

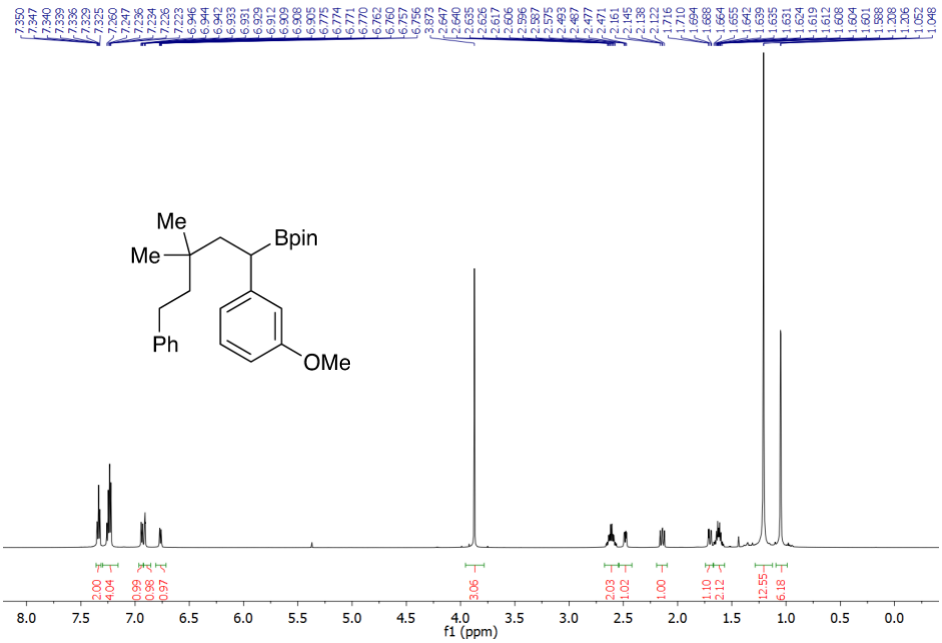

HRMS (DART) calcd for $C_{26}H_{38}BO_3$ $[M+H]^+$ *m/z* = 409.2914; found 409.2919.

5.4.g'

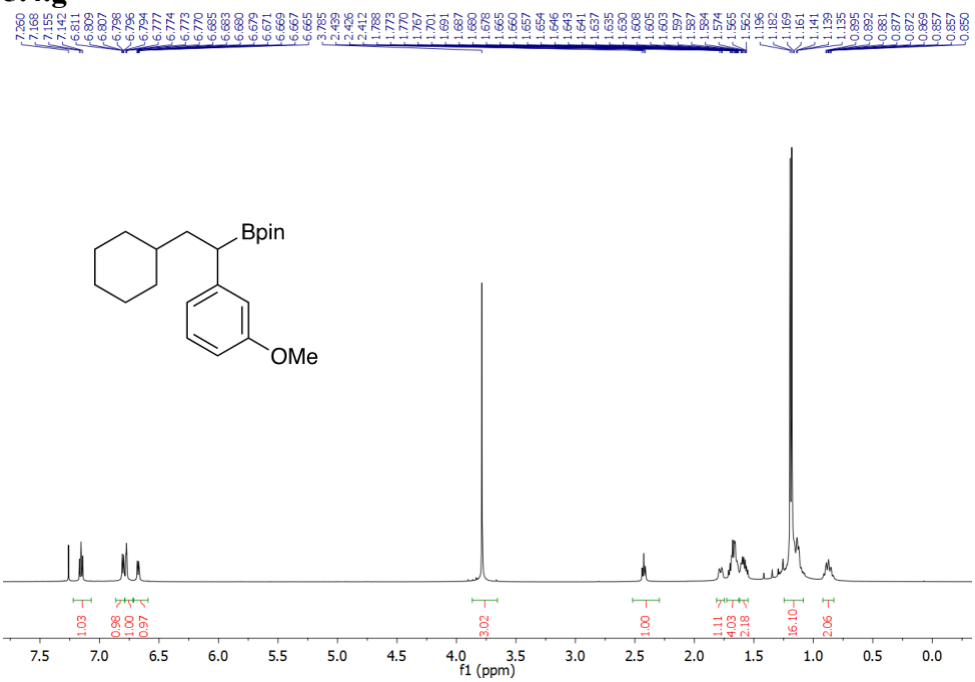

HRMS (DART) calcd for $C_{21}H_{34}BO_3$ $[M+H]^+$ *m/z* = 345.2601; found 345.2603.

5.4.h'

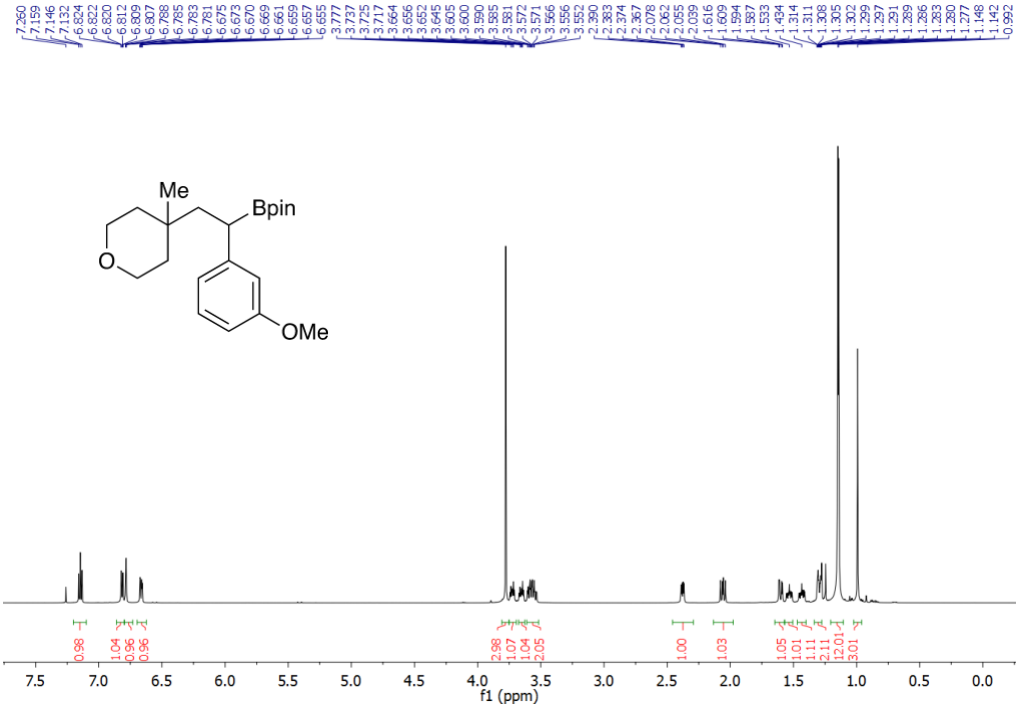

HRMS (DART) calcd for $C_{21}H_{33}BO_4$ $[M+H]^+$ *m/z* = 361.2550; found 361.2545.

5.4.i'

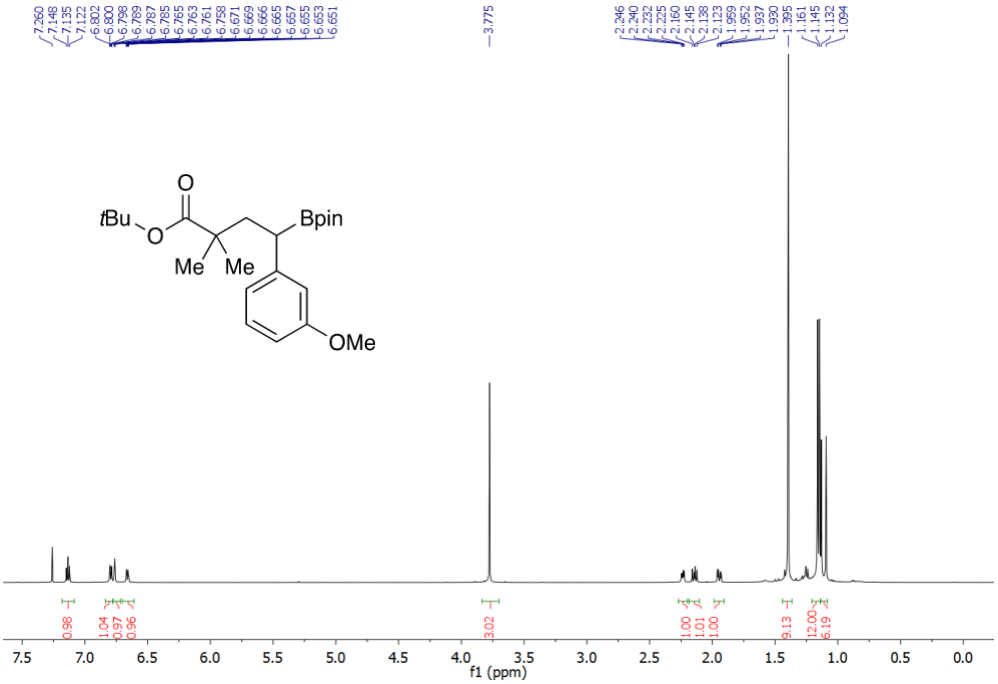

HRMS (DART) calcd for $C_{23}H_{38}BO_5$ $[M+H]^+$ *m/z* = 405.2812; found 405.2808.

5.4.j'

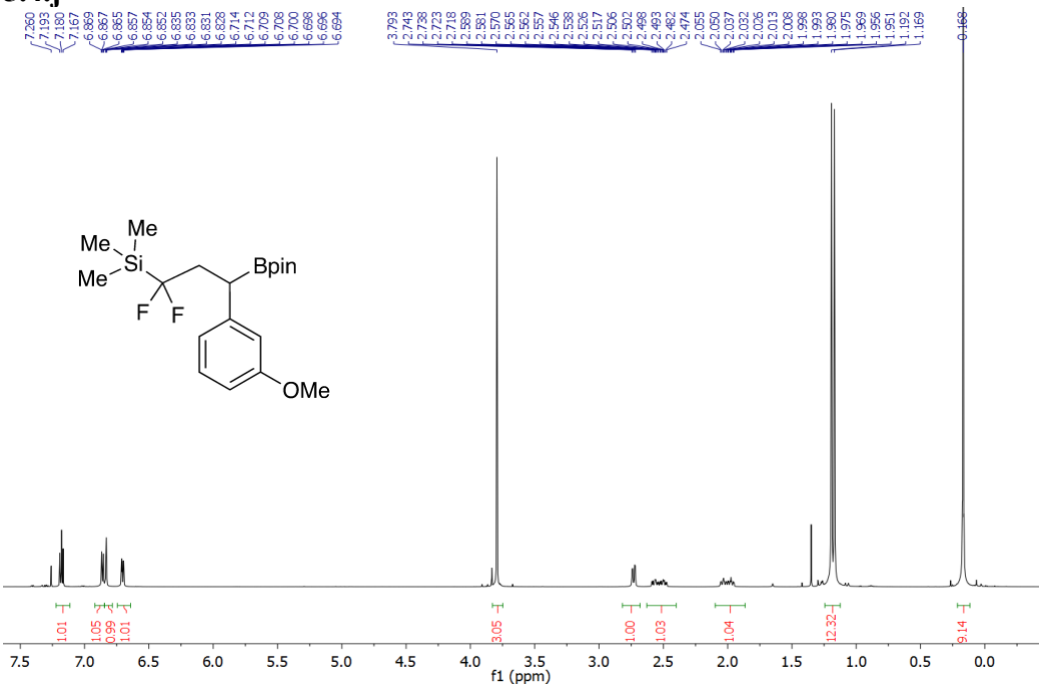

HRMS (DART) calcd for $C_{19}H_{32}BF_2O_3Si$ $[M+H]^+$ *m/z* = 385.2182; found 385.2188.

5.4.l'

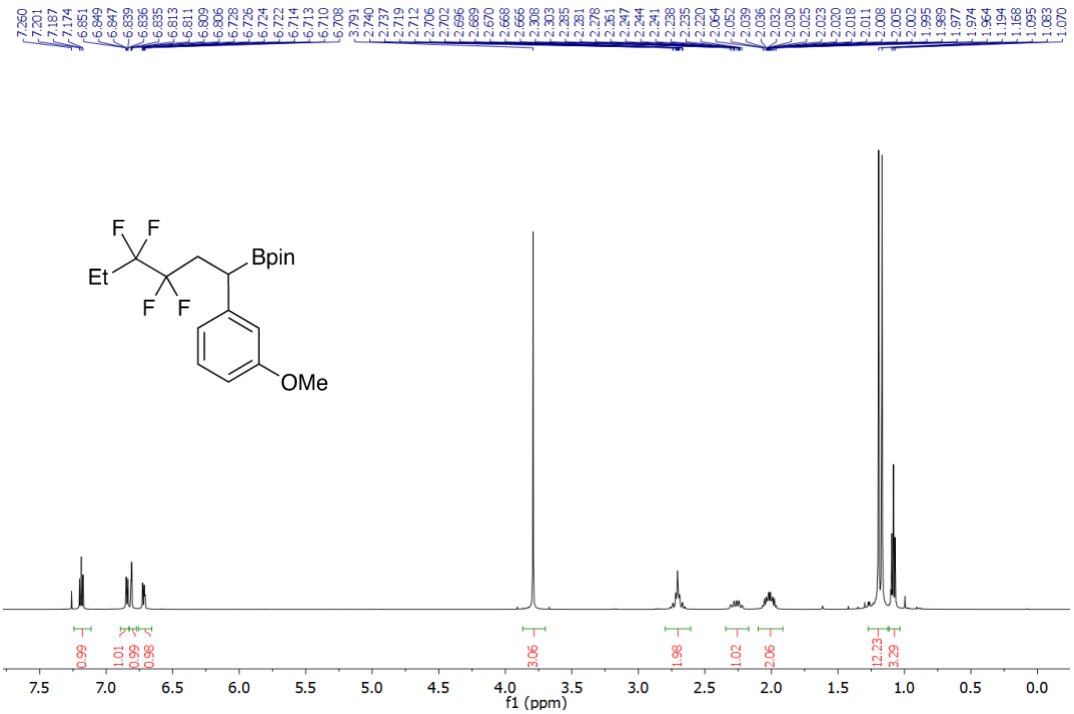

HRMS (DART) calcd for $C_{19}H_{28}BF_4O_3$ $[M+H]^+$ *m/z* = 391.2068; found 391.2068.

5.4.m'

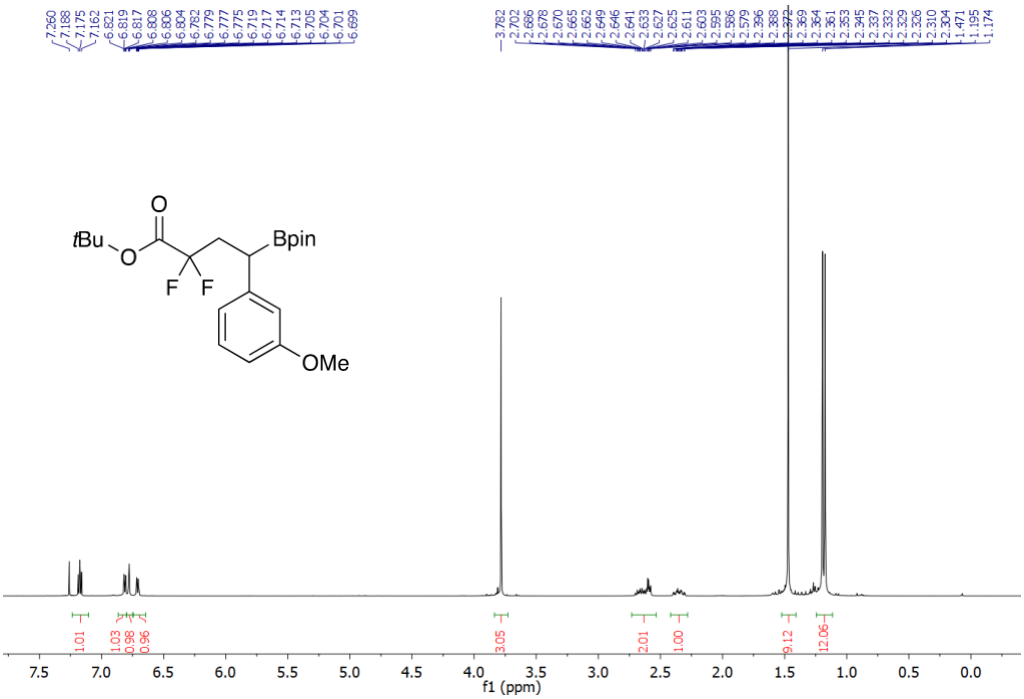

HRMS (DART) calcd for $C_{21}H_{35}BF_2NO_5$ $[M+NH_4]^+$ *m/z* = 430.2576; found 430.2573.

5.4.n'

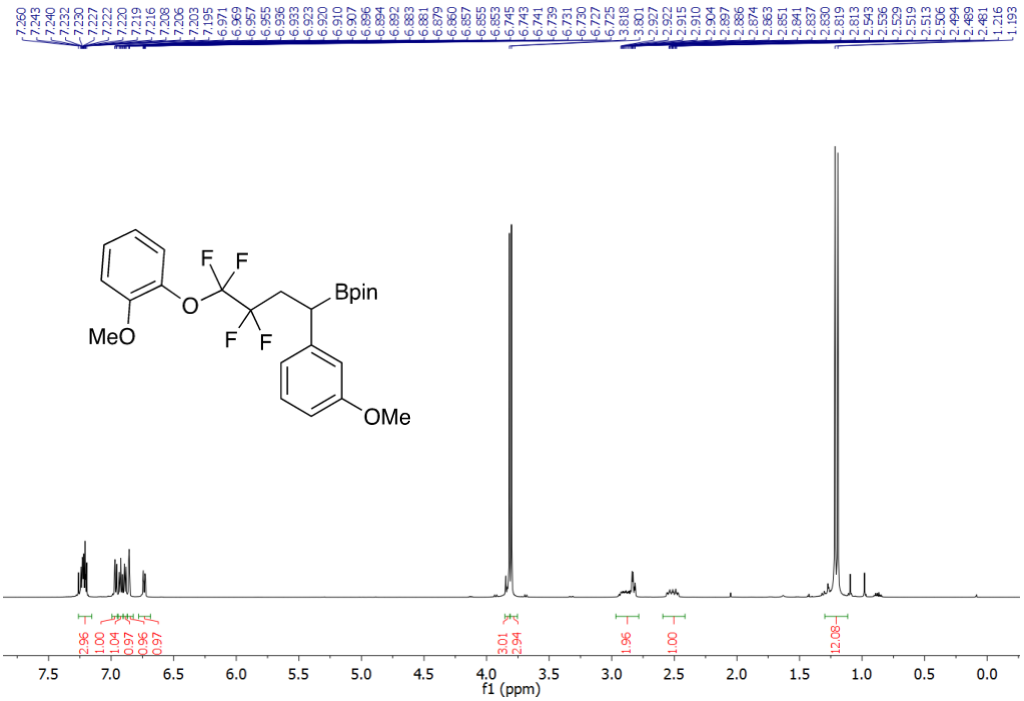

HRMS (DART) calcd for $C_{24}H_{30}BF_4O_5$ $[M+H]^+$ *m/z* = 485.2122; found 485.2115.

5.4.o'

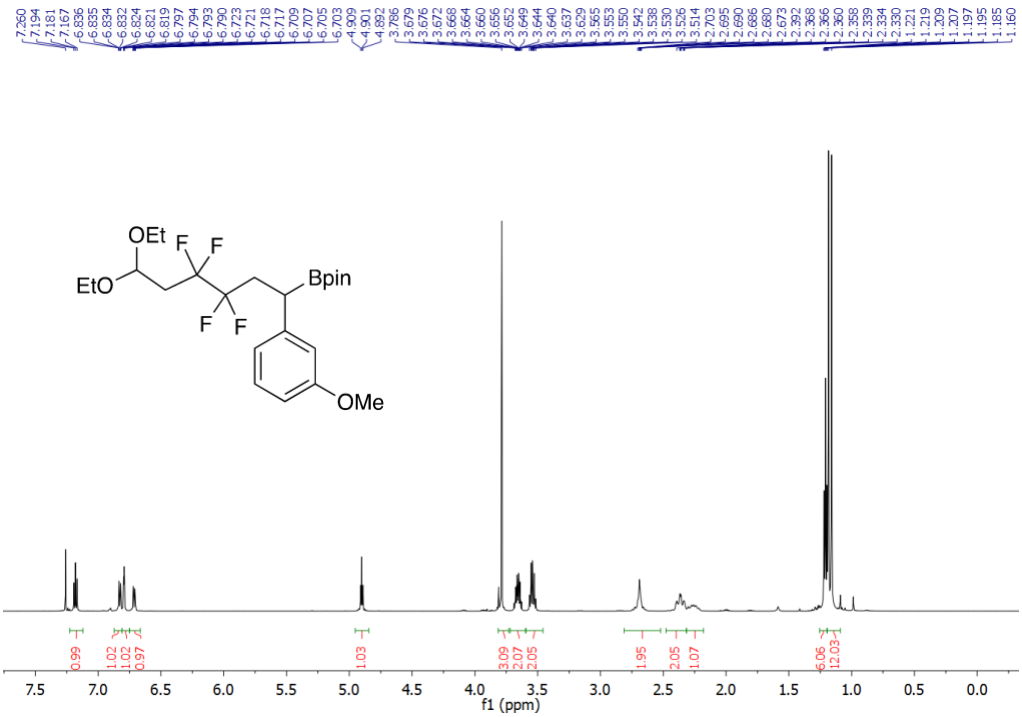

HRMS (DART) calcd for $C_{23}H_{39}BF_4NO_5$ $[M+NH_4]^+$ *m/z* = 496.2857; found 496.2862.

5.4.p'

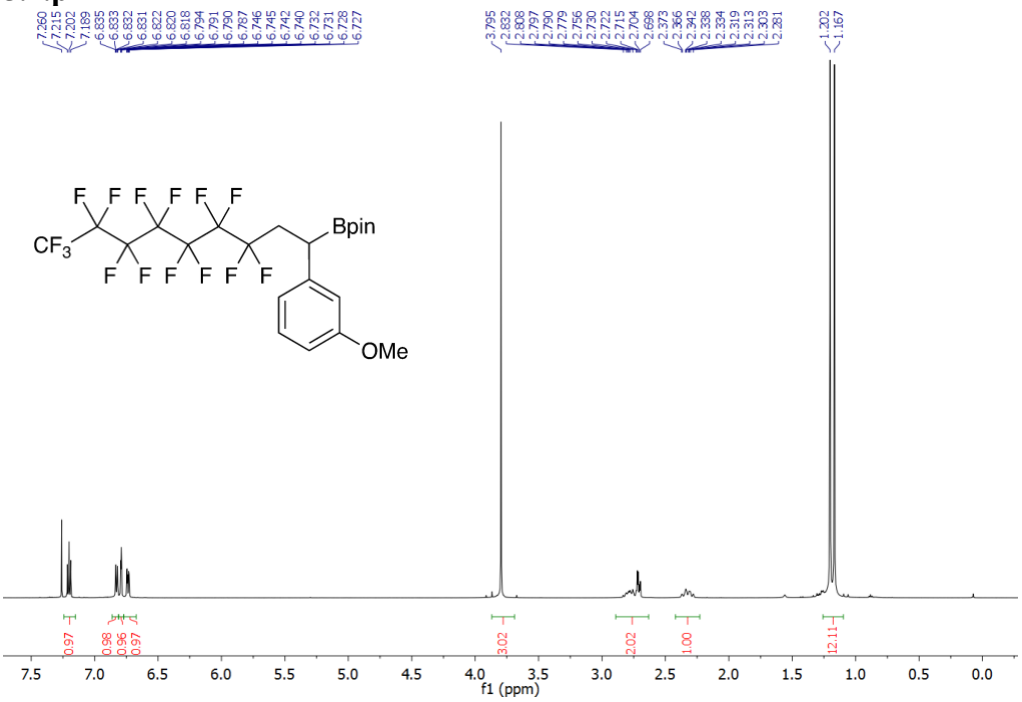

HRMS (DART) calcd for $C_{22}H_{23}BF_{15}O_3$ $[M+H]^+$ *m/z* = 631.1501; found 631.1488.

5.6.a

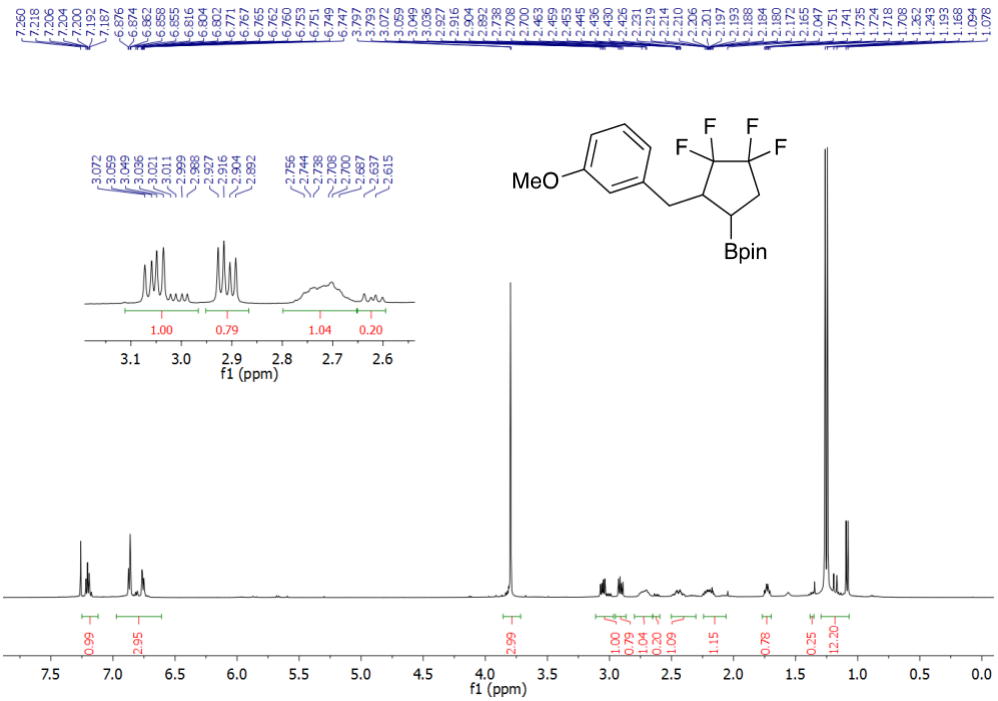

HRMS (DART) calcd for $C_{19}H_{26}BF_4O_3$ $[M+H]^+$ *m/z* = 389.1911; found 389.1914.

5.6.b

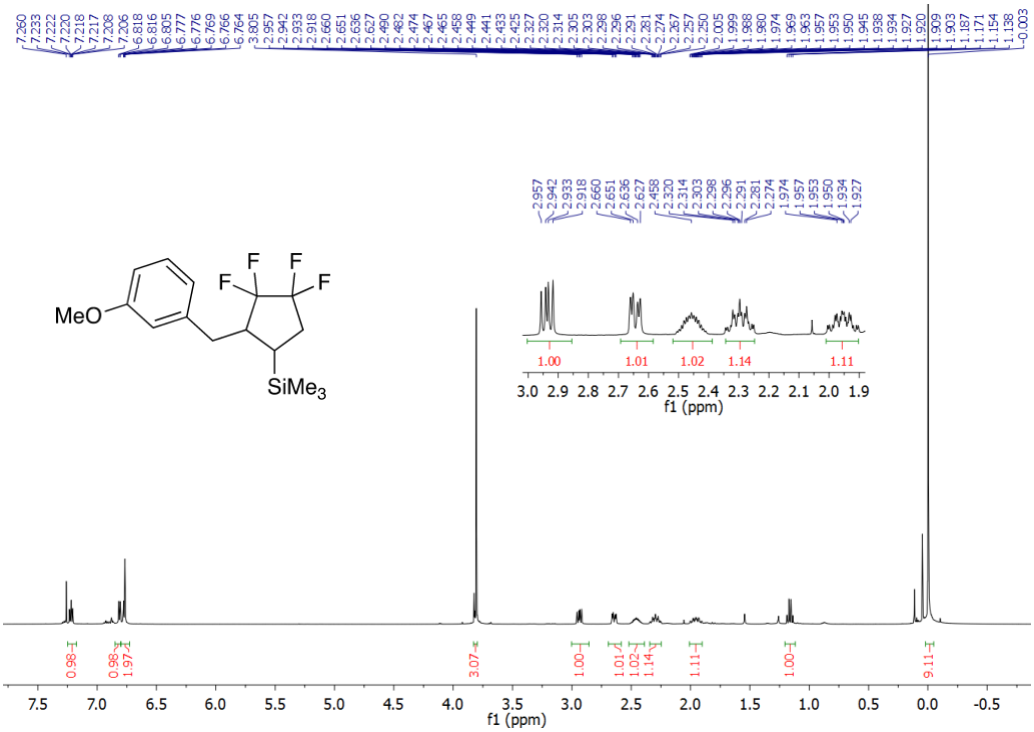

HRMS (DART) calcd for $C_{16}H_{23}F_4OSi$ $[M+H]^+$ *m/z* = 335.1454; found 335.1456.

5.6.c

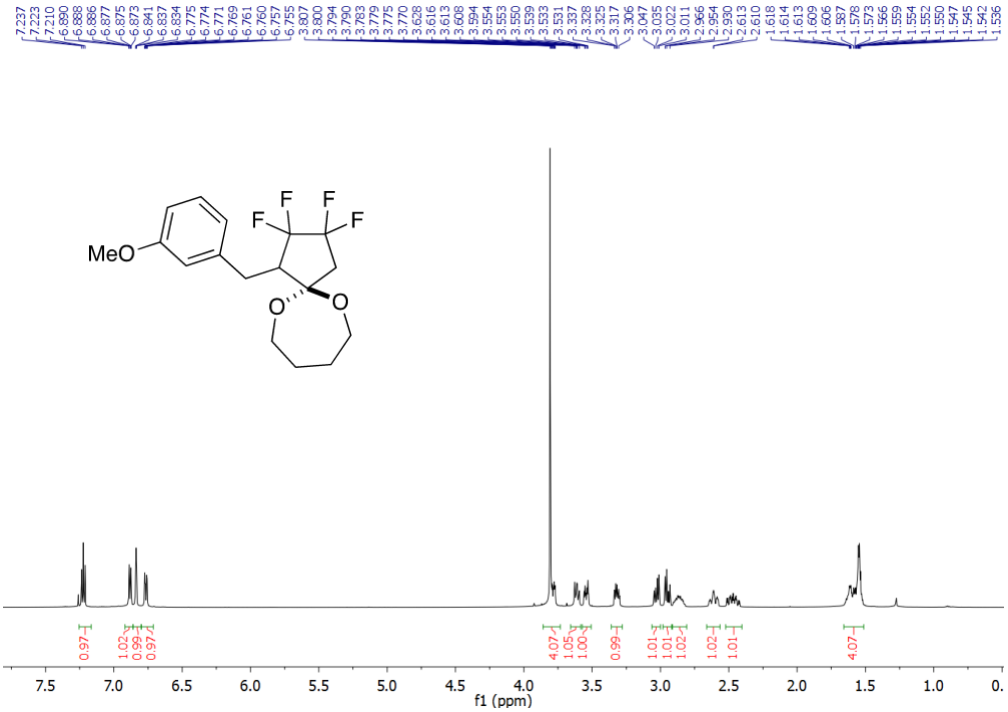

HRMS (DART) calcd for $C_{17}H_{24}F_4NO_3$ $[M+NH_4]^+$ *m/z* = 366.1692; found 366.1691.

5.6.d

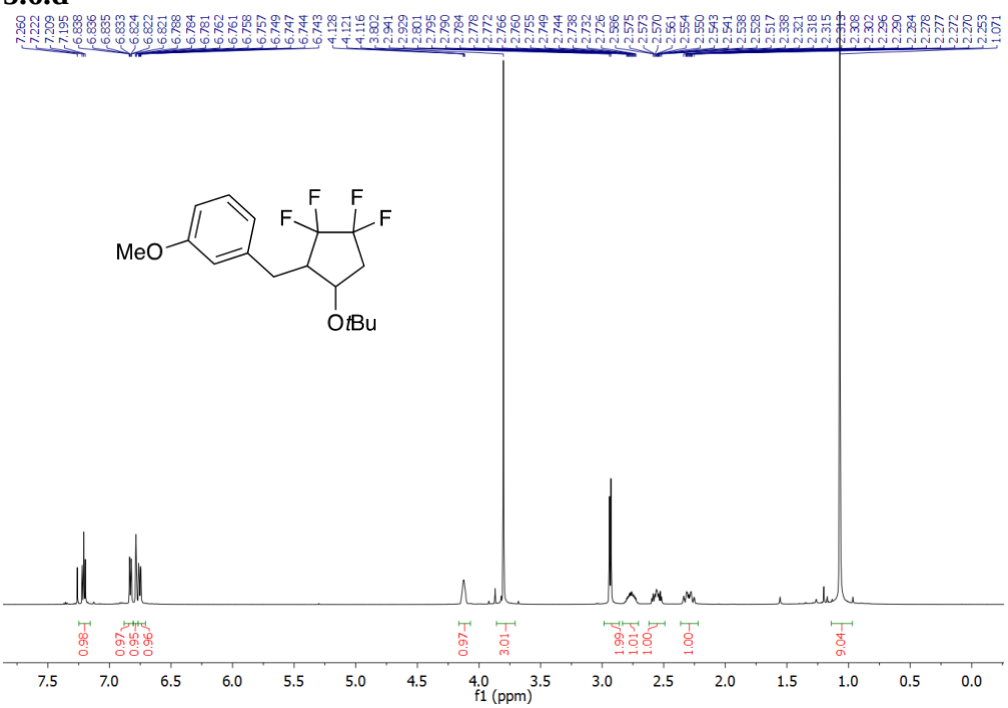

HRMS (DART) calcd for $C_{17}H_{23}F_4O_2$ $[M+H]^+$ *m/z* = 335.1634; found 335.1634.

5.6.e

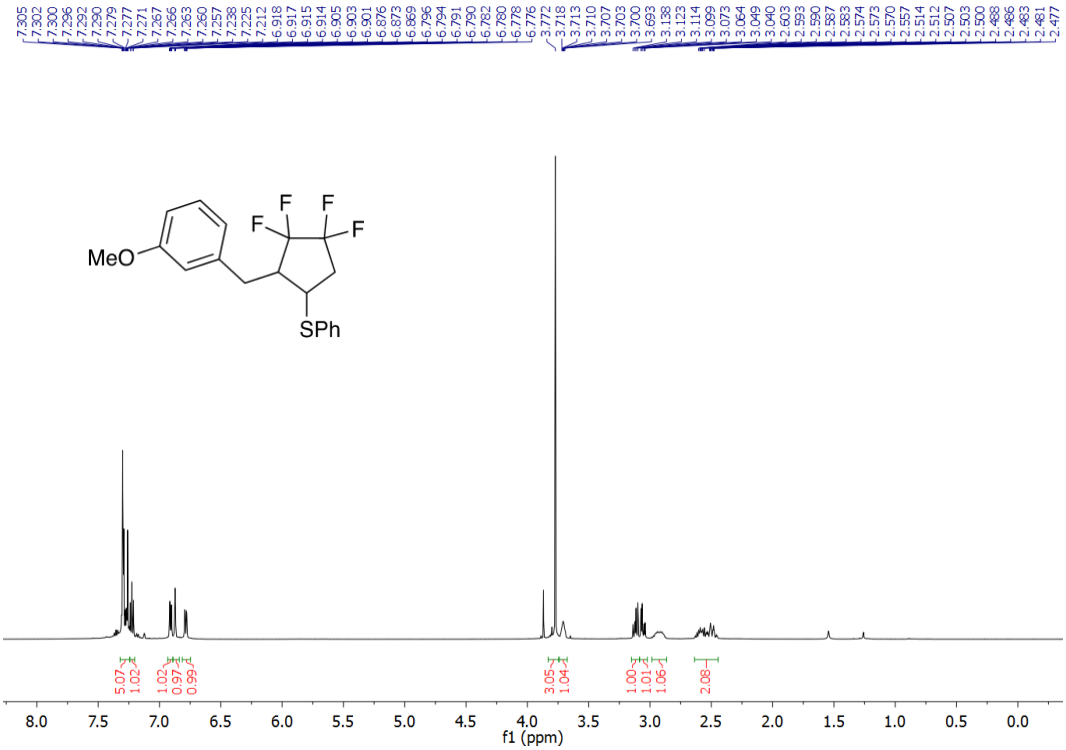

HRMS (DART) calcd for $C_{19}H_{19}F_4O_2S$ $[M+H]^+$ *m/z* = 371.1093; found 371.1090.

5.6.h

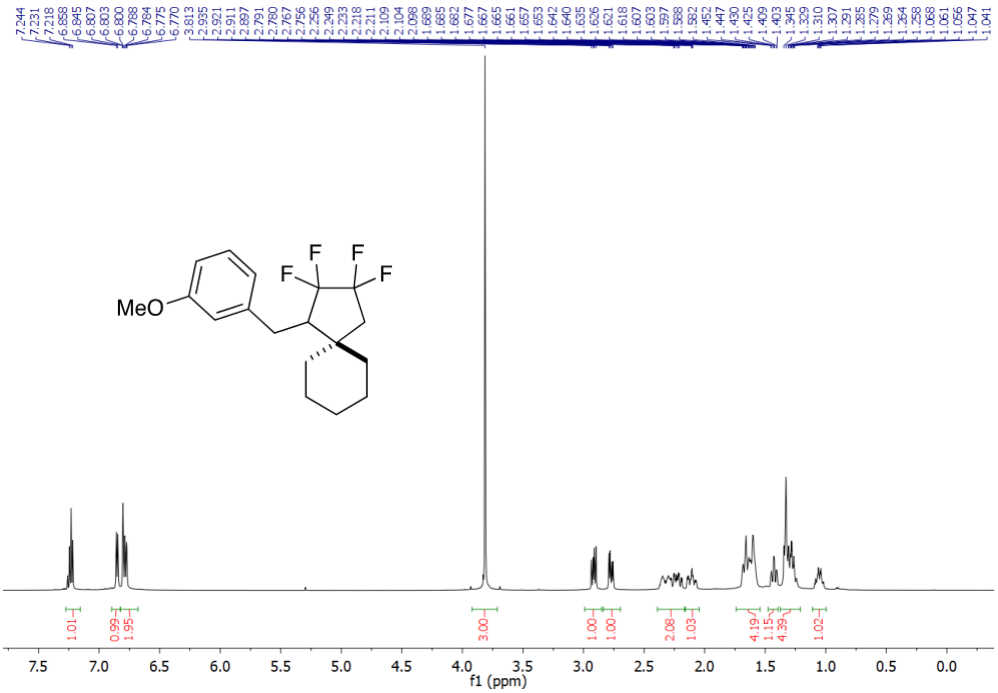

HRMS (DART) calcd for $C_{18}H_{23}F_4O$ $[M+H]^+$ *m/z* = 331.1685; found 331.1685.

5.6.i

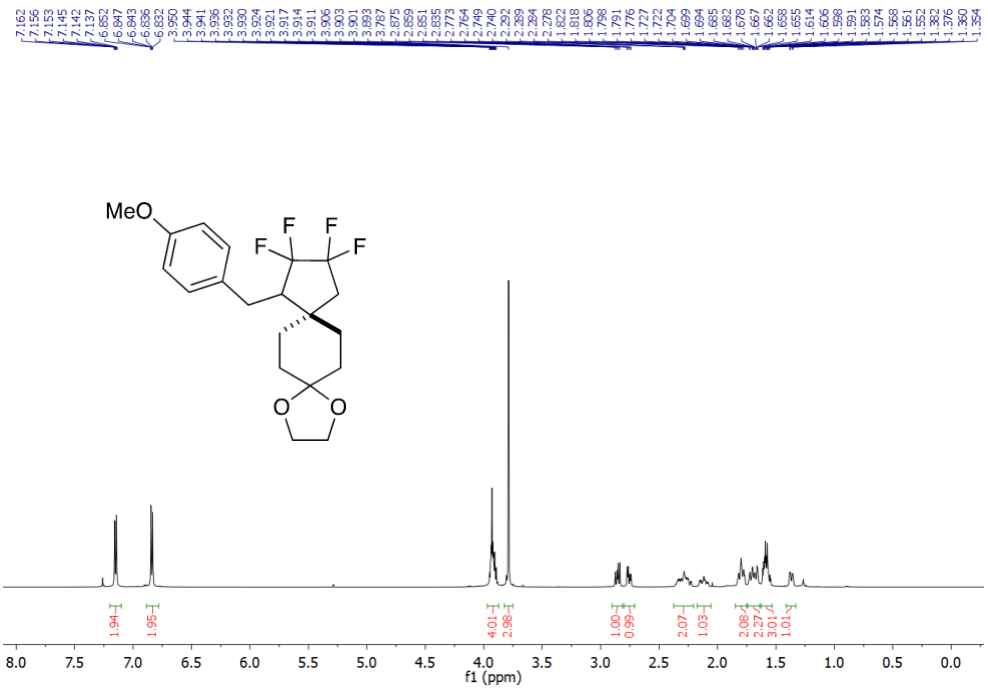

HRMS (DART) calcd for $C_{20}H_{25}F_4O_3$ $[M+H]^+$ *m/z* = 389.1740; found 389.1734.

5.6.f

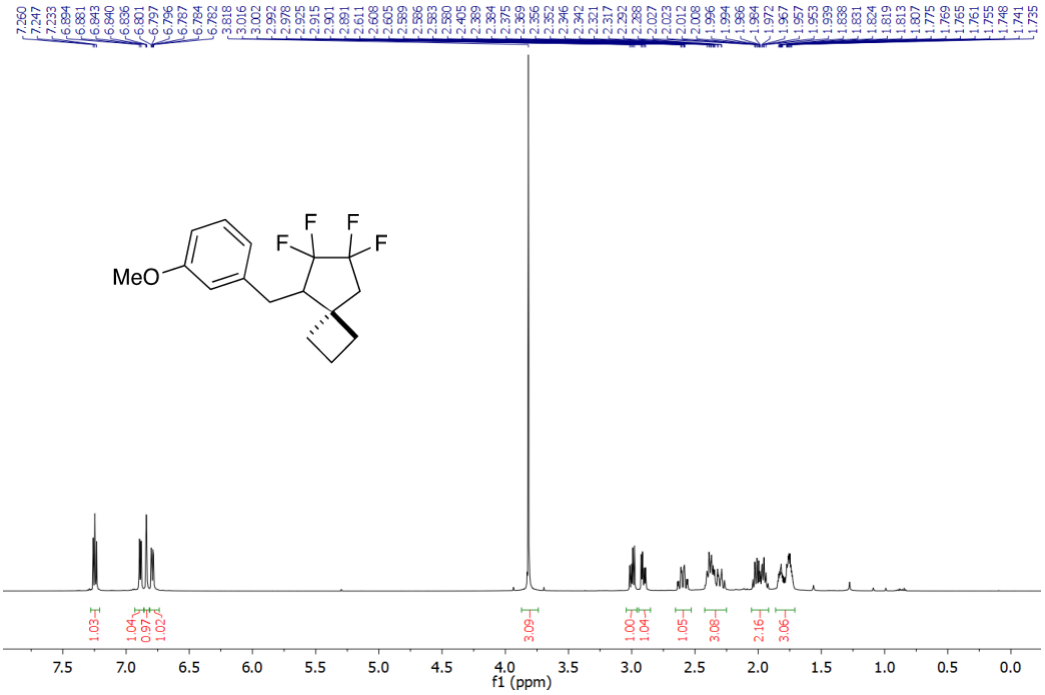

HRMS (DART) calcd for $C_{16}H_{19}F_4O$ $[M+H]^+$ *m/z* = 303.1372; found 303.1374.

5.6.j

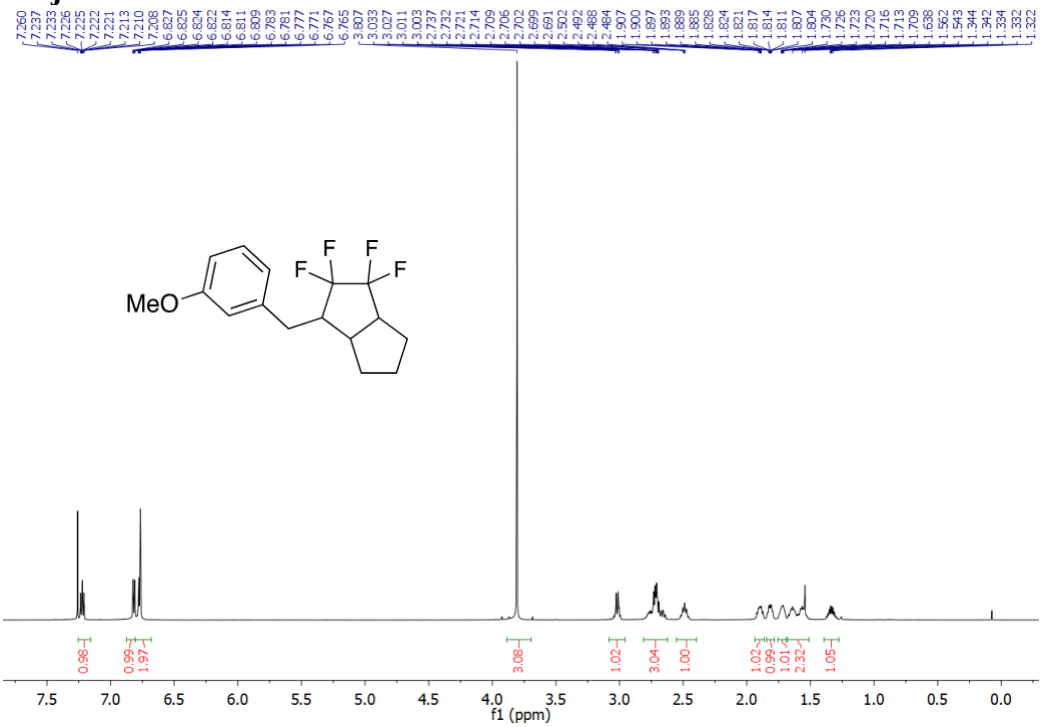

HRMS (DART) calcd for $C_{16}H_{19}F_4O$ $[M+H]^+$ *m/z* = 303.1372; found 303.1376.

5.6.l

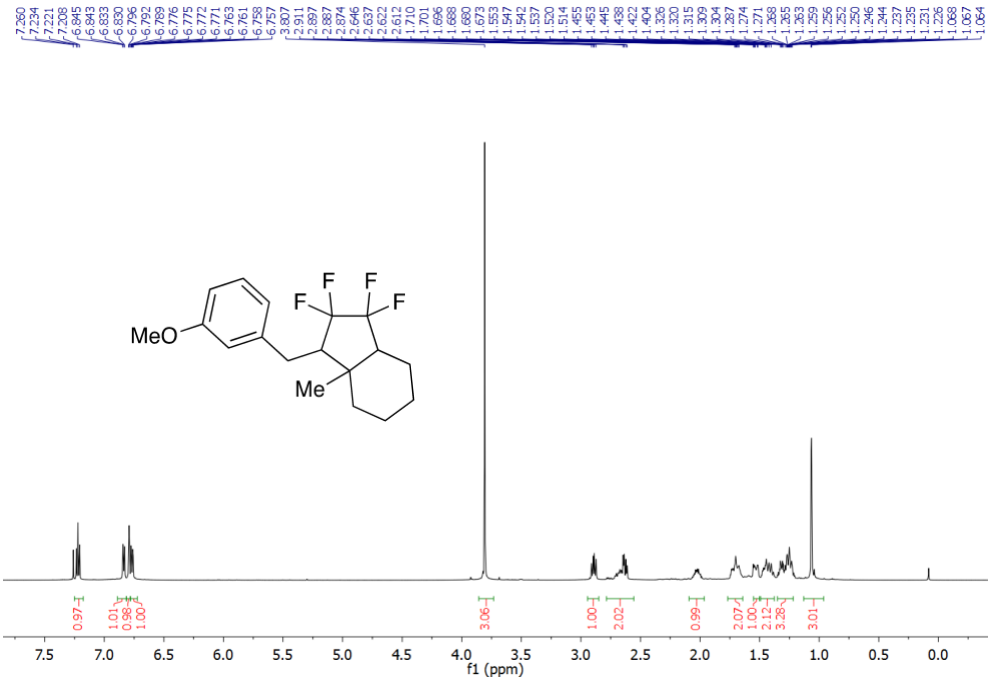

HRMS (DART) calcd for $C_{18}H_{23}F_4O$ $[M+H]^+$ *m/z* = 331.1685; found 331.1688.

5.6.k

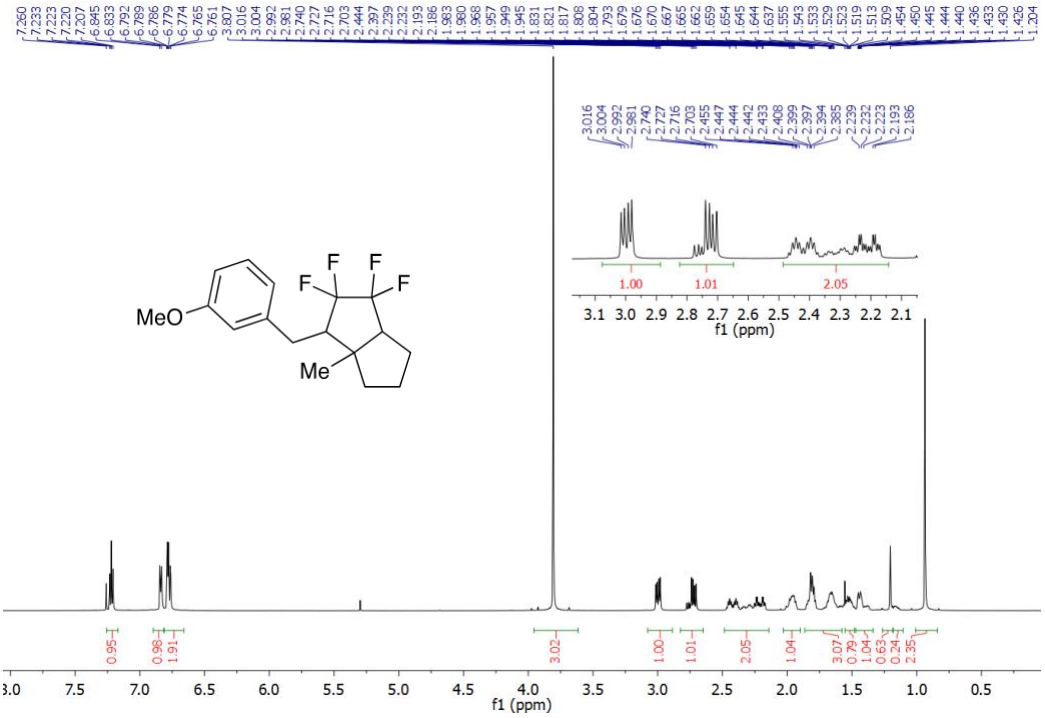

HRMS (DART) calcd for $C_{17}H_{21}F_4O$ $[M+H]^+$ *m/z* = 317.1529; found 317.1524.

5.6.m

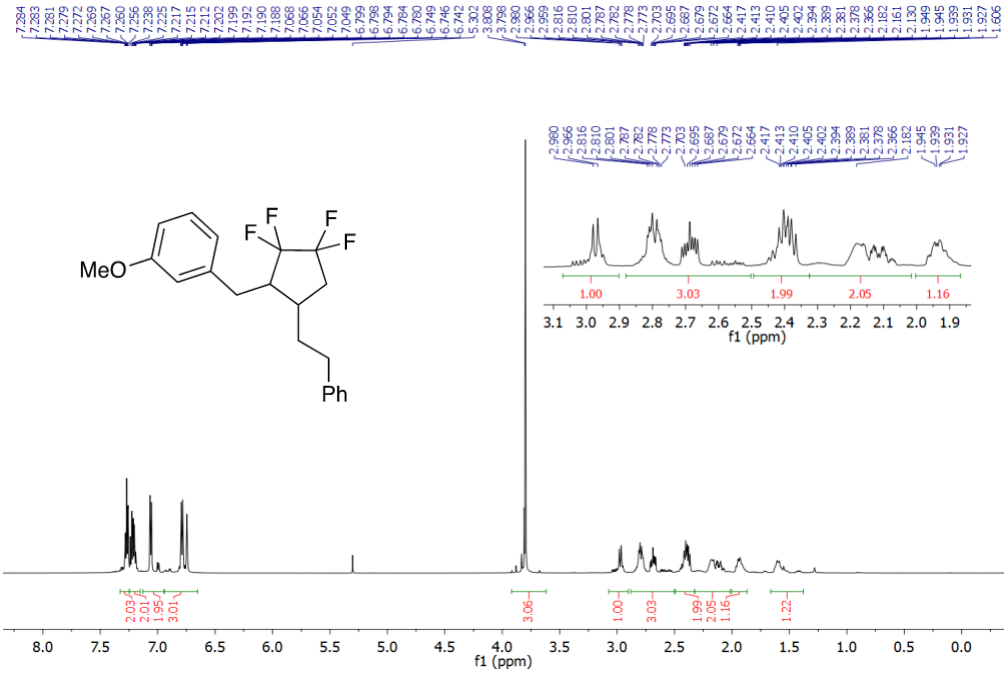

HRMS (DART) calcd for $C_{21}H_{23}F_4O$ $[M+H]^+$ *m/z* = 367.1685; found 367.1689.

5.6.n

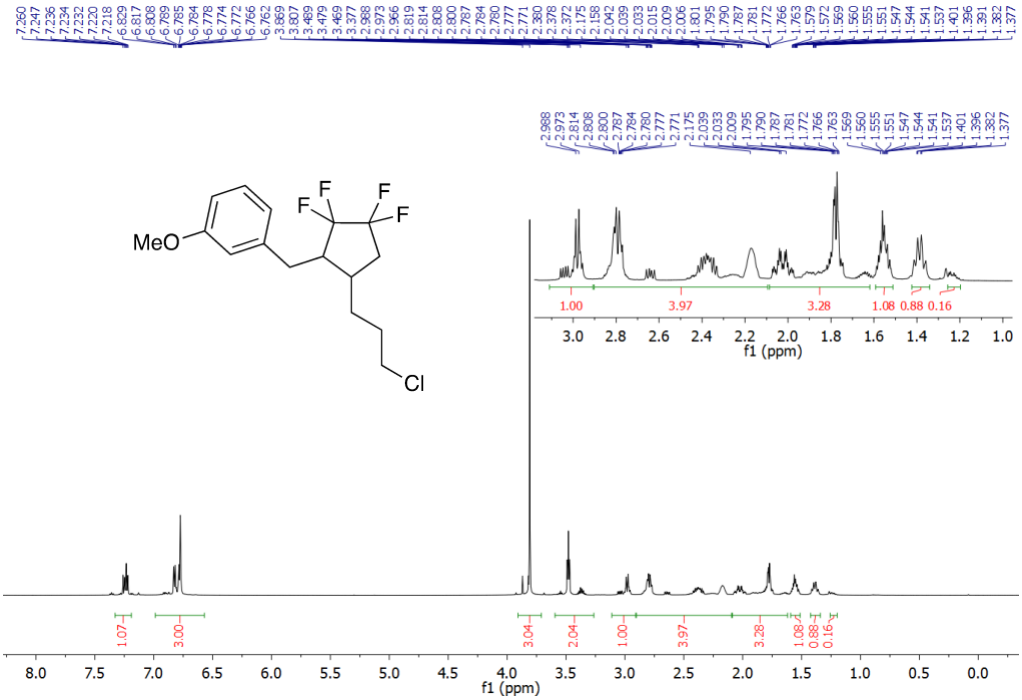

HRMS (DART) calcd for $C_{16}H_{20}ClF_4O$ $[M+H]^+$ *m/z* = 339.1139; found 339.1137.

5.6.o

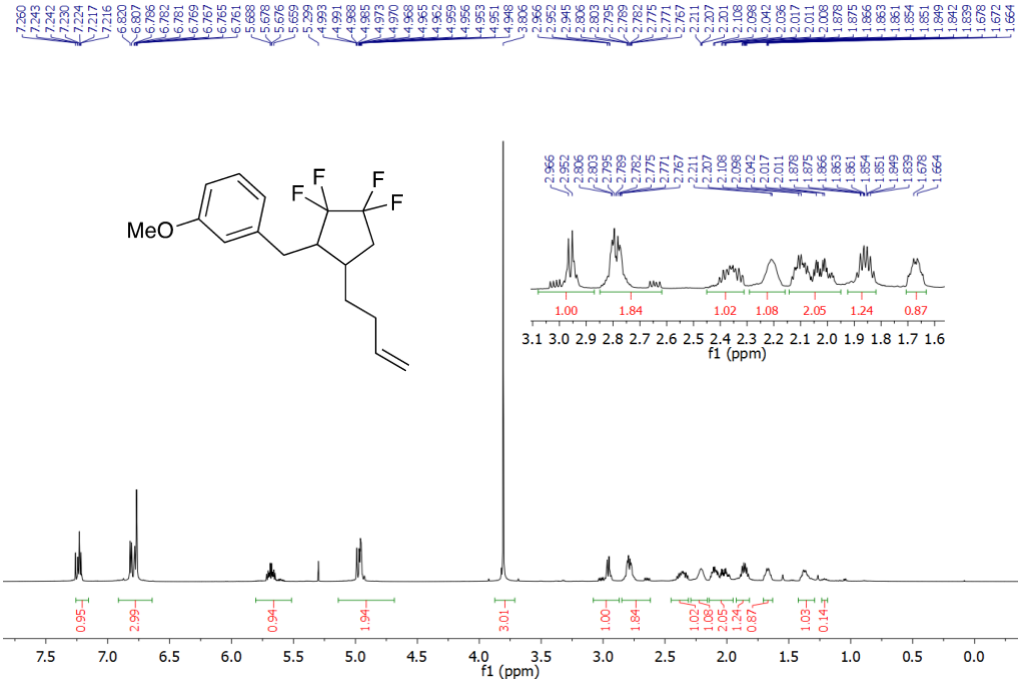

HRMS (DART) calcd for $C_{17}H_{21}F_4O$ $[M+H]^+$ *m/z* = 317.1529; found 317.1528.

5.6.p

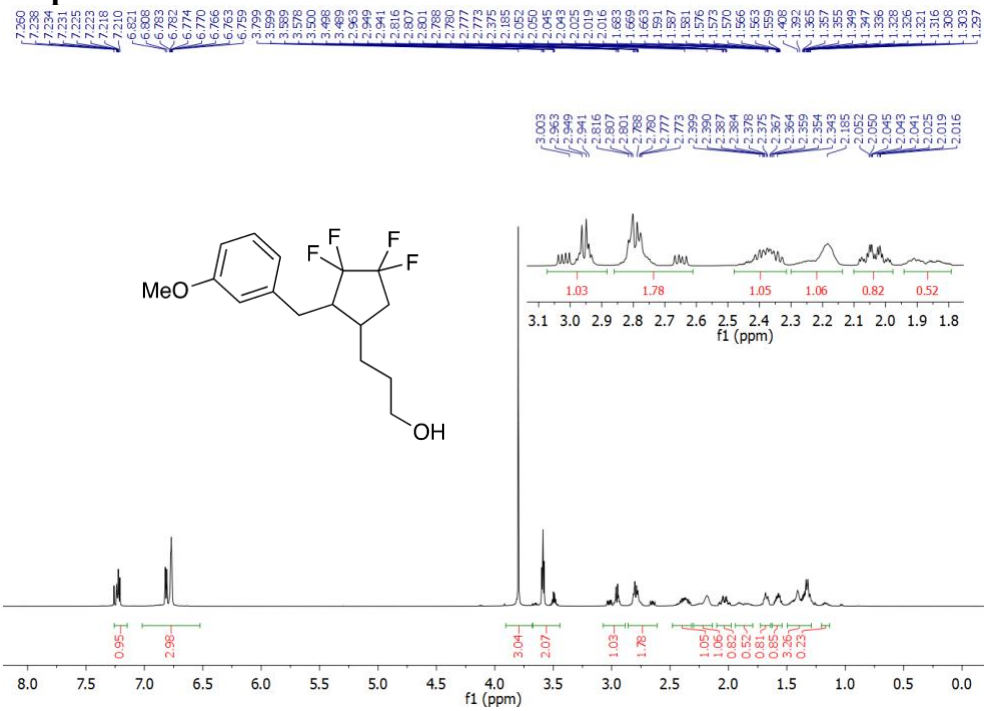

HRMS (DART) calcd for $C_{16}H_{21}F_4O_2$ $[M+H]^+$ *m/z* = 321.1478; found 321.1481.

5.6.q

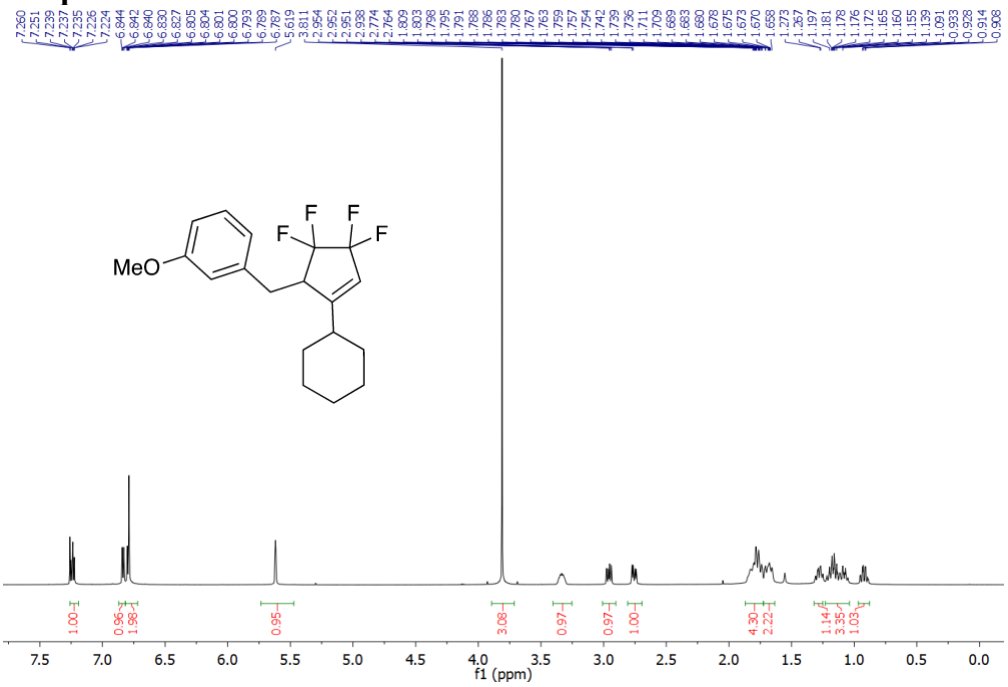

HRMS (DART) calcd for $C_{19}H_{23}F_4O$ $[M+H]^+$ *m/z* = 343.1685; found 343.1681.

5.6.r

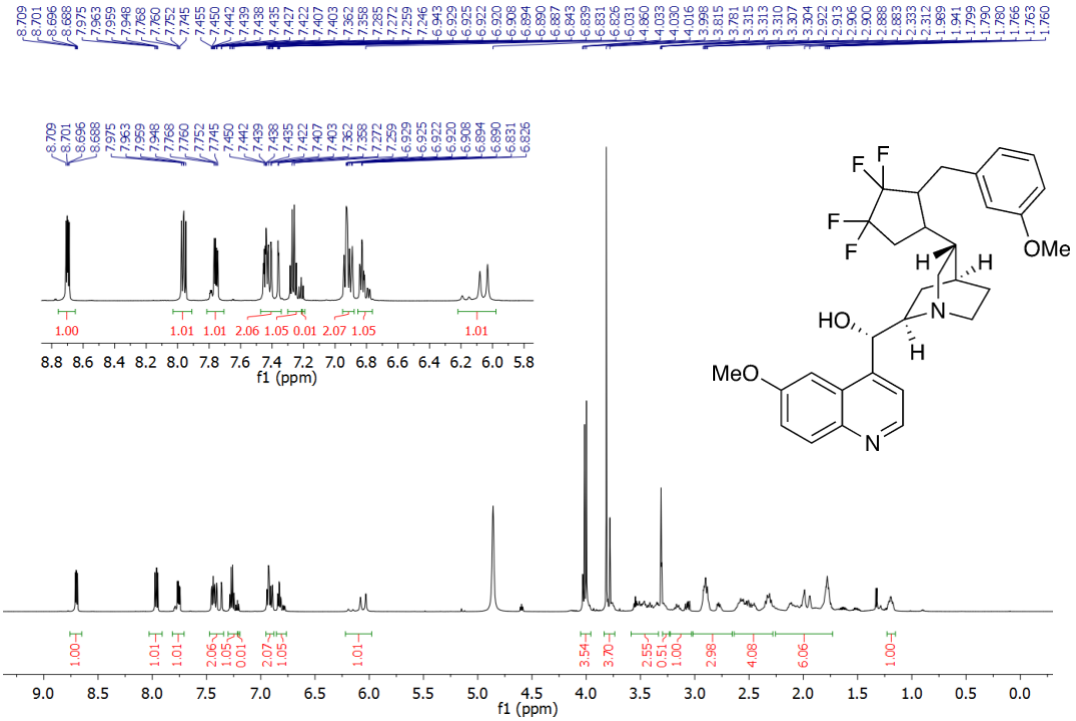

HRMS (DART) calcd for $C_{31}H_{35}F_4N_2O_3$ $[M+H]^+$ *m/z* = 559.2584; found 559.2583.

5.6.s

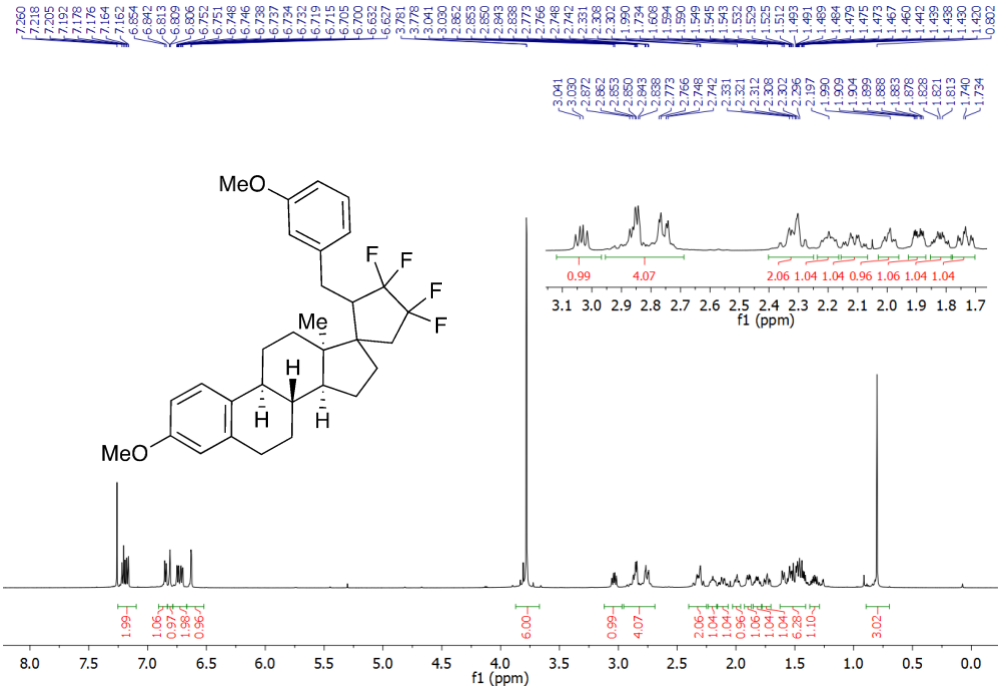

HRMS (DART) calcd for $C_{31}H_{37}F_4O_2$ $[M+H]^+$ *m/z* = 517.2730; found 517.2723.

5.6.t

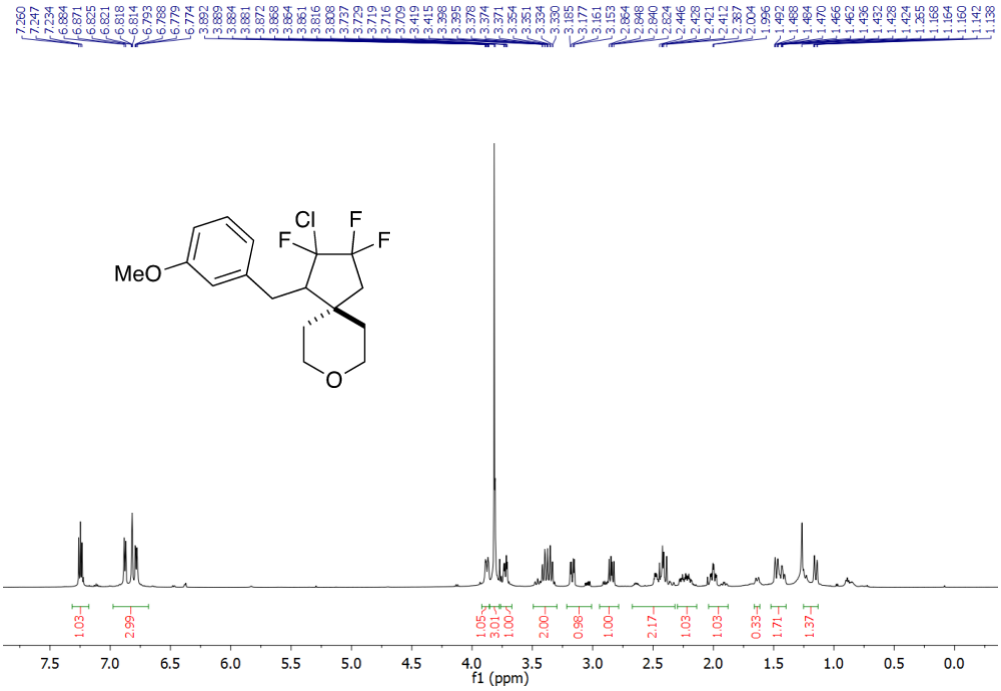

HRMS (DART) calcd for $C_{17}H_{21}ClF_3O_2$ $[M+H]^+$ *m/z* = 349.1182; found 349.1187.

5.6.u

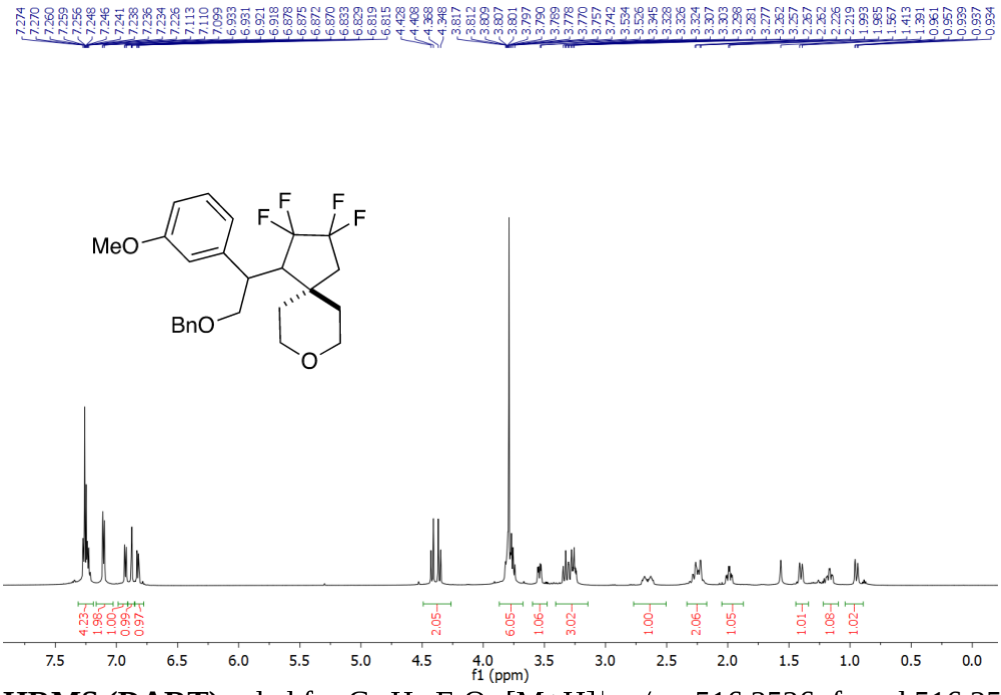

HRMS (DART) calcd for $C_{30}H_{34}F_4O_2$ $[M+H]^+$ *m/z* = 516.2526; found 516.2523.

5.6.v

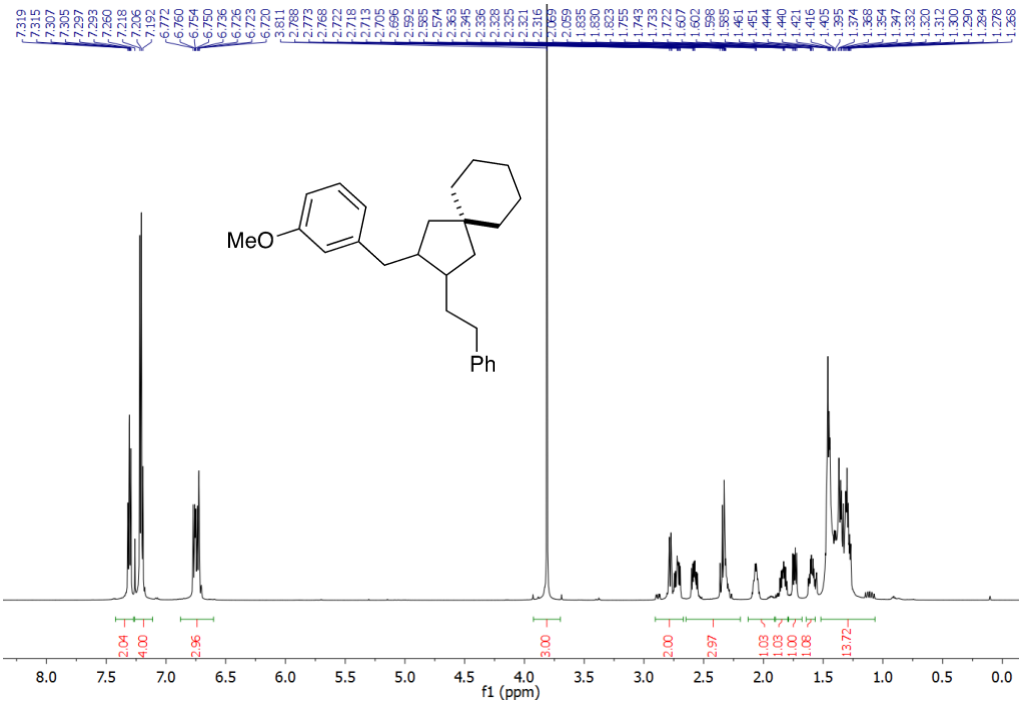

HRMS (DART) calcd for $C_{26}H_{35}O$ $[M+H]^+$ *m/z* = 363.2688; found 363.2693.

5.6.w

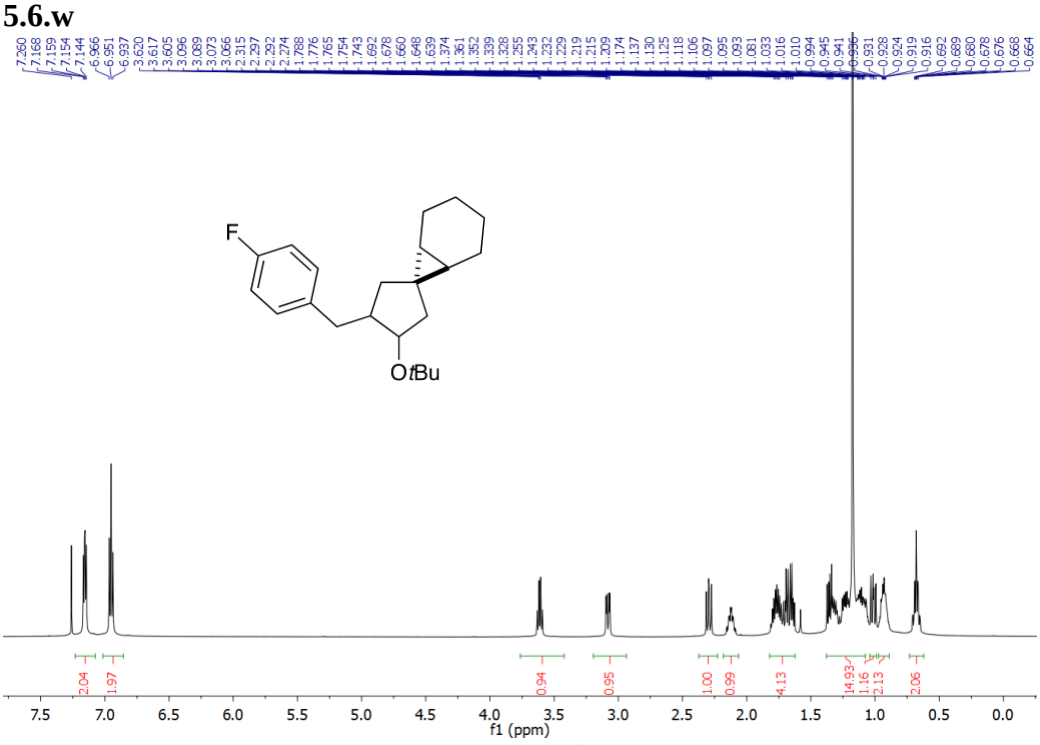

HRMS (DART) calcd for $C_{22}H_{32}FO$ $[M+H]^+$ *m/z* = 331.2437; found 331.2440.

5.7.a

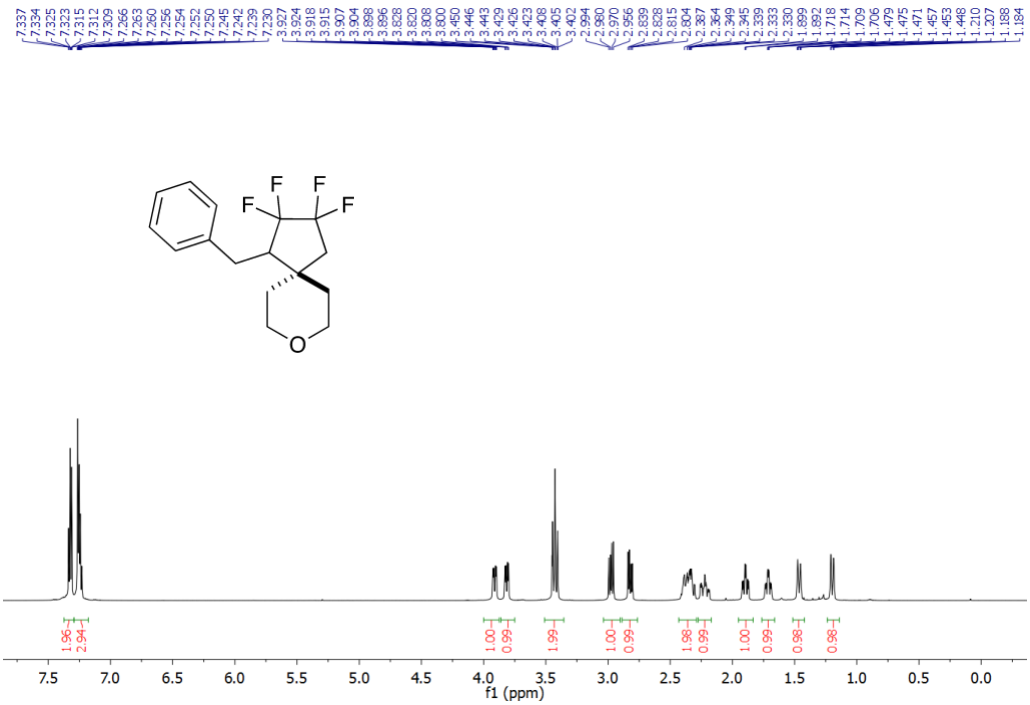

HRMS (DART) calcd for $C_{16}H_{19}F_4O$ $[M+H]^+$ *m/z* = 303.1372; found 303.1380.

5.7.b

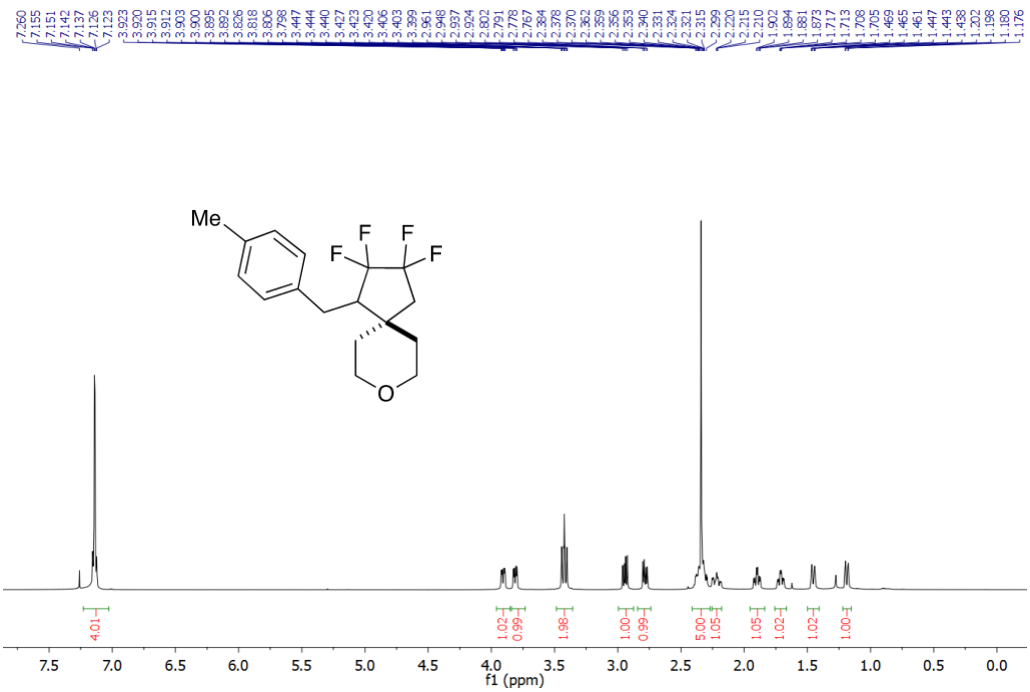

HRMS (DART) calcd for $C_{17}H_{21}F_4O$ $[M+H]^+$ *m/z* = 317.1529; found 317.1531.

5.7.c

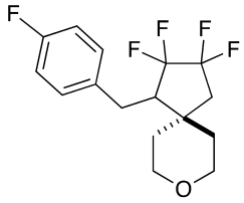

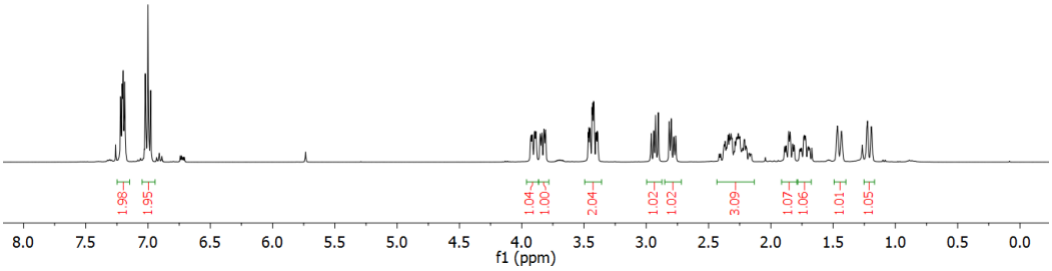

HRMS (DART) calcd for $C_{16}H_{18}F_5O$ $[M+H]^+$ *m/z* = 321.1278; found 321.1279.

5.7.d

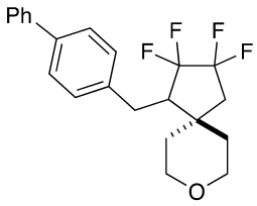

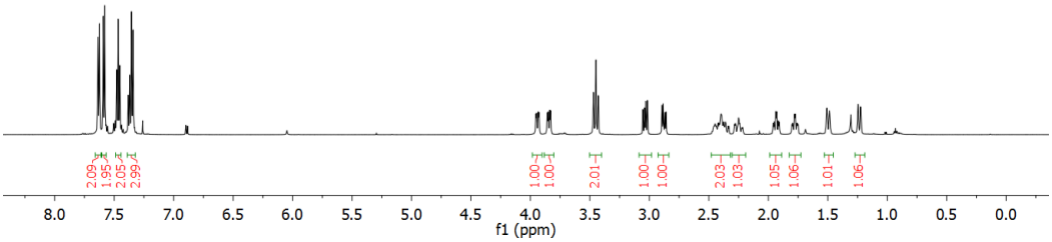

HRMS (DART) calcd for $C_{22}H_{23}F_4O$ $[M+H]^+$ *m/z* = 379.1685; found 379.1684.

5.7.e

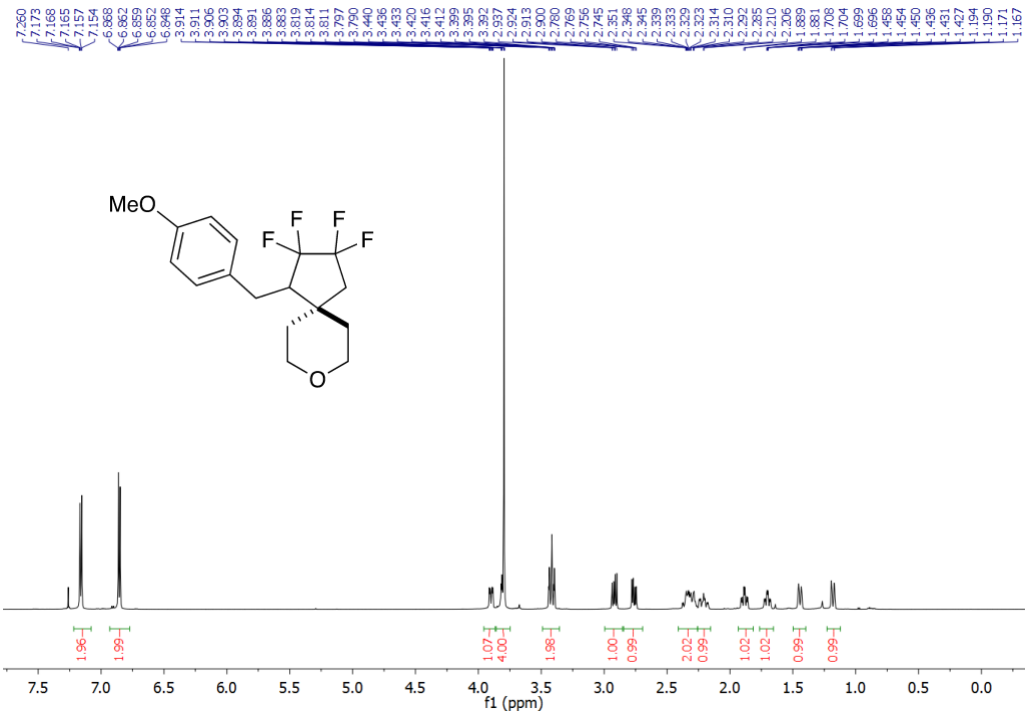

HRMS (DART) calcd for $C_{17}H_{21}F_4O_2$ $[M+H]^+$ *m/z* = 333.1478; found 333.1473.

5.7.h

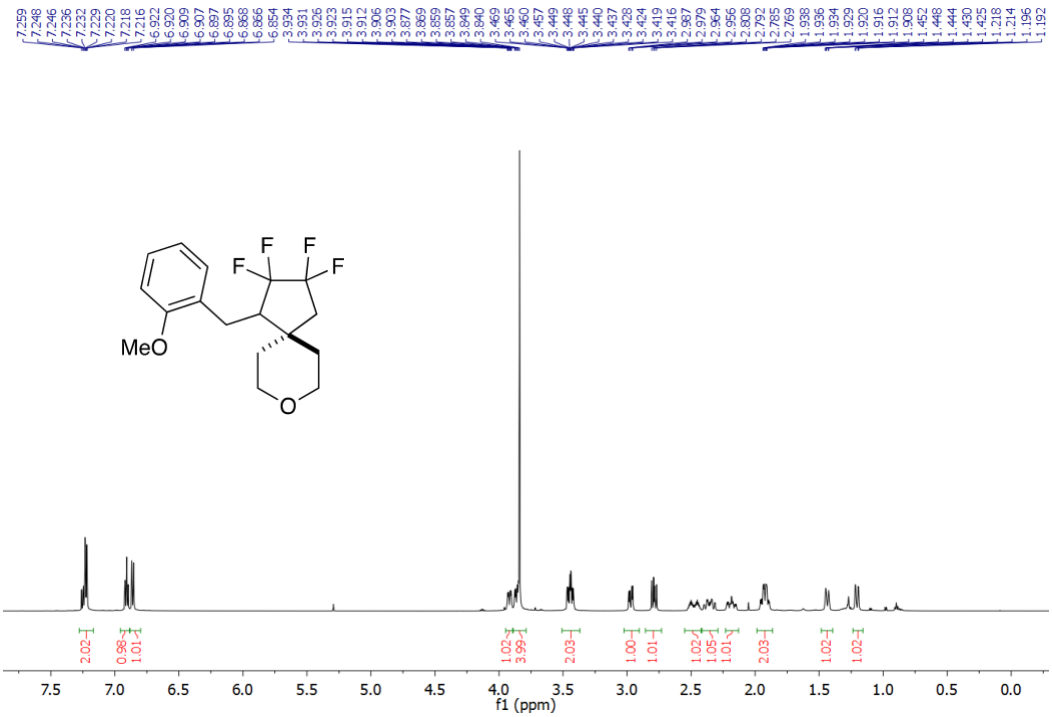

HRMS (DART) calcd for $C_{17}H_{21}F_4O_2$ $[M+H]^+$ *m/z* = 333.1478; found 333.1481.

5.7.j

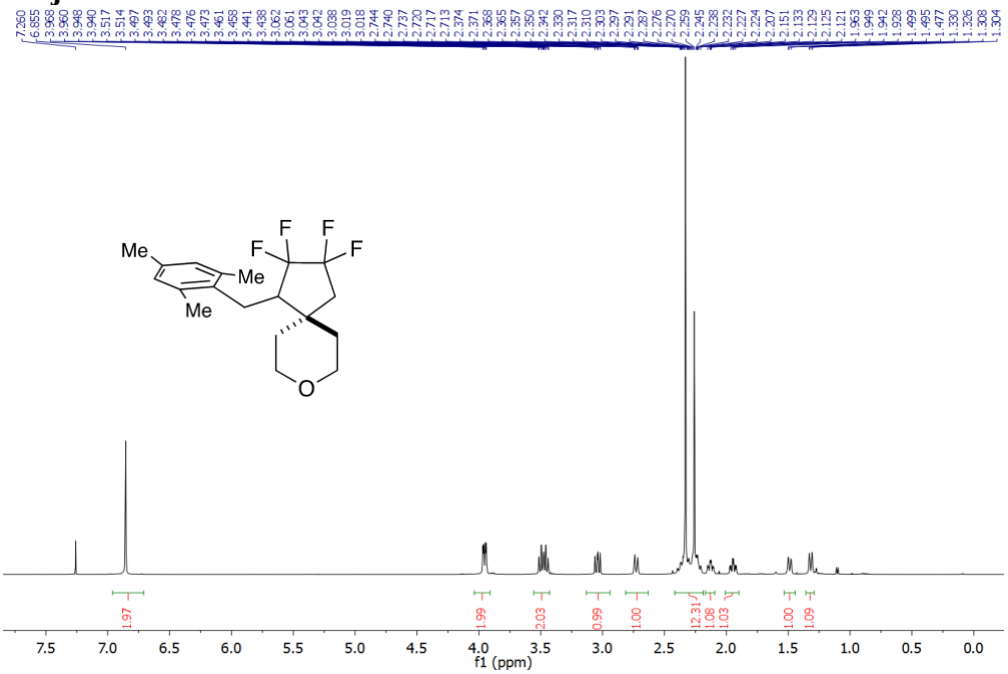

HRMS (DART) calcd for $C_{19}H_{25}F_4O$ $[M+H]^+$ *m/z* = 345.1842; found 345.1849.

5.7.g

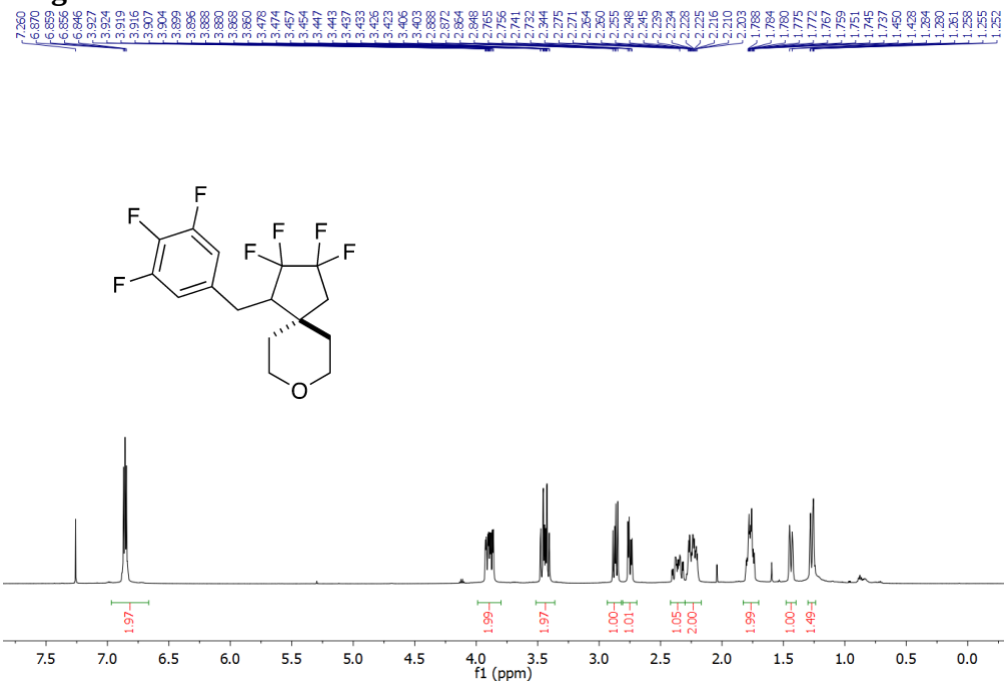

HRMS (DART) calcd for $C_{16}H_{16}F_7O$ $[M+H]^+$ *m/z* = 357.1089; found 357.1084.

5.7.f

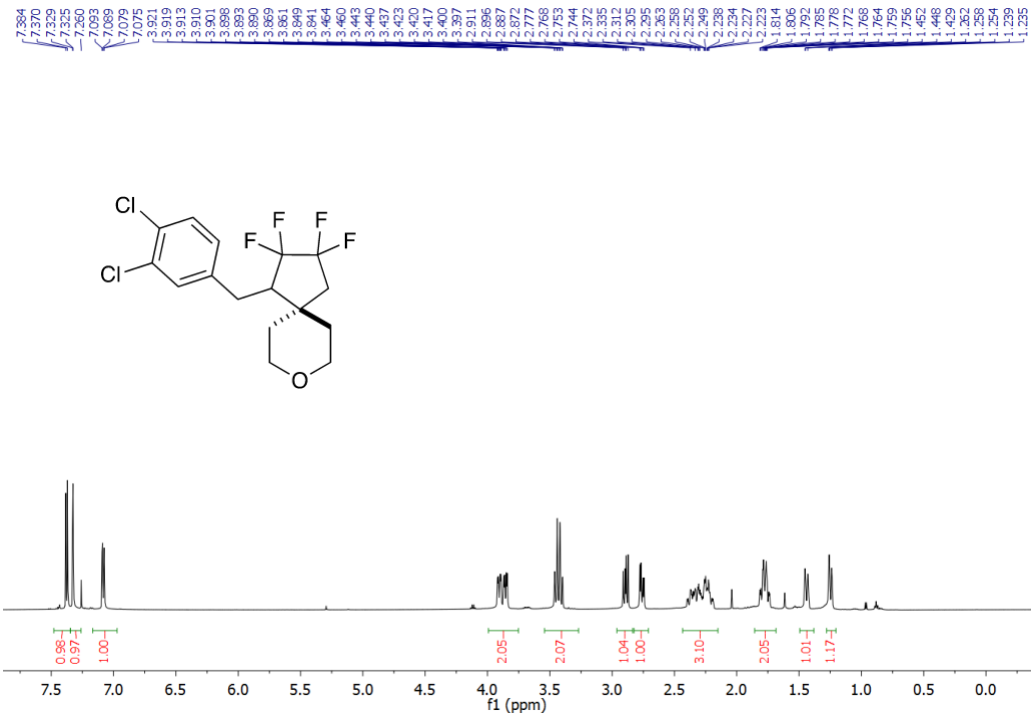

HRMS (DART) calcd for $C_{16}H_{17}Cl_2F_4O$ $[M+H]^+$ *m/z* = 371.0593; found 371.0592.

5.7.i

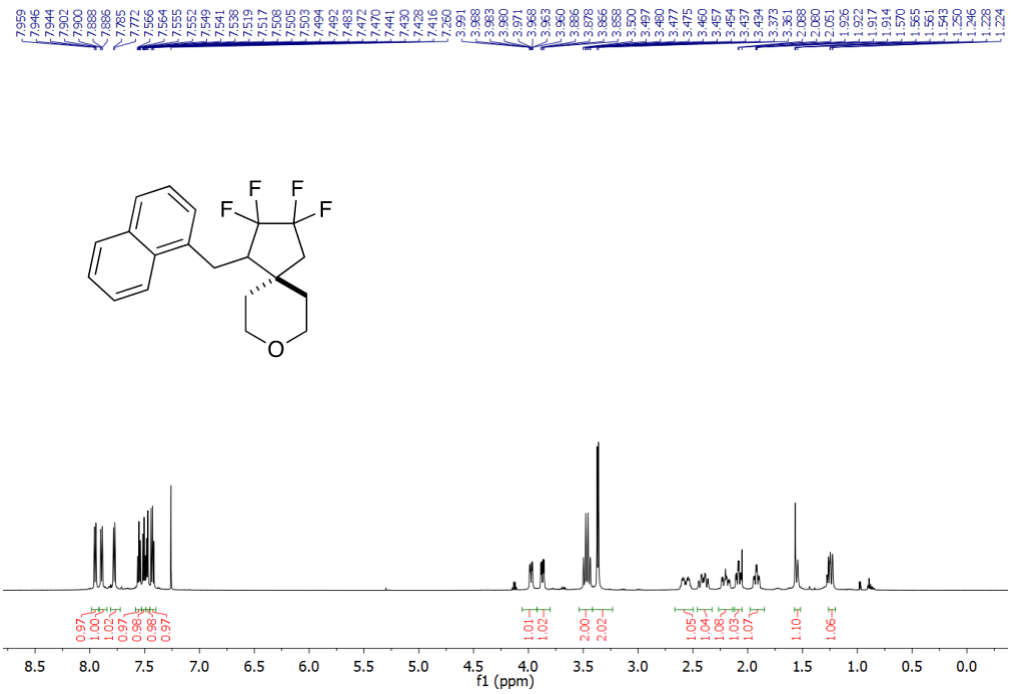

HRMS (DART) calcd for $C_{20}H_{21}F_4O$ $[M+H]^+$ *m/z* = 353.1529; found 353.1522.

5.7.k

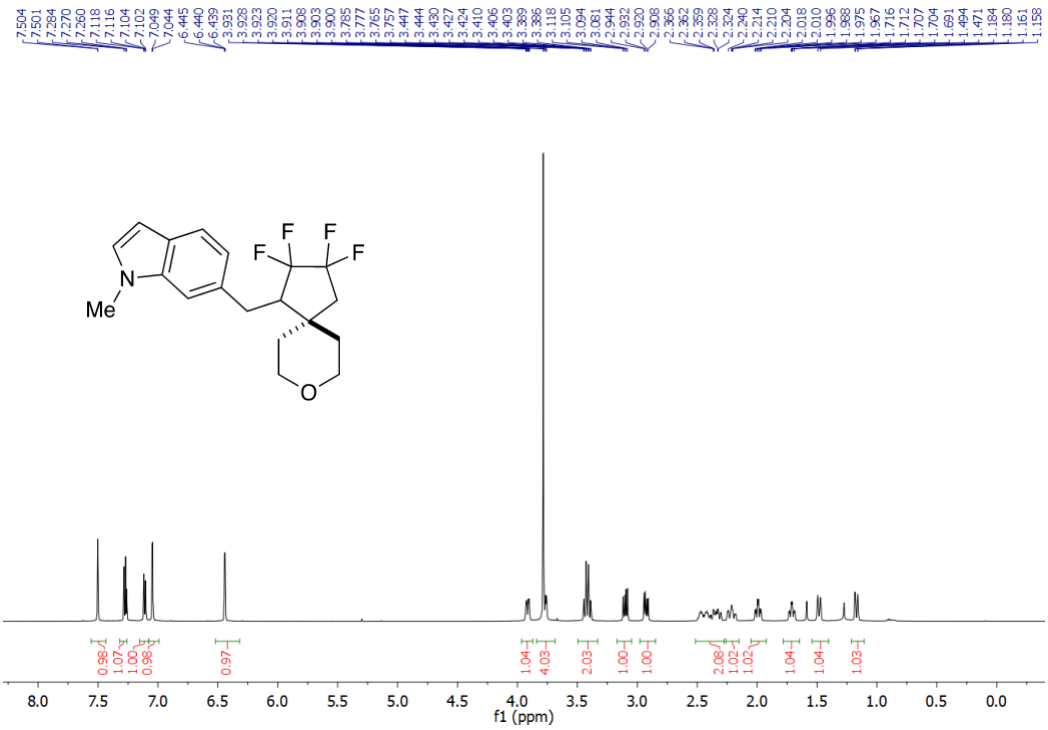

HRMS (DART) calcd for $C_{19}H_{22}F_4NO$ $[M+H]^+$ *m/z* = 356.1638; found 356.1636.

5.7.i

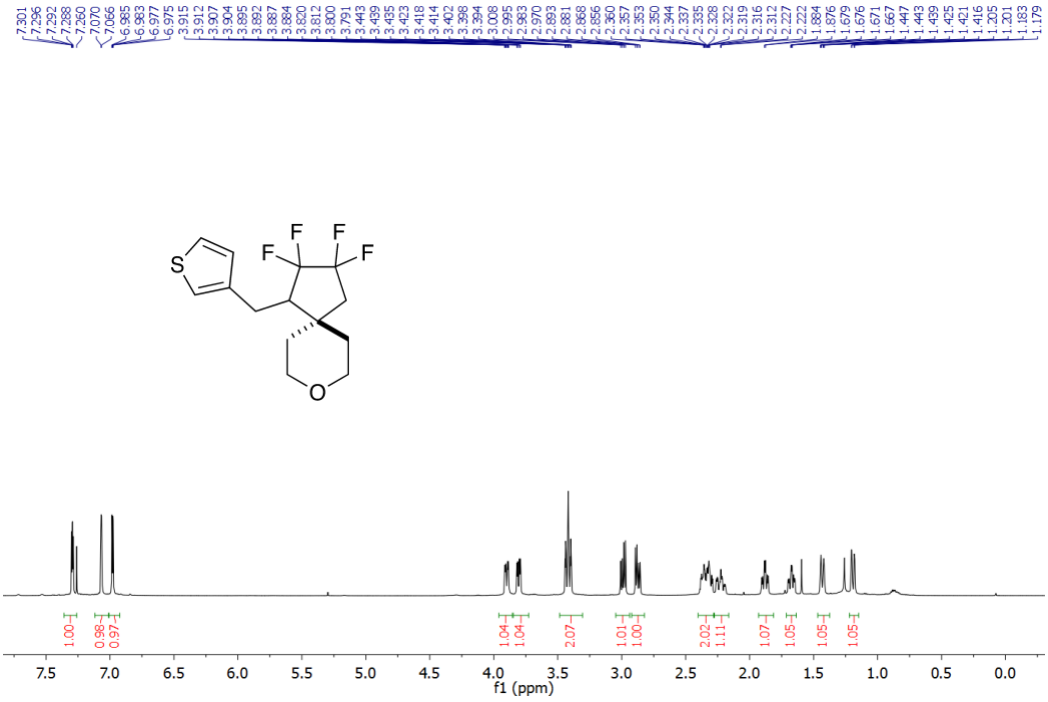

HRMS (DART) calcd for $C_{14}H_{17}F_4OS$ $[M+H]^+$ *m/z* = 309.0936; found 309.0937.

5.7.m

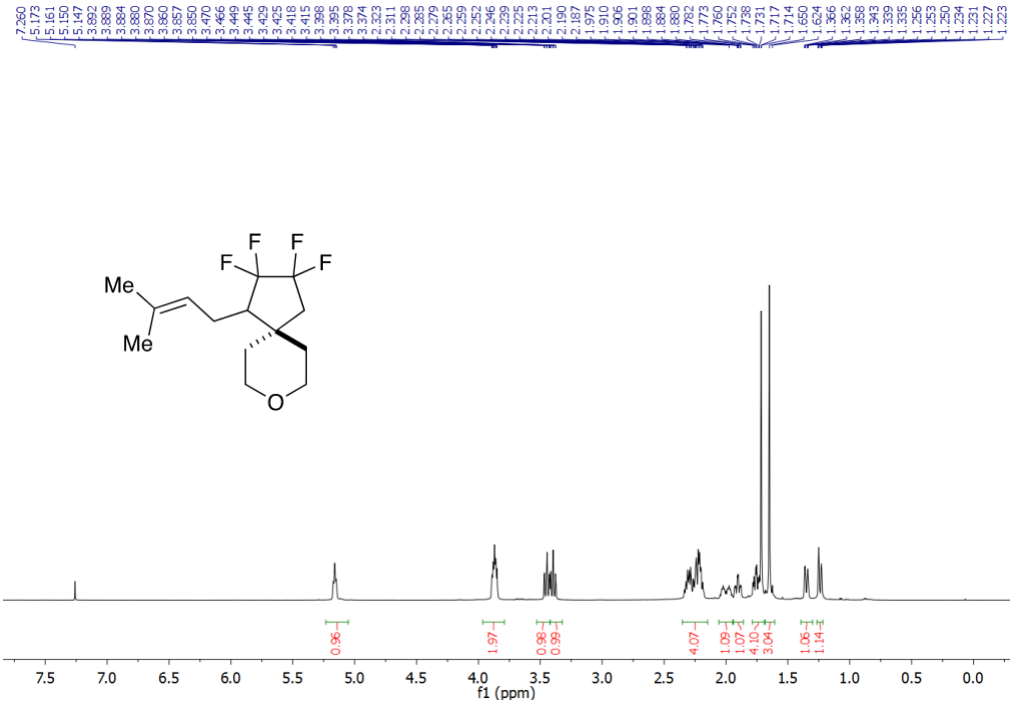

HRMS (DART) calcd for $C_{14}H_{21}F_4O$ $[M+H]^+$ *m/z* = 281.1529; found 281.1528.

5.7.n

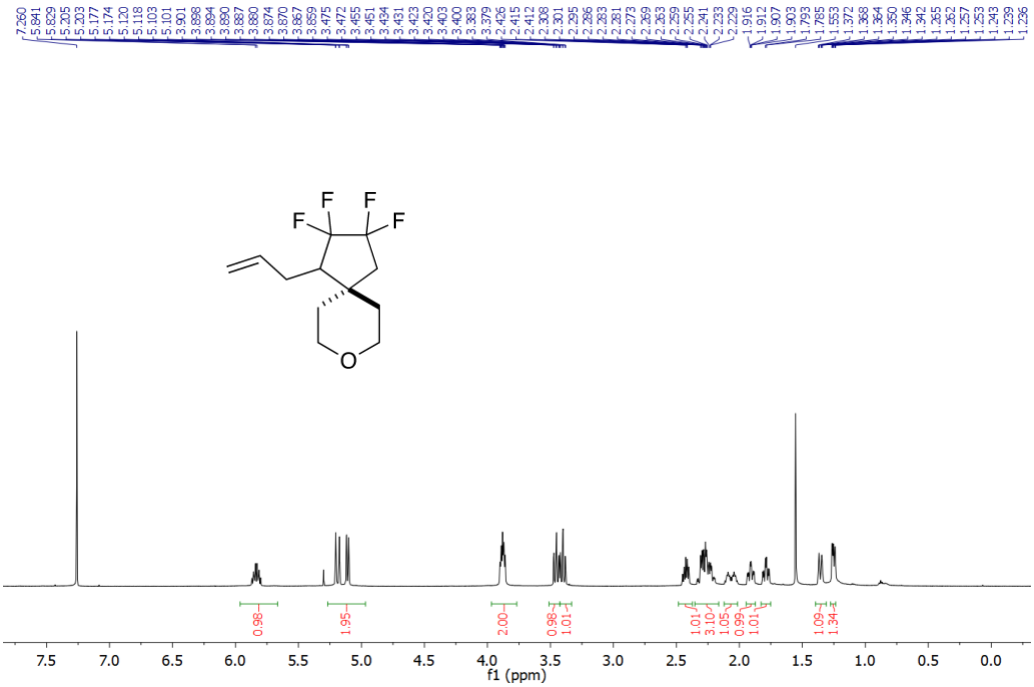

HRMS (DART) calcd for $C_{12}H_{17}F_4O$ $[M+H]^+$ *m/z* = 253.1216; found 253.1225.

7.10 NMR Spectra of Compounds in Chapter 6

6.2.d

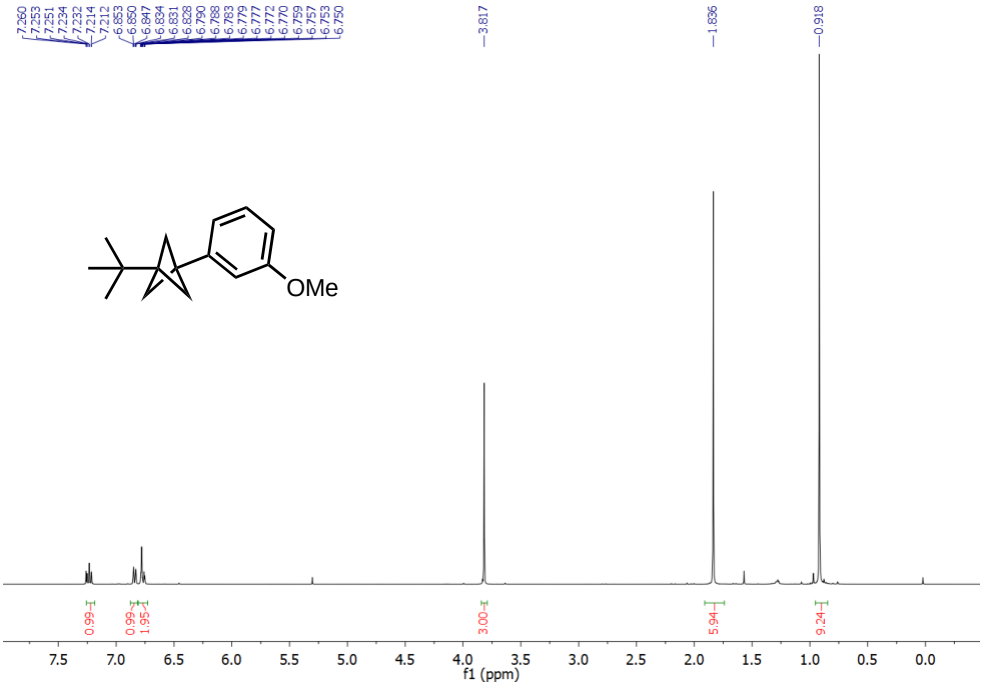

HRMS (DART) calcd for $C_{16}H_{23}O$ $[M+H]^+$ *m/z* = 231.1749; found 231.1768.

6.3.n

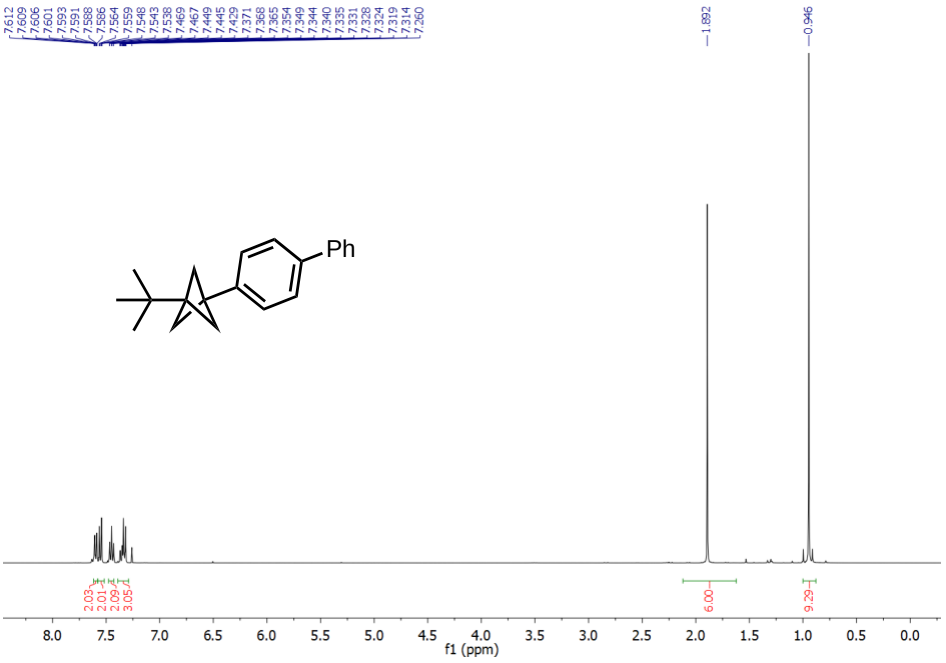

HRMS (DART) calcd for $C_{21}H_{25}$ $[M+H]^+$ *m/z* = 277.1956; found 277.1952.

6.3.o

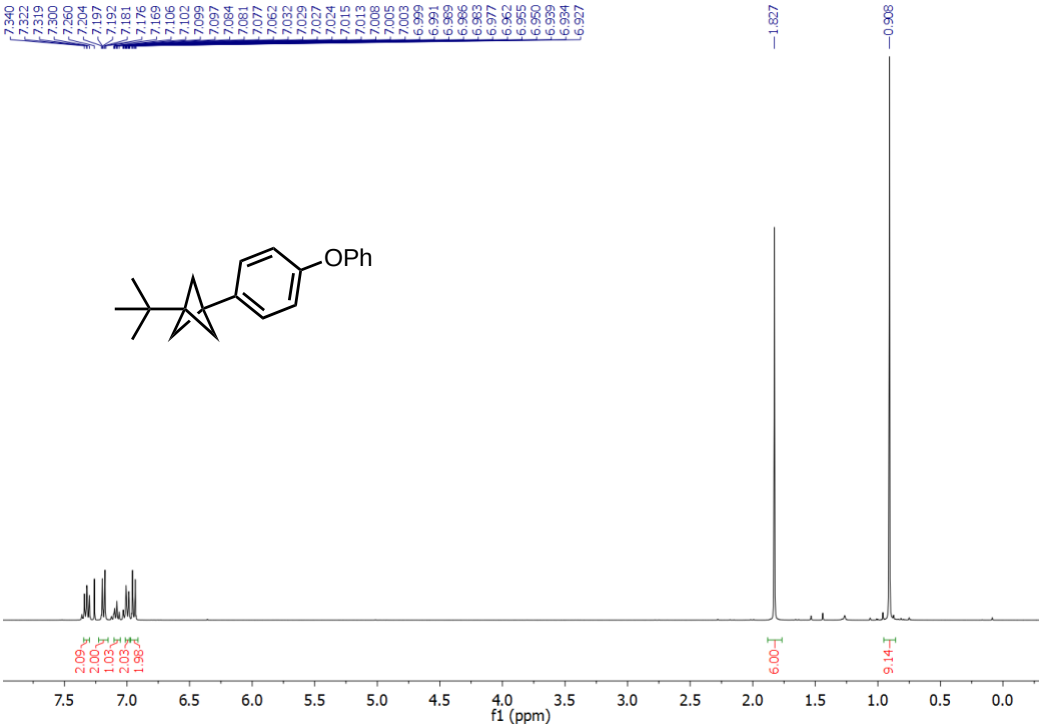

HRMS (DART) calcd for $C_{21}H_{25}O$ $[M+H]^+$ *m/z* = 293.1905; found 293.1905.

6.3.g

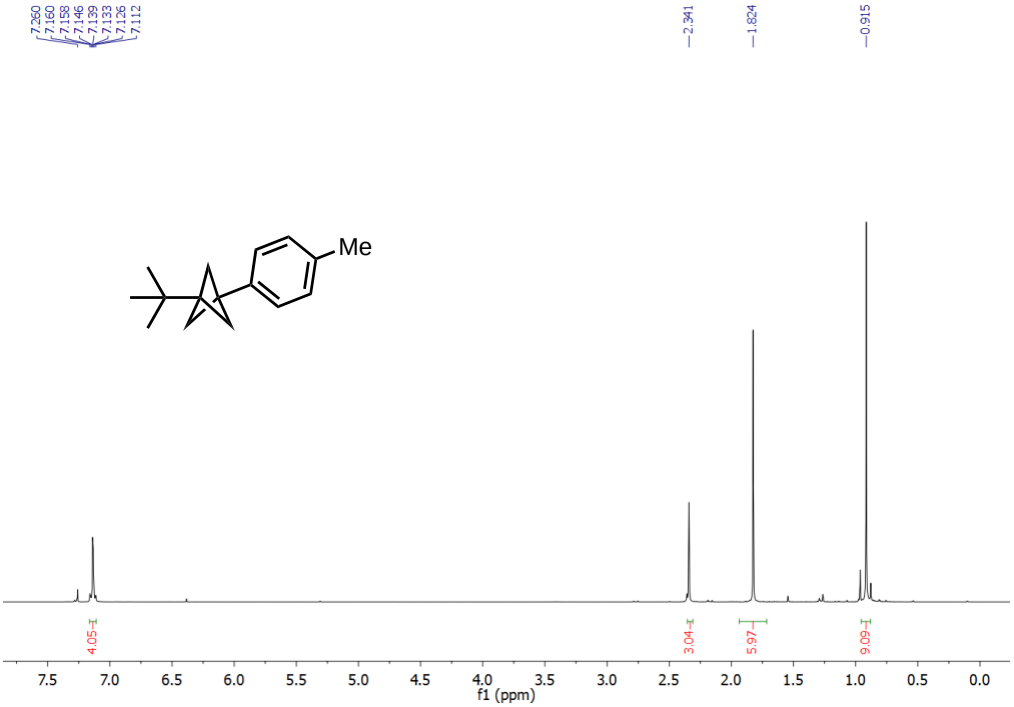

HRMS (DART) calcd for $C_{16}H_{23}$ $[M+H]^+$ *m/z* = 215.1800; found 215.1803.

6.3.j

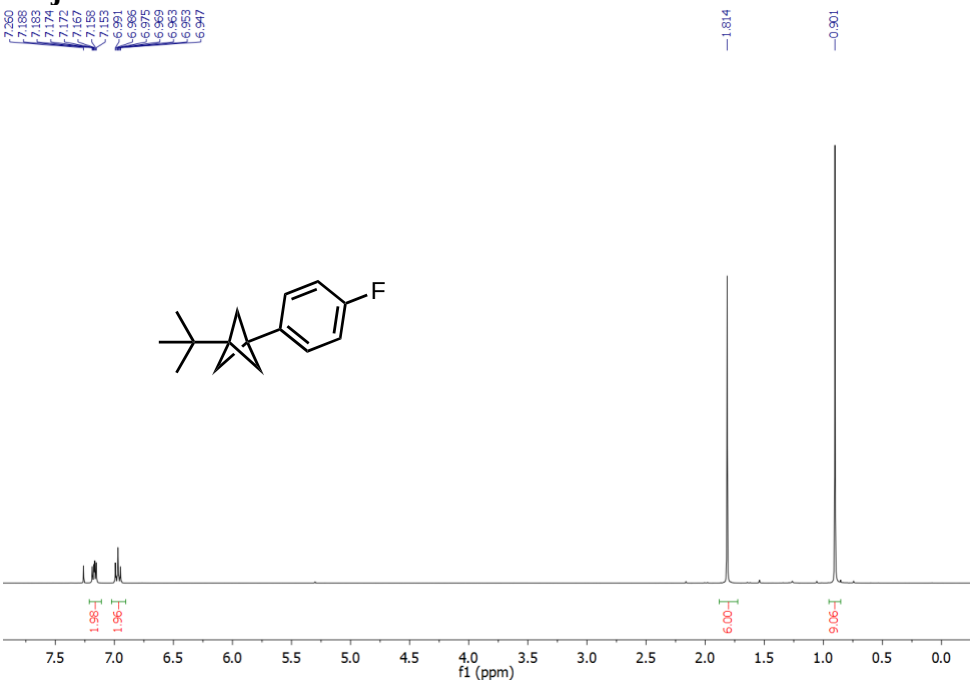

HRMS (DART) calcd for $C_{15}H_{20}F$ $[M+H]^+$ *m/z* = 219.1549; found 219.1572.

6.3.k

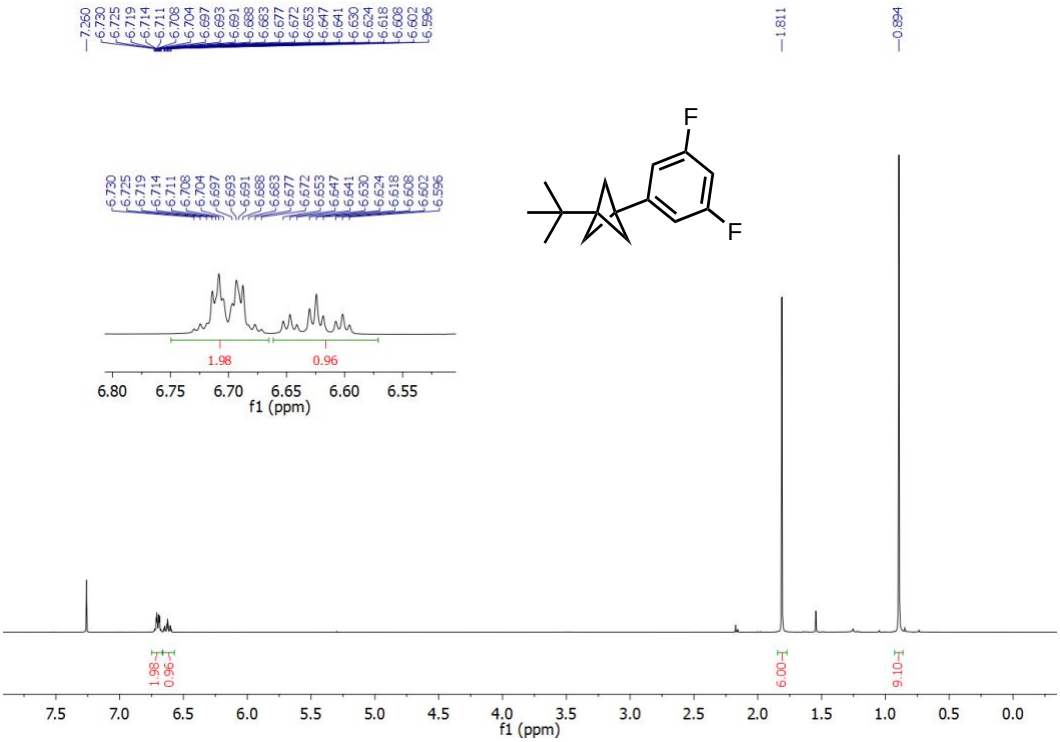

HRMS (DART) calcd for $C_{15}H_{19}F_2$ $[M+H]^+$ *m/z* = 237.1455; found 237.1457.

6.3.e

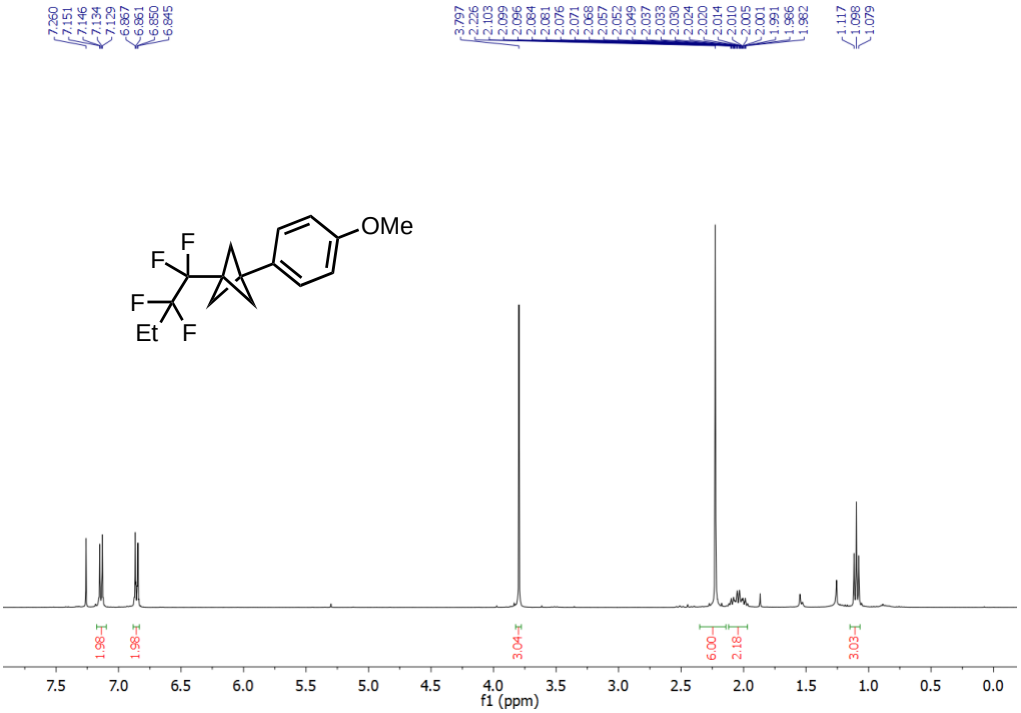

HRMS (DART) calcd for $C_{16}H_{19}F_4O$ $[M+H]^+$ *m/z* = 303.1372; found 303.1370.

6.3.m

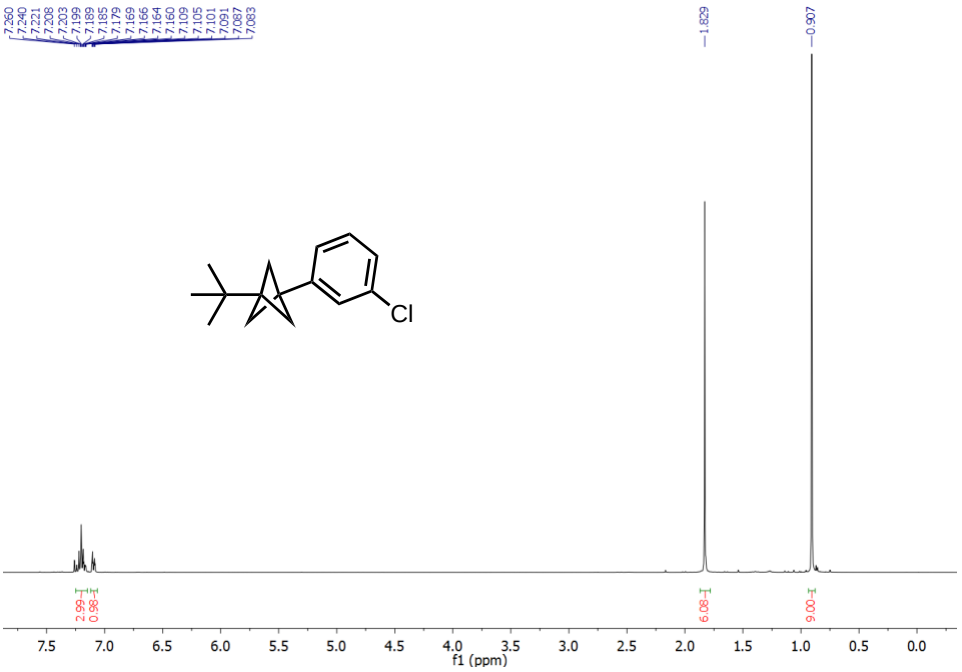

HRMS (DART) calcd for $C_{15}H_{20}Cl$ $[M+H]^+$ *m/z* = 235.1254; found 235.1247.

6.4.e

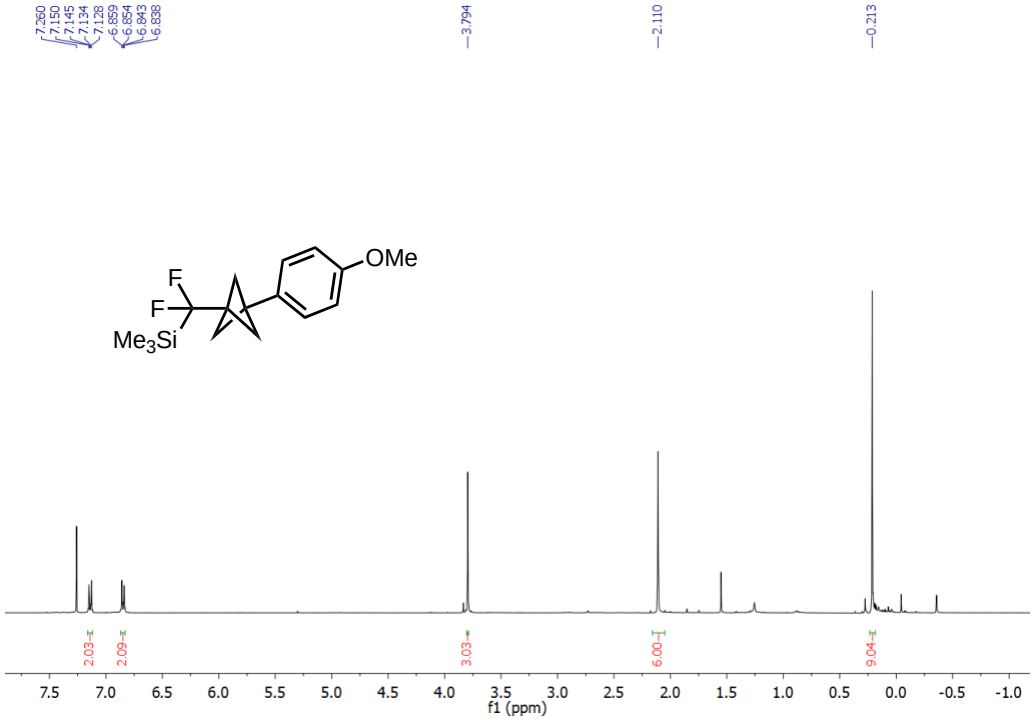

HRMS (DART) calcd for $C_{16}H_{23}F_2OSi$ $[M+H]^+$ *m/z* = 297.1486; found 297.1498.

6.3.l

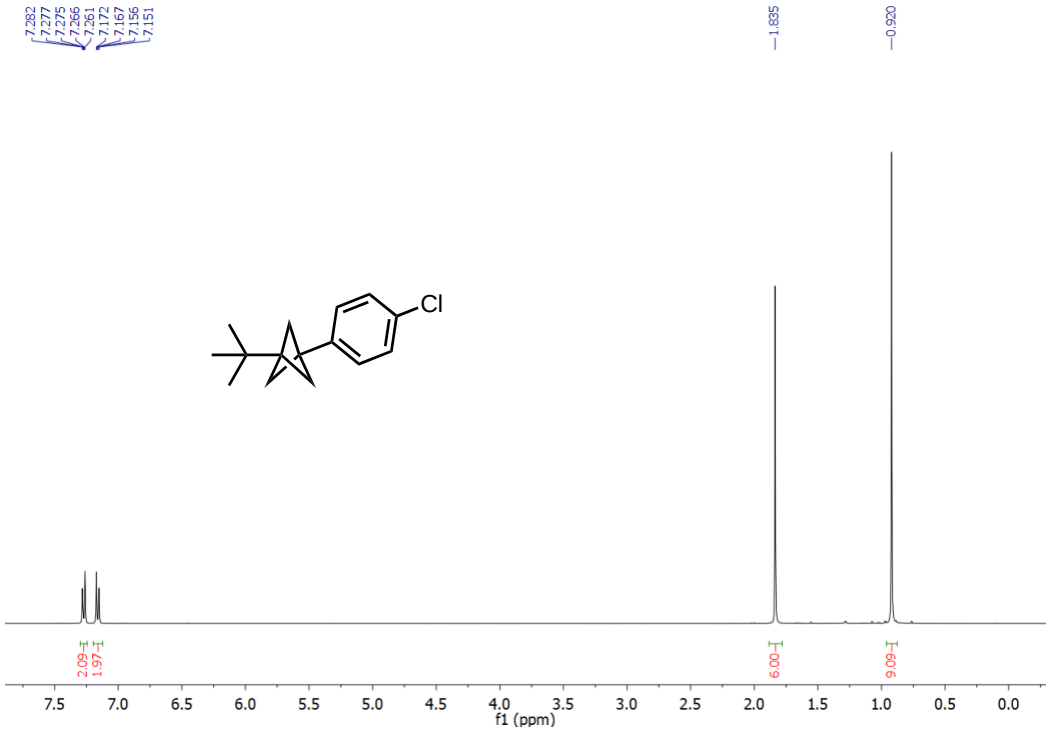

HRMS (DART) calcd for $C_{15}H_{20}Cl$ $[M+H]^+$ *m/z* = 235.1254; found 235.1228.

6.4.f

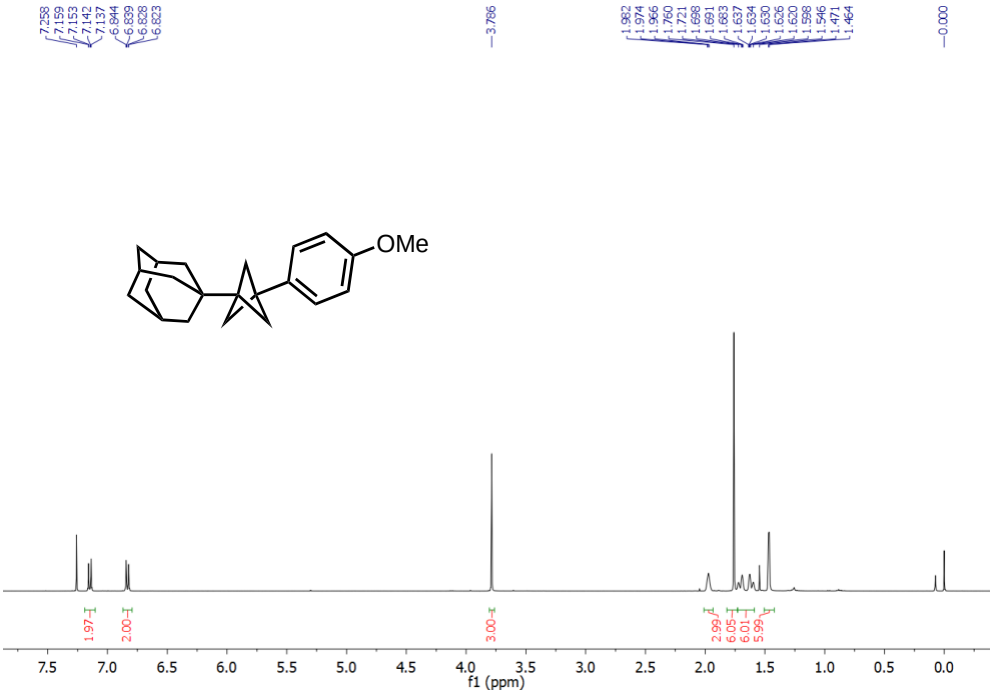

HRMS (DART) calcd for $C_{22}H_{29}O$ $[M+H]^+$ *m/z* = 309.2218; found 309.2217.

7.11 Computation Coordinates of Chapter 5

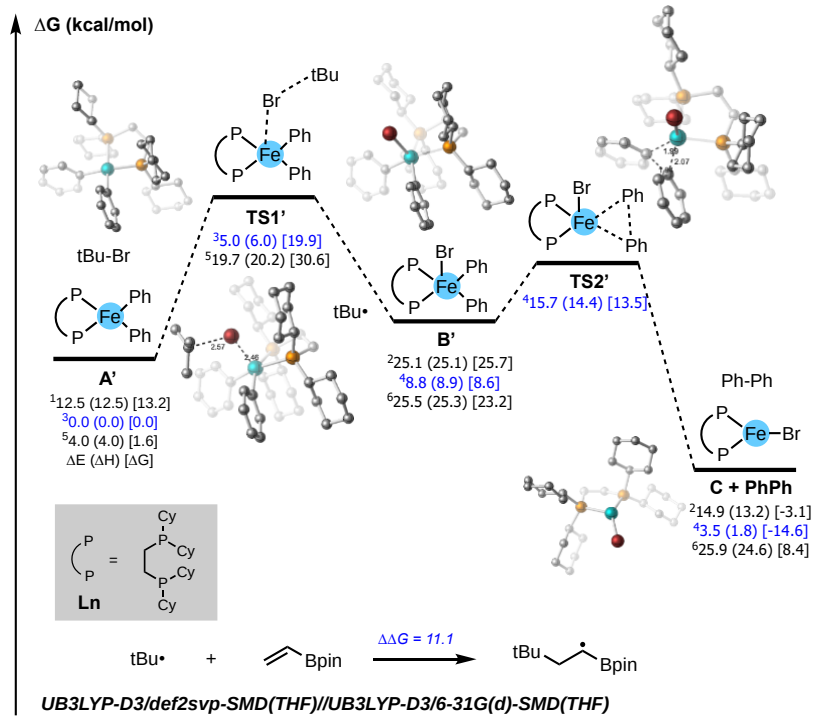

Figure 7.3. The active species iron(II)-diphenyl **A'** that can possibly generate the *tert*-butyl radical **tBu•** and further reacts with the vinylboronate.

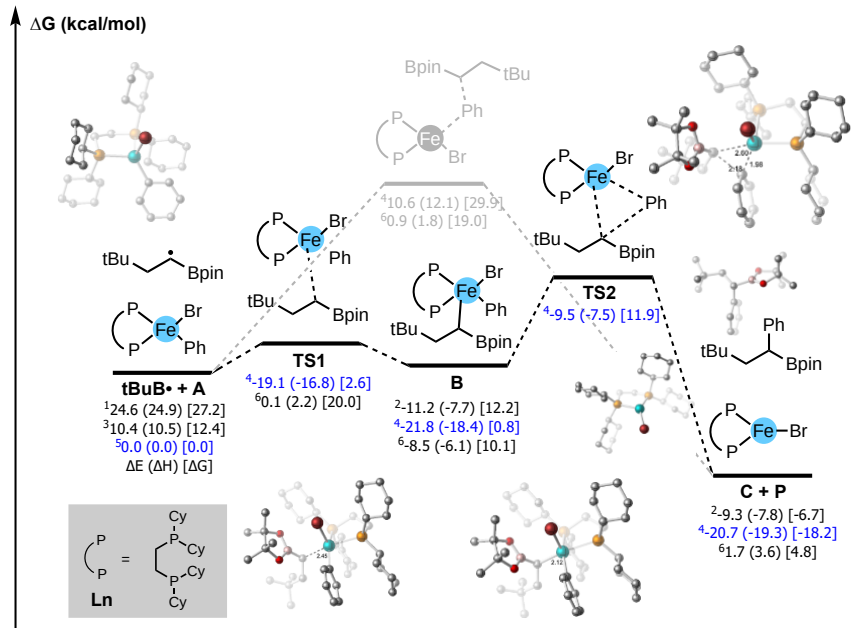

Figure 7.4. DFT calculations showing the vinylboronate radical **tBuB•** reacting with iron(II)-monophenyl **A** to undergo radical addition **TS1** and reductive elimination **TS2** to form the desired product **P**.

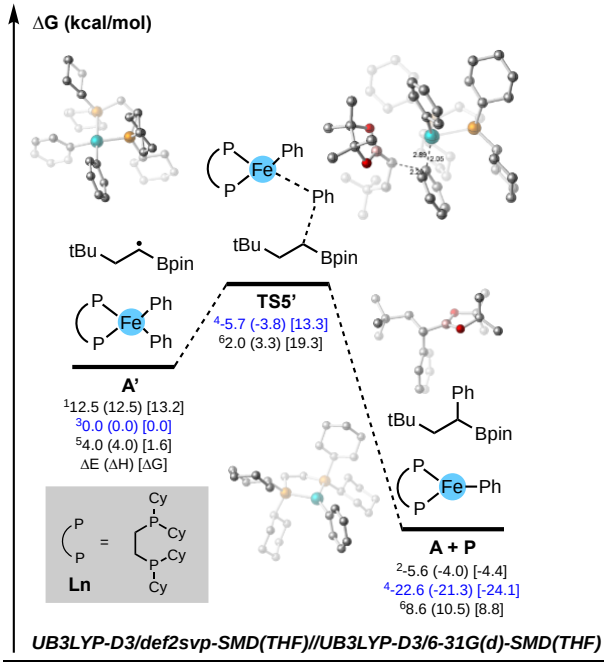

Figure 7.5. A proposed pathway to form the desired product **P**.

tBu-Br

UB3LYP-D3/6-31G(d)-SMD(THF)

Zero-point correction= 0.122896 (Hartree/Particle)
Thermal correction to Energy= 0.129503
Thermal correction to Enthalpy= 0.130447
Thermal correction to Gibbs Free Energy= 0.092331
Sum of electronic and zero-point Energies= -2729.466467
Sum of electronic and thermal Energies= -2729.459860
Sum of electronic and thermal Enthalpies= -2729.458916
Sum of electronic and thermal Free Energies= -2729.497032

UB3LYP-D3/def2svp-SMD(THF)//UB3LYP-D3/6-31G(d)-SMD(THF)

HF=-2731.6351

Br	-1.40517600	-1.00431100	0.00023100
C	-3.45621300	-1.00444600	0.00000800
C	-3.88565000	-0.31829200	1.29077500
H	-3.52217400	0.71275000	1.33633000
H	-4.98334000	-0.29727700	1.33069200
H	-3.52187100	-0.85707600	2.17089800
C	-3.88570200	-0.22988800	-1.23975100
H	-3.52196200	-0.70597100	-2.15529600
H	-4.98340300	-0.20623000	-1.27804800
H	-3.52236900	0.80184700	-1.21348100
C	-3.88576100	-2.46533800	-0.05108000
H	-4.98345700	-2.51020500	-0.05232800
H	-3.52248900	-2.95831000	-0.95788300
H	-3.52219000	-3.02045700	0.81893300

A'-singlet

UB3LYP-D3/6-31G(d)-SMD(THF)

Zero-point correction= 0.888601 (Hartree/Particle)
Thermal correction to Energy= 0.930576
Thermal correction to Enthalpy= 0.931520
Thermal correction to Gibbs Free Energy= 0.813718
Sum of electronic and zero-point Energies= -3428.610060
Sum of electronic and thermal Energies= -3428.568084
Sum of electronic and thermal Enthalpies= -3428.567140
Sum of electronic and thermal Free Energies= -3428.684943
HF=-3429.4986606

UB3LYP-D3/def2svp-SMD(THF)//UB3LYP-D3/6-31G(d)-SMD(THF)

HF=-3428.2450

Fe	5.46228900	11.62853600	3.77517400

P	3.82046400	10.47739800	2.64446400
P	3.72510600	12.62919100	4.91422900
C	2.16180600	10.77854000	3.45895400
H	1.34513700	10.64516000	2.73991600
H	2.04328300	10.00467100	4.22448300
C	2.09692700	12.17183200	4.10927100
H	1.27630100	12.22629300	4.83410600
H	1.89825500	12.93013000	3.34482700
C	4.04877900	8.63344100	2.74784800
H	4.93078200	8.44107200	2.12298800
C	4.41441900	8.21729300	4.18722700
H	3.58147900	8.45009100	4.86451800
H	5.27638400	8.80081000	4.53875200
C	4.72411400	6.71507400	4.26764000
H	5.62751500	6.50371200	3.67706500
H	4.95004200	6.43539600	5.30471800
C	3.55760600	5.87544500	3.72724500
H	3.81008800	4.80781200	3.76025300
H	2.68201000	6.01448500	4.37915500
C	3.18958500	6.29152000	2.29580700
H	2.33068100	5.70931600	1.93723200
H	4.03058800	6.06250300	1.62486900
C	2.87595400	7.79445200	2.20904900
H	2.65177300	8.07082500	1.17175500
H	1.97258600	8.00777100	2.79775800
C	3.50639300	10.83061500	0.83719500
H	2.51788600	10.41832600	0.58739200
C	4.55691600	10.17517000	-0.08254900
H	4.51717100	9.08418200	0.01273100
H	5.55963300	10.48518400	0.22973200
C	4.34112700	10.56698800	-1.55276600
H	5.12688100	10.11306400	-2.17039400
H	3.38298600	10.15454600	-1.90361000
C	4.33029400	12.09024000	-1.73519700
H	4.15882500	12.34903400	-2.78812100
H	5.31755700	12.49151900	-1.46319000
C	3.26057800	12.73564400	-0.84479600
H	3.27600000	13.82811300	-0.95264500
H	2.26526400	12.39835400	-1.17069000
C	3.46576200	12.35922500	0.62948100
H	2.67261000	12.80301900	1.24269100
H	4.41411300	12.78914100	0.98037700
C	3.78397100	14.48552000	4.80294300
H	4.64983000	14.75843700	5.42043600
C	2.54443400	15.21837500	5.34704600
H	1.66097400	14.92636600	4.76190200

H	2.34920300	14.92488100	6.38543200
C	2.72584600	16.74289500	5.25810900
H	1.82111300	17.24864100	5.61997400
H	3.54649400	17.04422900	5.92562000
C	3.05059500	17.18895100	3.82512200
H	3.21118800	18.27421000	3.79179100
H	2.18677100	16.97621200	3.17739400
C	4.28142000	16.45162200	3.27769900
H	5.16727300	16.73889600	3.86276300
H	4.47625200	16.74914500	2.23928700
C	4.09983400	14.92888600	3.36008700
H	3.28211900	14.62790000	2.69157600
H	5.00254300	14.41726800	2.99955000
C	3.45542500	12.25532700	6.72420300
H	2.43503300	12.57616700	6.97992100
C	3.55630900	10.73011700	6.93785500
H	4.53781200	10.38686100	6.58179500
H	2.80284700	10.21294100	6.33197300
C	3.39680700	10.34333500	8.41501600
H	3.51279400	9.25739100	8.52720000
H	2.37710900	10.58982700	8.74667300
C	4.40939800	11.08817300	9.29454500
H	4.26984200	10.81972500	10.34975000
H	5.42722800	10.77723500	9.01669500
C	4.27983900	12.60527300	9.10612600
H	5.02479700	13.13185700	9.71654100
H	3.29032000	12.93001800	9.46200300
C	4.44837800	13.00866500	7.63288200
H	5.47324800	12.79070700	7.31349300
H	4.30772500	14.09086900	7.53362400
C	6.82745600	12.34524100	4.99516700
C	7.25436700	13.68780200	5.10988300
H	6.87462700	14.43036200	4.40737000
C	8.13784300	14.11898000	6.10564200
C	8.63924900	13.21274100	7.04512200
H	9.31936000	13.54448600	7.82644800
C	8.26005100	11.86947900	6.95400100
H	8.65029600	11.14557800	7.66834400
C	7.38527900	11.45473600	5.94452300
H	7.11749300	10.39653500	5.90498600
C	6.86898200	11.07592800	2.51311800
C	7.42165300	9.78454500	2.35805800
H	7.13103500	8.99318800	3.05002600
C	8.32014600	9.46395800	1.33431200
C	8.70843100	10.43550700	0.40655100
H	9.39956300	10.18950300	-0.39647500

C	8.20211800	11.73287700	0.53781100
H	8.50344200	12.50706300	-0.16674900
C	7.31480600	12.03781900	1.57510800
H	6.94617700	13.06334500	1.64721100
H	8.43029000	15.16722400	6.15451100
H	8.71270900	8.45095500	1.25426500

A'-triplet

UB3LYP-D3/6-31G(d)-SMD(THF)

Zero-point correction= 0.888602 (Hartree/Particle)
Thermal correction to Energy= 0.930615
Thermal correction to Enthalpy= 0.931559
Thermal correction to Gibbs Free Energy= 0.812637
Sum of electronic and zero-point Energies= -3428.629945
Sum of electronic and thermal Energies= -3428.587932
Sum of electronic and thermal Enthalpies= -3428.586988
Sum of electronic and thermal Free Energies= -3428.705910
HF=-3429.5185471

UB3LYP-D3/def2svp-SMD(THF)//UB3LYP-D3/6-31G(d)-SMD(THF)

HF=-3428.2649282

Fe	5.47460700	11.62924200	3.77503300
P	3.82333400	10.47761200	2.64043700
P	3.72916000	12.62951000	4.91700200
C	2.16781700	10.77886000	3.45967700
H	1.34924300	10.64391400	2.74304800
H	2.05304800	10.00575200	4.22646600
C	2.10344100	12.17292200	4.10793700
H	1.28109700	12.22918500	4.83073300
H	1.90856500	12.93085100	3.34222000
C	4.05434400	8.63363100	2.74475500
H	4.93428700	8.44098900	2.11712200
C	4.42403300	8.21711500	4.18314700
H	3.59358000	8.45152900	4.86294400
H	5.28765400	8.79927300	4.53215200
C	4.73160200	6.71434800	4.26273000
H	5.63317400	6.50165400	3.66980300
H	4.96007800	6.43465900	5.29925400
C	3.56280900	5.87586700	3.72570400
H	3.81409100	4.80793300	3.75835100
H	2.68899300	6.01613300	4.37973900
C	3.19182900	6.29211200	2.29512600
H	2.33148100	5.71080400	1.93855800
H	4.03102600	6.06228000	1.62220200
C	2.87933700	7.79528600	2.20917800

H	2.65237300	8.07177100	1.17252700
H	1.97782300	8.00926700	2.80046600
C	3.50733200	10.83020000	0.83305900
H	2.51734800	10.41987300	0.58575100
C	4.55419300	10.17130400	-0.08842200
H	4.51287600	9.08054400	0.00854000
H	5.55836100	10.48019700	0.22019100
C	4.33484500	10.56116700	-1.55865400
H	5.11806500	10.10482500	-2.17773500
H	3.37500100	10.14977500	-1.90606100
C	4.32619500	12.08412100	-1.74364300
H	4.15176700	12.34136600	-2.79646700
H	5.31508700	12.48398800	-1.47556900
C	3.26066000	12.73312500	-0.85082200
H	3.27799900	13.82537800	-0.96056200
H	2.26360200	12.39737000	-1.17301300
C	3.46993900	12.35875400	0.62341500
H	2.67989200	12.80530100	1.23867600
H	4.42034500	12.78658500	0.97107400
C	3.79002000	14.48631500	4.80561800
H	4.65354700	14.75943300	5.42622600
C	2.54788300	15.21730800	5.34688300
H	1.66648100	14.92455400	4.75903300
H	2.35009200	14.92278100	6.38448200
C	2.72698800	16.74213400	5.25957700
H	1.82057500	17.24599000	5.61988500
H	3.54567900	17.04441900	5.92906600
C	3.05404000	17.18950800	3.82759400
H	3.21243400	18.27512100	3.79501700
H	2.19217700	16.97517100	3.17777600
C	4.28767000	16.45484000	3.28315800
H	5.17134500	16.74391300	3.87067400
H	4.48473800	16.75321000	2.24540100
C	4.10985400	14.93148600	3.36403300
H	3.29526800	14.62840200	2.69262200
H	5.01486800	14.42271200	3.00598400
C	3.45748400	12.25610700	6.72718800
H	2.43576700	12.57484600	6.98036600
C	3.56145700	10.73127600	6.94277900
H	4.54481700	10.39010500	6.59017600
H	2.81137500	10.21172500	6.33469200
C	3.39744500	10.34610100	8.41988900
H	3.51533600	9.26055200	8.53393200
H	2.37608100	10.59087000	8.74772800
C	4.40543000	11.09411900	9.30204400
H	4.26261300	10.82690600	10.35713500

H	5.42481800	10.78473400	9.02828300
C	4.27372800	12.61071800	9.11111700
H	5.01581500	13.13947400	9.72317100
H	3.28250500	12.93419300	9.46340500
C	4.44624400	13.01259500	7.63789500
H	5.47262200	12.79623500	7.32240000
H	4.30385200	14.09440100	7.53706100
C	6.84029900	12.34303700	5.00772800
C	7.25731700	13.68817600	5.12704700
H	6.88461000	14.42788500	4.41799100
C	8.12267700	14.12423900	6.13620900
C	8.61423700	13.22052000	7.08359500
H	9.28082800	13.55618700	7.87483300
C	8.24458700	11.87518900	6.98718500
H	8.62864400	11.15372400	7.70727400
C	7.38797600	11.45467600	5.96419500
H	7.12829100	10.39510600	5.91904400
C	6.88139700	11.07989700	2.50083800
C	7.42444700	9.78473900	2.34359300
H	7.14048200	8.99805100	3.04341300
C	8.30515500	9.45584400	1.30740200
C	8.68381400	10.42233500	0.37008900
H	9.36152000	10.16974000	-0.44227500
C	8.18698200	11.72282100	0.50414400
H	8.48218300	12.49278300	-0.20756100
C	7.31758600	12.03701100	1.55423100
H	6.95677600	13.06467200	1.62949800
H	8.40916600	15.17388000	6.18914800
H	8.69173800	8.44076500	1.22522100

A'-quintet

UB3LYP-D3/6-31G(d)-SMD(THF)

Zero-point correction= 0.887810 (Hartree/Particle)
Thermal correction to Energy= 0.930599
Thermal correction to Enthalpy= 0.931543
Thermal correction to Gibbs Free Energy= 0.808751
Sum of electronic and zero-point Energies= -3428.626505
Sum of electronic and thermal Energies= -3428.583717
Sum of electronic and thermal Enthalpies= -3428.582773
Sum of electronic and thermal Free Energies= -3428.705565
HF=-3429.5143154

UB3LYP-D3/def2svp-SMD(THF)//UB3LYP-D3/6-31G(d)-SMD(THF)

HF=-3428.2585719

Fe	5.74102500	11.73783400	3.78279100

P	3.91936700	10.70551000	2.42454100
P	3.83360300	12.48616800	5.16927600
C	2.28733800	10.92409900	3.31586000
H	1.46890200	10.97828900	2.58808000
H	2.12767100	10.01242600	3.89803500
C	2.23846700	12.15193300	4.24949300
H	1.41058400	12.04877000	4.96122600
H	2.03495300	13.04991000	3.65936100
C	3.99873800	8.86898600	2.08824900
H	4.94378100	8.74759100	1.54018000
C	4.13134200	8.06351100	3.39856000
H	3.21478500	8.17059500	3.99486000
H	4.95508200	8.45491300	4.00208800
C	4.35399800	6.57242700	3.10427000
H	5.31876100	6.45051800	2.59071900
H	4.42684600	6.01605200	4.04774400
C	3.22951300	6.00051900	2.22993100
H	3.42327100	4.94538500	1.99698800
H	2.28506600	6.03199100	2.79399300
C	3.06781100	6.80945300	0.93538700
H	2.22872700	6.42135100	0.34304600
H	3.97165500	6.69025200	0.31973400
C	2.85636700	8.30617300	1.22105700
H	2.78019100	8.85239900	0.27392400
H	1.90068800	8.44443600	1.74697700
C	3.64083500	11.49545600	0.75644200
H	2.69029700	11.12653600	0.34611800
C	4.78198600	11.11322600	-0.20802200
H	4.78100600	10.03199500	-0.38889000
H	5.74560700	11.35232500	0.26254100
C	4.67645700	11.85865600	-1.54760700
H	5.53084900	11.59350300	-2.18377600
H	3.77185100	11.52278900	-2.07622500
C	4.60652200	13.37804600	-1.34626700
H	4.50869200	13.88653400	-2.31414300
H	5.54528300	13.72918600	-0.89395400
C	3.43734900	13.74992900	-0.42557800
H	3.40883700	14.83464500	-0.25967200
H	2.48993100	13.47743500	-0.91434900
C	3.54035900	13.02707500	0.92557500
H	2.67329300	13.28160300	1.54639300
H	4.42952200	13.38801600	1.45977100
C	3.73948400	14.30883000	5.57148400
H	4.67721400	14.49854700	6.11328600
C	2.56652900	14.74132500	6.47127800
H	1.61848800	14.54289100	5.95082500

H	2.54890300	14.15798000	7.39892300
C	2.66139500	16.23956800	6.80929700
H	1.80210500	16.53791600	7.42416900
H	3.56071400	16.40777400	7.42015700
C	2.74142100	17.10741600	5.54528900
H	2.85929500	18.16429500	5.81773100
H	1.79298900	17.02676200	4.99312800
C	3.89050200	16.65770000	4.63181400
H	4.85276700	16.83631400	5.13359500
H	3.90121700	17.25200100	3.70899100
C	3.77585300	15.16530600	4.28769500
H	2.85277900	15.00883900	3.71258200
H	4.60877800	14.85880600	3.64813000
C	3.61762700	11.61988400	6.80674100
H	2.64964300	11.92018900	7.23171400
C	3.60347800	10.09141600	6.59509900
H	4.51283300	9.79305200	6.05726500
H	2.75433900	9.80551600	5.96424700
C	3.53225000	9.33030000	7.92724900
H	3.56292900	8.25006300	7.73462500
H	2.56784500	9.53942800	8.41395300
C	4.67237200	9.74115900	8.86761600
H	4.59071600	9.20771100	9.82345800
H	5.63232300	9.44658400	8.41920100
C	4.66552500	11.25753700	9.10209600
H	5.50242900	11.55029100	9.74914800
H	3.74269500	11.53640000	9.63231600
C	4.73919400	12.03693100	7.77957700
H	5.71380100	11.85477900	7.30473900
H	4.68603000	13.11271100	7.98417300
C	6.79890000	13.37356400	3.09263800
C	7.29098400	13.57137200	1.78314000
H	7.02443500	12.86398200	0.99893100
C	8.11122700	14.65112700	1.43276400
C	8.48212200	15.59038300	2.39867000
H	9.11581400	16.43389600	2.13324000
C	8.02910000	15.42976600	3.71174800
H	8.31177900	16.15219900	4.47614800
C	7.21012700	14.34342000	4.03872100
H	6.86426900	14.25825800	5.07025300
C	6.95638700	10.13598200	4.29587400
C	7.31223900	9.70216800	5.59190300
H	6.94799600	10.25210800	6.45897100
C	8.10799500	8.57299900	5.82474600
C	8.59078300	7.82462900	4.74835400
H	9.20245100	6.94164900	4.92078700

C	8.27921800	8.22733000	3.44547300
H	8.65240800	7.65542600	2.59707000
C	7.48224900	9.35799100	3.23668200
H	7.24422100	9.63192900	2.20748300
H	8.45951600	14.76123700	0.40667700
H	8.34621300	8.27381000	6.84460700

TS1'-triplet

UB3LYP-D3/6-31G(d)-SMD(THF)

Zero-point correction= 1.012533 (Hartree/Particle)
Thermal correction to Energy= 1.062685
Thermal correction to Enthalpy= 1.063629
Thermal correction to Gibbs Free Energy= 0.928710
Sum of electronic and zero-point Energies= -6158.104367
Sum of electronic and thermal Energies= -6158.054216
Sum of electronic and thermal Enthalpies= -6158.053272
Sum of electronic and thermal Free Energies= -6158.188190
HF=-6159.1169004

UB3LYP-D3/def2svp-SMD(THF)//UB3LYP-D3/6-31G(d)-SMD(THF)

HF=-6159.8920052

Fe	5.71014300	11.84255900	3.66034200
P	3.95804600	10.62945600	2.48838900
P	3.82830700	12.81634000	4.82416500
C	2.32624700	10.90163400	3.35770400
H	1.49822700	10.74794100	2.65514400
H	2.23099400	10.13525300	4.13024600
C	2.23900000	12.29564200	3.99719400
H	1.40785900	12.33906600	4.71044300
H	2.04401600	13.04957700	3.22868200
C	4.15679600	8.76222900	2.43362300
H	5.18986200	8.63978200	2.08411500
C	4.07449200	8.14878400	3.84656500
H	3.04549600	8.22713200	4.22299700
H	4.71048800	8.69959400	4.54224200
C	4.47133300	6.66583300	3.82869400
H	5.52087500	6.58129500	3.51454800
H	4.40738200	6.25208700	4.84383200
C	3.57825200	5.87052500	2.86768000
H	3.89737800	4.82099200	2.82529200
H	2.54628300	5.87302500	3.24989500
C	3.59721100	6.48836600	1.46349500
H	2.91260200	5.94692600	0.79735800
H	4.60536700	6.38083000	1.03702200
C	3.23003500	7.98334900	1.47923100

H	3.29746100	8.36931700	0.45750600
H	2.18483000	8.10391500	1.80021100
C	3.53717800	11.06295100	0.71384000
H	2.73629500	10.36335900	0.43754100
C	4.73654500	10.82227200	-0.22389200
H	5.11018400	9.79689200	-0.11743200
H	5.55003100	11.49118400	0.07022700
C	4.36462400	11.10350500	-1.68696600
H	5.24322600	10.95171400	-2.32756500
H	3.60173300	10.38290800	-2.01871100
C	3.82139500	12.52941900	-1.85113100
H	3.54170400	12.71581000	-2.89629400
H	4.61544300	13.24756600	-1.59972600
C	2.61730600	12.76447500	-0.92941400
H	2.25313500	13.79546300	-1.02949200
H	1.79248700	12.10642900	-1.24234500
C	2.95841000	12.48200600	0.54361400
H	2.05115800	12.59597500	1.14743700
H	3.68177600	13.22207900	0.89958400
C	3.59176200	14.66006000	5.03494600
H	4.44808200	14.96945300	5.64762300
C	2.29491900	15.04813400	5.77727200
H	1.42821200	14.74612800	5.17320000
H	2.21138600	14.52334900	6.73505200
C	2.23540300	16.56669800	6.01322800
H	1.30090800	16.82624800	6.52790600
H	3.05770000	16.85609600	6.68420100
C	2.35591800	17.34627200	4.69671200
H	2.35459800	18.42665100	4.89156200
H	1.47411300	17.13535300	4.07311700
C	3.62048500	16.94043200	3.92826400
H	4.50902000	17.24975700	4.49874700
H	3.66770700	17.46304900	2.96391100
C	3.68253300	15.42272600	3.69841400
H	2.85229500	15.12310800	3.04263800
H	4.59960000	15.15754500	3.16997000
C	3.67258700	12.13914600	6.57186500
H	2.61193500	12.22305900	6.84948600
C	4.06064400	10.64605200	6.58584800
H	5.08788300	10.54628100	6.20970400
H	3.41783400	10.08120900	5.90507900
C	3.98783800	10.03428300	7.99195300
H	4.31143500	8.98588600	7.95063400
H	2.94229200	10.03127900	8.33458900
C	4.84506900	10.82718200	8.98551500
H	4.76874200	10.39357800	9.99107600

H	5.90083100	10.76034900	8.68478100
C	4.42231900	12.30135200	9.00147200
H	5.05255500	12.87347800	9.69467100
H	3.38936800	12.37821100	9.37363300
C	4.51099000	12.92812900	7.60091300
H	5.55759300	12.94160900	7.28454800
H	4.18030500	13.97059000	7.65105100
C	6.94923600	12.59289900	5.06765300
C	7.03926300	14.00147200	5.18332000
H	6.51435900	14.62801400	4.46775900
C	7.77428000	14.63625200	6.18740600
C	8.46318700	13.88037300	7.14183100
H	9.03254500	14.36682400	7.93060200
C	8.40690800	12.48907100	7.05620300
H	8.93913000	11.87690200	7.78280600
C	7.66924300	11.87016200	6.03713700
H	7.66218900	10.78571600	6.01777900
C	6.96523300	10.33022600	3.23402700
C	7.21724000	9.24816100	4.10122100
H	6.78592600	9.24382300	5.10049300
C	7.98742500	8.13851000	3.73003600
C	8.55251200	8.06991400	2.45504300
H	9.15377700	7.21303200	2.15996500
C	8.32786100	9.12516700	1.56578100
H	8.75563900	9.09473900	0.56471300
C	7.54703400	10.21928300	1.95097800
H	7.37721200	11.00937200	1.22678400
H	7.80357900	15.72417900	6.22869300
H	8.14278500	7.32786400	4.44007300
Br	6.15577500	13.48938800	1.88175600
C	8.62082400	14.10685500	1.50335100
C	8.77022100	13.62261000	0.09140400
H	8.64947200	12.53673200	0.02031000
H	8.05069100	14.09862100	-0.58352600
H	9.78205400	13.86585100	-0.27933800
C	8.51449100	15.58933500	1.70365700
H	7.82271200	16.05058900	0.99037900
H	8.18519800	15.83303600	2.71903100
H	9.50374500	16.05825400	1.55453300
C	9.33183300	13.32557600	2.56328800
H	9.11956100	13.70972000	3.56291800
H	9.05662000	12.26660200	2.54634800
H	10.42197500	13.38754000	2.39472900

TS1'-quintet
UB3LYP-D3/6-31G(d)-SMD(THF)

Zero-point correction= 1.010660 (Hartree/Particle)
Thermal correction to Energy= 1.061782
Thermal correction to Enthalpy= 1.062727
Thermal correction to Gibbs Free Energy= 0.922226
Sum of electronic and zero-point Energies= -6158.088333
Sum of electronic and thermal Energies= -6158.037211
Sum of electronic and thermal Enthalpies= -6158.036266
Sum of electronic and thermal Free Energies= -6158.176767
HF=-6159.098993

UB3LYP-D3/def2svp-SMD(THF)//UB3LYP-D3/6-31G(d)-SMD(THF)
HF=-6159.8685748

C	-4.54340700	2.88308400	-1.60219600
C	-4.30032700	2.25847200	-2.99011000
P	-3.27512400	4.18774700	-1.13962700
P	-3.70515200	3.43591300	-4.31938600
Fe	-1.99496100	4.72227300	-3.22705500
C	-4.34410800	5.54927100	-0.43393200
C	-5.16684900	5.15795400	0.80871100
C	-3.58429300	6.86933100	-0.19435400
H	-5.05096600	5.73503500	-1.25433100
C	-6.14078900	6.28694200	1.18854600
H	-4.48881600	4.96503300	1.65080000
H	-5.72463700	4.23015800	0.63071000
C	-4.56635300	7.99355700	0.16599600
H	-2.86961200	6.74672100	0.62672600
H	-2.98820800	7.13365900	-1.07109100
C	-5.40953900	7.62176900	1.39483700
H	-6.69634200	6.01164500	2.09459500
H	-6.88301000	6.40205800	0.38458000
H	-4.01548300	8.92552200	0.34880000
H	-5.23187300	8.18187400	-0.69007300
H	-6.13083100	8.41789800	1.62043700
H	-4.74750200	7.53692900	2.26957500
C	-2.38478200	3.37640200	0.29459000
C	-1.50913400	2.23676300	-0.26284000
C	-1.53534300	4.35500300	1.12829700
H	-3.16064800	2.94294600	0.94301300
C	-0.72565300	1.51516000	0.84224300
H	-0.79860400	2.66305500	-0.98106800
H	-2.12565300	1.51674900	-0.81635400
C	-0.73796700	3.62545700	2.22114400
H	-0.85039100	4.88858400	0.46104500
H	-2.17669800	5.10784900	1.59654300
C	0.13325900	2.50674900	1.63721300

H	-0.09818200	0.73298600	0.39560100
H	-1.42746100	1.01165700	1.52403900
H	-0.11869200	4.35089600	2.76508300
H	-1.43625500	3.19369000	2.95427000
H	0.68088400	1.98911300	2.43549900
H	0.88439100	2.94872900	0.96589200
H	-3.50933400	1.50381600	-2.91259600
H	-5.20281100	1.74003900	-3.33530300
H	-5.53135900	3.34871200	-1.56304700
H	-4.54682500	2.09044400	-0.84518300
C	-3.21182700	2.22497700	-5.66101900
H	-2.61346000	1.49542200	-5.10103500
C	-2.27149500	2.82776800	-6.72400900
H	-2.79000500	3.60201500	-7.30184700
H	-1.42392300	3.30869600	-6.23026500
C	-1.76269300	1.73430400	-7.67669700
H	-1.12054700	2.18364000	-8.44531100
H	-1.13176000	1.03613900	-7.10773100
C	-2.91975200	0.96378600	-8.32689700
H	-3.49286700	1.64787100	-8.97077600
H	-2.53278600	0.16776400	-8.97635400
C	-3.85676500	0.37360800	-7.26377400
H	-3.31139800	-0.38200100	-6.67921900
H	-4.70093900	-0.14228900	-7.73995700
C	-4.38317800	1.46170600	-6.31267100
H	-5.02473500	1.00761900	-5.54786200
H	-5.01183600	2.15659300	-6.88396800
C	-5.27684200	4.26315000	-4.93033000
H	-5.98158200	3.43806500	-5.11103700
C	-5.06992200	5.02620500	-6.25585700
H	-4.30054300	5.79123300	-6.11747000
H	-4.70806400	4.34886400	-7.03442200
C	-6.36607100	5.69899300	-6.73308200
H	-6.16859000	6.24536800	-7.66434900
H	-7.11484400	4.92762400	-6.96928200
C	-6.93015500	6.64264500	-5.66521700
H	-6.21083100	7.45537400	-5.48874900
H	-7.86217900	7.10675300	-6.01311400
C	-7.16747700	5.88203400	-4.35599600
H	-7.95014800	5.12497600	-4.51453900
H	-7.53729900	6.55993200	-3.57536900
C	-5.88806800	5.18960400	-3.86047900
H	-6.12279500	4.62341900	-2.95626400
H	-5.15022800	5.95105500	-3.58538800
C	-2.35524800	6.37175900	-4.39137500
C	-1.80634300	6.40436400	-5.68738300

C	-3.07542800	7.51055000	-3.98861100
C	-1.98103300	7.49919000	-6.54233900
H	-1.23923100	5.55094500	-6.05221100
C	-3.27134300	8.60777800	-4.83435800
H	-3.49536500	7.55068300	-2.98621800
C	-2.72568100	8.60466900	-6.12200000
H	-3.84443200	9.46638300	-4.48790100
H	-2.87321400	9.45440600	-6.78468900
C	-0.53403800	3.35059400	-3.73399800
C	-0.54322200	1.94994100	-3.59297600
C	0.54916000	3.88154200	-4.46900000
C	0.44197000	1.12509900	-4.15166800
H	-1.34260100	1.46937400	-3.03298900
C	1.53365200	3.07433600	-5.04752600
H	0.62506100	4.95899100	-4.59654200
C	1.48484700	1.68534500	-4.89232000
H	0.39065000	0.04632800	-4.01194800
H	2.25004100	1.05215300	-5.33590400
H	-1.54448600	7.48511500	-7.53972200
H	2.34465800	3.52886200	-5.61459300
Br	-0.37399600	6.10353200	-1.99253700
C	0.67780100	8.11649100	-0.50559600
C	2.03207200	8.18455000	-1.13979200
H	2.59014900	7.25125200	-1.00413200
H	1.96520400	8.39414300	-2.21307700
H	2.63435100	8.99354900	-0.68523700
C	0.57635400	7.51960000	0.86353500
H	0.95523300	8.22705400	1.62493000
H	-0.46119400	7.28712100	1.12634600
H	1.16938300	6.60248500	0.95257400
C	-0.32258500	9.16511500	-0.88240700
H	-0.34210700	9.33822400	-1.96402700
H	-1.33466800	8.88929700	-0.56656800
H	-0.07733900	10.12844700	-0.39776200

tBu•

UB3LYP-D3/6-31G(d)-SMD(THF)

Zero-point correction= 0.117064 (Hartree/Particle)
Thermal correction to Energy= 0.123382
Thermal correction to Enthalpy= 0.124326
Thermal correction to Gibbs Free Energy= 0.087681
Sum of electronic and zero-point Energies= -157.690001
Sum of electronic and thermal Energies= -157.683683
Sum of electronic and thermal Enthalpies= -157.682739
Sum of electronic and thermal Free Energies= -157.719384
HF=-157.8070652

UB3LYP-D3/def2svp-SMD(THF)//UB3LYP-D3/6-31G(d)-SMD(THF)
HF=-157.6930095

C	-0.85854800	-1.02988100	0.27843500
C	-0.22041700	-0.12742200	1.28836500
H	0.87396700	-0.12097900	1.19848400
H	-0.57862400	0.90664500	1.19779600
H	-0.44695500	-0.44684000	2.32433500
C	-2.32106700	-0.86957400	0.00103400
H	-2.61471100	0.18725700	-0.05079800
H	-2.61514000	-1.35431100	-0.93936300
H	-2.94155900	-1.32755400	0.79591100
C	-0.22028500	-2.35558500	0.00145900
H	-0.58003100	-2.79505100	-0.93833400
H	0.87397400	-2.28034500	-0.05121800
H	-0.44461700	-3.09255400	0.79716300

B'-doublet
UB3LYP-D3/6-31G(d)-SMD(THF)
Zero-point correction= 0.893357 (Hartree/Particle)
Thermal correction to Energy= 0.936761
Thermal correction to Enthalpy= 0.937705
Thermal correction to Gibbs Free Energy= 0.818214
Sum of electronic and zero-point Energies= -6000.388038
Sum of electronic and thermal Energies= -6000.344635
Sum of electronic and thermal Enthalpies= -6000.343690
Sum of electronic and thermal Free Energies= -6000.463181
HF=-6001.2813954

UB3LYP-D3/def2svp-SMD(THF)//UB3LYP-D3/6-31G(d)-SMD(THF)
HF=-6002.1669846

Fe	5.86806700	11.64693000	3.84438200
P	4.08707300	10.47366000	2.56013500
P	3.90706000	12.75319900	4.82148400
C	2.41819500	10.86323300	3.30930300
H	1.63411900	10.73160700	2.55401600
H	2.22799200	10.12629000	4.09216400
C	2.35716800	12.27689100	3.90561100
H	1.48727500	12.37685400	4.56465500
H	2.24383200	13.01824800	3.10980900
C	4.16616900	8.59659500	2.55798000
H	5.21610300	8.39529000	2.31098800
C	3.90126800	8.01993900	3.96459900
H	2.84592500	8.16838900	4.22944500

H	4.49364700	8.54449100	4.71705500
C	4.20160200	6.51496100	4.00681500
H	5.26856000	6.35713800	3.79705800
H	4.01309600	6.12664300	5.01635100
C	3.35434900	5.75974200	2.97450100
H	3.60675200	4.69147100	2.97736200
H	2.29313900	5.83553000	3.25557900
C	3.54740000	6.34681100	1.57038300
H	2.89334500	5.83891700	0.84957000
H	4.58144200	6.16444400	1.24299800
C	3.28211500	7.86284000	1.52930700
H	3.47195200	8.22242700	0.51368400
H	2.22212900	8.05942300	1.74721700
C	3.82891300	10.90383200	0.75694900
H	2.99946200	10.25754400	0.43719000
C	5.06982600	10.55887300	-0.09044600
H	5.36334100	9.51296500	0.05948700
H	5.90422900	11.17938400	0.24774600
C	4.81208000	10.82946700	-1.58007000
H	5.71658400	10.60135500	-2.15880500
H	4.02266000	10.15528600	-1.94605800
C	4.38278700	12.28515400	-1.80861400
H	4.18150900	12.46297000	-2.87315500
H	5.20904300	12.95215800	-1.52364200
C	3.14448300	12.62910200	-0.97007400
H	2.86493100	13.68117000	-1.11332600
H	2.29391100	12.02537600	-1.32158000
C	3.37211800	12.35894300	0.52691100
H	2.43955900	12.55374900	1.06811100
H	4.13062400	13.04511600	0.91495300
C	3.78711200	14.61422400	4.90528600
H	4.62853600	14.90804000	5.54537500
C	2.47906900	15.12439300	5.54726300
H	1.62850300	14.83453700	4.91512700
H	2.31361200	14.67009200	6.53013700
C	2.50471900	16.65619700	5.68285900
H	1.56204100	17.00470500	6.12462800
H	3.30600900	16.93880800	6.38144000
C	2.74667400	17.33804300	4.32921500
H	2.80462400	18.42680600	4.45650100
H	1.88804400	17.14092700	3.66986100
C	4.02241100	16.80682600	3.66189500
H	4.89685700	17.09805900	4.26260700
H	4.15494800	17.26140700	2.67160500
C	3.99740500	15.27643500	3.52880700
H	3.18109700	14.98940500	2.85081900

H	4.92032700	14.91709300	3.06892700
C	3.62097000	12.17053500	6.58133200
H	2.55311700	12.32234500	6.79459800
C	3.93101300	10.66181800	6.68409200
H	4.97411600	10.49649600	6.38071400
H	3.30279300	10.09344200	5.99195300
C	3.74459500	10.12573100	8.11066100
H	4.01169600	9.06130000	8.13845400
H	2.68216000	10.19436300	8.38762100
C	4.58489700	10.92181700	9.11621700
H	4.42328900	10.54499300	10.13430400
H	5.65129700	10.78138300	8.88688300
C	4.24857200	12.41617200	9.03640500
H	4.87320400	12.98712100	9.73535200
H	3.20349500	12.57008800	9.34477200
C	4.44868100	12.96476300	7.61490700
H	5.50945200	12.90359700	7.35625600
H	4.17730900	14.02507600	7.59479800
C	7.04074400	12.45004000	5.22913100
C	7.19541700	13.85013400	5.32305200
H	6.78201000	14.48429100	4.54534000
C	7.85494300	14.45788300	6.39454500
C	8.40346700	13.67962700	7.41804600
H	8.91566900	14.14801700	8.25522700
C	8.29470900	12.29057100	7.33913200
H	8.72995900	11.66409900	8.11564900
C	7.62955500	11.69385200	6.26054100
H	7.57741800	10.61090000	6.23843900
C	6.99798000	10.05993800	3.47703000
C	7.03795500	9.01531000	4.42072300
H	6.47996300	9.09747000	5.35075300
C	7.75985100	7.83679500	4.20186600
C	8.48002500	7.66751500	3.01702600
H	9.04095100	6.75332600	2.83784600
C	8.47379700	8.69489300	2.06988900
H	9.03636700	8.58436900	1.14449900
C	7.74596700	9.86722000	2.30008000
H	7.76118900	10.64976000	1.54904700
H	7.93802800	15.54269100	6.43087200
H	7.75612000	7.05265400	4.95649700
Br	6.57815200	13.12199700	2.05390600

B'-quartet

UB3LYP-D3/6-31G(d)-SMD(THF)

Zero-point correction= 0.893213 (Hartree/Particle)

Thermal correction to Energy= 0.936765

Thermal correction to Enthalpy= 0.937709
Thermal correction to Gibbs Free Energy= 0.816920
Sum of electronic and zero-point Energies= -6000.414197
Sum of electronic and thermal Energies= -6000.370645
Sum of electronic and thermal Enthalpies= -6000.369701
Sum of electronic and thermal Free Energies= -6000.490490
HF=-6001.3074102

UB3LYP-D3/def2svp-SMD(THF)//UB3LYP-D3/6-31G(d)-SMD(THF)
HF=-6002.192913

Fe	5.85913000	11.67502800	3.78058400
P	4.06455200	10.46844500	2.55766500
P	3.90709300	12.77794600	4.80469500
C	2.40321000	10.87733500	3.30921200
H	1.61783100	10.74582900	2.55534600
H	2.20853000	10.14722800	4.09758300
C	2.35467700	12.29768400	3.89227800
H	1.48592500	12.40917600	4.55084200
H	2.24530300	13.03147300	3.08884900
C	4.15717500	8.59481000	2.56571100
H	5.20880700	8.40232100	2.31814700
C	3.89967500	8.02566300	3.97656300
H	2.84528200	8.17439000	4.24539200
H	4.49545900	8.55640100	4.72173200
C	4.20509700	6.52196600	4.02614200
H	5.27220000	6.36724300	3.81502000
H	4.02033400	6.13903000	5.03835200
C	3.35885500	5.75772100	2.99981700
H	3.61529300	4.69048400	3.00864600
H	2.29779800	5.83127900	3.28197500
C	3.54807000	6.33699200	1.59192300
H	2.89546800	5.82214100	0.87483800
H	4.58257300	6.15732000	1.26466000
C	3.27561400	7.85144000	1.54194800
H	3.46286400	8.20648500	0.52419300
H	2.21511200	8.04432500	1.76045500
C	3.81817400	10.89571400	0.75309200
H	2.99288200	10.24383100	0.43410700
C	5.06514800	10.55104300	-0.08510300
H	5.36026100	9.50646700	0.07051300
H	5.89642300	11.17537300	0.25464100
C	4.81327700	10.81462800	-1.57712800
H	5.72181200	10.58837200	-2.15004100
H	4.02916000	10.13466500	-1.94370000
C	4.37784400	12.26709800	-1.81444100

H	4.18005000	12.43830000	-2.88067200
H	5.19935000	12.93952000	-1.52907500
C	3.13423500	12.60931300	-0.98316100
H	2.85051100	13.65935600	-1.13230500
H	2.28772800	12.00003300	-1.33483000
C	3.35694800	12.34787400	0.51612800
H	2.42147600	12.54143900	1.05256300
H	4.11187000	13.03882200	0.90311300
C	3.78277100	14.63793600	4.89919800
H	4.62109300	14.92838500	5.54516500
C	2.47045100	15.13785600	5.54122900
H	1.62343100	14.85101200	4.90311200
H	2.30271400	14.67412500	6.51920800
C	2.48997000	16.66838500	5.69046200
H	1.54476100	17.00897800	6.13294600
H	3.28839400	16.94808200	6.39345400
C	2.73231700	17.36245400	4.34321600
H	2.78509900	18.45036300	4.47953100
H	1.87628200	17.16687700	3.68004500
C	4.01225800	16.84235900	3.67529700
H	4.88368400	17.13264300	4.28079300
H	4.14552200	17.30534700	2.68904400
C	3.99536400	15.31295500	3.52936100
H	3.18348000	15.02700500	2.84551500
H	4.92207900	14.96267600	3.07012400
C	3.62338800	12.18288600	6.56219700
H	2.55329600	12.32561400	6.77100400
C	3.94224000	10.67531000	6.65608300
H	4.98373900	10.51606500	6.34590500
H	3.31281800	10.10942000	5.96332000
C	3.76059300	10.12857500	8.07936700
H	4.03926200	9.06690300	8.09990300
H	2.69737100	10.18358700	8.35641400
C	4.59075200	10.92639600	9.09182900
H	4.43224100	10.54005600	10.10685100
H	5.65895900	10.80075400	8.86281900
C	4.23639400	12.41699900	9.02227700
H	4.85088500	12.99029700	9.72827400
H	3.18809600	12.55586800	9.32690500
C	4.43777600	12.97812700	7.60591300
H	5.50027200	12.92989000	7.35378800
H	4.15522500	14.03566500	7.59195200
C	7.01335300	12.39681700	5.27137500
C	7.18945600	13.79518700	5.35096000
H	6.76828200	14.43137700	4.57879000
C	7.88451700	14.40081700	6.40118800

C	8.43766100	13.62189600	7.42134200
H	8.97418800	14.08841100	8.24421400
C	8.29898300	12.23467900	7.35959700
H	8.73390100	11.60772400	8.13586600
C	7.60544500	11.64012500	6.29750500
H	7.53063500	10.55869600	6.28832900
C	7.01356900	10.05569500	3.51171500
C	7.05548100	8.98870100	4.42788300
H	6.49335800	9.04634000	5.35714700
C	7.78579100	7.82060400	4.18151800
C	8.51273000	7.68474500	2.99658100
H	9.08050400	6.77900800	2.79727800
C	8.50404700	8.73572100	2.07609800
H	9.07132200	8.65344000	1.15059300
C	7.76678100	9.89717300	2.33214300
H	7.77989100	10.69730000	1.59904500
H	7.98751700	15.48420800	6.42518600
H	7.78340600	7.01792800	4.91649900
Br	6.58583500	13.20634700	1.98921400

B'-sextet

UB3LYP-D3/6-31G(d)-SMD(THF)

Zero-point correction= 0.892444 (Hartree/Particle)
Thermal correction to Energy= 0.936557
Thermal correction to Enthalpy= 0.937502
Thermal correction to Gibbs Free Energy= 0.813645
Sum of electronic and zero-point Energies= -6000.390164
Sum of electronic and thermal Energies= -6000.346051
Sum of electronic and thermal Enthalpies= -6000.345107
Sum of electronic and thermal Free Energies= -6000.468963
HF=-6001.2826083

UB3LYP-D3/def2svp-SMD(THF)//UB3LYP-D3/6-31G(d)-SMD(THF)

HF=-6002.166422

Fe	6.19429700	11.79849600	3.77888400
P	4.03020200	10.42603900	2.46356300
P	3.96184500	12.75199900	4.82352900
C	2.42012300	10.84900100	3.30615800
H	1.57813300	10.73239200	2.61237200
H	2.27016500	10.12177100	4.10865000
C	2.41736500	12.27189200	3.89338100
H	1.54745800	12.40572300	4.54705000
H	2.32432900	13.00694600	3.08850100
C	4.09242600	8.54801000	2.46496000
H	5.11187900	8.33533500	2.11470500

C	3.97707600	7.98194300	3.89588100
H	2.96611400	8.16419100	4.28509700
H	4.67696300	8.48856700	4.56564900
C	4.23681900	6.46844900	3.91383000
H	5.27175000	6.27971200	3.59596700
H	4.14492800	6.08860900	4.93996200
C	3.26648200	5.73217800	2.98064900
H	3.48642200	4.65675200	2.96872600
H	2.24221300	5.84179100	3.36786400
C	3.33132500	6.30352800	1.55813600
H	2.59593600	5.80668500	0.91166300
H	4.32253600	6.09251800	1.13052700
C	3.09956900	7.82499200	1.53362200
H	3.19685700	8.18086900	0.50283100
H	2.07080000	8.04658800	1.85377000
C	3.71896900	10.86495900	0.66903900
H	2.86115500	10.26402000	0.33552800
C	4.94791300	10.49381500	-0.18702100
H	5.18748200	9.42908600	-0.07743900
H	5.81310200	11.05727100	0.18109500
C	4.72354600	10.83255600	-1.66809300
H	5.62312400	10.58177800	-2.24520200
H	3.90739000	10.21080700	-2.06610500
C	4.36747400	12.31437600	-1.84731900
H	4.18509700	12.53957800	-2.90621800
H	5.22248500	12.92999100	-1.53257500
C	3.13998800	12.68753500	-1.00543900
H	2.91411500	13.75683100	-1.11063500
H	2.26375700	12.14012500	-1.38434700
C	3.34236800	12.34924800	0.48124000
H	2.42079500	12.57836500	1.02838600
H	4.13592300	12.98273400	0.89390000
C	3.79539600	14.61015600	4.92903300
H	4.58544400	14.90606900	5.63048600
C	2.44230400	15.09987000	5.48572300
H	1.63895200	14.81672100	4.79240500
H	2.21491200	14.62390300	6.44645900
C	2.44619400	16.62949500	5.64555700
H	1.47367400	16.96582700	6.02809400
H	3.19758800	16.90897200	6.39873500
C	2.77071500	17.33042800	4.31884700
H	2.80845500	18.41808500	4.46194400
H	1.96007600	17.13293900	3.60144400
C	4.09446800	16.82221800	3.73128300
H	4.92272400	17.11602800	4.39308200
H	4.28733600	17.29098700	2.75769000

C	4.09810000	15.29303100	3.57968700
H	3.34058400	15.00263700	2.83765200
H	5.05929300	14.95447800	3.18458600
C	3.66750500	12.12508700	6.56522300
H	2.58409400	12.17851300	6.74550600
C	4.11153600	10.64947700	6.63906900
H	5.17464000	10.60052400	6.36759300
H	3.56633400	10.04765600	5.90569600
C	3.92798600	10.05467100	8.04194400
H	4.29223300	9.01912900	8.05174900
H	2.85490800	10.01658300	8.28121900
C	4.65555600	10.89485600	9.09869500
H	4.49219800	10.47655300	10.10018200
H	5.73793200	10.85722400	8.90738500
C	4.18888600	12.35518100	9.04451400
H	4.73426800	12.95889900	9.78125000
H	3.12398400	12.40622900	9.31704100
C	4.38686300	12.96076000	7.64572500
H	5.45796500	13.00270400	7.42368100
H	4.02063200	13.99251000	7.64234600
C	7.18656200	12.71432200	5.37961400
C	7.23006800	14.11793200	5.50473100
H	6.80594900	14.73718600	4.71716300
C	7.79418600	14.74857600	6.61809300
C	8.34886900	13.98277100	7.64838000
H	8.78343600	14.46692100	8.51991300
C	8.35273800	12.58989800	7.53958200
H	8.79776800	11.98396700	8.32681600
C	7.78343300	11.97355200	6.41826900
H	7.80868000	10.88786300	6.36225800
C	7.13905200	9.96558900	3.49189000
C	7.22425000	8.98477300	4.49847700
H	6.80036000	9.17629500	5.48328200
C	7.82341300	7.73874200	4.27756100
C	8.36089600	7.43597500	3.02402500
H	8.82355100	6.46837700	2.84393600
C	8.30052700	8.39188800	2.00545900
H	8.71896000	8.16880000	1.02564200
C	7.70221900	9.63409800	2.24272100
H	7.66334500	10.35677200	1.43137200
H	7.80008100	15.83510800	6.68449000
H	7.86491300	7.00485400	5.08020000
Br	6.76301600	13.18408300	1.92870500

TS2’
UB3LYP-D3/6-31G(d)-SMD(THF)

Zero-point correction= 0.891261 (Hartree/Particle)
Thermal correction to Energy= 0.934684
Thermal correction to Enthalpy= 0.935628
Thermal correction to Gibbs Free Energy= 0.813687
Sum of electronic and zero-point Energies= -6000.399457
Sum of electronic and thermal Energies= -6000.356034
Sum of electronic and thermal Enthalpies= -6000.355090
Sum of electronic and thermal Free Energies= -6000.477031
HF=-6001.2907179

UB3LYP-D3/def2svp-SMD(THF)//UB3LYP-D3/6-31G(d)-SMD(THF)
HF=-6002.181952

Fe	5.89849800	11.77721600	3.64042300
P	4.15013700	10.37359900	2.61422500
P	3.97050300	12.90498100	4.76246600
C	2.48787400	10.92950500	3.25877600
H	1.72048900	10.79979300	2.48659500
H	2.22313100	10.25302100	4.07497100
C	2.48371100	12.39155500	3.74905600
H	1.55587400	12.60627200	4.29317900
H	2.50486500	13.05115400	2.87600200
C	4.12789000	8.51989000	2.87505700
H	5.06308100	8.18382800	2.40718300
C	4.19373900	8.15444300	4.37144400
H	3.26470300	8.46500700	4.86602900
H	5.00306600	8.69744100	4.87052600
C	4.37231300	6.64140600	4.56337000
H	5.33672600	6.33463500	4.13209600
H	4.41336600	6.40426400	5.63434400
C	3.23708900	5.86281600	3.88474000
H	3.39821000	4.78208700	3.98837500
H	2.29033500	6.09292300	4.39590500
C	3.11413400	6.24302200	2.40299000
H	2.26259800	5.72360300	1.94448200
H	4.01464400	5.90768300	1.86767900
C	2.96083900	7.76204200	2.20990800
H	2.90576400	7.98345300	1.13899500
H	2.01154400	8.09297100	2.65479700
C	4.07061400	10.54964600	0.75560200
H	3.37351600	9.79107200	0.37526000
C	5.47342000	10.26439300	0.17294200
H	5.79461300	9.24932700	0.43750400
H	6.19941100	10.94879400	0.62753000
C	5.49767500	10.43894900	-1.35257000
H	6.51908400	10.28027300	-1.72248100

H	4.86660900	9.66816200	-1.82081100
C	4.98700900	11.82680800	-1.76290600
H	4.99481300	11.92922800	-2.85611700
H	5.66594000	12.59261800	-1.36181000
C	3.57505400	12.07345700	-1.21376300
H	3.22420900	13.07498300	-1.49593200
H	2.87808000	11.35332900	-1.66929100
C	3.53729000	11.92847400	0.31590700
H	2.50945800	12.06732500	0.67376400
H	4.15123400	12.71636600	0.76303400
C	3.78065300	14.78036200	4.87396800
H	4.75684100	15.10495400	5.26318000
C	2.68033800	15.28234800	5.83499500
H	1.69941300	14.95467900	5.46083600
H	2.79390500	14.85927500	6.83699700
C	2.69924500	16.81702800	5.94754300
H	1.89518000	17.14671300	6.61888900
H	3.64642400	17.12330200	6.41600500
C	2.57044400	17.49863200	4.57995900
H	2.64309800	18.58877100	4.68903600
H	1.57383800	17.28730800	4.16385100
C	3.63815700	16.97846600	3.60986500
H	4.63456600	17.28306400	3.96302300
H	3.50515500	17.42739500	2.61666900
C	3.59141400	15.44716200	3.49397900
H	2.61375600	15.16200100	3.08103000
H	4.35753000	15.09771200	2.80008800
C	3.63931900	12.35263300	6.51865000
H	2.66717600	12.75825800	6.82914400
C	3.57153000	10.82063900	6.64488500
H	4.49886900	10.38527300	6.25529800
H	2.75184500	10.42470700	6.03882100
C	3.38083000	10.37848700	8.10411600
H	3.36481500	9.28164500	8.15566600
H	2.39966100	10.72652800	8.46021000
C	4.47959100	10.94310400	9.01274200
H	4.30455000	10.64557200	10.05485600
H	5.44694900	10.51553700	8.71560500
C	4.55350100	12.47120100	8.89758400
H	5.37746200	12.86029200	9.50974300
H	3.62629500	12.91088100	9.29491400
C	4.74299300	12.91962800	7.44039500
H	5.71851900	12.57225200	7.08167000
H	4.76461800	14.01409900	7.39550700
C	7.36053800	11.50782600	4.97038700
C	8.08404800	12.71091300	5.17119200

H	8.16170200	13.42681300	4.35855500
C	8.67351700	13.00039800	6.39946900
C	8.59643900	12.09177100	7.46207700
H	9.06939800	12.31458700	8.41457100
C	7.91637800	10.88476400	7.27184300
H	7.85652400	10.16036700	8.08096800
C	7.30990200	10.59680900	6.04977000
H	6.79783700	9.64673600	5.93138200
C	7.57351800	10.62131900	3.26347100
C	7.47702400	9.21319000	3.27639300
H	6.77817500	8.72849000	3.94634700
C	8.24367400	8.41392000	2.43094500
C	9.17218900	8.99347800	1.56004300
H	9.76906800	8.37472400	0.89512900
C	9.33577900	10.38112300	1.58013100
H	10.07105900	10.85312300	0.93179300
C	8.57152100	11.17573900	2.43485900
H	8.72271800	12.24793600	2.42672700
H	9.20222100	13.94265200	6.52696700
H	8.11124200	7.33415600	2.45181500
Br	6.31865400	13.62450400	2.02403900

C-doublet

UB3LYP-D3/6-31G(d)-SMD(THF)

Zero-point correction= 0.708749 (Hartree/Particle)
Thermal correction to Energy= 0.742061
Thermal correction to Enthalpy= 0.743005
Thermal correction to Gibbs Free Energy= 0.640901
Sum of electronic and zero-point Energies= -5537.238085
Sum of electronic and thermal Energies= -5537.204773
Sum of electronic and thermal Enthalpies= -5537.203829
Sum of electronic and thermal Free Energies= -5537.305933
HF=-5537.9468337

UB3LYP-D3/def2svp-SMD(THF)//UB3LYP-D3/6-31G(d)-SMD(THF)

HF=-5539.1778703

C	-5.31612100	3.27599100	-1.58224300
C	-5.17041100	2.55529300	-2.93533400
P	-3.76857800	4.24678300	-1.14232200
P	-3.96580700	3.46343300	-4.05514000
Fe	-2.65611200	4.82145100	-2.94762600
C	-4.49332500	5.59342500	-0.06421300
C	-5.02529300	5.13934100	1.30694700
C	-3.55151000	6.80548900	0.07057400
H	-5.35218600	5.92883500	-0.66692400

C	-5.70819700	6.30159500	2.04746200
H	-4.19067400	4.76872900	1.91760300
H	-5.72720200	4.30401200	1.18804500
C	-4.24294100	7.96032200	0.81061900
H	-2.64590700	6.51873300	0.62069900
H	-3.22203000	7.12378300	-0.92683400
C	-4.77013000	7.51012900	2.18125000
H	-6.04564700	5.96781200	3.03765500
H	-6.60813800	6.60246200	1.49079300
H	-3.54728500	8.80169000	0.92589700
H	-5.08356600	8.32528700	0.20167900
H	-5.28721200	8.33868200	2.68254700
H	-3.91830400	7.23497700	2.82126700
C	-2.82774100	3.08281500	-0.02093400
C	-2.37302800	1.85873500	-0.84599900
C	-1.61283100	3.78676700	0.61519700
H	-3.49934000	2.73755100	0.77770900
C	-1.50177000	0.89726500	-0.02441500
H	-1.79952400	2.21144000	-1.71868800
H	-3.24215800	1.32094300	-1.24014200
C	-0.74598000	2.81580600	1.43143100
H	-1.00285100	4.23601500	-0.18353200
H	-1.94383400	4.61025700	1.25634900
C	-0.29372100	1.61805000	0.58681100
H	-1.17278700	0.06315700	-0.65800200
H	-2.10977400	0.46178900	0.78239000
H	0.12297400	3.34871800	1.83885200
H	-1.32659200	2.45228800	2.29244300
H	0.29981300	0.92269900	1.19431600
H	0.36218200	1.97356800	-0.22204700
H	-4.77055300	1.54712400	-2.78744600
H	-6.14510000	2.44123500	-3.42361900
H	-6.12556400	4.01191600	-1.63642100
H	-5.57446300	2.57037100	-0.78389000
C	-3.13930200	2.04242200	-4.94367100
H	-2.89283000	1.36358100	-4.11183300
C	-1.79975000	2.45958500	-5.58451100
H	-1.97592300	3.19327600	-6.38131000
H	-1.17536500	2.96597900	-4.83651200
C	-1.06371400	1.24403800	-6.16748200
H	-0.13167600	1.56629500	-6.64964100
H	-0.77924200	0.56886100	-5.34639000
C	-1.94618100	0.47941300	-7.16504300
H	-2.15389300	1.12604100	-8.03076400
H	-1.41390400	-0.40087800	-7.54826300
C	-3.27579200	0.05916100	-6.52180000

H	-3.07530900	-0.66235600	-5.71573000
H	-3.91038500	-0.45469500	-7.25586000
C	-4.02316400	1.26986600	-5.93860100
H	-4.95033400	0.94248300	-5.45052900
H	-4.31589500	1.93755600	-6.76022200
C	-5.09978100	4.30995800	-5.27633500
H	-5.77893200	3.55480100	-5.69730400
C	-4.30145800	4.96918100	-6.41704900
H	-3.53209100	5.61816000	-5.97637200
H	-3.77555900	4.20516000	-7.00033100
C	-5.20151900	5.79677500	-7.34744900
H	-4.58859800	6.27920500	-8.12012700
H	-5.89969900	5.12565600	-7.87029700
C	-6.00185000	6.84618600	-6.56591500
H	-5.30398200	7.56552700	-6.11197100
H	-6.65301200	7.41546800	-7.24202600
C	-6.82911100	6.18141700	-5.45824800
H	-7.58118700	5.52033800	-5.91457400
H	-7.37967100	6.93703200	-4.88247300
C	-5.93750300	5.36076100	-4.51529800
H	-6.55402900	4.87534600	-3.74937900
H	-5.25264100	6.03967600	-3.98488200
Br	-1.45855300	6.53725100	-3.95165900

C-quartet

UB3LYP-D3/6-31G(d)-SMD(THF)

Zero-point correction= 0.708547 (Hartree/Particle)
Thermal correction to Energy= 0.741997
Thermal correction to Enthalpy= 0.742941
Thermal correction to Gibbs Free Energy= 0.640742
Sum of electronic and zero-point Energies= -5537.264891
Sum of electronic and thermal Energies= -5537.231440
Sum of electronic and thermal Enthalpies= -5537.230496
Sum of electronic and thermal Free Energies= -5537.332695
HF=-5537.9734374

UB3LYP-D3/def2svp-SMD(THF)//UB3LYP-D3/6-31G(d)-SMD(THF)

HF=-5539.1961257

C	-5.31743600	3.44984000	-1.60987500
C	-5.18004800	2.66308100	-2.93102800
P	-3.76250300	4.39045500	-1.11163600
P	-3.96919700	3.47353000	-4.11910600
Fe	-2.59026800	4.95359400	-2.98518500
C	-4.50234900	5.65036700	0.06083600
C	-5.03084000	5.09039300	1.39506100

C	-3.57169600	6.85787300	0.28685900
H	-5.36588000	6.02281800	-0.51263500
C	-5.72009600	6.18706500	2.22430800
H	-4.19455200	4.67930300	1.97641300
H	-5.72813100	4.26260900	1.21419500
C	-4.26958300	7.94507700	1.11879800
H	-2.66013300	6.53859800	0.80789800
H	-3.25123300	7.26191000	-0.68175200
C	-4.78844600	7.38606400	2.45161800
H	-6.05469400	5.77434500	3.18529900
H	-6.62217000	6.52584000	1.69348300
H	-3.57950600	8.78014500	1.29662300
H	-5.11548100	8.35020200	0.54352300
H	-5.30815300	8.16983600	3.01798700
H	-3.93300000	7.06596800	3.06541700
C	-2.81021300	3.15852700	-0.07021400
C	-2.30699900	2.00872600	-0.97195800
C	-1.62209200	3.83366000	0.64414900
H	-3.48771100	2.73769100	0.68610900
C	-1.44336200	1.00129000	-0.19865800
H	-1.71132700	2.43496400	-1.79540300
H	-3.15196100	1.48939300	-1.43450400
C	-0.76190100	2.81911300	1.41349500
H	-0.99934100	4.34509900	-0.10535500
H	-1.97908000	4.60570000	1.33292900
C	-0.26540000	1.69213400	0.49925200
H	-1.08323200	0.22200900	-0.88301800
H	-2.06704600	0.49826300	0.55507700
H	0.08596600	3.33489100	1.88264500
H	-1.35966500	2.38610600	2.22941100
H	0.32117400	0.96284200	1.07271000
H	0.40800600	2.11447800	-0.26162800
H	-4.80034900	1.65590600	-2.73217900
H	-6.16227800	2.54077800	-3.40289100
H	-6.08946500	4.21956500	-1.72026900
H	-5.64066300	2.78538000	-0.79947200
C	-3.17747800	1.99965600	-4.94937700
H	-2.95938900	1.33240800	-4.10077800
C	-1.81963300	2.36651000	-5.58366700
H	-1.96762600	3.08633600	-6.39854400
H	-1.18845300	2.87299500	-4.84100100
C	-1.11099500	1.11837500	-6.13123100
H	-0.16589300	1.40468000	-6.61045000
H	-0.85314100	0.45485800	-5.29205900
C	-2.00346300	0.35495300	-7.12083900
H	-2.18510600	0.98689600	-8.00305200

H	-1.49061400	-0.54736800	-7.47827900
C	-3.35006700	-0.01576200	-6.48268900
H	-3.17690800	-0.72367900	-5.65844200
H	-3.99058900	-0.52939800	-7.21166200
C	-4.07129000	1.22718400	-5.93570600
H	-5.01102700	0.93638800	-5.44850500
H	-4.33873300	1.88240600	-6.77569000
C	-5.08571100	4.30044900	-5.36722700
H	-5.77149900	3.54511600	-5.77695100
C	-4.25944800	4.91610200	-6.51311600
H	-3.49137400	5.57138600	-6.07879100
H	-3.73151400	4.12947700	-7.06359700
C	-5.13611200	5.72126300	-7.48462500
H	-4.50567800	6.17296100	-8.26164900
H	-5.83144600	5.03951700	-7.99741100
C	-5.93982000	6.80254100	-6.75127800
H	-5.24371500	7.53237600	-6.31198900
H	-6.57665600	7.35252800	-7.45637600
C	-6.78900500	6.18271600	-5.63413000
H	-7.54092400	5.51359800	-6.07888000
H	-7.34022700	6.96215900	-5.09185600
C	-5.91986300	5.38545000	-4.65066500
H	-6.55373100	4.93172200	-3.87953600
H	-5.23517500	6.07361600	-4.13248700
Br	-1.47641200	6.72944600	-4.05188500

C-sextet

UB3LYP-D3/6-31G(d)-SMD(THF)

Zero-point correction= 0.709122 (Hartree/Particle)
Thermal correction to Energy= 0.742553
Thermal correction to Enthalpy= 0.743497
Thermal correction to Gibbs Free Energy= 0.641631
Sum of electronic and zero-point Energies= -5537.223317
Sum of electronic and thermal Energies= -5537.189886
Sum of electronic and thermal Enthalpies= -5537.188942
Sum of electronic and thermal Free Energies= -5537.290808
HF=-5537.932439

UB3LYP-D3/def2svp-SMD(THF)//UB3LYP-D3/6-31G(d)-SMD(THF)

HF=-5539.1603167

C	-4.90242500	2.96854900	-1.61554200
C	-4.65712900	2.24166400	-2.95684200
P	-3.47915500	4.05890500	-1.05708500
P	-3.69318200	3.23941400	-4.21050500
Fe	-1.88530800	4.30642800	-2.93206600

C	-4.37157800	5.51770300	-0.29875500
C	-5.13529700	5.20404100	1.00132300
C	-3.46735200	6.75643800	-0.13947700
H	-5.10988000	5.76445200	-1.07699700
C	-5.94461000	6.42402400	1.47169900
H	-4.41804500	4.92772100	1.78612200
H	-5.79988000	4.34206100	0.85919100
C	-4.28601800	7.96680900	0.33685500
H	-2.67235900	6.55233600	0.58898800
H	-2.97872200	6.97943100	-1.09340800
C	-5.04892400	7.66063900	1.63354300
H	-6.45332500	6.19227000	2.41669700
H	-6.73061800	6.64016900	0.73294400
H	-3.62403600	8.83114100	0.47706500
H	-5.00456100	8.24376000	-0.44927400
H	-5.64982600	8.52754000	1.93772000
H	-4.32555800	7.47703600	2.44219200
C	-2.72615400	3.06738600	0.33900900
C	-2.18573600	1.73317000	-0.21810000
C	-1.60386000	3.86227700	1.03232100
H	-3.51930500	2.84884800	1.06768700
C	-1.47150100	0.90777400	0.86204200
H	-1.47775600	1.95522200	-1.03438400
H	-2.99920500	1.14314900	-0.65794400
C	-0.88329600	3.02642700	2.10148500
H	-0.87936800	4.18696900	0.26861800
H	-2.00954700	4.77016000	1.49114100
C	-0.34488700	1.71176300	1.52368700
H	-1.07597700	-0.01531700	0.41847500
H	-2.19990700	0.60434700	1.62902300
H	-0.06833500	3.61554600	2.54162700
H	-1.58704100	2.80117100	2.91688900
H	0.13873800	1.11775900	2.30994100
H	0.42670300	1.93635400	0.77254000
H	-4.05320100	1.34432400	-2.77977500
H	-5.61034400	1.90727000	-3.38381100
H	-5.77866000	3.61736300	-1.69430300
H	-5.13280400	2.23160400	-0.83688900
C	-3.10220500	1.92739100	-5.39985200
H	-2.73232700	1.14393400	-4.71975200
C	-1.88525900	2.41308000	-6.21496300
H	-2.17836500	3.23496900	-6.87952100
H	-1.13042300	2.82287300	-5.52796300
C	-1.30019200	1.26990900	-7.05647300
H	-0.45797100	1.63941200	-7.65561400
H	-0.89712200	0.49763500	-6.38441300

C	-2.36838800	0.64233700	-7.96485100
H	-2.70239000	1.39184000	-8.69793500
H	-1.94048400	-0.19088400	-8.53726900
C	-3.57940600	0.16094300	-7.15205700
H	-3.26595000	-0.65699600	-6.48653700
H	-4.34826700	-0.25062800	-7.81899600
C	-4.17651500	1.29752900	-6.30480800
H	-5.01228300	0.92045700	-5.70154800
H	-4.58800200	2.06356400	-6.97526600
C	-4.97416200	4.27112500	-5.10575400
H	-5.75798400	3.58946200	-5.46756700
C	-4.35044700	5.00428600	-6.31233800
H	-3.49834100	5.59902100	-5.96045800
H	-3.96658300	4.28292600	-7.04038200
C	-5.36328400	5.93076500	-7.00317100
H	-4.87317100	6.45151200	-7.83613500
H	-6.17222300	5.32567100	-7.44002900
C	-5.96379200	6.94017500	-6.01745600
H	-5.16623000	7.59887900	-5.64443200
H	-6.69880700	7.58036800	-6.52259000
C	-6.61139000	6.21264300	-4.83354600
H	-7.46545600	5.62076500	-5.19591700
H	-7.01164800	6.93454000	-4.10944000
C	-5.61195700	5.28304500	-4.12789900
H	-6.12635100	4.75639500	-3.31855300
H	-4.81468900	5.88590400	-3.67404700
Br	-1.95975500	6.60434600	-3.71322500

PhPh

UB3LYP-D3/6-31G(d)-SMD(THF)

Zero-point correction= 0.182221 (Hartree/Particle)
Thermal correction to Energy= 0.191057
Thermal correction to Enthalpy= 0.192001
Thermal correction to Gibbs Free Energy= 0.147731
Sum of electronic and zero-point Energies= -463.151993
Sum of electronic and thermal Energies= -463.143157
Sum of electronic and thermal Enthalpies= -463.142213
Sum of electronic and thermal Free Energies= -463.186484
HF=-463.3342142

UB3LYP-D3/def2svp-SMD(THF)//UB3LYP-D3/6-31G(d)-SMD(THF)

HF=-463.0053373

C	-1.05607000	-0.54627600	-0.38676400
C	0.33893700	-0.54590000	-0.38681900
C	1.06113300	0.59704700	0.00022400

C	0.33848900	1.73994000	0.38659000
C	-1.05651700	1.74022900	0.38518200
C	-1.76065700	0.59695500	-0.00113400
H	-1.59313800	-1.43913800	-0.69669700
H	0.87513000	-1.43328000	-0.71194000
H	0.87431300	2.62735100	0.71223300
H	-1.59394100	2.63305500	0.69460200
H	-2.84748600	0.59692000	-0.00165900
C	2.54710300	0.59711800	0.00091600
C	3.26963800	1.73956800	-0.38696200
C	3.26940900	-0.54524600	0.38947300
C	4.66464500	1.73999200	-0.38555300
H	2.73373600	2.62650100	-0.71377800
C	4.66441700	-0.54548600	0.38942100
H	2.73330800	-1.43225200	0.71576600
C	5.36889500	0.59729900	0.00227800
H	5.20198100	2.63246000	-0.69615700
H	5.20156700	-1.43788600	0.70053800
H	6.45572300	0.59737000	0.00280500

Vinylboronate

UB3LYP-D3/6-31G(d)-SMD(THF)

Zero-point correction= 0.225635 (Hartree/Particle)
Thermal correction to Energy= 0.237539
Thermal correction to Enthalpy= 0.238484
Thermal correction to Gibbs Free Energy= 0.189012
Sum of electronic and zero-point Energies= -489.086573
Sum of electronic and thermal Energies= -489.074668
Sum of electronic and thermal Enthalpies= -489.073724
Sum of electronic and thermal Free Energies= -489.123196
HF=-489.3122074

UB3LYP-D3/def2svp-SMD(THF)//UB3LYP-D3/6-31G(d)-SMD(THF)

HF=-488.9562882

C	-1.04736500	0.35363600	0.21056500
H	-0.70073800	0.39106400	1.24250000
H	-1.83330300	-0.37059900	-0.00158700
C	-0.52762500	1.15688300	-0.72816500
H	-0.91042500	1.08243400	-1.74791400
C	2.26100500	3.70515300	-0.77772800
C	2.00309200	3.53052700	0.76512800
B	0.59600800	2.18631900	-0.42375500
O	1.19293100	2.31648600	0.80830700
O	1.08869600	3.05898000	-1.36348300
C	2.31668700	5.14926300	-1.26247100

H	3.13785100	5.68582000	-0.77422400
H	2.49202600	5.17004900	-2.34344600
H	1.38309400	5.68002600	-1.06091000
C	3.48269500	2.92805700	-1.27852200
H	3.48172200	2.92948300	-2.37335900
H	4.41633200	3.38401500	-0.93359600
H	3.45618100	1.88698600	-0.94042100
C	1.14672400	4.64993900	1.36597400
H	0.84139900	4.36094700	2.37687500
H	1.70326600	5.59060800	1.42893000
H	0.24141000	4.81845400	0.77351700
C	3.25513500	3.31244300	1.60660700
H	3.92525800	4.17573900	1.52784300
H	2.97686000	3.19296100	2.65921900
H	3.79969600	2.41712200	1.29716200

VinylboronateRadical

UB3LYP-D3/6-31G(d)-SMD(THF)

Zero-point correction= 0.117064 (Hartree/Particle)
Thermal correction to Energy= 0.123382
Thermal correction to Enthalpy= 0.124326
Thermal correction to Gibbs Free Energy= 0.087681
Sum of electronic and zero-point Energies= -157.690001
Sum of electronic and thermal Energies= -157.683683
Sum of electronic and thermal Enthalpies= -157.682739
Sum of electronic and thermal Free Energies= -157.719384
HF=-157.8070652

UB3LYP-D3/def2svp-SMD(THF)//UB3LYP-D3/6-31G(d)-SMD(THF)

HF=-157.6930095

C	-0.85854800	-1.02988100	0.27843500
C	-0.22041700	-0.12742200	1.28836500
H	0.87396700	-0.12097900	1.19848400
H	-0.57862400	0.90664500	1.19779600
H	-0.44695500	-0.44684000	2.32433500
C	-2.32106700	-0.86957400	0.00103400
H	-2.61471100	0.18725700	-0.05079800
H	-2.61514000	-1.35431100	-0.93936300
H	-2.94155900	-1.32755400	0.79591100
C	-0.22028500	-2.35558500	0.00145900
H	-0.58003100	-2.79505100	-0.93833400
H	0.87397400	-2.28034500	-0.05121800
H	-0.44461700	-3.09255400	0.79716300

A-singlet

UB3LYP-D3/6-31G(d)-SMD(THF)

Zero-point correction= 0.801176 (Hartree/Particle)
Thermal correction to Energy= 0.839627
Thermal correction to Enthalpy= 0.840571
Thermal correction to Gibbs Free Energy= 0.729959
Sum of electronic and zero-point Energies= -5768.825229
Sum of electronic and thermal Energies= -5768.786778
Sum of electronic and thermal Enthalpies= -5768.785834
Sum of electronic and thermal Free Energies= -5768.896446
HF=-5769.6264047

UB3LYP-D3/def2svp-SMD(THF)//UB3LYP-D3/6-31G(d)-SMD(THF)

HF=-5770.6824841

Br	8.98717500	5.42731000	10.23205400
Fe	9.15704100	6.55432400	12.33315900
P	8.46999200	8.69388900	11.68172200
P	10.69570200	7.57261500	13.54213600
C	9.36163800	9.95159800	12.72756100
H	9.46330500	10.90579300	12.19861800
H	8.73959800	10.13664200	13.60809900
C	10.73619400	9.40922900	13.15670000
H	11.12205500	9.96764200	14.01629400
H	11.45604900	9.54367600	12.34441200
C	6.65360300	8.97377600	11.98919800
H	6.43407300	10.03271200	11.79337100
C	6.29630800	8.66352500	13.45848900
H	6.61187600	7.63957500	13.69641800
H	6.84460800	9.32584200	14.13759200
C	4.78797600	8.79449200	13.71622800
H	4.57121300	8.53380000	14.76012700
H	4.48635600	9.84380600	13.58089700
C	3.97877100	7.90808600	12.76094700
H	2.90348900	8.03221700	12.94264100
H	4.21577300	6.85237400	12.96040600
C	4.31521000	8.23370600	11.30009700
H	3.99623400	9.26255500	11.07602800
H	3.75882400	7.57466900	10.62138100
C	5.82052900	8.10095900	11.02515800
H	6.03144500	8.36911600	9.98374100
H	6.12101900	7.05022500	11.14060300
C	8.75507300	9.16181000	9.90628500
H	8.26625800	8.34901400	9.35212600
C	8.15125000	10.50704400	9.46503000

H	7.07276200	10.53157800	9.65898200
H	8.60065100	11.32105200	10.05198500
C	8.41157300	10.75806100	7.96938200
H	7.86931300	10.00185100	7.38304700
H	8.00306500	11.73528300	7.68060200
C	9.90701700	10.68118400	7.63138600
H	10.43393900	11.50310900	8.13929100
H	10.06065700	10.82511500	6.55411300
C	10.50857700	9.34355300	8.08428400
H	11.58646800	9.31775900	7.87767200
H	10.05503900	8.52398000	7.50819600
C	10.25927500	9.09727600	9.57905200
H	10.79406800	9.86213700	10.16032600
H	10.66117900	8.12349300	9.87514300
C	12.44994700	7.05691000	13.14836000
H	13.11213200	7.77563000	13.65256900
C	12.72277900	7.12348200	11.63103500
H	12.01274600	6.46433700	11.11186400
H	12.54864400	8.13454600	11.24883200
C	14.15800500	6.68959600	11.29605100
H	14.30699500	6.72398500	10.20904600
H	14.86541500	7.40812100	11.73651500
C	14.46040800	5.28555800	11.83454800
H	13.81931100	4.55664600	11.31711000
H	15.49969900	5.00724400	11.61700900
C	14.18966400	5.21007400	13.34258200
H	14.89543000	5.86651700	13.87326400
H	14.36396200	4.19176200	13.71333300
C	12.75290000	5.64093400	13.67458900
H	12.59025500	5.58500100	14.75705400
H	12.05128700	4.93714800	13.20566000
C	10.56448300	7.47359400	15.39621900
H	10.60385600	6.39751000	15.60153600
C	11.68435500	8.15343300	16.20359800
H	11.69008000	9.23310700	15.99845900
H	12.66580600	7.76693000	15.90488000
C	11.47800300	7.93119900	17.71212600
H	11.58102200	6.85829600	17.93152100
H	12.26682700	8.44659400	18.27554500
C	10.09300400	8.40913700	18.17077500
H	9.95664500	8.20697300	19.24104700
H	10.02875800	9.50044800	18.04386600
C	8.97714500	7.74218800	17.35447200
H	8.97340300	6.66044600	17.55280200
H	7.99519100	8.12430800	17.66263700
C	9.17510900	7.96363800	15.84797500

H	9.06858900	9.03412300	15.62095800
H	8.39672900	7.43428000	15.28783600
C	8.67040600	5.13368100	13.61938000
C	9.37331800	4.35517500	14.56090300
H	10.45807000	4.40674900	14.59806200
C	8.72827900	3.50016000	15.46203800
C	7.33432200	3.39918900	15.46257300
H	6.82875000	2.74574100	16.17000600
C	6.60090400	4.13982000	14.53199600
H	5.51526700	4.06075900	14.50559900
C	7.26454500	4.97220600	13.62430400
H	6.65749400	5.50616500	12.89208800
H	9.31493300	2.91668500	16.16987600

A-triplet

UB3LYP-D3/6-31G(d)-SMD(THF)

Zero-point correction= 0.800928 (Hartree/Particle)
Thermal correction to Energy= 0.839222
Thermal correction to Enthalpy= 0.840166
Thermal correction to Gibbs Free Energy= 0.728895
Sum of electronic and zero-point Energies= -5768.846380
Sum of electronic and thermal Energies= -5768.808086
Sum of electronic and thermal Enthalpies= -5768.807142
Sum of electronic and thermal Free Energies= -5768.918413
HF=-5769.6473078

UB3LYP-D3/def2svp-SMD(THF)//UB3LYP-D3/6-31G(d)-SMD(THF)

HF=-5770.7050472

Br	10.33200200	4.42236000	13.95688800
Fe	9.38766200	6.41763200	12.96487100
P	8.42045100	8.39491500	12.27734400
P	11.15968800	7.74774600	13.71887700
C	9.40985400	9.82808800	12.95809300
H	9.26370900	10.72114600	12.34069700
H	8.98506100	10.05414300	13.94153200
C	10.90334900	9.48909500	13.09758500
H	11.40867700	10.21954800	13.73893600
H	11.39154000	9.53866300	12.11845500
C	6.68485100	8.81789300	12.81265700
H	6.58002400	9.90785300	12.70500000
C	6.52094800	8.45293000	14.30407900
H	6.73454800	7.38344900	14.42868000
H	7.25375600	8.99442900	14.91285000
C	5.10261100	8.74800600	14.81308900
H	5.01769800	8.43872000	15.86287200

H	4.92548200	9.83364600	14.78634000
C	4.04587700	8.04095100	13.95498800
H	3.03733600	8.27913100	14.31702200
H	4.17293700	6.95278900	14.04901600
C	4.19278700	8.43611100	12.48022600
H	3.98560200	9.51147300	12.37086700
H	3.45321400	7.90650200	11.86600700
C	5.60353600	8.13233300	11.95234700
H	5.67977100	8.46092900	10.90993500
H	5.76767700	7.05039100	11.95899500
C	8.44803200	8.55773800	10.42585700
H	7.70009900	7.82150200	10.10418300
C	8.04589500	9.93470200	9.86945500
H	7.07370000	10.24690500	10.26865000
H	8.77986800	10.68776900	10.18770800
C	8.00007900	9.90041400	8.33214500
H	7.20220100	9.21384100	8.01366000
H	7.73699800	10.89348200	7.94561100
C	9.33793200	9.43406700	7.73933700
H	10.11302700	10.17979700	7.97155900
H	9.26999100	9.37902600	6.64537300
C	9.76211500	8.07491900	8.31521200
H	10.74347300	7.78084900	7.92151600
H	9.04654700	7.30352700	7.99532800
C	9.80477500	8.10992100	9.84961600
H	10.58713600	8.80920200	10.17229300
H	10.07728000	7.12331800	10.24720800
C	12.90459100	7.37718800	13.16299800
H	13.48000600	8.31035900	13.25775400
C	12.86867700	6.96979600	11.67356500
H	12.21054900	6.09512300	11.56632700
H	12.42912900	7.77062100	11.06859400
C	14.26503300	6.62137900	11.13861400
H	14.18951700	6.30486700	10.09018600
H	14.89462700	7.52366200	11.15343400
C	14.92679800	5.52765100	11.98607600
H	14.34046800	4.60096600	11.89954900
H	15.93332400	5.30614600	11.60810600
C	14.98686800	5.94685200	13.46047200
H	15.64149600	6.82609500	13.56001900
H	15.43488500	5.14931000	14.06740800
C	13.59184100	6.28544300	14.00871800
H	13.68100100	6.60849300	15.05203900
H	12.96330200	5.38743600	14.00554500
C	11.21457500	7.83696900	15.57628400
H	11.55944800	6.83064800	15.85136000

C	12.17879900	8.87302300	16.17915200
H	11.84360700	9.88435500	15.90934100
H	13.18824900	8.75274000	15.76807000
C	12.21399900	8.75121400	17.71234100
H	12.63488700	7.77180000	17.98277600
H	12.88524800	9.51158400	18.13243100
C	10.80970200	8.88491500	18.31990000
H	10.85248100	8.75079700	19.40842800
H	10.43705000	9.90485000	18.14116400
C	9.83087700	7.87843400	17.69725900
H	10.13690200	6.85586200	17.96205100
H	8.82197400	8.02371400	18.10474200
C	9.79996200	8.00209200	16.16706800
H	9.39958300	8.98753600	15.89308700
H	9.12287300	7.25093300	15.74023900
C	7.82937000	5.41114200	12.30719200
C	6.87187400	4.87803000	13.20011600
H	7.01378400	5.01737300	14.27167800
C	5.74155500	4.18181400	12.76545500
C	5.52885400	3.96973500	11.39745300
H	4.64850300	3.43195600	11.05242100
C	6.46936300	4.45271100	10.48518300
H	6.32530200	4.28900700	9.41802600
C	7.59003200	5.16041700	10.93998700
H	8.29235300	5.54006500	10.19713200
H	5.02396700	3.80053100	13.49077400

A-quintet

UB3LYP-D3/6-31G(d)-SMD(THF)

Zero-point correction= 0.800065 (Hartree/Particle)
Thermal correction to Energy= 0.839022
Thermal correction to Enthalpy= 0.839966
Thermal correction to Gibbs Free Energy= 0.725722
Sum of electronic and zero-point Energies= -5768.864176
Sum of electronic and thermal Energies= -5768.825219
Sum of electronic and thermal Enthalpies= -5768.824275
Sum of electronic and thermal Free Energies= -5768.938519
HF=-5769.6642413

UB3LYP-D3/def2svp-SMD(THF)//UB3LYP-D3/6-31G(d)-SMD(THF)

HF=-5770.721638

Br	9.95839300	5.29932800	10.35502400
Fe	9.24521900	6.32267500	12.41256100
P	8.44807300	8.55475700	11.76616600
P	11.01580400	7.59156300	13.53171000

C	9.37732500	9.82243700	12.77431800
H	9.37432000	10.79530900	12.26913600
H	8.81581800	9.94860900	13.70414500
C	10.83012800	9.40026500	13.09349600
H	11.23189100	10.02500000	13.89966500
H	11.46379000	9.57128500	12.21933400
C	6.64497700	8.84944000	12.13167500
H	6.40451300	9.90672600	11.95311400
C	6.33488000	8.51014200	13.60660000
H	6.67304800	7.48688400	13.81744700
H	6.88986100	9.17449000	14.27921300
C	4.83189000	8.60732300	13.90812200
H	4.65125400	8.33457700	14.95587700
H	4.50089500	9.64986900	13.78828800
C	4.01929000	7.70488400	12.97089700
H	2.94658900	7.79630100	13.18527300
H	4.29596000	6.65643300	13.15398200
C	4.30220300	8.05297900	11.50392200
H	3.94635700	9.07358900	11.29801000
H	3.74603300	7.38313200	10.83541600
C	5.80207800	7.96813300	11.18337800
H	5.97252900	8.25385100	10.13901900
H	6.13540400	6.92618100	11.28397100
C	8.70271800	9.04097500	9.98488100
H	8.24859800	8.21222300	9.42350900
C	8.03438000	10.35864100	9.54953700
H	6.95939300	10.34132500	9.76101300
H	8.46000000	11.19138200	10.12792700
C	8.25812500	10.61510500	8.04890700
H	7.73939000	9.83319700	7.47502800
H	7.80147400	11.57187400	7.76356300
C	9.74914100	10.60353400	7.68350300
H	10.24606600	11.45523100	8.17218500
H	9.87601200	10.74183600	6.60196400
C	10.42255800	9.30196700	8.14076200
H	11.49754300	9.32843600	7.91937800
H	10.00410300	8.45404600	7.57935600
C	10.20706300	9.06239700	9.64214400
H	10.69370300	9.87499500	10.19895800
H	10.68017000	8.12425500	9.94780700
C	12.79162500	7.18557300	13.14389000
H	13.43845400	7.90291400	13.66857600
C	13.06751700	7.28905500	11.62834300
H	12.36619300	6.63746900	11.09238900
H	12.89039000	8.31043100	11.27164200
C	14.50661100	6.86937600	11.29166000

H	14.66190800	6.93093400	10.20672300
H	15.21183000	7.57606700	11.75445000
C	14.80563200	5.45110900	11.79504400
H	14.16236800	4.73727600	11.25994400
H	15.84410900	5.17546800	11.57012600
C	14.53814300	5.33831800	13.30141800
H	15.24596400	5.98199400	13.84484600
H	14.71457600	4.31162900	13.64715000
C	13.10349800	5.76133300	13.65287500
H	12.95645100	5.69798400	14.73744500
H	12.39371600	5.05735700	13.19377700
C	10.88051500	7.52419500	15.39209300
H	10.91363800	6.44853400	15.61657100
C	12.00731100	8.21080000	16.18523600
H	12.01444400	9.28616900	15.95734600
H	12.98628100	7.81526900	15.89226800
C	11.80447300	8.01188900	17.69798000
H	11.90690700	6.94179000	17.93097800
H	12.59748300	8.53246100	18.25041400
C	10.42336700	8.49857200	18.15978800
H	10.29050800	8.30107600	19.23125300
H	10.36387200	9.58948700	18.02895900
C	9.29944500	7.83630800	17.35006600
H	9.28243200	6.75663900	17.55871900
H	8.32208100	8.23268600	17.65405600
C	9.50346500	8.05283700	15.84401100
H	9.44223400	9.12890000	15.63241700
H	8.70107600	7.56803200	15.27747600
C	7.98868100	5.12441600	13.50206100
C	8.10166000	4.85178500	14.88262700
H	8.95810700	5.23471600	15.43603300
C	7.15008400	4.10356600	15.58690200
C	6.03244200	3.59380900	14.92201800
H	5.28498000	3.01785900	15.46327600
C	5.88947000	3.82546500	13.55006500
H	5.02805500	3.42451400	13.01839000
C	6.85322600	4.57265300	12.86442300
H	6.71440600	4.72974300	11.79481800
H	7.27849800	3.92143900	16.65275300

TS1-doublet

UB3LYP-D3/6-31G(d)-SMD(THF)

Zero-point correction= 1.153879 (Hartree/Particle)
Thermal correction to Energy= 1.210344
Thermal correction to Enthalpy= 1.211288
Thermal correction to Gibbs Free Energy= 1.063918

Sum of electronic and zero-point Energies= -6415.674791
Sum of electronic and thermal Energies= -6415.618326
Sum of electronic and thermal Enthalpies= -6415.617382
Sum of electronic and thermal Free Energies= -6415.764752
HF=-6416.8286699

Br	9.31356400	6.24341300	9.33092100
Fe	8.80930400	6.21993000	11.72351000
P	8.27056800	8.69509900	11.82728800
P	10.87852100	6.95448600	12.78591400
C	9.63080600	9.52293300	12.80631600
H	9.71663200	10.57454100	12.50830400
H	9.32830000	9.51911600	13.85607800
C	10.98686800	8.81070300	12.64974900
H	11.70717300	9.19810300	13.37882000
H	11.40760100	9.00868600	11.66026600
C	6.68666000	9.28658600	12.62374600
H	6.69812400	10.38459500	12.58172900
C	6.56855100	8.88125900	14.10655200
H	6.63088000	7.79149900	14.19428000
H	7.39777300	9.29779800	14.68883400
C	5.23710600	9.36300200	14.70669500
H	5.16549100	9.03222500	15.75111600
H	5.22732800	10.46325500	14.72166500
C	4.03314900	8.85821000	13.90019800
H	3.09929100	9.24235800	14.33092500
H	3.98934300	7.76184800	13.96334900
C	4.15160900	9.26484800	12.42549600
H	4.09805300	10.36099300	12.34256300
H	3.30969800	8.86020600	11.84929700
C	5.47272100	8.76869800	11.81984500
H	5.54096400	9.07485600	10.76968300
H	5.48127200	7.67483900	11.82770400
C	8.31126700	9.57939600	10.16341700
H	7.76091400	8.90181000	9.49780100
C	7.63803500	10.96797500	10.12792200
H	6.60558900	10.92495500	10.48518800
H	8.17925800	11.65308200	10.79700100
C	7.63924200	11.53959100	8.69840900
H	7.01252100	10.89636800	8.06343400
H	7.17178100	12.53305700	8.69995200
C	9.05136900	11.61221000	8.10438400
H	9.64218400	12.35008900	8.66784400
H	9.00975100	11.96653700	7.06614300
C	9.74847100	10.24839300	8.18237400
H	10.78024900	10.32308000	7.81429200

H	9.23117600	9.52923200	7.53143100
C	9.75135400	9.70757300	9.61930300
H	10.31442500	10.40690300	10.25239800
H	10.26251700	8.74375400	9.64965200
C	12.58446900	6.44094000	12.20957700
H	13.26606800	7.21638500	12.59186200
C	12.64330600	6.43530800	10.66783700
H	11.95722800	5.66442000	10.30544400
H	12.29478700	7.38844000	10.25286900
C	14.06256400	6.12936600	10.16700100
H	14.06698200	6.11193400	9.06907900
H	14.74707500	6.93448800	10.47498100
C	14.56694300	4.79104700	10.72332400
H	13.93899600	3.98174100	10.32447700
H	15.59483400	4.59705800	10.38983000
C	14.48740700	4.76914100	12.25568700
H	15.18318200	5.51464700	12.66957500
H	14.80490200	3.79133100	12.64106100
C	13.06203200	5.07490900	12.74540900
H	13.03628200	5.04552100	13.84025500
H	12.39259200	4.29165500	12.37404400
C	10.83962200	6.59331100	14.62007500
H	11.00610100	5.51040600	14.67627700
C	11.93056100	7.28493200	15.45712700
H	11.78710600	8.37353800	15.42059300
H	12.92576400	7.08011400	15.04521800
C	11.86012600	6.82413900	16.92317700
H	12.08581000	5.74880200	16.97229500
H	12.63159000	7.33720800	17.51182000
C	10.47080800	7.08005700	17.52527200
H	10.43117700	6.71581200	18.55977800
H	10.29130000	8.16502000	17.56397900
C	9.36872000	6.41865800	16.68548500
H	9.47610900	5.32651300	16.73880000
H	8.37824700	6.65911200	17.09316700
C	9.44408400	6.86244800	15.21745000
H	9.22023800	7.93336700	15.16362500
H	8.67620900	6.34807500	14.62854800
C	6.94157800	5.49598600	11.83711000
C	6.22102500	5.39674300	13.04164100
H	6.71637800	5.59497000	13.98996000
C	4.86904900	5.03745200	13.07877300
C	4.18630000	4.75857500	11.89218300
H	3.13473700	4.48169300	11.91173700
C	4.88087400	4.83057900	10.68119600
H	4.36875500	4.60481000	9.74710500

C	6.23245700	5.19044200	10.65845800
H	6.74809000	5.24098600	9.70448000
H	4.35148600	4.97605600	14.03468600
C	8.11714800	1.56210500	15.22656200
H	7.74812100	2.32802300	15.92153600
H	7.26005300	1.19882700	14.64528400
H	8.49703800	0.72330100	15.82462800
C	9.68150000	1.02433600	13.34242100
H	10.53275200	1.35888200	12.73902600
H	8.88179800	0.72997300	12.65440800
H	10.00219700	0.13523000	13.90132700
C	9.21129100	2.12981500	14.30368200
C	10.40247400	2.58530800	15.16577900
H	10.10432800	3.36979100	15.87248200
H	10.80386400	1.74694600	15.75011100
H	11.22065300	2.97866900	14.55155100
C	8.59046900	3.33632500	13.52727500
C	9.49935900	4.00468700	12.51504200
C	9.33580300	2.05152200	9.26620600
C	10.87595600	2.45318100	9.35592900
B	9.71784600	3.32520800	11.15072600
O	10.92608900	3.36631900	10.47985300
O	8.79254900	2.51783000	10.52654100
C	8.56216200	2.76738100	8.15437400
H	8.89373900	2.44513200	7.16108900
H	7.49803400	2.52726400	8.25628200
H	8.67233400	3.84941700	8.23988000
C	9.07545700	0.54696700	9.17785500
H	7.99479600	0.36773700	9.18009200
H	9.48688700	0.13061700	8.25147700
H	9.50560500	0.00777500	10.02544300
C	11.41439800	3.19145700	8.13085600
H	12.47108000	3.43529800	8.28862700
H	11.34006200	2.57186300	7.23013900
H	10.87387000	4.12693200	7.97536300
C	11.80351200	1.28506300	9.70859400
H	11.85104000	0.54647600	8.90132100
H	12.81362300	1.67362300	9.87817700
H	11.48089400	0.78195900	10.62493300
H	7.67744200	2.99094500	13.03031100
H	8.26484700	4.05522400	14.29204400
H	10.43926600	4.30698300	12.96666800

TS1-quartet

UB3LYP-D3/6-31G(d)-SMD(THF)

Zero-point correction= 1.154286 (Hartree/Particle)

Thermal correction to Energy= 1.210557
Thermal correction to Enthalpy= 1.211501
Thermal correction to Gibbs Free Energy= 1.064445
Sum of electronic and zero-point Energies= -6415.710028
Sum of electronic and thermal Energies= -6415.653757
Sum of electronic and thermal Enthalpies= -6415.652813
Sum of electronic and thermal Free Energies= -6415.799869
HF=-6416.864314

UB3LYP-D3/def2svp-SMD(THF)//UB3LYP-D3/6-31G(d)-SMD(THF)
HF=-6417.4445215

Br	9.31356400	6.24341300	9.33092100
Fe	8.80930400	6.21993000	11.72351000
P	8.27056800	8.69509900	11.82728800
P	10.87852100	6.95448600	12.78591400
C	9.63080600	9.52293300	12.80631600
H	9.71663200	10.57454100	12.50830400
H	9.32830000	9.51911600	13.85607800
C	10.98686800	8.81070300	12.64974900
H	11.70717300	9.19810300	13.37882000
H	11.40760100	9.00868600	11.66026600
C	6.68666000	9.28658600	12.62374600
H	6.69812400	10.38459500	12.58172900
C	6.56855100	8.88125900	14.10655200
H	6.63088000	7.79149900	14.19428000
H	7.39777300	9.29779800	14.68883400
C	5.23710600	9.36300200	14.70669500
H	5.16549100	9.03222500	15.75111600
H	5.22732800	10.46325500	14.72166500
C	4.03314900	8.85821000	13.90019800
H	3.09929100	9.24235800	14.33092500
H	3.98934300	7.76184800	13.96334900
C	4.15160900	9.26484800	12.42549600
H	4.09805300	10.36099300	12.34256300
H	3.30969800	8.86020600	11.84929700
C	5.47272100	8.76869800	11.81984500
H	5.54096400	9.07485600	10.76968300
H	5.48127200	7.67483900	11.82770400
C	8.31126700	9.57939600	10.16341700
H	7.76091400	8.90181000	9.49780100
C	7.63803500	10.96797500	10.12792200
H	6.60558900	10.92495500	10.48518800
H	8.17925800	11.65308200	10.79700100
C	7.63924200	11.53959100	8.69840900
H	7.01252100	10.89636800	8.06343400

H	7.17178100	12.53305700	8.69995200
C	9.05136900	11.61221000	8.10438400
H	9.64218400	12.35008900	8.66784400
H	9.00975100	11.96653700	7.06614300
C	9.74847100	10.24839300	8.18237400
H	10.78024900	10.32308000	7.81429200
H	9.23117600	9.52923200	7.53143100
C	9.75135400	9.70757300	9.61930300
H	10.31442500	10.40690300	10.25239800
H	10.26251700	8.74375400	9.64965200
C	12.58446900	6.44094000	12.20957700
H	13.26606800	7.21638500	12.59186200
C	12.64330600	6.43530800	10.66783700
H	11.95722800	5.66442000	10.30544400
H	12.29478700	7.38844000	10.25286900
C	14.06256400	6.12936600	10.16700100
H	14.06698200	6.11193400	9.06907900
H	14.74707500	6.93448800	10.47498100
C	14.56694300	4.79104700	10.72332400
H	13.93899600	3.98174100	10.32447700
H	15.59483400	4.59705800	10.38983000
C	14.48740700	4.76914100	12.25568700
H	15.18318200	5.51464700	12.66957500
H	14.80490200	3.79133100	12.64106100
C	13.06203200	5.07490900	12.74540900
H	13.03628200	5.04552100	13.84025500
H	12.39259200	4.29165500	12.37404400
C	10.83962200	6.59331100	14.62007500
H	11.00610100	5.51040600	14.67627700
C	11.93056100	7.28493200	15.45712700
H	11.78710600	8.37353800	15.42059300
H	12.92576400	7.08011400	15.04521800
C	11.86012600	6.82413900	16.92317700
H	12.08581000	5.74880200	16.97229500
H	12.63159000	7.33720800	17.51182000
C	10.47080800	7.08005700	17.52527200
H	10.43117700	6.71581200	18.55977800
H	10.29130000	8.16502000	17.56397900
C	9.36872000	6.41865800	16.68548500
H	9.47610900	5.32651300	16.73880000
H	8.37824700	6.65911200	17.09316700
C	9.44408400	6.86244800	15.21745000
H	9.22023800	7.93336700	15.16362500
H	8.67620900	6.34807500	14.62854800
C	6.94157800	5.49598600	11.83711000
C	6.22102500	5.39674300	13.04164100

H	6.71637800	5.59497000	13.98996000
C	4.86904900	5.03745200	13.07877300
C	4.18630000	4.75857500	11.89218300
H	3.13473700	4.48169300	11.91173700
C	4.88087400	4.83057900	10.68119600
H	4.36875500	4.60481000	9.74710500
C	6.23245700	5.19044200	10.65845800
H	6.74809000	5.24098600	9.70448000
H	4.35148600	4.97605600	14.03468600
C	8.11714800	1.56210500	15.22656200
H	7.74812100	2.32802300	15.92153600
H	7.26005300	1.19882700	14.64528400
H	8.49703800	0.72330100	15.82462800
C	9.68150000	1.02433600	13.34242100
H	10.53275200	1.35888200	12.73902600
H	8.88179800	0.72997300	12.65440800
H	10.00219700	0.13523000	13.90132700
C	9.21129100	2.12981500	14.30368200
C	10.40247400	2.58530800	15.16577900
H	10.10432800	3.36979100	15.87248200
H	10.80386400	1.74694600	15.75011100
H	11.22065300	2.97866900	14.55155100
C	8.59046900	3.33632500	13.52727500
C	9.49935900	4.00468700	12.51504200
C	9.33580300	2.05152200	9.26620600
C	10.87595600	2.45318100	9.35592900
B	9.71784600	3.32520800	11.15072600
O	10.92608900	3.36631900	10.47985300
O	8.79254900	2.51783000	10.52654100
C	8.56216200	2.76738100	8.15437400
H	8.89373900	2.44513200	7.16108900
H	7.49803400	2.52726400	8.25628200
H	8.67233400	3.84941700	8.23988000
C	9.07545700	0.54696700	9.17785500
H	7.99479600	0.36773700	9.18009200
H	9.48688700	0.13061700	8.25147700
H	9.50560500	0.00777500	10.02544300
C	11.41439800	3.19145700	8.13085600
H	12.47108000	3.43529800	8.28862700
H	11.34006200	2.57186300	7.23013900
H	10.87387000	4.12693200	7.97536300
C	11.80351200	1.28506300	9.70859400
H	11.85104000	0.54647600	8.90132100
H	12.81362300	1.67362300	9.87817700
H	11.48089400	0.78195900	10.62493300
H	7.67744200	2.99094500	13.03031100

H	8.26484700	4.05522400	14.29204400
H	10.43926600	4.30698300	12.96666800

TS1-sextet

UB3LYP-D3/6-31G(d)-SMD(THF)

Zero-point correction= 1.153670 (Hartree/Particle)
Thermal correction to Energy= 1.210242
Thermal correction to Enthalpy= 1.211186
Thermal correction to Gibbs Free Energy= 1.061414
Sum of electronic and zero-point Energies= -6415.683072
Sum of electronic and thermal Energies= -6415.626500
Sum of electronic and thermal Enthalpies= -6415.625556
Sum of electronic and thermal Free Energies= -6415.775328
HF=-6416.8367419

UB3LYP-D3/def2svp-SMD(THF)//UB3LYP-D3/6-31G(d)-SMD(THF)

HF=-6417.4138317

Br	9.31356400	6.24341300	9.33092100
Fe	8.80930400	6.21993000	11.72351000
P	8.27056800	8.69509900	11.82728800
P	10.87852100	6.95448600	12.78591400
C	9.63080600	9.52293300	12.80631600
H	9.71663200	10.57454100	12.50830400
H	9.32830000	9.51911600	13.85607800
C	10.98686800	8.81070300	12.64974900
H	11.70717300	9.19810300	13.37882000
H	11.40760100	9.00868600	11.66026600
C	6.68666000	9.28658600	12.62374600
H	6.69812400	10.38459500	12.58172900
C	6.56855100	8.88125900	14.10655200
H	6.63088000	7.79149900	14.19428000
H	7.39777300	9.29779800	14.68883400
C	5.23710600	9.36300200	14.70669500
H	5.16549100	9.03222500	15.75111600
H	5.22732800	10.46325500	14.72166500
C	4.03314900	8.85821000	13.90019800
H	3.09929100	9.24235800	14.33092500
H	3.98934300	7.76184800	13.96334900
C	4.15160900	9.26484800	12.42549600
H	4.09805300	10.36099300	12.34256300
H	3.30969800	8.86020600	11.84929700
C	5.47272100	8.76869800	11.81984500
H	5.54096400	9.07485600	10.76968300
H	5.48127200	7.67483900	11.82770400
C	8.31126700	9.57939600	10.16341700

H	7.76091400	8.90181000	9.49780100
C	7.63803500	10.96797500	10.12792200
H	6.60558900	10.92495500	10.48518800
H	8.17925800	11.65308200	10.79700100
C	7.63924200	11.53959100	8.69840900
H	7.01252100	10.89636800	8.06343400
H	7.17178100	12.53305700	8.69995200
C	9.05136900	11.61221000	8.10438400
H	9.64218400	12.35008900	8.66784400
H	9.00975100	11.96653700	7.06614300
C	9.74847100	10.24839300	8.18237400
H	10.78024900	10.32308000	7.81429200
H	9.23117600	9.52923200	7.53143100
C	9.75135400	9.70757300	9.61930300
H	10.31442500	10.40690300	10.25239800
H	10.26251700	8.74375400	9.64965200
C	12.58446900	6.44094000	12.20957700
H	13.26606800	7.21638500	12.59186200
C	12.64330600	6.43530800	10.66783700
H	11.95722800	5.66442000	10.30544400
H	12.29478700	7.38844000	10.25286900
C	14.06256400	6.12936600	10.16700100
H	14.06698200	6.11193400	9.06907900
H	14.74707500	6.93448800	10.47498100
C	14.56694300	4.79104700	10.72332400
H	13.93899600	3.98174100	10.32447700
H	15.59483400	4.59705800	10.38983000
C	14.48740700	4.76914100	12.25568700
H	15.18318200	5.51464700	12.66957500
H	14.80490200	3.79133100	12.64106100
C	13.06203200	5.07490900	12.74540900
H	13.03628200	5.04552100	13.84025500
H	12.39259200	4.29165500	12.37404400
C	10.83962200	6.59331100	14.62007500
H	11.00610100	5.51040600	14.67627700
C	11.93056100	7.28493200	15.45712700
H	11.78710600	8.37353800	15.42059300
H	12.92576400	7.08011400	15.04521800
C	11.86012600	6.82413900	16.92317700
H	12.08581000	5.74880200	16.97229500
H	12.63159000	7.33720800	17.51182000
C	10.47080800	7.08005700	17.52527200
H	10.43117700	6.71581200	18.55977800
H	10.29130000	8.16502000	17.56397900
C	9.36872000	6.41865800	16.68548500
H	9.47610900	5.32651300	16.73880000

H	8.37824700	6.65911200	17.09316700
C	9.44408400	6.86244800	15.21745000
H	9.22023800	7.93336700	15.16362500
H	8.67620900	6.34807500	14.62854800
C	6.94157800	5.49598600	11.83711000
C	6.22102500	5.39674300	13.04164100
H	6.71637800	5.59497000	13.98996000
C	4.86904900	5.03745200	13.07877300
C	4.18630000	4.75857500	11.89218300
H	3.13473700	4.48169300	11.91173700
C	4.88087400	4.83057900	10.68119600
H	4.36875500	4.60481000	9.74710500
C	6.23245700	5.19044200	10.65845800
H	6.74809000	5.24098600	9.70448000
H	4.35148600	4.97605600	14.03468600
C	8.11714800	1.56210500	15.22656200
H	7.74812100	2.32802300	15.92153600
H	7.26005300	1.19882700	14.64528400
H	8.49703800	0.72330100	15.82462800
C	9.68150000	1.02433600	13.34242100
H	10.53275200	1.35888200	12.73902600
H	8.88179800	0.72997300	12.65440800
H	10.00219700	0.13523000	13.90132700
C	9.21129100	2.12981500	14.30368200
C	10.40247400	2.58530800	15.16577900
H	10.10432800	3.36979100	15.87248200
H	10.80386400	1.74694600	15.75011100
H	11.22065300	2.97866900	14.55155100
C	8.59046900	3.33632500	13.52727500
C	9.49935900	4.00468700	12.51504200
C	9.33580300	2.05152200	9.26620600
C	10.87595600	2.45318100	9.35592900
B	9.71784600	3.32520800	11.15072600
O	10.92608900	3.36631900	10.47985300
O	8.79254900	2.51783000	10.52654100
C	8.56216200	2.76738100	8.15437400
H	8.89373900	2.44513200	7.16108900
H	7.49803400	2.52726400	8.25628200
H	8.67233400	3.84941700	8.23988000
C	9.07545700	0.54696700	9.17785500
H	7.99479600	0.36773700	9.18009200
H	9.48688700	0.13061700	8.25147700
H	9.50560500	0.00777500	10.02544300
C	11.41439800	3.19145700	8.13085600
H	12.47108000	3.43529800	8.28862700
H	11.34006200	2.57186300	7.23013900

H	10.87387000	4.12693200	7.97536300
C	11.80351200	1.28506300	9.70859400
H	11.85104000	0.54647600	8.90132100
H	12.81362300	1.67362300	9.87817700
H	11.48089400	0.78195900	10.62493300
H	7.67744200	2.99094500	13.03031100
H	8.26484700	4.05522400	14.29204400
H	10.43926600	4.30698300	12.96666800

B-doublet

UB3LYP-D3/6-31G(d)-SMD(THF)

Zero-point correction= 1.156111 (Hartree/Particle)
Thermal correction to Energy= 1.212434
Thermal correction to Enthalpy= 1.213378
Thermal correction to Gibbs Free Energy= 1.066967
Sum of electronic and zero-point Energies= -6415.689617
Sum of electronic and thermal Energies= -6415.633295
Sum of electronic and thermal Enthalpies= -6415.632351
Sum of electronic and thermal Free Energies= -6415.778762
HF=-6416.8457286

UB3LYP-D3/def2svp-SMD(THF)//UB3LYP-D3/6-31G(d)-SMD(THF)

HF=-6417.431825

Br	9.98586500	5.43544500	9.77107600
Fe	9.13935500	5.53903800	12.07370200
P	8.31126800	7.90910900	11.94419400
P	11.04182500	6.69368200	13.07033000
C	9.39928100	9.01280700	12.99116400
H	9.33339200	10.04323500	12.62190500
H	8.97288000	9.01371200	13.99599900
C	10.86274200	8.54921200	13.04167200
H	11.37395500	8.98202700	13.90938100
H	11.39410900	8.90155300	12.15686300
C	6.61632600	8.39430800	12.58499500
H	6.60285100	9.49388000	12.54965600
C	6.40325200	7.97637300	14.05612800
H	6.44588500	6.88500600	14.13130900
H	7.19588400	8.37151900	14.70076600
C	5.04082600	8.46511400	14.57590400
H	4.90056700	8.12854800	15.61149100
H	5.03930800	9.56523600	14.59742700
C	3.88604100	7.97519800	13.69194500
H	2.93039200	8.36888800	14.06199100
H	3.82597500	6.87898800	13.75162500
C	4.10488500	8.37988200	12.22798100

H	4.06743700	9.47643800	12.14108700
H	3.29810000	7.98290500	11.59840800
C	5.45772200	7.86684800	11.71177600
H	5.59193800	8.15146400	10.66305300
H	5.45380800	6.77636900	11.73834900
C	8.42340800	8.68530500	10.23606800
H	8.00854800	7.91640700	9.57046600
C	7.64041800	10.00053900	10.03395100
H	6.58750000	9.89700300	10.30677000
H	8.06344700	10.77740400	10.68750100
C	7.72841500	10.46055500	8.56697700
H	7.22282700	9.71504900	7.93584900
H	7.17867800	11.40295700	8.44346500
C	9.17914300	10.62259600	8.09415200
H	9.64271500	11.46009500	8.63702600
H	9.20434900	10.88443000	7.02828100
C	9.99101800	9.34766800	8.35770300
H	11.04373400	9.50036200	8.08513600
H	9.61616200	8.52914800	7.72693600
C	9.89385900	8.92666700	9.83022200
H	10.30512700	9.73586900	10.44887000
H	10.49596200	8.03547600	10.00463300
C	12.79398800	6.42959000	12.45303800
H	13.43722700	6.98592800	13.15028200
C	13.03167400	6.99554900	11.03644800
H	12.34907800	6.50024800	10.33971800
H	12.81054100	8.06777800	10.99919500
C	14.48235500	6.76752400	10.58223400
H	14.60937400	7.15875600	9.56430800
H	15.16436200	7.33990200	11.22936400
C	14.86096500	5.28212500	10.63683800
H	14.23331700	4.72512700	9.92559600
H	15.90409100	5.13921600	10.32582700
C	14.63679700	4.72114000	12.04619100
H	15.32251700	5.21654900	12.75018200
H	14.87078000	3.64902200	12.07531100
C	13.18585600	4.93811700	12.50069200
H	13.05389800	4.53695600	13.51340400
H	12.52111500	4.37154300	11.83850100
C	11.08646100	6.25075500	14.88341800
H	11.10015100	5.15593200	14.88136700
C	12.30233800	6.73777900	15.69110700
H	12.34018800	7.83647300	15.67974900
H	13.23415900	6.37975100	15.23973600
C	12.22017200	6.24506200	17.14714300
H	12.29834500	5.14825300	17.15456800

H	13.07806400	6.62637800	17.71589900
C	10.90549600	6.66180000	17.82146500
H	10.85873300	6.26114900	18.84214000
H	10.87715700	7.75824700	17.90964000
C	9.69010200	6.19394800	17.00851200
H	9.64810600	5.09596000	17.00944200
H	8.75951500	6.54737500	17.47110300
C	9.77292900	6.69700700	15.56072000
H	9.72436400	7.79353300	15.57040000
H	8.90475400	6.34784700	14.98635500
C	7.28307500	4.92190800	11.76108700
C	6.43485500	4.63200500	12.84823300
H	6.79688900	4.74891200	13.86709100
C	5.11624300	4.19614900	12.67782700
C	4.59521500	4.03471400	11.39148100
H	3.57087500	3.69785000	11.24930800
C	5.41263400	4.31046600	10.29182500
H	5.02397700	4.18789400	9.28209200
C	6.72811300	4.74589700	10.47901800
H	7.34500000	4.94349500	9.60906700
H	4.49820500	3.98478800	13.54867800
C	8.62811700	1.71387600	15.87673400
H	8.40460200	2.58484100	16.50751600
H	7.68334700	1.37075900	15.43567500
H	9.00178200	0.91553300	16.53133800
C	9.90761000	0.82193900	13.91510900
H	10.71750600	0.99730900	13.19969100
H	9.01301100	0.54428100	13.34683000
H	10.19797100	-0.03323100	14.53969600
C	9.65474000	2.06678700	14.78345500
C	10.97439800	2.47434700	15.46021900
H	10.82768300	3.31869900	16.14372100
H	11.38138000	1.64157100	16.04881300
H	11.73591300	2.75964900	14.72525700
C	9.04960400	3.23024700	13.93448800
C	9.85645800	3.72330700	12.72718600
C	9.27898700	1.36404800	9.79468300
C	10.87081600	1.46426700	9.84907300
B	9.92461900	2.75080600	11.51905800
O	11.11696900	2.42688200	10.90065400
O	8.85615200	2.06015200	10.99161700
C	8.64494600	2.09964100	8.60853800
H	8.90796800	1.62991000	7.65429300
H	7.55563500	2.07225600	8.71848800
H	8.95358100	3.14631100	8.59755100
C	8.72538400	-0.05964200	9.86442500

H	7.63086500	-0.01888500	9.88472300
H	9.02751900	-0.64421400	8.98816800
H	9.05690200	-0.58256000	10.76504400
C	11.51862000	2.00751400	8.57431000
H	12.60267200	2.07448600	8.72172500
H	11.33089000	1.35100200	7.71725400
H	11.14979600	3.01106000	8.35298500
C	11.56589200	0.16475700	10.26928000
H	11.45842000	-0.61595700	9.50846300
H	12.63415700	0.36360600	10.40844800
H	11.17138100	-0.21396800	11.21631800
H	8.06752000	2.89427600	13.59073600
H	8.85628500	4.05824100	14.63683200
H	10.88462100	3.90900300	13.04285300

B-quartet

UB3LYP-D3/6-31G(d)-SMD(THF)

Zero-point correction= 1.155727 (Hartree/Particle)
Thermal correction to Energy= 1.212229
Thermal correction to Enthalpy= 1.213173
Thermal correction to Gibbs Free Energy= 1.065832
Sum of electronic and zero-point Energies= -6415.717080
Sum of electronic and thermal Energies= -6415.660578
Sum of electronic and thermal Enthalpies= -6415.659634
Sum of electronic and thermal Free Energies= -6415.806975
HF=-6416.8728075

UB3LYP-D3/def2svp-SMD(THF)//UB3LYP-D3/6-31G(d)-SMD(THF)

HF=-6417.4487846

Br	10.04799400	5.44148600	9.64679300
Fe	9.16302900	5.55337400	11.99475300
P	8.31055100	7.94628600	11.96017200
P	11.05199400	6.70224600	13.04257100
C	9.41968300	9.03468400	12.99652600
H	9.35655600	10.06576800	12.62872700
H	9.00672200	9.03719800	14.00688700
C	10.88001900	8.55868900	13.02175700
H	11.40810500	8.98618800	13.88188400
H	11.39868900	8.90841000	12.12850400
C	6.61864700	8.41516200	12.61349900
H	6.59727100	9.51497900	12.59194700
C	6.42021900	7.97395200	14.07967900
H	6.48496900	6.88236900	14.14033200
H	7.20965900	8.37604300	14.72397500
C	5.05226000	8.43092700	14.61337800

H	4.92352200	8.07590200	15.64420900
H	5.03196400	9.53037900	14.65203100
C	3.90180200	7.93505800	13.72729500
H	2.94130700	8.30527400	14.10872700
H	3.86172700	6.83714000	13.76840100
C	4.10548600	8.36905600	12.26966600
H	4.04978300	9.46620000	12.20258200
H	3.30194300	7.97011400	11.63729800
C	5.46314300	7.88772900	11.73592300
H	5.58689800	8.19711500	10.69299900
H	5.47661800	6.79690100	11.73950600
C	8.41110300	8.71738100	10.24967000
H	7.97949600	7.95306200	9.58942500
C	7.63789800	10.04032600	10.05970200
H	6.58792400	9.94680200	10.34756600
H	8.07833400	10.81241900	10.70724700
C	7.71093400	10.49839600	8.59125200
H	7.18910300	9.75775800	7.96772900
H	7.16944000	11.44637300	8.47459900
C	9.15693300	10.64501200	8.09885000
H	9.63598100	11.47869000	8.63409300
H	9.17004100	10.90522200	7.03238700
C	9.96011900	9.36253500	8.35272400
H	11.01051900	9.50488100	8.06619400
H	9.56971000	8.54648300	7.72852500
C	9.87896200	8.94361300	9.82670700
H	10.30497300	9.74970200	10.43939300
H	10.47452400	8.04626900	9.99360700
C	12.80154800	6.42808200	12.42739400
H	13.45009700	6.96913400	13.13150900
C	13.04711900	7.00548200	11.01692500
H	12.35551700	6.53053000	10.31484000
H	12.84563700	8.08213900	10.99303800
C	14.49275300	6.75572100	10.55782600
H	14.62508200	7.15556200	9.54394000
H	15.18684100	7.30789500	11.20969700
C	14.84358100	5.26292700	10.59522200
H	14.20391900	4.72518700	9.88003600
H	15.88296400	5.10410100	10.27939400
C	14.61410100	4.69123100	11.99936900
H	15.31218700	5.16600000	12.70544900
H	14.82768400	3.61459000	12.01618700
C	13.16972100	4.93012200	12.46330000
H	13.03768600	4.52585100	13.47487700
H	12.49111700	4.37774600	11.80349300
C	11.08900300	6.25269100	14.85495100

H	11.10646800	5.15803700	14.85095400
C	12.30193200	6.74154300	15.66645700
H	12.33819400	7.84030100	15.65668100
H	13.23572200	6.38541500	15.21762100
C	12.21649200	6.24758000	17.12186900
H	12.29561500	5.15084400	17.12877400
H	13.07270400	6.62939300	17.69282800
C	10.89978600	6.66292400	17.79295900
H	10.85137300	6.26307700	18.81387900
H	10.86981000	7.75944100	17.88018200
C	9.68720800	6.19241600	16.97746300
H	9.64616200	5.09468100	16.98055100
H	8.75495600	6.54561800	17.43696800
C	9.77220500	6.69386800	15.52911400
H	9.72096500	7.79005800	15.54074200
H	8.90761100	6.34165400	14.95208300
C	7.27867600	4.91965200	11.72066700
C	6.41888300	4.61951900	12.79329600
H	6.77016800	4.72303700	13.81668100
C	5.10055500	4.19331700	12.59729200
C	4.59670300	4.05437200	11.30143300
H	3.57277000	3.72489600	11.14045000
C	5.42929000	4.34224100	10.21655100
H	5.05354300	4.23675400	9.20010600
C	6.74455900	4.76897300	10.42734800
H	7.37524600	4.97727700	9.56939300
H	4.46912200	3.97224000	13.45599000
C	8.59712300	1.68298300	15.89084100
H	8.36124400	2.54881300	16.52409800
H	7.65865400	1.33332000	15.44150100
H	8.97342200	0.88494000	16.54429700
C	9.90021200	0.81069400	13.93636600
H	10.71390600	0.99668100	13.22816800
H	9.01286500	0.52568400	13.36034700
H	10.19465100	-0.04361800	14.56021100
C	9.62820900	2.05013700	14.80640200
C	10.93879900	2.46875600	15.49459000
H	10.77906800	3.31286800	16.17535100
H	11.34739000	1.63992900	16.08764600
H	11.70459600	2.75956000	14.76613800
C	9.01896300	3.21235400	13.95958000
C	9.83472200	3.72324700	12.76496700
C	9.29876100	1.35724500	9.82696200
C	10.88946600	1.46447100	9.89777700
B	9.92034300	2.75450100	11.55184700
O	11.11954500	2.43692800	10.94537500

O	8.85977000	2.06157900	11.01403600
C	8.67454900	2.08044200	8.62844600
H	8.94783800	1.60146800	7.68165300
H	7.58418700	2.05101100	8.72784100
H	8.98187600	3.12742700	8.60966400
C	8.75019700	-0.06805300	9.90368800
H	7.65537900	-0.03154400	9.91142100
H	9.06445200	-0.65910700	9.03611200
H	9.07371400	-0.58158700	10.81257100
C	11.54984100	1.99975000	8.62629200
H	12.63268600	2.06517600	8.78338300
H	11.36897100	1.33793200	7.77184700
H	11.18511000	3.00280700	8.39688700
C	11.58527200	0.17127900	10.33602200
H	11.49228600	-0.61385700	9.57784900
H	12.65047700	0.37670900	10.48832600
H	11.18023100	-0.20522100	11.27932600
H	8.04409800	2.86888300	13.60173900
H	8.81029700	4.03440500	14.66268200
H	10.85695500	3.91695700	13.09331200

B-sextet

UB3LYP-D3/6-31G(d)-SMD(THF)

Zero-point correction= 1.153175 (Hartree/Particle)
Thermal correction to Energy= 1.210616
Thermal correction to Enthalpy= 1.211561
Thermal correction to Gibbs Free Energy= 1.059371
Sum of electronic and zero-point Energies= -6415.699852
Sum of electronic and thermal Energies= -6415.642411
Sum of electronic and thermal Enthalpies= -6415.641467
Sum of electronic and thermal Free Energies= -6415.793656
HF=-6416.8530271

UB3LYP-D3/def2svp-SMD(THF)//UB3LYP-D3/6-31G(d)-SMD(THF)

HF=-6417.4275634

Br	9.98559100	5.30829600	9.60024000
Fe	9.20702800	5.23702300	11.86488900
P	8.25053700	8.10914600	11.88670700
P	11.04710800	6.68778300	12.98416400
C	9.43645300	9.09538100	12.94383900
H	9.44709800	10.14755400	12.63357000
H	9.03780800	9.07734800	13.96063000
C	10.87586100	8.54584700	12.93579200
H	11.45045700	8.97489500	13.76567000
H	11.37659100	8.86120700	12.01871100

C	6.58838600	8.61649100	12.60141000
H	6.55953000	9.71543100	12.63637100
C	6.40508700	8.09205100	14.04160000
H	6.48844300	6.99866200	14.03828000
H	7.19380500	8.47107100	14.70158800
C	5.03369500	8.48996100	14.61234700
H	4.92312900	8.08000900	15.62500500
H	4.98740000	9.58523300	14.70769700
C	3.88652400	8.01098600	13.71278300
H	2.92057500	8.33736200	14.12009100
H	3.87436900	6.91201300	13.69881900
C	4.06464300	8.52286100	12.27758300
H	3.97438100	9.61968400	12.26707500
H	3.26721700	8.13221700	11.63200200
C	5.43252800	8.11781700	11.70708900
H	5.53522500	8.50274200	10.68598900
H	5.48050400	7.02622100	11.63666700
C	8.31291200	8.98212700	10.21987900
H	7.73352900	8.32094000	9.55868400
C	7.69437900	10.39354300	10.16152200
H	6.65935700	10.39135000	10.51710500
H	8.25721700	11.06416000	10.82711000
C	7.73156300	10.95163500	8.72753300
H	7.08513700	10.33014700	8.09038800
H	7.30839100	11.96482500	8.71269800
C	9.15315200	10.95753900	8.14961300
H	9.76949500	11.67071000	8.71767600
H	9.13999600	11.30964400	7.10983100
C	9.79111600	9.56457700	8.23907100
H	10.82730400	9.59349300	7.87679400
H	9.24667200	8.86742400	7.58549600
C	9.75816800	9.03097400	9.67893000
H	10.35543700	9.70298000	10.31048700
H	10.21780300	8.04050700	9.72381200
C	12.81045400	6.43855400	12.39146600
H	13.44671800	7.02440000	13.07084600
C	13.03366600	6.96253600	10.95513600
H	12.35602000	6.43576400	10.27564800
H	12.79504700	8.02911600	10.88164000
C	14.48525500	6.74088200	10.50028900
H	14.60217300	7.10160300	9.47006400
H	15.16033500	7.34394400	11.12614300
C	14.88627700	5.26375800	10.60029600
H	14.26619100	4.67530100	9.90793700
H	15.93085400	5.12746500	10.29149700
C	14.67355200	4.74232600	12.02666300

H	15.35388900	5.26757500	12.71383600
H	14.92175900	3.67479400	12.08681700
C	13.22113000	4.95381400	12.47916700
H	13.09436300	4.57731900	13.50172500
H	12.56317300	4.36156000	11.83198200
C	11.04944900	6.23645000	14.79705600
H	11.11325600	5.14194700	14.79195900
C	12.21504300	6.77549800	15.64465600
H	12.20252000	7.87464200	15.63831300
H	13.17623900	6.46287600	15.22136900
C	12.10614400	6.27440800	17.09613200
H	12.22931800	5.18168800	17.10446400
H	12.92804800	6.68929400	17.69376600
C	10.75352400	6.63582700	17.72639100
H	10.69001500	6.23345700	18.74547500
H	10.67739400	7.73016400	17.81233700
C	9.58511800	6.11822300	16.87548600
H	9.58542200	5.01980700	16.88061400
H	8.62658800	6.43623700	17.30558200
C	9.69339000	6.61961900	15.42869300
H	9.59229500	7.71195800	15.43296400
H	8.86360300	6.22709400	14.82638300
C	7.17540500	4.85537600	11.74876200
C	6.35105700	4.61642400	12.86553900
H	6.77262700	4.65534900	13.86828400
C	4.98666900	4.33022400	12.74060000
C	4.39857400	4.27170800	11.47416400
H	3.33852500	4.05189200	11.36994800
C	5.19041500	4.49353600	10.34400900
H	4.74557200	4.44694900	9.35143300
C	6.55269300	4.77876700	10.48512100
H	7.14525000	4.94992800	9.58988500
H	4.38401400	4.15341700	13.62964800
C	8.56646300	1.63860800	15.94273500
H	8.32678100	2.55076000	16.50569100
H	7.63847100	1.28003300	15.47884400
H	8.89601200	0.87906800	16.66380200
C	9.92890000	0.60841900	14.10798700
H	10.77045600	0.73061100	13.41711200
H	9.05883700	0.29783500	13.51961200
H	10.18649600	-0.20396000	14.80043200
C	9.64799800	1.90903400	14.88004100
C	10.93919700	2.35722400	15.58632600
H	10.77186800	3.25823900	16.18793700
H	11.30686100	1.57283900	16.26091600
H	11.73798000	2.57453500	14.86747100

C	9.10683800	3.02420100	13.93009400
C	9.99961800	3.43610300	12.75781500
C	9.48587600	1.06356800	9.85197000
C	11.06182600	1.26202400	9.84944700
B	10.11172000	2.46379200	11.57024000
O	11.27081800	2.30346400	10.83316600
O	9.08173000	1.66372800	11.10875600
C	8.76110400	1.83179200	8.74143800
H	8.98450900	1.41816800	7.75179100
H	7.68128100	1.76082500	8.91048500
H	9.03384500	2.88845900	8.75824600
C	9.02512500	-0.39316300	9.85058700
H	7.93112100	-0.42750100	9.89586000
H	9.34315900	-0.90317800	8.93416500
H	9.41379700	-0.94479900	10.71013200
C	11.64168800	1.75172600	8.52364500
H	12.72515800	1.88106600	8.62626600
H	11.45896300	1.03066200	7.71884800
H	11.21463700	2.71789300	8.24580200
C	11.83740900	0.03536200	10.34263100
H	11.77283100	-0.79936100	9.63645600
H	12.89209500	0.30711900	10.45935200
H	11.46852600	-0.30088200	11.31668100
H	8.14039000	2.68610800	13.53963500
H	8.88328800	3.89400700	14.56923200
H	10.99565400	3.71385400	13.10596300

TS2-quartet

UB3LYP-D3/6-31G(d)-SMD(THF)

Zero-point correction= 1.153615 (Hartree/Particle)
Thermal correction to Energy= 1.209959
Thermal correction to Enthalpy= 1.210904
Thermal correction to Gibbs Free Energy= 1.063823
Sum of electronic and zero-point Energies= -6415.693705
Sum of electronic and thermal Energies= -6415.637361
Sum of electronic and thermal Enthalpies= -6415.636417
Sum of electronic and thermal Free Energies= -6415.783497
HF=-6416.8473205

UB3LYP-D3/def2svp-SMD(THF)//UB3LYP-D3/6-31G(d)-SMD(THF)

HF=-6417.4291204

Br	9.31475500	6.06132300	9.58773600
Fe	8.84046900	6.40150700	11.95729200
P	8.14435100	8.79259500	11.87570400
P	10.83644300	7.33883600	12.98789400

C	9.33415600	9.77831000	12.92834900
H	9.35211400	10.82897000	12.61394800
H	8.92464500	9.75988700	13.94103300
C	10.77008500	9.20535100	12.94681700
H	11.32508800	9.61461300	13.79964200
H	11.30505700	9.51738200	12.04797800
C	6.44945000	9.32509600	12.44907800
H	6.32799800	10.38749000	12.19932800
C	6.22534400	9.18063200	13.96657700
H	6.40050000	8.14110300	14.26491400
H	6.93424500	9.80242400	14.52517900
C	4.79110000	9.58791900	14.34703300
H	4.64270500	9.44759500	15.42594100
H	4.66040400	10.66220800	14.14761000
C	3.73933200	8.79611700	13.55730400
H	2.73048200	9.14163700	13.81878600
H	3.79897900	7.73659600	13.83932900
C	3.97130300	8.91815100	12.04521300
H	3.79934600	9.95867300	11.73090000
H	3.24979700	8.29747200	11.49830300
C	5.40086000	8.50384500	11.66759900
H	5.55181100	8.61541300	10.58649200
H	5.54377200	7.44063900	11.89709500
C	8.29066800	9.51540500	10.14663800
H	7.85584800	8.73168900	9.51234700
C	7.54625100	10.83670600	9.87737800
H	6.48101900	10.74594200	10.11375000
H	7.95222000	11.62721700	10.52606200
C	7.69103100	11.25543400	8.40266800
H	7.17991900	10.51025100	7.77550000
H	7.17729500	12.21184000	8.23814000
C	9.15931600	11.35424100	7.96789800
H	9.64284700	12.17870600	8.51353900
H	9.22320500	11.60160800	6.90016600
C	9.90917300	10.04925500	8.26588500
H	10.97131900	10.14814500	8.00502900
H	9.50397800	9.23789900	7.64475800
C	9.77217000	9.66129700	9.74419700
H	10.23440300	10.44974000	10.35438200
H	10.31422700	8.73392000	9.93910800
C	12.51176300	6.90071700	12.29609100
H	13.28718300	7.36565100	12.92092900
C	12.68914500	7.39794800	10.84599800
H	11.86295100	7.01674200	10.23432700
H	12.64803600	8.49259400	10.80285400
C	14.01996000	6.91448100	10.24830100

H	14.10575100	7.26957600	9.21290600
H	14.85709900	7.35948600	10.80736900
C	14.13004800	5.38513600	10.30017600
H	13.33546300	4.95042600	9.67670000
H	15.08813400	5.05342800	9.87886400
C	13.97009300	4.87831900	11.73917000
H	14.81496500	5.23469200	12.34781400
H	14.00007300	3.78099300	11.76455400
C	12.64909500	5.36511700	12.35053000
H	12.56343900	5.00527100	13.38390800
H	11.82068700	4.92323700	11.78675000
C	10.92651000	6.91198000	14.80738400
H	10.75910900	5.82801600	14.83085500
C	12.25359800	7.19678400	15.53205300
H	12.45730300	8.27729100	15.51485400
H	13.08908400	6.70539700	15.02188100
C	12.18948800	6.70449700	16.98955800
H	12.10002900	5.60822300	16.98650400
H	13.12942300	6.94255200	17.50429400
C	10.99874700	7.30497900	17.75072800
H	10.95112600	6.89221000	18.76664200
H	11.14883900	8.38987100	17.85635700
C	9.67736000	7.05569200	17.00920100
H	9.45949300	5.97767800	16.99677500
H	8.84538400	7.54165200	17.53522200
C	9.75715200	7.57207600	15.56589600
H	9.91064200	8.65924300	15.59192000
H	8.80926500	7.40228300	15.04232600
C	7.38149500	5.25189200	12.64585500
C	6.78554500	5.58672100	13.88648500
H	7.40578400	5.95901700	14.69755800
C	5.41795600	5.42957800	14.11186900
C	4.58741300	4.92258800	13.10687000
H	3.52262700	4.79418200	13.28320700
C	5.15366900	4.57206100	11.87370800
H	4.52405400	4.17005000	11.08200400
C	6.52095600	4.72147500	11.65016500
H	6.94139900	4.42494500	10.69679600
H	4.99829400	5.70806800	15.07661600
C	9.15395400	4.01045800	12.92698100
C	8.95752400	1.83368900	9.81465200
C	10.50806000	2.17867300	9.87591800
B	9.38977000	3.20128600	11.61620600
O	10.58851000	3.16362900	10.94021200
O	8.44996700	2.35526400	11.07269200
C	8.20083100	2.56147900	8.69839300

H	8.49931200	2.19859000	7.70886400
H	7.12788000	2.37699200	8.82105600
H	8.37103500	3.63876400	8.75077700
C	8.63613200	0.34101900	9.76211300
H	7.54942000	0.20358200	9.76752400
H	9.03112200	-0.11086900	8.84540700
H	9.04635900	-0.19558300	10.62115700
C	11.07238100	2.81401100	8.60590200
H	12.14349000	3.00298100	8.73934600
H	10.95130500	2.14686300	7.74504000
H	10.58712900	3.76954500	8.40187800
C	11.39192400	0.99922300	10.29517800
H	11.43653500	0.23650800	9.51039700
H	12.40804900	1.36680600	10.47440500
H	11.03689200	0.53048800	11.21598000
H	10.05017800	4.53212200	13.25716800
C	8.56266500	3.20697700	14.08657800
C	9.53157900	2.23677500	14.83098500
H	8.16747800	3.88217500	14.85407100
H	7.70433100	2.62919400	13.72068400
C	10.17331300	1.21784200	13.87582500
H	9.41192100	0.69389200	13.28605200
H	10.86010000	1.70891200	13.17992500
H	10.74782300	0.46737600	14.43446600
C	10.64399000	3.02415600	15.54767000
H	11.29457500	3.54356300	14.83491900
H	10.22249000	3.77296300	16.23048600
H	11.27815200	2.35179000	16.13997200
C	8.69868000	1.48276800	15.88503000
H	7.90963000	0.88514000	15.41096900
H	9.32830700	0.80176800	16.47223500
H	8.21644200	2.17883700	16.58375300

TS2-sextet

UB3LYP-D3/6-31G(d)-SMD(THF)

Zero-point correction= 1.151333 (Hartree/Particle)
Thermal correction to Energy= 1.208271
Thermal correction to Enthalpy= 1.209215
Thermal correction to Gibbs Free Energy= 1.058626
Sum of electronic and zero-point Energies= -6415.680915
Sum of electronic and thermal Energies= -6415.623977
Sum of electronic and thermal Enthalpies= -6415.623032
Sum of electronic and thermal Free Energies= -6415.773622
HF=-6416.8322477

UB3LYP-D3/def2svp-SMD(THF)//UB3LYP-D3/6-31G(d)-SMD(THF)

HF=-6417.4125604

Br	9.08889600	6.18242600	9.49307400
Fe	8.76891200	6.61752600	11.83129600
P	8.20845300	9.01161400	11.76056800
P	10.79439900	7.43893800	12.93514800
C	9.39673700	9.94507200	12.85721300
H	9.46968700	10.99287500	12.54261100
H	8.96032700	9.94710400	13.85907400
C	10.80822000	9.30851900	12.90180200
H	11.36475200	9.69294000	13.76490200
H	11.37114700	9.59969000	12.01234000
C	6.49077400	9.44513200	12.33116800
H	6.33498100	10.52816000	12.23569200
C	6.26289500	9.04221700	13.80145200
H	6.49865600	7.97721800	13.92001200
H	6.93434800	9.59926400	14.46565000
C	4.80552900	9.27775200	14.22975300
H	4.67213200	8.94778500	15.26837700
H	4.59114100	10.35683900	14.20926600
C	3.82137400	8.54603300	13.30698600
H	2.78734300	8.75542500	13.61075900
H	3.97312900	7.46206100	13.40670600
C	4.04040700	8.94675600	11.84257600
H	3.79795600	10.01230700	11.71345200
H	3.36286400	8.38496800	11.18680400
C	5.49373100	8.70268000	11.41179800
H	5.63135900	9.00647400	10.36703700
H	5.70856700	7.62516200	11.45909700
C	8.37935800	9.78140600	10.06593800
H	7.86897400	9.06431800	9.40917200
C	7.73390500	11.16752700	9.88281000
H	6.67157200	11.14417500	10.14854200
H	8.21718500	11.88916600	10.55791300
C	7.87918700	11.64771800	8.42741400
H	7.29738600	10.97824500	7.77696100
H	7.44135100	12.64902600	8.32206100
C	9.34250500	11.65208400	7.96402300
H	9.90052900	12.40674800	8.53870400
H	9.40528600	11.94856000	6.90893900
C	9.99443900	10.27892100	8.17679800
H	11.05476800	10.30972500	7.89344900
H	9.51299200	9.53579900	7.52511600
C	9.85981800	9.82538600	9.63695500
H	10.39891900	10.54043800	10.27362800
H	10.32761700	8.84684500	9.77355800

C	12.44102100	6.89747200	12.25866300
H	13.24221700	7.33407700	12.87102900
C	12.63208000	7.35215200	10.79593400
H	11.78357800	6.99676500	10.19737900
H	12.64151200	8.44614900	10.72574300
C	13.93446400	6.79000900	10.20468900
H	14.03264300	7.11573800	9.16090100
H	14.79397300	7.20760800	10.75046300
C	13.96999200	5.25878000	10.29282900
H	13.15545400	4.84968300	9.67846300
H	14.91066600	4.87179000	9.87971300
C	13.78587700	4.79091400	11.74217700
H	14.64884300	5.11520200	12.34322400
H	13.75915300	3.69433700	11.79013600
C	12.49321400	5.35717900	12.34578600
H	12.39273200	5.02347700	13.38627000
H	11.64002200	4.94673400	11.79440300
C	10.81134600	6.99851800	14.75150800
H	10.56155200	5.92994400	14.76589800
C	12.14460900	7.18585700	15.49786900
H	12.42122800	8.25022300	15.49150800
H	12.95353000	6.64233800	14.99817400
C	12.02205400	6.69047300	16.95055400
H	11.85611600	5.60344200	16.93803800
H	12.96804400	6.85925700	17.48123400
C	10.86416100	7.36838300	17.69732100
H	10.76838800	6.94968400	18.70733600
H	11.09042900	8.43836700	17.81802400
C	9.54158700	7.22387200	16.93042500
H	9.24478700	6.16521900	16.90125400
H	8.73811900	7.76494100	17.44669100
C	9.68494600	7.74631500	15.49421700
H	9.92592900	8.81709900	15.53327800
H	8.73415700	7.65793700	14.95740400
C	7.53096500	5.19999200	12.73690200
C	7.01536000	5.47150200	14.05619200
H	7.68633600	5.89766300	14.79917500
C	5.71224000	5.18701000	14.44030100
C	4.80512200	4.62533500	13.52424200
H	3.78236100	4.40700500	13.82063900
C	5.24537800	4.36128900	12.21264600
H	4.54990100	3.94379300	11.48561300
C	6.54906000	4.64270400	11.83413800
H	6.85180800	4.43679700	10.81147300
H	5.38370900	5.41905400	15.45275100
C	9.03238000	3.73152000	13.06037000

C	8.88471900	1.73754600	9.85257200
C	10.38462600	2.22711800	9.85792800
B	9.28218800	3.02563700	11.70916700
O	10.38481400	3.23490500	10.90431500
O	8.44075500	2.05498300	11.19965200
C	7.99327800	2.52956100	8.89000000
H	8.21213000	2.28157400	7.84553600
H	6.94603000	2.27971400	9.09101200
H	8.12515900	3.60532500	9.02818500
C	8.69884000	0.24029100	9.62429300
H	7.63153600	-0.00532100	9.65297200
H	9.08861600	-0.05428600	8.64331800
H	9.20139000	-0.35278200	10.39253500
C	10.85137500	2.87457100	8.55723200
H	11.91298700	3.13417400	8.63430500
H	10.73317300	2.18370600	7.71453300
H	10.29604200	3.79246200	8.35819700
C	11.37791400	1.14300400	10.29065300
H	11.49411200	0.37377700	9.51960700
H	12.35470400	1.60795500	10.46269300
H	11.06468200	0.66104000	11.22100100
H	9.82695900	4.40717000	13.37242800
C	8.51526400	2.85313000	14.18573500
C	9.59786300	2.06626900	14.98741200
H	7.95904400	3.45238600	14.91875400
H	7.79717500	2.13127700	13.77424100
C	10.44910200	1.18250100	14.06020800
H	9.81534500	0.51741000	13.46114900
H	11.04377100	1.78986400	13.36906900
H	11.14374400	0.55959300	14.63919400
C	10.51791500	3.04194400	15.74502100
H	11.09785500	3.66664700	15.05628400
H	9.93648800	3.70762200	16.39627300
H	11.23270700	2.49717900	16.37558500
C	8.86957900	1.17344900	16.00866000
H	8.21826000	0.44793700	15.50456700
H	9.58328500	0.61145100	16.62534100
H	8.24337100	1.77213500	16.68300900

P

UB3LYP-D3/6-31G(d)-SMD(THF)

Zero-point correction= 0.444142 (Hartree/Particle)
Thermal correction to Energy= 0.466250
Thermal correction to Enthalpy= 0.467195
Thermal correction to Gibbs Free Energy= 0.392973
Sum of electronic and zero-point Energies= -878.441476

Sum of electronic and thermal Energies= -878.419367
Sum of electronic and thermal Enthalpies= -878.418423
Sum of electronic and thermal Free Energies= -878.492645
HF=-878.8856177

UB3LYP-D3/def2svp-SMD(THF)//UB3LYP-D3/6-31G(d)-SMD(THF)
HF=-878.2509234

C	-6.15174100	3.29995000	-2.56298000
H	-5.96692500	4.14311200	-3.24112000
H	-5.78647200	2.38888800	-3.05474900
H	-7.23788300	3.20083400	-2.44059000
C	-5.81751800	2.32528700	-0.28657800
H	-5.42292300	1.38283000	-0.68660500
H	-5.41933300	2.45041800	0.72390100
H	-6.90786300	2.22379100	-0.20511000
C	-5.45932600	3.51233500	-1.20145600
C	-5.98510700	4.81529400	-0.57381000
H	-5.70989800	5.68869800	-1.17958100
H	-7.07961100	4.79360000	-0.49605500
H	-5.58767800	4.96715800	0.43628200
C	-3.93261200	3.60442400	-1.47321500
H	-3.79141900	4.32790800	-2.28908200
H	-3.58910500	2.64136500	-1.87223000
C	-2.99381100	4.03805800	-0.31791400
C	0.54309300	5.18298500	-1.15397000
C	0.49046700	3.74088100	-1.78103500
B	-1.52210800	4.26238300	-0.84699000
O	-0.94572100	3.47101600	-1.81063200
O	-0.67200200	5.21226200	-0.34122600
C	1.73978300	5.44852900	-0.24848900
H	2.67556900	5.34944500	-0.80979400
H	1.68594300	6.46908000	0.14551400
H	1.76500300	4.75950000	0.59913700
C	0.39989600	6.29918900	-2.19286800
H	0.24056900	7.25042300	-1.67474700
H	1.29903200	6.38904500	-2.81094700
H	-0.45890000	6.12157100	-2.84862700
C	1.11406900	2.66696800	-0.88380400
H	0.86840400	1.67946200	-1.28779500
H	2.20394500	2.76186000	-0.84378600
H	0.71894100	2.72198300	0.13572100
C	1.03727800	3.63350000	-3.19915800
H	2.09747700	3.90901500	-3.22349700
H	0.94585900	2.60103000	-3.55311500
H	0.49203400	4.27834300	-3.89257700

C	-2.29395700	0.82988200	1.66456100
C	-2.60579400	1.22034100	2.97013500
C	-3.03881100	2.52666100	3.20875100
C	-3.16634300	3.42936000	2.15005800
C	-2.87139000	3.04747300	0.83299700
C	-2.42000500	1.73502200	0.61016100
H	-1.94761700	-0.18174000	1.46677000
H	-2.50853100	0.51543100	3.79177800
H	-3.28029900	2.84496600	4.22008700
H	-3.50819400	4.44344500	2.34513300
H	-2.16187500	1.42618500	-0.39897100
H	-3.34687300	4.99078500	0.09279800

TS5'

UB3LYP-D3/6-31G(d)-SMD(THF)

Zero-point correction= 1.241213 (Hartree/Particle)
Thermal correction to Energy= 1.301435
Thermal correction to Enthalpy= 1.302379
Thermal correction to Gibbs Free Energy= 1.146969
Sum of electronic and zero-point Energies= -4075.450800
Sum of electronic and thermal Energies= -4075.390579
Sum of electronic and thermal Enthalpies= -4075.389634
Sum of electronic and thermal Free Energies= -4075.545044
HF=-4076.6920131

UB3LYP-D3/def2svp-SMD(THF)//UB3LYP-D3/6-31G(d)-SMD(THF)

HF=-4074.9664202

Fe	8.80188900	6.36713600	11.74535600
P	8.12372200	8.83012100	11.82362200
P	10.78831900	7.29364400	12.93614800
C	9.37096700	9.79710400	12.82681200
H	9.43608500	10.82898000	12.46057300
H	8.97951000	9.85263100	13.84475000
C	10.77964500	9.16072500	12.84379400
H	11.36933700	9.57441700	13.67105600
H	11.30896500	9.42114800	11.92457600
C	6.45849100	9.39943500	12.45417500
H	6.37054700	10.48187100	12.28869400
C	6.27112500	9.13217300	13.96068300
H	6.43343300	8.06721600	14.16016200
H	7.01148500	9.68791000	14.54790500
C	4.85768200	9.51882500	14.42662300
H	4.74699600	9.28695300	15.49422900
H	4.72708000	10.60665600	14.32385000
C	3.77622100	8.79986400	13.60869200

H	2.77721100	9.11431900	13.93825500
H	3.84867800	7.71785000	13.78764600
C	3.95483300	9.06878900	12.10893200
H	3.78812200	10.13763500	11.90699500
H	3.20477500	8.51554300	11.52895200
C	5.36338600	8.67755000	11.63800400
H	5.47366300	8.89666300	10.56889600
H	5.49332100	7.59235100	11.75418000
C	8.24320900	9.57765800	10.10749600
H	7.65577500	8.88830700	9.48886000
C	7.67628300	10.99641300	9.92032300
H	6.63038400	11.04676100	10.24213800
H	8.23839200	11.70591200	10.54546100
C	7.76666700	11.42602100	8.44405400
H	7.10634900	10.77761500	7.84961100
H	7.38793000	12.45058100	8.33150500
C	9.19674300	11.32152100	7.89557400
H	9.83504100	12.05498300	8.41137100
H	9.21331700	11.58320400	6.82946800
C	9.77336600	9.91601000	8.11443200
H	10.81498100	9.87126100	7.76962600
H	9.21037100	9.18430200	7.51827800
C	9.69668800	9.51882700	9.59522300
H	10.31421000	10.21722400	10.17649800
H	10.11259100	8.51719200	9.73832400
C	12.50424100	6.82277400	12.36349700
H	13.23894200	7.32877400	13.00501700
C	12.75911600	7.26033700	10.90676600
H	11.97322800	6.84749300	10.26299700
H	12.70263200	8.35068100	10.81185000
C	14.12949400	6.77831500	10.40385000
H	14.26073200	7.07646300	9.35548200
H	14.92133300	7.28236200	10.97791200
C	14.28847600	5.25958400	10.55383300
H	13.55768300	4.75374200	9.90552700
H	15.28468900	4.94547800	10.21610200
C	14.05131300	4.82733700	12.00661500
H	14.83891300	5.25184600	12.64720500
H	14.12187200	3.73541900	12.09776400
C	12.67510700	5.29472700	12.50189400
H	12.52935300	4.98226500	13.54303600
H	11.90310000	4.78895000	11.91039000
C	10.78690500	6.92888400	14.77872000
H	10.54123800	5.86141700	14.83764300
C	12.10985500	7.14972500	15.53704700
H	12.37941100	8.21529200	15.50065600

H	12.93150700	6.59726400	15.07046600
C	11.97367200	6.69883200	17.00333000
H	11.81560500	5.61071900	17.02181100
H	12.91313400	6.88984600	17.53831600
C	10.80404800	7.39008000	17.71824300
H	10.69758200	6.99727900	18.73764500
H	11.02413700	8.46389600	17.81375700
C	9.49296100	7.22033800	16.93742000
H	9.19760800	6.16080700	16.93473700
H	8.68149900	7.77484400	17.42647400
C	9.65721700	7.70210900	15.48939500
H	9.90694500	8.77136000	15.50382600
H	8.71269700	7.60888500	14.94493200
C	7.42163500	5.17631700	12.67502700
C	6.93440300	5.54188000	13.95597700
H	7.61895900	5.98009200	14.67731800
C	5.60847900	5.33924900	14.34321900
C	4.70026000	4.73993400	13.46386900
H	3.66731400	4.57620800	13.76101300
C	5.15287400	4.33659900	12.19896700
H	4.46551800	3.85373500	11.50596100
C	6.47899400	4.54014300	11.82263800
H	6.80425900	4.20254300	10.84437600
H	5.28190300	5.65343300	15.33340700
C	9.21002700	3.78217400	12.97351900
C	9.01696800	1.68757500	9.83627600
C	10.52310900	2.14000100	9.83235700
B	9.42974200	3.05447700	11.63277300
O	10.51583900	3.23955000	10.78701800
O	8.58394400	2.06052300	11.17268900
C	8.14921900	2.47314900	8.84667600
H	8.36938700	2.19555400	7.81027900
H	7.09577500	2.24984900	9.04569700
H	8.29741200	3.55003900	8.95896700
C	8.79704900	0.18897900	9.65599100
H	7.72453200	-0.03205300	9.68768500
H	9.18417000	-0.14498200	8.68660100
H	9.28375000	-0.38981100	10.44500600
C	11.04188900	2.63917400	8.48915900
H	12.08065900	2.97274300	8.59626800
H	11.02108300	1.83014100	7.74973000
H	10.45410200	3.47487400	8.11150200
C	11.47836400	1.07603300	10.38677000
H	11.60567500	0.24730600	9.68222900
H	12.45775500	1.53564600	10.55834000
H	11.12189800	0.67213600	11.33751400

H	10.01907300	4.43520700	13.28989900
C	8.61468300	2.97566900	14.11286100
C	9.62232700	2.13005400	14.95273100
H	8.09692600	3.63103200	14.82451200
H	7.84902300	2.30084900	13.70852500
C	10.44095300	1.18204100	14.06227000
H	9.78425000	0.55911200	13.44359800
H	11.10036100	1.74320000	13.39131800
H	11.07018200	0.51758600	14.66911600
C	10.58135300	3.05211600	15.72785300
H	11.21104700	3.63900700	15.04990700
H	10.02668000	3.75267700	16.36539400
H	11.24953400	2.46836600	16.37452400
C	8.80668000	1.29941200	15.96049400
H	8.12965400	0.60661600	15.44448000
H	9.46406200	0.70532600	16.60885900
H	8.19586300	1.94550300	16.60451300
C	8.67208200	6.17911800	9.66924200
C	9.72497400	5.95791300	8.75721800
C	7.39914800	6.34334700	9.07360100
C	9.54114500	5.92112800	7.36832800
H	10.73055100	5.78881900	9.13574100
C	7.18576400	6.29584900	7.69168500
H	6.53495200	6.51797300	9.71481500
C	8.26465300	6.08940400	6.82586200
H	10.39293500	5.75272600	6.71062700
H	6.18230900	6.42577000	7.28837900
H	8.11235600	6.05863300	5.74907100

7.12 References

(1) Lee, W.; Zhou, J.; Gutierrez, O. *J. Am. Chem. Soc*. **2017**, *139*, 16126–16133.

(2) Liu, L.; Lee, W.; Zhou, J.; Bandyopadhyay, S.; Gutierrez, O. *Tetrahedron*, **2019**, *75*, 129–136.

(3) Liu, L.; Lee, W.; Yuan, M.; Acha, C.; Geherty, M. B.; Williams, B. Gutierrez, O. *Chem. Sci*. **2020**, *11*, 3146–3151.

(4) Liu, L.; Lee, W.; Youshaw, C. R.; Yuan, M.; Geherty, M. B.; Zavalij, P. Y.; Gutierrez, O. *Chem. Sci*. **2020**, *11*, 8301–8305.